Mechanisms of cellular senescence and the use of repurposed drugs as senotherapeutic compounds.

Submitted by

Laura Rosemary Bramwell, BSc (Hons), MSc by Res,

to the University of Exeter as a thesis for the degree of

PhD Medical Studies

November 2022

Abstract

The mechanisms of cellular ageing underpin the pathologies of many age-related diseases, but are not yet fully understood. Cellular senescence and mRNA splicing factor dysregulation are particularly interesting as recent evidence suggests they may be druggable targets. Compounds that are already prescribed for other diseases may be “senotherapeutic” with the ability to affect cellular senescence. Methods for improving existing models and techniques for assessing senescence were developed, including the improvement of human *in vitro* tissue culture models, techniques for medium-throughput senescence screening and a tool for analysis of fluorescence imaging of nuclear staining (FINS). Diseases of premature ageing, progeroid syndromes, represent an important avenue of research for treating disease and for basic ageing science. mRNA splicing factor dysregulation was found to occur in progeroid cells, providing more evidence supporting it as a hallmark of cellular ageing. Progeroid cells were affected by trametinib treatment, a drug known to reverse some aspects of senescence in normal circumstances, but the more severe phenotypes were not rescued. This suggested that senomorphic compounds can only rescue less senescent cell cultures. As many compounds have never been investigated for senotherapeutic ability, a medium-throughput screen studied 240 drugs for altered gene expression of the senescence marker, *CDKN2A*. 32 compounds were screened further for senescence-associated beta galactosidase (SAB) activity (the “gold standard” measure of senescence). Compounds that either decreased or induced senescence were identified for further validation. Bioinformatic association of structure and function identified a

potential common molecular substructure within compounds that decreased *CDKN2A* gene expression. Some synthetic female hormones affected senescence in the screen, so were used in further experiments to measure senescence and aspects of the senescence phenotype in male and female treated cells. Such treatment affected senescence in male cells and some senescence characteristics in both sexes, suggesting a sex-specific senomorphic effect and that sex differences in the context of ageing and cellular senescence may be important. This thesis contributes several new methods for studying human-relevant models of cellular ageing, evidence of the basic mechanisms of cellular ageing, potential candidates for the treatment of age-related disease, and identifies sex as being an important factor in the response of cells to senotherapeutic treatment. Senotherapeutic compounds that can target the underlying mechanisms of cellular ageing could treat many different diseases.

Contents

List of Tables

List of Figures

Author Declaration

Many of the data chapters for this thesis have been prepared as articles for submission to primary research journals. These articles are collaborative works with other authors, however I was the lead author for each article and was responsible for the majority of the work going into the articles. The author contributions are listed within the bounds of the article format, however my exact contribution is detailed further for clarity in a short introductory section at the beginning of each chapter.

Abbreviations

3'	3-prime end of a nucleic acid molecule
5'	5-prime end of a nucleic acid molecule
ACF	Animal component-free
ADC	Antibody drug conjugation
ADMET	Absorption, distribution, metabolism, excretion, and toxicity
ADS	Antibody diluent solution
ADST	Antibody diluent solution - triton
AKT	Protein kinase B
ALK	Anaplastic lymphoma kinase
AMP	Adenosine monophosphate
AMPK	AMP-activated protein kinase
ANOVA	Analysis of variance
BPE	Bovine pituitary extract
BSA	Bovine serum albumin
C. elegans	*Caenorhabditis elegans*
C. medius	*Cheirogaleus medius*
Cas9	CRISPR-associated protein 9
CDK	Cyclin dependent kinase
cDNA	Complementary DNA
cGAS-STING	Cyclic GMP-AMP synthase-stimulator of interferon genes pathway
COX	Cyclooxygenase
cPDL	Cumulative population doublings
CRISPR	Clustered regularly interspersed short palindromic repeats
C_T	Cycle threshold
D. melanogaster	*Drosophila melanogaster*
DAPI	4′,6-diamidino-2-phenylindole
DDR	DNA damage response
dH_2O	Distilled water
DMEM	Dulbecco's modified eagle medium
DMSO	Dimethylsulfoxide
DNA	Deoxyribonucleic acid
DNA-SCARS	DNA segments with chromatin alterations reinforcing senescence
DNN	Deep neural network
DPBS	Dulbecco's phosphate buffered saline
dUTP	Deoxyuridine triphosphate
ECM	Extracellular matrix
EDTA	Ethylenediaminetetraacetic acid
EGF	Epidermal growth factor
EMA	European Medical Agency
ERK	Extracellular signal-regulated kinase

ESE	Exonic splicing enhancer
ESS	Exonic splicing silencer
FAM	Fluorescein amidites
FBS	Foetal bovine serum
FCS	Foetal calf serum
FDA	USA Food and Drug Administration
FGF	Fibroblast growth factor
FINS	Fluorescence Imaging of Nuclear Staining algorithm
FOXO	Forkhead box O
GABA	Gamma-aminobutyric acid
GMP	Guanosine monophosphate
GOI	Gene of interest
GPCR	G protein coupled receptor
GTP	Guanosine triphosphate
H. glaber	*Heterocephalus glaber*
H. sapiens	*Homo sapiens*
HAoEC	Human aortic endothelial cell
HCFU	1-hexylcarboamoyl-5-fluorouracil
HCV	Hepatitis C virus
HDAC	Histone deacetylase
HIV	Human influenza virus
hnRNP	Heterogeneous nuclear ribonucleoprotein
HS	Human serum
Hsp90	Heat shock protein 90
HUF	Human uterine fibroblast
IGF-1	Insulin-like growth factor 1
IIS	Insulin and insulin-like growth factor signalling
IKK	Inhibitor of nuclear factor kappa B kinase
ISE	Intronic splicing enhancer
ISS	Intronic splicing silencer
JAK	Janus kinase
LSD	Least significant difference
M. musculus	*Mus musculus*
MAPK	Mitogen-activated protein kinase
MEK	Mitogen-activated protein kinase kinase
miRNA	MicroRNA
mRNA	Messenger RNA
mtDNA	Mitochondrial DNA
mTOR	Mechanistic target of rapamycin
NAD	Nicotinamide adenine dinucleotide
NF-κB	Nuclear factor kappa-light-chain-enhancer of activated B cells
nHDF	Normal human dermal fibroblast
NO	Nitric oxide
PBMC	Peripheral blood mononuclear cell
PBS	Phosphate buffered saline
PCR	Polymerase chain reaction

PD	Population doubling
PI3K	Phosphoinositide 3-kinase
POLG	DNA polymerase subunit gamma
PPAR	Peroxisome Proliferation
pre-mRNA	Precursor messenger RNA
RAF	Rapidly accelerated fibrosarcoma family of protein kinases
RAR	Retinoid acid receptor
RAS	Rat sarcoma protein
REC	Retinal endothelial cell
RNA	Ribonucleic acid
RNP	Ribonucleoprotein
ROCK	Rho-associated protein kinase
ROS	Reactive oxygen species
RPMI	Roswell Park Memorial Institute medium
RT	Reverse transcription
RT-qPCR	Real-time quantitative polymerase chain reaction
RTK	Receptor tyrosine kinase
RXR	Retinoid X Receptor
S. microcephalus	*Somniosus microcephalus*
SAHF	Senescence-associated heterochromatin foci
SASP	Senescence-associated secretory phenotype
SCAP	Senescent cell anti-apoptotic pathway
SDF	Structure-data file
SEM	Standard error of the mean
Smad	“Small mothers against decapentaplegic” family of proteins
SMILES	Simplified molecular input line entry system
SR	Serine and arginine-rich
STAT	Signal transducer and activator of transcription
Taq polymerase	*Thermus aquaticus* DNA polymerase
TGF	Transforming growth factor
TRP	Transient receptor potential channel
TUNEL	Terminal deoxynucleotidyl transferase dUTP nick-end labelling
TV	Total variation
UV	Ultraviolet
VEGF	Vascular endothelial growth factor
VEGFR	Vascular endothelial growth factor receptor
ΔC_T	Delta C_T value
$\Delta\Delta C_T$	Delta delta C_T value

Acknowledgements

Firstly, I would like to gratefully acknowledge the generosity of Animal Free Research UK and all of their supporters. This project would not have been possible without you.

I would like to thank my wonderful supervisor, Professor Lorna Harries, for her faith in me, her infectious enthusiasm and her incredible mind. Without her guidance I would be in a very different situation. My thanks go to my second supervisors, Dr Brandon Invergo and Dr Jack Spencer, for their patience, help and expertise.

I'd like to thank members of Team RNA, Senisca Ltd, and the wider UoE/NHS RILD research laboratory teams, past and present, for doing the groundwork for my project, and for their help and friendship in the laboratory. Particular thanks for their willingness to help, their collaboration, mentorship and camaraderie go to Dr Ben Lee, Dr Nicola Jeffery, Dr Shahnaz Haque, Emad Manni, Ryan Frankum, Fred Mou, Merlin Davies and Dr Sam Gould.

I'd like to thank the scientists across the globe and the people of our NHS who all reacted speedily and amazingly during the Covid-19 pandemic to create vaccines, develop tests and/or treatments and analyse public health data. The world can't thank you enough for limiting the impact of this virus. Without you, I would not have achieved this PhD.

To all my friends, diving buddies and students, for helping me to take my mind off work and find some calm beneath the waves. My thanks go to my friends from Exeter University SAC, Reading University BSAC, Berkshire Alumni Diving SAC, and the wider BSAC community.

I'd like to say thank you to my family for their support and inspiration. My mother, Dr Kathleen Bramwell, for her proofreading and for never letting me doubt that I was capable of being a scientist by her own example. My grandmother, Mary Briggs, for helping my mum by reading and typing up my mum's handwritten PhD thesis thus setting the precedent! My father, John Bramwell, for his ability to keep me grounded and for many late-night discussions over cups of tea. My sister, Rowanne Bramwell for her understanding, supply of coffee and for letting me vent frustrations when needed.

My partner, Lt James Sinclair RN - thank you for listening to every one of my issues even when you're wildly sleep-deprived at sea in a different time zone, trying to get away to finish preparing for an underwater bomb disposal exercise or some other equally outrageous scenario! Thank you for fixing far too many little inconsequential things, for weathering the storms with me, and for being my favourite diving buddy.

Chapter 1: Introduction

Ageing

Why research ageing and age-related disease?

People are now living longer than they ever have before. This brings with it new challenges in healthcare research due to the additional burden posed by an increased lifespan and an increase in age-related diseases. This burden is exacerbated by the fact that people tend to spend a longer time in a period of ill health towards the end of their lives with less compression of morbidity [1,2]. To help combat this, research into age-related disease can improve the length of time that a person is living without disease, their "healthspan" [3].

A baby girl born in the UK today can expect a life expectancy of 92.6 years with reasonable chances of surviving past 100 years [4]. In 1991, there were 9.1 million people aged 65 years or over, representing 15.8% of the UK's population. 25 years later, in 2016, there were 11.8 million in this age category which represents 18% of the total population of the UK. Fifty years after these estimates, in 2066, the proportion of older people is projected to increase to approximately 26% of the population (20.4 million people) [5].

The vast majority of UK health care expenditure is for persons in the older age categories [4]. For example, 41% of adult hospital admissions in the UK in 2018 were for people over age 65 [6]. Given the projected increases in population, this trend is set to continue. The reason for this disparity in healthcare spending by age group is because, as we age, our risk of age-related disease increases. Many

diseases are age-related and, as a whole, age-related disease makes up the bulk of healthcare spending. Many common diseases are age-related, such as type two diabetes, dementia, osteoarthritis and cardiovascular disease, to name a few [6,7]. Naturally these diseases disproportionately affect the older population, for example, it is thought that one in six people over the age of 80 have dementia [6,8,9]. It is clear that age-related disease will become more problematic as the population continues to age. Aside from research into individual disease pathologies, one approach to combat this problem is to target medical research into ageing itself. It is well evidenced that there are many cellular and molecular mechanisms which are altered during ageing and underpin the root causes and/or exacerbation of many age-related diseases [10].

Ageing as a disease or disease process

Ageing is generally defined as being a universal, intrinsic, progressive and deleterious process that encapsulates the change in an organism over time. For example, in humans, we might expect to feel frailer, lose mobility, and find remembering things more difficult, as well as suffering from some form of age-related disease, e.g. age-related macular degeneration. There is much debate about whether or not ageing should be classed as a disease *per se*, as it fulfils many criteria for a disease, but also meets criteria for being a process that underpins diseases [11,12]. Ultimately, this classification is only relevant in the context of its use, for instance, it may be useful to categorise ageing as a disease when making provisions for healthcare or medical research, but it would not be appropriate to diagnose a patient with ageing as a disease. Ageing is a process

that happens at the organismal scale by definition, however there is a molecular basis for the process [3].

The molecular basis of ageing

Theories of ageing

There are many theories as to how and why organisms age, and inevitably many theories overlap with each other. It is likely that ageing as a process includes elements from all theories [13]. Generally the theories attempt either to explain why ageing happens (evolutionary ageing theories), or the mechanisms that drive ageing as a process (programmed ageing or damage accumulation theories). Evolutionary ageing theories include antagonistic pleiotropy and the disposable soma theory [14]. Antagonistic pleiotropy is the idea that a trait is evolutionarily selected for in early life due to it increasing the odds of an organism surviving to successfully reproduce, despite it offering deleterious effects after the age of reproduction. The trait persists because any negative selective pressure comes after the age at which the trait would have already been passed onto offspring. The disposable soma theory builds on the concept of antagonistic pleiotropy to suggest that, as life tends to have limited resources, an organism's genetics will push towards reproduction and the survival of the gene rather than maintaining the body (or soma) of the organism [14]. Many other concepts interleave with these basic theories, such as the idea that cellular senescence (a hallmark of ageing) is an evolutionary trade off that offers protection against cancers [15].

Programmed ageing theories suggest that ageing is programmed into our DNA. There is evidence that epigenetic patterns correlate with age, i.e. the Horvath clock [16,17]. The reproductive-cell cycle theory links ageing and the sex hormones that control reproduction via a programmed mechanism (as DNA can determine biological sex). The theory suggests that reproduction comes at the cost of ageing in a form of antagonistic pleiotropy [18]. Damage accumulation theories suggest that the negative effects of ageing are due to the build-up over time of damage caused by specific inducers like free radicals or DNA damage-inducing compounds, or through the increased chance of random DNA replication errors over an extended period of time [13,19,20]. The theories of ageing, despite their differences, broadly share common molecular processes termed the “Hallmarks of Ageing”.

Hallmarks of ageing

There are now fourteen widely accepted “Hallmarks of Ageing”, illustrated as symbols in Figure 1 [21]. The hallmarks of ageing were first described in a landmark paper by López-Otín *et al.* that drew on previous works regarding hallmarks of cancer [22,23]. The hallmarks are all interrelated, but each hallmark must fulfil three criteria. Firstly, the hallmark must happen during normal ageing. Secondly, ageing should be accelerated when the hallmark is experimentally aggravated. Finally, ageing should slow when the hallmark is experimentally ameliorated. One would also expect to see hallmarks present across multiple species.

López-Otín *et al.* categorised their hallmarks into three categories: primary hallmarks (that characterise ageing *per se*), antagonistic hallmarks (where it is thought that the process initially provides a benefit but in a chronic situation can become the opposite), and integrative hallmarks (which are the higher level of hallmark and are generally caused by the other hallmarks). Many review articles discuss the evidence for each hallmark in great detail, so here I will simply discuss the basic concepts of each individual hallmark, followed by a brief illustration of some of the evidence that shows it fulfils the criteria for being termed a hallmark of ageing [21–29]. The hallmarks are ordered by their aforementioned categories.

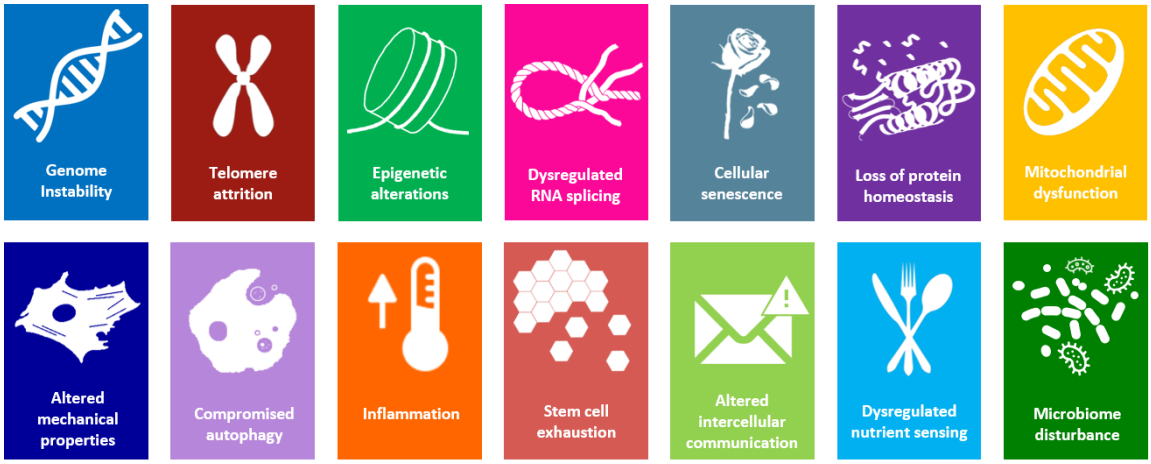

Figure 1: The 14 "Hallmarks of Ageing". The hallmarks of ageing include genome instability, telomere attrition, epigenetic alterations, dysregulated RNA splicing, cellular senescence, loss of protein homeostasis, mitochondrial dysfunction, altered mechanical properties, compromised autophagy, inflammation, stem cell exhaustion, altered intercellular communication, dysregulated nutrient sensing, and microbiome disturbance [21].

López-Otín *et al.*'s initial primary hallmarks were genome instability, epigenetic changes, a loss of protein homeostasis and attrition of the telomeres. Then, the antagonistic hallmarks included cellular senescence, a dysregulation in nutrient sensing and mitochondrial dysfunction. The final integrative hallmarks were alterations in intercellular communication and an exhaustion of the supply of stem cells needed to replenish tissues. In 2022, following a conference in Copenhagen,

a revised list of fourteen hallmarks was published. Five new hallmarks were added: splicing dysregulation, compromised autophagy, altered mechanical properties, inflammation and disturbance in the microbiome [21].

Genome instability

Instability of the genome is probably the most obvious of the hallmarks of ageing, considering DNA's role in biology and that a theory of ageing speculates that accumulation of DNA damage is the cause of ageing. As a hallmark, this process encapsulates any form of damage to the genome or increase in instability. It therefore includes mutations (substitutions, insertions, deletions, inversions) in the nucleotide sequence, DNA damage accumulation from lesions (caused by exogenous or endogenous factors, e.g. UV radiation, reactive oxygen species (ROS) etc.) and impairment of the DNA damage repair pathways (e.g. base excision repair, non-homologous end joining, and mismatch repair etc.) [19]. The mitochondrial genome can be affected as well as the nuclear genome. Changes in the location of DNA within the cell and the genome's organisation are also associated with ageing and/or senescence. For example, the presence of cytoplasmic chromatin fragments and altered chromosome positioning during interphase have both been linked with senescence [30,31]. The key evidence for genomic instability as a hallmark of ageing comes from observations that mutations accumulate in aged organisms including humans [32]. Further evidence comes from a unique source: diseases that cause a premature ageing phenotype, termed progeroid diseases. These syndromes mostly occur as a result of defects in genes associated with DNA repair or via closely linked mechanisms, e.g.

laminopathies decrease the defence of the nucleus against DNA damage-inducing agents resulting in more DNA damage accumulation [33]. Baker *et al.*'s *BubR1* mouse studies are an animal model of progeria disease and show that when genomic instability is manipulated it can increase ageing when aggravated and decrease ageing when ameliorated. Mice that underexpress *BubR1*, a cell cycle checkpoint that checks for correct chromosomal segregation, subsequently exhibit shorter lifespan as well as earlier onset of age-related issues such as sarcopenia, cardiac arrhythmia and dermal thinning. When *BubR1* is overexpressed, the mice show a longer, healthier lifespan and later onset of age-related phenotypes [34].

Telomere attrition

Although DNA damage is recognised under the hallmark of genome instability, the chromosomal end regions, the telomeres, are particularly susceptible to age-related decline [35]. Most somatic cells will lose a certain number of base pairs from the telomeric end of the chromosome with every cell division. This is the molecular basis for the proposed "Hayflick" limit. Hayflick and Moorhead discovered in the early days of *in vitro* cell culture that most primary cells have a limited number of mitotic divisions that can occur before cell death or senescence [36]. The later theory of replicative senescence builds on this and suggests that telomeric attrition is the primary reason for a cell entering a replicative senescent state [37]. The shelterin complex, formed of six protein subunits, protects the ends of chromosomes from being recognised as DNA breaks by DNA repair proteins [38]. As a result of this protection, any damage to telomeres is very persistent and

will normally induce senescence or apoptosis [39]. There is sufficient evidence that telomeric attrition is a hallmark in its own right. Telomeric shortening is observed in humans and other species during normal ageing [40]. Shorter telomeres are linked to earlier ageing [41]. The experimentally induced impairment of shelterin components accelerates ageing [42]. The telomeres can be lengthened by the telomerase protein, a DNA polymerase. Telomerase is not universally expressed; most mammalian adult cells do not express it in normal circumstances. Telomerase-deficient mice are prematurely aged, but their ageing phenotype is rescued with the reactivation of telomerase [43].

Epigenetic changes

Complex epigenetic patterns of DNA modifications, post-translational histone modifications and chromatin remodelling are present at all stages of life and can affect the transcription of genes by altering the binding sites of regulatory factors. However, there are certain epigenetic changes that are associated with age, such as particular histone acetylation/methylation patterns. A collection of DNA methylation changes are identified as being associated with ageing, and together contribute to a measure of ageing: Horvath's "epigenetic clock" [17]. Age is also associated with a reduction in global heterochromatin, an increase in senescence-associated heterochromatin foci (SAHFs), re-localisation of chromatin modifiers, nucleosome remodelling and loss, and an increased activation of transposons and non-coding RNAs [44]. These epigenetic alterations are present across multiple species [44]. Sirtuins are a class of protein that act as nicotinamide adenine dinucleotide (NAD+)-dependent deacetylases, and early

studies linked the sirtuin genes with lifespan in the context of dietary restriction [45,46]. The sirtuins have been targeted experimentally using genetic engineering to increase or decrease gene expression, as well as the use of sirtuin-targeting compounds like resveratrol [47–49]. Similarly, other epigenetic mechanisms have been targeted experimentally and provide further evidence supporting epigenetic changes as a hallmark of ageing. For example, the experimental inhibition of histone demethylases increases ageing in flies, and experimental restoration of altered histone acetylation of H4K12 leads to recovery of cognitive abilities in aged mice [50,51].

Dysregulation of alternative splicing

The dysregulation of alternative splicing is one of the newer hallmarks of ageing, but it no less fulfils the criteria as a hallmark of ageing. Most of the primary hallmarks of ageing are involved in the heavily regulated processes of gene expression and subsequent protein production. Alternative splicing is the process that an immature transcript of mRNA (pre-mRNA) undergoes in order to remove introns (non-coding regions of a gene). Exons may also be spliced differently to give different transcripts which can then result in different protein isoforms. Splicing is governed by splicing factors, and these splicing factors are also regulated by the same process [27,52]. Splicing is noted as being defective in several diseases of ageing such as cardiac myopathy and Alzheimer's disease, however its first direct link with ageing *per se* was identified from work on transcriptomics [53–55]. Sequencing RNA transcripts revealed differences in the splicing patterns of young and old blood and changes in the gene expression of

splicing factors across several cohorts and several species [56–60]. Although splicing factor dysregulation has been shown to affect multiple species, it has not yet been investigated in the context of the diseases of premature ageing (progeroid diseases). Evidence for the mechanistic basis of how RNA splicing dysregulation affects ageing mainly comes from *in vitro* studies. Knockdowns of splicing factor genes *SRSF2* and *HNRNPD* render endothelial cells unresponsive to compounds that reduce senescence (such as hydrogen sulphide donors) [61]. Similarly, targeted knockdown of the downstream targets of splicing factors, *FOXO1* and *ETV6*, showed that splicing factor dysregulation attenuates senescence phenotypes [62]. Small molecules such as resveratrol, trametinib and mitochondria-targeted hydrogen sulphide donors are capable of restoring splicing factor gene expression in senescent cell cultures back to the levels observed in earlier passage cells [61,63].

Cellular senescence

Cellular senescence in particular interfaces with many of the other hallmarks. For instance, it has been mentioned above in the evidence supporting splicing factor dysregulation as a hallmark of ageing. It is a process defined by Terzi *et al*. as a state of irreversible, cell cycle arrest [64]. Cells in a senescent state are thought to be in either of the G1 or G2 phases of the cell cycle, unlike quiescent cells which are in the G0 phase of the cell cycle. Quiescent cells are functional, can respond to mitogenic signals and re-enter the cell cycle easily, but senescent cells are different because they don’t respond to normal mitogenic signals and don’t function as normal [65]. This means that senescent cells place a burden on a tissue

due to their use of resources in the absence of proper cell function. However, recent studies now show that the senescent phenotype can be somewhat reversible [63,66].

Generally, senescence is induced as a result of replication (via telomeric attrition), a cellular stressor (such as UV-induced DNA damage), or an oncogene (such as via the p53 pathway), but other triggers are also proposed (as discussed later in this thesis) [37,67,68]. Senescent cells exhibit several characteristic traits *in vitro*: an enlarged irregular morphology ("fried egg shape" morphology), secretion of senescence-associated secretory phenotype (SASP) factors, dysregulated splicing factors, increased senescence-associated beta galactosidase (SAB) activity, reduced proliferation, increased levels of DNA damage, increased levels of SAHFs, increased levels of DNA segments with chromatin alterations reinforcing senescence (DNA-SCARS), altered apoptosis (due to activation of senescent cell anti-apoptotic pathways (SCAPs), and increased gene expression of proteins such as p16, p21 and p53 [69–71]. An increase in senescence is linked with normal ageing and with many age-related diseases, such as Alzheimer's disease, Parkinson's disease and atherosclerosis [72,73]. Senescence can be induced by conditional expression of the $p16^{Ink4a}$ locus (a locus within the *CDKN2A* gene). When senescence is induced in mice via this locus, the mice exhibit a clear ageing phenotype with a decreased lifespan and increases in characteristics such as skin wrinkling, fur loss, reduction in subcutaneous fat and cataracts [74,75]. The strongest experimental evidence for the inclusion of cellular senescence as a hallmark of ageing comes from the *in vivo* mouse studies by Baker *et al.* who showed that restoring p16 function in these prematurely aged

p16-deficient mice could restore the normal ageing phenotype with a 27% increase in lifespan and clear improvements in fur density and mobility, and decreased incidence of tumorigenesis [66,75].

The loss of proteostasis

Proteostasis is the careful balance of the correct levels of correctly functioning proteins to meet the requirements of a cell. It involves the coordination of the stabilisation of correctly folded proteins (including chaperone-mediated folding), the regulation of protein degradation (by the proteasome/lysosomes) and other quality control mechanisms regarding protein production [76,77]. In the initial nine hallmarks of ageing, the loss of proteostasis covered how autophagy was affected by ageing, but now enough evidence exists to identify compromised autophagy as a hallmark in its own right [21]. The loss of proteostasis as ageing occurs is evidenced by the accumulation of unfolded, misfolded or aggregated proteins and their associated diseases, such as Alzheimer's and Parkinson's diseases [78]. The two main proteolytic systems, autophagy-lysosomal and ubiquitin-proteosomal, both decline with age [79,80]. Evidence regarding the former system will be discussed in the section on the hallmark of compromised autophagy. In *Caenorhabditis elegans* (*C. elegans*), the increase in expression of ubiquitin-proteosome system components extends lifespan, and experimental aggravation (via repression of chaperome proteins that aggregate proteins) can decrease lifespan [81–83]. Deubiquitylase inhibitors can increase clearance of waste proteins *in vitro* in human cells and extend lifespan in yeast [84,85].

Mitochondrial dysfunction

Mitochondria are the cellular organelles responsible for the production of chemical energy in the form of adenosine triphosphate (ATP) via the oxidative phosphorylation cascade, but their ability to respond to the energy demands of the cell are compromised as people age [86]. Although mitochondrial dysfunction has long been suspected to influence ageing, there is still much discussion as to its mechanisms. Mitochondrial dysfunction is thought to be caused by several mechanisms, such as a reduction in the biogenesis of mitochondria, instability of the mitochondrial genome, oxidation of mitochondrial proteins (caused by the free radicals and reactive oxygen species (ROS) that accumulate with the energy conversion process), alterations in the response to unfolded proteins and subsequent changes to the populations of haematopoietic stem cells, and impaired mitophagy (similar to autophagy but at the level of the mitochondrial organelle rather than the cell) [26,87]. Experimentally, mutations in mitochondrial DNA (mtDNA) have been shown to contribute to premature aging in a mouse knockout of mitochondria DNA polymerase γ (POLG) which lacks proper proofreading responses and so accumulates mtDNA mutations [88]. More recently, a study using a form of mitochondria-targeted Coenzyme Q10 was able to show restoration of aspects of mitochondrial function in old haematopoietic stem cells [89].

The mitochondria in older people are larger, less efficient and are associated with increased production of free radicals and oxidative damage [90]. ROS are thought to form due to leakage from the mitochondrial electron transport chain and can

cause oxidative stress. Oxidative stress can cause mutations in DNA, so it was thought that mtDNA suffered from more oxidative stress due to the proximity of ROS, and this became cyclical with the instability of mtDNA exacerbating the production of ROS. Paradoxically, rises in ROS appeared to increase lifespan in model organisms. Similarly unexpected were observations that genetic disruption of mitochondrial function actually leads to lifespan increases in several model organisms [26]. This has lead to the conceptualisation of mitochondrial hormesis or mitohormesis. This is the suggestion that a small perturbation that would be expected to have a deleterious effect actually results in an overall beneficial effect when the cell responds to the small challenge [22,26].

Altered mechanical properties

A cell's shape and motility are governed by the constant remodelling of intracellular scaffolding and the extracellular matrix (ECM) proteins. Cell morphology is also one of the key determinants of the senescence phenotype [70]. Changes in the way these structural proteins function to provide motility and mechanical support to the cell are now considered a hallmark of ageing [21]. It may come as no surprise that our skin loses tensile strength with wrinkles appearing as we age. This is due to impairment of ECM proteins, such as collagen and elastin, and taking oral supplements of collagen can reduce wrinkles and increase the laying of the ECM in skin [91]. Experimentally aggravating mechanical dysfunction can worsen symptoms of ageing, for example, mice that are engineered to be deficient in lumican, a small leucine-rich proteoglycan, exhibit early ageing and increased susceptibility to cardiac fibrosis [92]. Nuclear structural

proteins can also be affected in ageing and senescence, e.g. the loss of Lamin B1, a structural protein in the nuclear lamina, is associated with several types of senescence [93]. Further experimental evidence comes from the progeroid syndrome, Hutchinson-Gilford Progeroid Syndrome (HGPS). HGPS is usually caused by the activation of a cryptic splice site in the *LMNA* gene. Instead of the cells producing the Lamin A protein (an integral nuclear lamina protein), they produce a dysfunctional toxic protein called progerin with a retained farnesyl group, which ultimately serves to induce a widespread premature ageing phenotype. Inhibition of a farnesyltransferase can reverse the phenotype *in vitro*, and more recently *in vivo* human clinical trials of lonafarnib (a farnesyltransferase inhibitor) show promise with a lower mortality rate of patients with HGPS [94,95].

Compromised autophagy

Originally encapsulated by the loss of proteostasis, compromised autophagy has fulfilled the criteria to become a hallmark. Unlike the antagonistic hallmark of the loss of proteostasis, compromised autophagy is proposed as an integrative hallmark [21]. Autophagy is the delivery/recycling process of cellular proteins and molecules in a specialised organelle, the lysosome. Autophagy can be mediated in several different ways: macroautophagy produces a double-membraned autophagosome to deliver molecules to the lysosome for degradation; microautophagy is thought to be the encapsulation of molecules directly from the cytoplasm using the membrane of the lysosome itself; chaperone-mediated autophagy uses chaperone proteins to aid translocation of a substrate into the lysosome; and RN/DNautophagy delivers nucleic acids into the lysosome via a

nucleic acid transporter protein [96]. The autophagy-lysosome system declines with age [79]. A conditional knockout of chaperone-mediated autophagy in the livers of transgenic mice compromises the ability of the mice to maintain metabolism and gives a reduction in peripheral adiposity, both of which are associated with ageing [97,98]. There are more studies investigating improving autophagy in ageing-related outcomes. For example, the age-related decline in autophagy can be rescued with compounds such as spermidine or in transgenic organisms targeting autophagy receptors, and results in improvement in longevity and age-related outcomes [99–101].

Inflammation

As the body ages, its ability to respond appropriately to infection, via the innate and adaptive immune responses and their associated inflammatory response, is impaired. As a result, ageing is often associated with chronically low levels of inflammation and inflammatory markers, so much so that Francheschi *et al*.'s portmanteau of "inflammageing" is often discussed [102]. Many cytokines produced by the body show shifts that are associated with ageing, such as increases in IL1, IL6, IL8, IL10, IL12 and TNFα, and decreases in IL2 and IFNγ [103]. Many of these cytokines are also part of the SASP. The SASP is mentioned in the context of cellular senescence above and is discussed further for its role in altered intercellular communication below. As one might therefore expect, there is much overlap in the experimental evidence between inflammation and both these hallmarks, as well as others such as disturbances in the microbiome. For example, mice that are raised in germ-free conditions are protected from

inflammation associated with ageing and have a longer average lifespan, but when they are housed with conventionally raised old mice (and therefore are exposed to a microbiome associated with age) they show increased levels of pro-inflammatory cytokines [104]. Further evidence for inflammation as a hallmark can come from progeroid models. Nuclear factor kappa-light-chain-enhancer of activated B cells (NF-κB) regulates many inflammatory markers. NF-κB is activated as ageing occurs and its experimental inhibition can improve symptoms associated with ageing in a mouse model of XFE progeria (a form of the progeria, xeroderma pigmentosum, which is caused by mutations in *Ercc1*, a DNA repair endonuclease) [105].

Exhaustion of stem cell supply

Stem cells in adults are cells that have retained some degree of pluripotency, multipotency or oligopotency after their differentiation from the totipotent stem cells of the developing embryo, that is to say that they have retained their ability to differentiate [106]. Stem cells remain largely quiescent in the G0 phase of the cell cycle, but can re-enter the cell cycle to be able to proliferate and differentiate when needed [29]. The banks of stem cells that exist in an adult are essential for tissue maintenance, as they serve to provide new cells that can replace dysfunctional/apoptotic cells of different lineages, such as haematopoietic or mesenchymal stem cells, but over time these stem cell pools become depleted. This is particularly noticeable in the pool of haematopoietic stem cells with their ability to replace immune cells waning over time [103,107]. Norddahl *et al.* show that inducing mitochondrial DNA mutations can drive haematopoietic cells to

prematurely age [108]. Florian *et al.* demonstrate the importance of stem cell exhaustion in a set of experiments that causally link the RhoGTPase Cdc42 and a lack of polar distribution of microtubules (which is associated with an aged pool of haematopoietic stem cells); they show that increasing the activity of Cdc42 induces ageing in young cells and inhibiting it can rescue this phenotype [109]. Other experiments link the expression of autophagy proteins and stem cell ageing with compounds such as spermidine and rapamycin which are able to reactivate autophagy in muscle stem cells [110].

Altered cell-cell communication

The hallmark of altered intercellular communication originally encompassed four major pathways of cell-cell communication: the neuroendocrine pathway, “inflammageing”, immunosenescence and bystander effects [22]. “Inflammageing” is discussed separately above as inflammation has now been proposed as one of the new hallmarks [21]. The neuroendocrine system concerns signalling pathways like the insulin and the insulin-like growth factor 1 (IGF-1) signalling pathway (IIS), and the steroid sex hormone signalling pathways. There is much experimental evidence for the roles of these pathways in ageing and both of them have been extensively studied in the regulation of lifespan across many model organisms: *C. elegans*, *D. melanogaster* and *M. musculus* [111]. Experimental interventions such as caloric restriction increase longevity, and experiments in *C. elegans* that use gene interference studies show how the experimental amelioration or aggravation of genes in these pathways can cause increases or decreases in lifespan [111,112].

Immunosenescence is the term used to describe the aged immune system and how its ageing affects the health of other tissues. “Inflammageing” and immunosenescence are quite intrinsically linked and are often discussed in parallel: both concern the way the body responds to infection or damage, but “inflammageing” covers how inflammation accumulates with age whereas immunosenescence is how the immune system becomes impaired and how its inability to function normally affects other cells [113]. Nevertheless, much of the evidence overlaps for how these two concepts are important to ageing. For example, there are changes in inflammatory markers as we age and there is also general impairment of both innate and adaptive immune responses as we age [103]. Some experimental evidence comes from parabiotic experiments: pairing the circulatory and immune systems of young and old mice has shown improvements in age-related outcomes for the older mouse and the opposite effect for the younger mouse [114]. In humans, there is experimental evidence that the application of hyperbaric oxygen therapy, which is used to help treat the symptoms of many age-related diseases, can decrease the levels of senescent immune cells [115].

Bystander effects are the paracrine signals caused by a senescent cell, namely the senescence-associated secretome or SASP as mentioned earlier in the information on cellular senescence [116]. SASP is induced by persistent DNA damage, dysfunctional mitochondria and other aspects of the senescence phenotype often as a result of the production of cytoplasmic chromatin fragments which activate pathways such as the cGAS-STING pathway [31,117,118]. A

senescent cell will often signal to other nearby cells via the SASP that they too should become senescent and secrete SASP factors. In certain circumstances, such as in tumorigenesis or wound healing, this process is beneficial to the organism, but, in many cases, it causes cells to become senescent and dysfunctional unnecessarily [119]. The SASP is a dynamic collection of chemokines and cytokines associated with ageing, such as the interleukins (including the inflammatory markers mentioned by name in the section on inflammation as a hallmark of ageing), matrix metalloproteinases, TNFα and TNFβ [119]. However, more candidate SASP proteins are being discovered and identified as being age-associated [120]. The SASP is a very diverse set of chemicals, but it is possible to target individual SASP factors experimentally to determine their importance in ageing. For example, IL10 knockout mice are frailer than wild-type mice and exhibit cardiovascular dysfunction [121]. Similarly, inhibition of IL6 activity using the drug tocilizumab in a progeroid mouse model improves several aspects of their premature ageing phenotype [122].

Nutrient sensing dysregulation

Cells must sense and adapt to changing macronutrient levels through nutrient sensing pathways. Many age-related diseases have problems with nutrient sensing pathways and metabolic decline, e.g. type two diabetes [112]. It is suggested that there are four main nutrient sensing pathways linked with dysregulation in ageing: 1. The IIS pathway (mentioned above within the hallmark of altered cell-cell communication), 2. The mammalian target of rapamycin (mTOR) pathway, 3. Sirtuin signalling (mentioned in the context of the hallmark

of epigenetic changes), and 4. the AMP kinase (AMPK) pathway. All four pathways are interrelated: the mTOR pathway is activated by the IIS pathway (via PI3K and Akt signalling) and inhibited by AMPK which is regulated by sirtuin signalling [22]. Also of note within these pathways are the FOXO proteins, a family of forkhead box transcription factors, that regulate cell fate pathways [123]. Collectively the pathways interact via phosphorylation cascade signalling and altered gene transcription that ultimately serve to adjust cell fate in response to scarcity or abundance of nutrients. Many dietary restriction experiments show increases in lifespan of model organisms [112]. In humans, many low calorie or restrictive diets, such as intermittent fasting, the Mediterranean diet and the Okinawan diet, are associated with a longer average lifespan, improved health and improvements in other age-related outcomes [124]. The reverse is true with obesity and poor diet linked to a shorter lifespan and worsened outcomes of age-related disease [125]. Investigating individual components of the pathways reveals a similar story, that these pathways are intrinsically linked with ageing. For example, centenarians have lower levels of circulating IGF-1, and targeting mTOR with rapamycin shows a reduction in lifespan in mice and other model organisms [126,127].

Microbiome disturbances

Many of the pathways by which cells communicate and interact with their microenvironment are affected by ageing, and this extends to the way that the plethora of bacteria (roughly a trillion organisms inhabit just one gram of luminal material in the gut) that constitute the human microbiome cause effects on the

rest of the body [128]. In particular the microbiome of the gut is thought to be important in ageing with differences in the composition of microbiota correlating with ageing and frailty [129,130]. The gut microbiome has many species of bacteria, and changes in the proportions of bacteria from many genera, e.g. *Bacteroides*, *Roseburia*, *Faecalibacterium*, *Prevotella*, *Proteobacteria*, *Alistipes*, *Akkermansia* and *Paracteroides*, have all been implicated in ageing and poorer age-related outcomes [130–132]. In a mouse model, the inoculation of a young mouse with gut microbiota from an old mouse induced inflammation associated with ageing [132]. Therapeutic reduction of the levels of tumour necrosis factors (TNF) in old mice rescued the age-associated changes to their microbiome, and genetically engineered TNF-deficient mice do not have the normal age-associated changes in microbiome composition nor any changes in age-associated inflammation [104].

Targeting molecular ageing

With fourteen hallmarks to choose from (and indications that, in due course, more processes that meet the criteria of a hallmark of ageing will come to the fore), there are many potential avenues of investigation for therapies targeting molecular ageing [21]. However, many novel therapies fail at translation into humans during the clinical trial pipeline: strikingly illustrated by the fact that an estimated 85% of new therapies in the pipeline fail to become FDA-approved in the USA [133].

Reliance on animals in ageing research

There are several reasons why so few therapies make it all the way from early stage basic science research into success at efficacy trials in humans, but one key factor is the use of animals in research [134]. There are several ways to reduce the reliance on animal models in drug discovery including drug repurposing (identifying new uses for compounds that are in use for an alternative disease/symptom and have already undergone clinical safety trials in humans). However, the problem with translation into humans also filters out from early stage *in vitro* research. *In vitro* cell culture models are essential for drug discovery research as they provide a quick and easy way to test hypotheses regarding how a drug might affect cellular processes. *In vitro* two-dimensional cell culture experiments are easier to conduct and quicker than most *in vivo* experiments, but do still have the risk of not translating into a clinically relevant therapy [135]. Many new *in vitro* techniques, such as three-dimensional cell culture and co-culture models, are becoming more commonplace and are often more similar to the human microenvironment than traditional two-dimensional cell culture, yet the benefits of two-dimensional cell culture, e.g. the ease of use and accessibility, mean that two-dimensional cell culture experiments remain important for the early stages of drug discovery research [135]. Regardless of the complexity of the model, many *in vitro* techniques use animal-derived products. Making *in vitro* studies more similar to the human microenvironment has been shown to enable the identification of nuanced species-specific cell processes that would otherwise have been missed [136]. Small increases in the relevance of any *in vitro* cell culture model to the human microenvironment may improve the likelihood of any findings translating into a future clinical therapy.

Much research regarding the hallmarks of ageing was completed using animal models, however animals can age at very different rates to humans. The reasons for different rates of ageing across the animal kingdom can be due to size (as one might intuitively think), selective pressures, and differing reproductive behaviours [137,138]. However, many animal species do not follow these patterns, e.g. the Greenland shark (*Somniosus microcephalus*) is extremely long-lived (estimates suggest a maximum lifespan of 500 years) and the naked mole-rat (*Heterocephalus glaber*) exhibits little to no signs of ageing [139]. Although parallels can be drawn from closer relatives such as mice (*Mus musculus*), even closer evolutionary relatives can still show major differences in the way they age compared to humans, e.g. the common marmoset (*Callithrix jacchus*) is very short-lived for a primate (with an estimated maximum lifespan of 16 years) while a fat-tailed dwarf lemur (*Cheirogaleus medius*) is hibernatory affecting its ageing process [139,140]. In addition to the differing signs of ageing, the naked mole-rat has negligible levels of senescence and maintains excellent splicing regulation in comparison to humans and other animals [60]. Animals clearly exhibit differences in ageing *per se* as well as in the hallmarks of ageing, so when considering that the hope of early stage medical research is the eventual translation into therapies for humans, it is important before research begins to consider how any improvements could be made to increase its human-relevance, e.g. reducing animal biomaterial in the *in vitro* microenvironment.

Targeting the hallmarks of ageing

Research is ongoing for many of the hallmarks, but our research team has specialised in cellular senescence and helped to drive the evidence in support of the dysregulation of alternative splicing as a novel hallmark. Cellular senescence is one hallmark that arguably could be defined as integrative as well as antagonistic because it interfaces with almost all of the hallmarks directly. Senescence can be indicated by many biomarkers and characteristics (explained in Figure 2 and also discussed in further detail later in this thesis), and many of these characteristics show links with the other hallmarks of ageing. The following brief set of examples of the links between senescence and each of the other hallmarks highlights just how linked cellular senescence is with them. Senescent cells typically have morphological changes which clearly links with the hallmark of altered mechanical properties [141]. A rise in DNA damage biomarkers is linked with the hallmark of genomic instability [141]. Telomeric attrition is thought to drive the state of replicative senescence [37]. RNA splicing dysregulation is shown in senescent cell cultures [56,63]. The appearance of SAHFs in senescence is linked with epigenetic changes to histone proteins [44]. Increased lysozyme activity indicates an imbalance in proteostasis and compromised autophagy [70,141]. The secretion of the SASP is linked with inflammation and altered cell-cell communication, both of which also feed into disturbances in the microbiome [71,104]. Compounds that affect senescence also affect many nutrient sensing pathways, and compounds that target mitochondria can affect senescence [61,142]. Given that cellular senescence is such an integral hallmark, it seems to be an ideal starting point for research into potential therapies.

Targeting senescence

Cellular senescence can be targeted by certain compounds that decrease the proportion of senescent cells within a tissue: these compounds are termed “senotherapeutic”. There are two main ways in which the proportion of senescent cells within a tissue may be reduced. The first way is via compounds known as “senolytic” compounds that induce selective lysis of senescent cells, and the second is via compounds known as “senomorphic” compounds that change cells back from their senescent state into a more normal functional proliferative state [65,71,143]. Senolytic compounds could be very useful to remove the burden of senescent cells without risking any senescent cells that are damaged being returned into the normal cell cycle. The restoration of a senescent cell to a functioning proliferative cell may seem more difficult to achieve without the risk of damaged cells re-entering the cell cycle, compared to the targeted ablation of the cells offered by senolytic compounds. However, there are many potential benefits offered by the senomorphic approach. For example, in certain tissues, using a senolytic may reduce the total number of cells too much, compromising the functioning cells in the tissue. The potential usefulness of the senomorphic approach becomes clearer when we consider that there are different types of senescence and that the senescence phenotype is heterogeneous. A senomorphic compound may not actually affect the more damaged cells.

Types of senescence and the heterogeneity of the senescence phenotype

There are many biomarkers that indicate a cell is senescent, as discussed previously and illustrated here in Figure 2, but senescent cells do not necessarily display every characteristic. For example, cells that are engineered to overexpress p21 or $p16^{Ink4a}$ don't secrete SASP despite lower levels of proliferation and other aspects of the senescence phenotype [144]. Additionally, SAHFs are not present in every type of senescence and their presence in some types of senescence is dependent on the cell type [145]. The phenotype is very heterogeneous, but it would be reasonable to expect that different types of senescence might have their own unique signatures. However, as yet, no unique signatures have emerged [68,141,146].

Senescence can be induced by a variety of means which result in multiple types of senescence. Replicative senescence, oncogene-induced senescence, and stress-induced premature senescence are described earlier, but Sikora *et al.* argue for another three types of senescence (when categorised according to what caused the cells to become senescent) [68]. These additional three are: secondary senescence, therapy-induced senescence and post-mitotic cell senescence. They describe secondary senescence as the induction of senescence following paracrine signals from other senescent cells. This is also commonly referred to as SASP-induced, and arguably falls under the bracket of stress-induced senescence. Similarly, it is arguable that therapy-induced senescence, e.g. when an anticancer drug induces senescence, is also a form of stress-induced senescence. Many progenitor cell types differentiate into a cell type that cannot

proliferate itself (post-mitotic), and these post-mitotic cells can show senescence in a similar manner to the way a normal proliferative cell might become senescent. It is disputable as to whether the cell's differentiation status or other normal inducers of senescence is/are the primary cause of the observed post-mitotic cell senescence phenotype. These different types of senescence can be associated with different aspects of the senescence phenotype, for example, polyploidisation is associated with anticancer treatment [68]. However, no unique signature of senescence has yet been identified for either senescence in general or for any type of senescence [68,141].

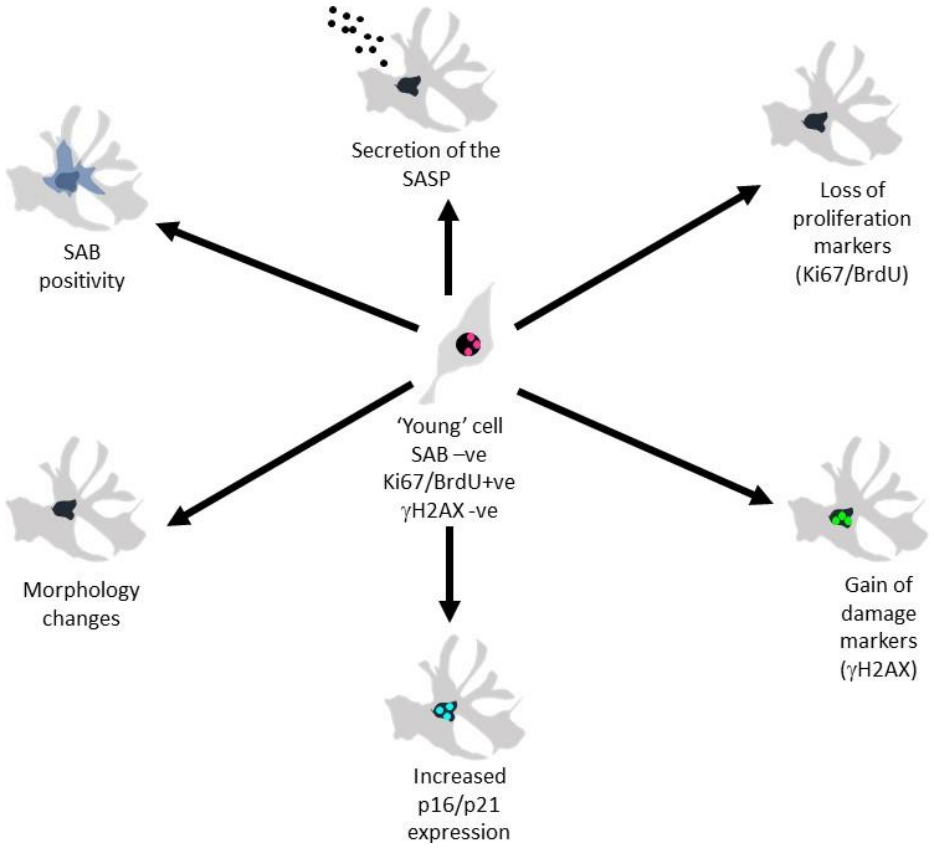

Figure 2: Biomarkers to identify senescent cells. Senescent cells undergo a number of functional, morphological and biochemical changes. These include the development of senescence-associated beta galactosidase (SAB) positivity (senescence), secretion of the senescence associated secretory phenotype (SASP), loss of proliferation markers such as Ki67 or BrdU, gain of markers of DNA damage such as γH2AX, gain of p16 and p21 positivity (cell cycle arrest) and characteristic morphology changes ('fried egg' morphology, gain of heterochromatic foci). Please note this figure is replicated from Figure 1 in the article 'Targeting Alternative Splicing for Reversal of Cellular Senescence in the Context of Aesthetic Aging' by Bramwell and Harries published in Plastic Surgery and Reconstruction in 2021. The original published article is attached in the appendix of this thesis.

Different stages of senescence have also been suggested, but again no stage defines a particular set of characteristics as yet. There are calls for definitions to aid in identifying a signature of senescence that discuss concepts like acute or chronic levels of senescence. Different stages of senescence are also mentioned, such as a pre-senescent stage in which the senescence phenotype is partially reversible, and/or a committed deep senescence/post-senescence/"gero stage" after which cells cannot be returned to their normal function using senomorphic compounds [68,141]. It is widely accepted that the SASP is highly variable among senescent cells, but some researchers suggest that senomorphic compounds may only affect the type of senescence that is induced by the SASP, while others term this particular type of compound "senostatic" [117,143,147].

The identification of the mechanisms that underlie senescence is an area of research worth considering for future studies. Much of the research that contributes to the evidence behind each hallmark of ageing uses models (often mouse models) of progeroid diseases (diseases that cause premature ageing). These diseases are particularly interesting with regard to identifying underlying mechanisms of senescence, because cells from people with these diseases have high levels of senescence and can be used as models of accelerated *in vitro* ageing [25]. As previously discussed, senescence interfaces with and can be targeted via other hallmarks. In the context of the novel hallmark of ageing, alternative splicing dysregulation, no progeroid models have yet been examined, but it would be worthwhile doing so to see if alternative splicing is dysregulated in these diseases (as it is in normal replicative senescence). If alternative splicing

were to be affected in progeroid diseases, this would give further clues about the mechanisms of senescence and pose a subsequent question: how might senotherapeutic compounds affect this dysregulation and the senescence phenotype in progeroid diseases.

Known senotherapeutic compounds

Many senotherapeutic compounds have been identified, but the field is still relatively new with the first few senolytic compounds currently undergoing clinical trials [71,148]. Most approaches remain in the experimental phase of research. Dasatinib and quercetin (in combination) are the furthest along with clinical trials for effects on two age-related diseases: diabetic kidney disease and idiopathic pulmonary fibrosis [149,150]. In addition to dasatinib and quercetin, there are many candidate senolytic approaches and compounds emerging, such as fisetin, piperlongumine, and Bcl-2 and Hsp90 protein inhibitors [143,151]. Similarly emerging are senomorphic approaches and compounds such as rapamycin, resveratrol, trametinib, mitochondria-targeted hydrogen sulphide donors, and compounds targeting signalling pathways such as Akt, MEK/ERK, JAK-STAT and ATM [143,151,152]. Many compounds that affect pathways such as cell fate pathways may also offer senotherapeutic potential. For example, metformin is a diabetes drug, but it is thought to offer senotherapeutic benefit and is now being repurposed in a clinical trial to test its beneficial effects on ageing [153].

Drug repurposing and *in silico* screening are efficient approaches to medical research [134]. Drug screening studies can use either bioinformatic approaches

and/or can use *in vitro* methods [154–156]. To our knowledge, no major *in vitro* drug repurposing studies have screened compounds for effects on senescence, representing untapped potential. As senescence is a heterogeneous phenotype, no single biomarker will be able to prove that a repurposed drug would offer senotherapeutic benefit: a combination of biomarkers is needed. Therefore, any initial screen will require optimisation of the process to identify the most appropriate biomarker(s) for use in a high or medium-throughput drug screen. Certain techniques for assaying the biomarkers in senescence rely on time-consuming manual image analysis, so this is a particular area for optimisation. Following the emergence of any candidate senotherapeutic drugs, the drugs would need to be investigated for effects on the remainder of the senescence phenotype. After cementing a drug as a potential senotherapeutic drug, many further validation studies would be needed before clinical benefit could be assessed. However, results from a screen of this nature could also be used to inform bioinformatic *in silico* screens.

Bioinformatics approaches using artificial intelligence techniques, such as deep neural networking, and structure/ligand-based virtual design and screening, can be used for generalised drug discovery [155]. Structural similarities may give compounds similar functions and so could give further future targets for drug development. A recent study from Olascoaga-Del Angel *et al.* investigated structural motifs of senomorphic and senolytic compounds, identifying some common substructures, but ultimately found more structural similarities than differences between the two categories of senotherapeutic effects [152]. Any newly

identified senotherapeutic compounds could be analysed in a similar manner for any functional associations of chemical substructures.

As discussed earlier, investigating the effects of senotherapeutic drugs on the senescence phenotype in progeroid cells could be useful in identifying mechanisms of senescence. Whilst many senotherapeutic compounds could be used, one suitable senotherapeutic would be the MEK inhibitor, trametinib. Trametinib is a senomorphic compound that is more specific than other senomorphic compounds such as rapamycin or resveratrol, and it has been shown to affect senescence and rescue dysregulated splicing factor gene expression in primary human cells in previous work from our research group [63]. Given their overlap, senescence and splicing factor dysregulation can be targeted by the same or similar method(s).

Targeting splicing factor dysregulation

With 95% of genes in humans alternatively spliced, control and regulation of alternative splicing is very important in normal cell function [157]. Constitutive splicing is the process of excising introns from pre-mRNA to give a mature mRNA which is ready to export and translate into a polypeptide chain. Mature mRNA is translated into a polypeptide chain by the recruitment and polymerisation of amino acid residues using tRNAs. Polypeptide chains may be combined and/or further processed in order to form the fully mature protein.

Alternative splicing enables different transcripts to be formed from the same gene which enables the production of far more proteins than are directly coded for in the human genome [158]. Figure 3 illustrates the concept of normal constitutive splicing and the alternative splicing of a cassette exon [70]. The pattern of alternative splicing is tightly governed by the spliceosome and by factors that can act to increase or decrease the usage of a particular splice site. The spliceosome consists of nucleic acids and nucleoproteins that catalyse the excision of the sequence of RNA at a splice site flanked by a GU and an AG residue, with an A residue branch point site and a polypyrimidine tract [52]. *Cis* and *trans* acting elements can enhance or silence splice site usage (intronic splicing enhancers (ISE), intronic splicing silencers (ISS), exonic splicing enhancers (ESE), and exonic splicing silencers (ESS) [158]. Splicing factors such as serine/arginine rich splicing factors (SRSFs) and heterogeneous nuclear ribonucleoproteins (HNRNPs) usually serve to enhance or silence splice site usage respectively. These splicing factors can also regulate their own splicing and their gene expression is associated with age [56,159]. Measuring the gene expression of these splicing factors is a good way to determine if alternative splicing is dysregulated in a cell.

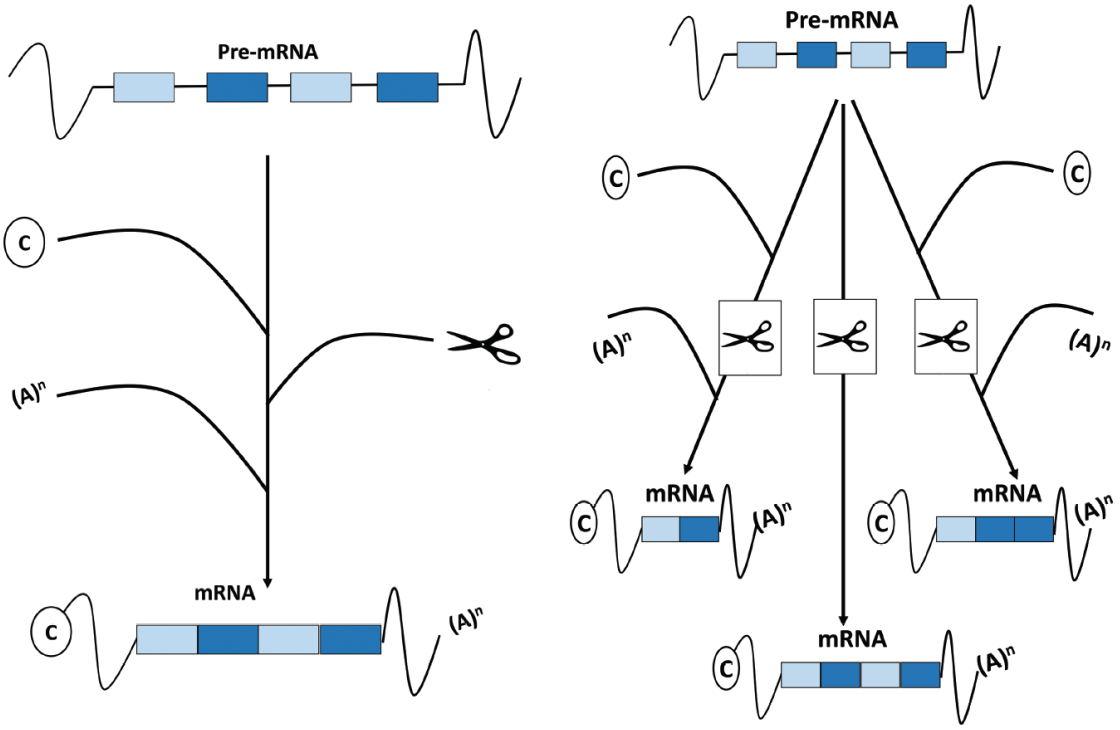

Figure 3: Illustration of constitutive and alternative splicing. (Left) Constitutive splicing. Before it can be translated, a pre-mRNA must undergo capping (indicated with by the circle-enclosed "C"), spliced (indicated by the scissor graphic), and polyadenylated (indicated by $(A)^n$). The result of this is a spliced and processed mRNA. Introns and untranslated regions are indicated by black lines, exons by light or dark blue boxes. (Right) Alternative splicing. This is the production of multiple mRNA isoforms from a single gene. Alternatively-expressed isoforms are independently processed as indicated (the addition of the 5' cap, given here by a circle-enclosed "C," splicing, indicated by the scissors and polyadenylation, shown by $(A)^n$), but undergo differential removal of exons (blue boxes) to produce distinct mRNA species, which may be temporally or spatially regulated. Please note this figure is replicated from Figure 2 in the article 'Targeting Alternative Splicing for Reversal of Cellular Senescence in the Context of Aesthetic Aging' by Bramwell and Harries published in Plastic Surgery and Reconstruction in 2021. The original published article is attached in the appendix of this thesis.

Splicing can be targeted specifically with splice-switching oligonucleotides, using microRNAs (miRNAs) to disrupt splicing, by inducing nonsense-mediated decay as well as via compounds that target ageing pathways and act to alter the gene expression of splicing factors [160–164]. Recent work from our research group has shown that several small molecules can modulate both splicing factor gene expression and senescence *in vitro* using compounds such as homologues of resveratrol, mitochondria-targeted hydrogen sulphide donors, and ERK and Akt inhibitors (such as the aforementioned trametinib) [61,63,70]. Small molecules are of

particular interest in the context of this work as they can target both cellular senescence and the dysregulation of splicing.

Conclusion

Ageing is a complex process that underpins many other diseases. The molecular basis of ageing gives many potential therapeutic targets, but cellular senescence and RNA splicing dysregulation are particularly promising. Our team's research has focused on these two hallmarks using traditional methods, however these methods can be improved by ensuring the model is human-relevant, by identifying higher throughput screening methods, and by the creation of new image analysis tools. The novel hallmark of the dysregulation of alternative splicing is intrinsically linked with senescence: many senotherapeutic compounds affect splicing factor gene expression. Progeroid diseases are important to study in their own right for future therapies and for the mechanistic insight into the hallmarks of ageing that they can provide. Therefore, it could be useful to explore splicing factor gene expression and apply senotherapeutic compounds to cells from people with progeroid diseases. Senotherapeutic compounds can be used to improve senescence, but as the concept is relatively new, many compounds will not have been tested for effects on senescence. Screening compounds that are already prescribed for other therapies could quickly identify new compounds for further evaluation. Using screens of this nature can also inform bioinformatic analysis of any links between a molecular structure and its function as a senotherapeutic compound. Compounds identified as affecting senescence need to be fully characterised in terms of their effects on senescence, i.e. is the

compound senomorphic or senolytic? Targeting senescence could be worthwhile for the possibility of therapies to improve healthy ageing and aid in treating age-related diseases.

Research hypothesis

We believe that cellular senescence is a fundamental process that underpins ageing and age-related disease, and that understanding the biological mechanisms of ageing could provide new targets and therapies for age-related disease. Many drugs could have previously undiscovered senotherapeutic effects and could be used to ameliorate some aspects of the senescence phenotype. Repurposed senotherapeutic compounds could become promising candidates for the treatment of age-related disease.

Aims and objectives of thesis

Chapter 3: Development of methods for assessment of senescence in human-relevant cell culture.

The overarching objective for this chapter was to improve the methods of measuring senescence in a human-relevant way so that they would be ready for use in the rest of the thesis data chapters.

The specific aims for this chapter were:

1. To improve the human-relevance of cell culture models by removing all animal-derived components from the culture process.
2. To optimise a more suitable medium-throughput method for assessing senescence to enable a screen of potential senotherapeutic compounds in a later chapter.
3. To help automate the counting of images of stained cells for further use.

Chapter 4: Senescence, alternative splicing and effects of trametinib treatment in progeroid syndromes.

The objective for this chapter was to investigate the mechanisms of senescence further by examining if splicing factor expression was altered in cells from people

with progeroid syndromes, and if a senotherapeutic compound could alter the senescence phenotype in these cells.

The specific aims of this chapter were:

1. To compare splicing factor expression in dermal fibroblasts from a control donor and three donors with progeroid syndromes.
2. To apply a senomorphic compound, trametinib, and identify any changes in the senescence phenotype in the cells from donors with progeroid syndromes.

Chapter 5: A medium-throughput screen of repurposed drugs for senotherapeutic activity and identification of structure-function associations.

The objective of this chapter was to perform a screen using methods developed in chapter three for any senotherapeutic effects of repurposed drugs and to perform a bioinformatic analysis of structure-function from the screen results.

The specific aims were:

1. To perform a high to medium-throughput screen for effects on senescence from repurposed drugs.
2. To use the screen results to inform further validation in chapter six.
3. To use the screen results to inform *in silico* structure-function analysis of the compounds and identify any structure associated with senescence.

Chapter 6: Synthetic female hormones exert sex-specific effects on cellular senescence in human dermal fibroblasts.

The overall objective for this chapter was to validate any senotherapeutic effects observed in the previous chapter's drug screen. As several synthetic versions of sex hormones showed a senotherapeutic effect, the validation was completed in cells from male and female donors.

The specific aims of this chapter were:

1. To validate if three synthetic female hormones (diethylstilboestrol, ethynyl estradiol and levonorgestrel) had an effect on senescence *in vitro*.
2. To identify the type of senotherapeutic effect (i.e. senomorphic or senolytic) and to characterise any changes to the senescence phenotype caused by the compounds.
3. To identify if the sex of the donor of the cells affected the cells' response to the three synthetic female hormones.

Chapter 2: Methods

This chapter details the general methods that I used in the acquisition, analysis and curation of data for this thesis. The data chapters are prepared in the format of journal articles, and so contain the specific details of the materials and methods used including reagent sources, cycling conditions etc. However, where possible, repetition has been omitted to meet submission requirements for this thesis. Here I give an overview of each technique, the rationale for its use in the context of this thesis, and any additional details needed.

Tissue culture

In vitro growth of cells permits many experiments that would be impossible to perform *in vivo*. In this thesis, several cell types are cultured to act as models for senescence. Chapter three describes the rationale and development of human-relevant tissue culture practices within our team. In this chapter, I cultured the human dermal fibroblasts (three normal fibroblast lines (nHDFs)) and human uterine fibroblasts in preparation for the use of the models in later chapters. Tissue culture conditions, standard passaging/freezing protocols and donor details are described in chapter three for these four cell types. The same male and female nHDFs were used in the other chapters following the same standard practices for passaging and freezing as detailed in chapter three.

Primary dermal fibroblasts can be grown to replicative senescence by repeated passaging and extended time in culture. Cells are grown from an early passage and monitored for increases in senescence levels. Using knowledge from preliminary experimentation within our team (data not shown) for

senescence-associated beta galactosidase (SAB) activity staining at early and late passages, experiments could be designed with an appropriate baseline level of senescence to be able to detect changes. For experimentation, the cells were grown until they reached the desired passage number (informed by previous experiments) that would give adequate results for the research question at hand. For older passages, this roughly correlated with their population doubling (PD) time having routinely slowed to half its original speed, and morphological changes (described previously within the introduction) to have begun to occur. PD time can be a variable measure with primary cells that do not necessarily grow linearly in the same way as an immortalised cell line, however it is a useful measure for identifying general trends in cell growth. The PD time is used in chapter three for identifying if there is any difference in the speed of cell growth in different culture media. An estimate of the number of accumulated population doublings (cumulative population doublings, cPDL) is given in each chapter's methods as this measure is more comparable and consistent between cell types/experiments.

For experiments in chapter four, we selected human dermal fibroblasts from people with three different progeroid syndromes. These cells are useful as a disease model in their own right, and as a model of premature cellular senescence. The details of the cells and diseases are discussed further in chapter four. For these lines, the culture conditions and donor details are described in the methods of chapter four, and follow the same passaging and freezing protocols as described for the nHDFs in chapter three.

Measurement of cellular senescence

At pH 6, lysosomal beta galactosidase activity is confined to senescent cells and is referred to as senescence-associated activity (SAB). SAB activity can be assayed using a staining method. Cells are fixed and a pH 6-buffered staining solution containing an X-gal substrate is applied. The yellow colour of X-gal is replaced by a blue coloured product as the substrate is used up by the SAB enzyme. Cells exhibiting blue staining are considered senescent [165]. Measuring SAB activity in this way is considered the "gold standard" of measuring senescence [166,167]. I use this method across the thesis by using a Senescence Cells Histochemical Staining kit from Merck. The kit provides a protocol in which cells are washed twice in DPBS, fixed for 15 minutes at 4°C, washed again in DPBS, and stained. The plate is incubated at 37°C for 24 hours protected from CO_2 to enable the stain to develop appropriately. The acquisition of staining images and count data is described later in this chapter. In chapter three, a fluorescence-based assay for SAB is described as part of an attempt to optimise for use in a medium-throughput drug screen. The reasons it was not used are discussed in chapter three, and the alternative method of examining *CDKN2A* gene expression is described in the same section. Techniques for measuring gene expression are discussed later in this chapter.

Measurement of protein biomarkers

Immunocytochemical staining of Ki67 and γH2AX

The technique of immunofluorescent or immunocytochemical staining enables visualisation of antibody-tagged proteins under a fluorescence microscope. The process is described in full in chapters four and six. Cells are fixed on coverslips with 4% paraformaldehyde. The coverslips are washed in DPBS, blocked for any non-specific binding using a mix of proteins (usually in the form of cow's milk, serum albumin or serum). After blocking, another wash is performed, followed by incubation with specific antibodies against the protein of interest. Multiple proteins can be tagged at once as long as each antibody is not produced by the same species. It should be noted that synthetic primary antibodies are produced without animals, but are named for the specific species in which the structure of the antibody was identified. I.e. a mouse antibody may be produced in a fully synthetic manner, but is still described as a "mouse antibody" because the structure is species-specific. After incubation with the primary antibodies, the coverslips are washed, and secondary antibodies applied. The secondary antibodies are conjugated with a fluorophore and specifically target the primary antibodies. For multiplex staining for multiple proteins, multiple primary and secondary antibodies are used, but care must be taken that the secondary antibodies do not target each other or each other's targets. The fluorophores must also be chosen so that they do not both fluoresce at a similar range of wavelengths. A nuclear stain such as 4′,6-diamidino-2-phenylindole (DAPI) can be incubated alongside the secondary antibodies to aid visualisation and analysis. The coverslips are mounted to slides with Dako mounting medium for

imaging on a fluorescence microscope. The exact details of staining and imaging protocols and materials are recorded in each data chapter's methods section.

This method is used in the context of senescence as it can aid in the analysis of characteristics such as cellular proliferation and DNA damage. Ki67 is a nuclear protein that is associated with cellular proliferation due to its functions during the cell cycle: protection against the aggregation of heterochromatin during the G1 stage of the cell cycle, and the later re-localisation to the nucleolus [166–170]. It is not usually identified in cells that are in G0 stage (i.e. it is widely regarded not to be present in quiescent or senescent cells), but recent studies suggest a very low level of Ki67 expression is sometimes retained by quiescent cells [171,172]. Nevertheless, measuring Ki67 is useful as it identifies changes in the levels of proliferation within a cell culture. γH2AX is a histone protein that becomes phosphorylated in the presence of double-stranded DNA breaks. It acts as a biomarker for the initiation of DNA damage repair, but is often considered a direct biomarker of DNA damage itself [173,174]. This is useful to measure as it can indicate changes in DNA damage repair.

Antibodies were sourced from Abcam: Rb anti-Ki67 (ab15580, ab16667), Ms anti-γH2AX (ab26350), Alexa Fluor R 555 Goat pAb to Rb (ab150078, ab150086) and Alexa Fluor R 488 Goat pAb to Ms (ab150117). Fluorescence at 405 nm, 488 nm and 555 nm was captured for DAPI, γH2AX and Ki67 respectively using the Leica DM4 B Upright Microsope at 10 × magnification and its associated image capture software: Leica Application Suite X (LASX) 2019 3.7.1.21655v software (Leica Microsystems, Wetzlar, Germany).

Terminal deoxynucleotidyl transferase dUTP nick-end labelling (TUNEL) staining

TUNEL staining is another method of detecting double-stranded DNA breaks [173]. The assay is widely used for detecting fragmented DNA in cells undergoing apoptosis. It uses a modified dUTP (usually a fluorophore) to identify the 3'-OH section of the fragmented DNA. On the incorporation of the dUTP into the DNA, a reaction serves to make the fluorophore detectable on a fluorescence microscope. The Click-iT® TUNEL Alexa Fluor® Imaging Assay from ThermoFisher was performed according to manufacturer's instructions and is detailed in chapter six's methods section. This kit used a similar blocking and washing approach as the immunocytochemical staining protocol above, but uses the kit components in place of antibodies and Hoescht stain instead of DAPI.

Analysis of staining

Manual counting methods

Chapter three discusses why many image analysis tools are not used in practice. In our team, multiple manual methods of counting cells from SAB activity staining and immunocytochemical staining (including TUNEL staining) experiments were used. We began to investigate the creation of custom image analysis tools and this is detailed in chapter three. In the meantime, image data for the other

chapters in this thesis had to be acquired via manual counting. For all staining in this thesis, five images per biological replicate were taken and counted. The exact method of analysis is detailed in each data chapter's methods section. A Zeiss AxioCam ERC55 PrimoVert brightfield microscope was used to take images during general tissue culture and for the images for SAB activity staining. The Leica DM4 B Upright Microsope was used to take images of fluorescently stained cells. For SAB activity staining, the cell counter plugin tool on ImageJ 1.47v software was used to keep track of the count and the cells were manually identified as being either "stained" or "not stained". The counter image was saved and the counts recorded in a spreadsheet. The Leica Application Suite X 2019 3.7.1.21655v software is used to control the Leica DM4 B Upright Microsope, and has a similar counter annotation tool. For fluorescently stained images, I viewed each different channel to ensure the stain of interest was co-localised with the nuclear stain. I counted the cells using the annotation tool while I manually identified each cell as being "stained" for the protein(s)/dye of interest or "not stained", and recorded the counts in a spreadsheet. This approach is of course subjective, but the creation of the image analysis tool will hopefully remedy this issue in the case of fluorescent nuclear staining.

Fluorescence Imaging of Nuclear Stains (FINS) image analysis algorithm

The development of the FINS algorithm is described in detail in chapter three. The algorithm is run using Matlab software version R2017b. The algorithm is able to count cells that have been stained for DAPI, Ki67 and γH2AX (using the immunocytochemical staining techniques described above) straight from .liff files

produced by the Leica Application Suite X 2019 3.7.1.21655v software. The FINS algorithm counts nuclei using DAPI and then only counts any signal for Ki67 and γH2AX that is co-localised to a nucleus.

Measurement of gene expression

RNA extraction

To enable downstream analysis of gene expression, RNA must be extracted from cell cultures. It can be extracted from cells in several different ways. In chapter four and chapter six, I used the following method for RNA extraction: using TRI reagent and a phenol-chloroform extraction. TRI reagent contains guanidine isothiocyanate and phenol which causes phase separation of RNA, DNA and proteins, when chloroform is added. The RNA is contained within an aqueous phase from which it can be subsequently precipitated in isopropanol and washed in ethanol.

The protocol is adapted from the TRI reagent manufacturer's instructions to include adjustments, namely the addition of 10 mM $MgCl_2$, to improve recovery of miRNAs should we have wished to investigate any miRNA expression [175]. Cells were washed twice in DPBS (14190136, Gibco™) and removed from the culture plate by cell scraping in TRI Reagent Solution (AM9738, Invitrogen™) supplemented with 10 mM $MgCl_2$ (AM9530G, Invitrogen™). A cell scraper is used to aid the detachment and lysis of the cells. The TRI mixture is removed and stored at -80°C until the day of extraction. The TRI mixture is thawed before the

addition of 10 µl of 10 mM $MgCl_2$ per ml of TRI reagent. These extractions are all from cells, so the TRI fraction is spun at 13870 × g for 20 minutes at 4°C (all centrifugation steps are done at 4°C to reduce the risk of RNA degradation during extraction). For every 1 ml of TRI reagent, 200 µl of chloroform (C/4920/08, Fisher Chemical) is added and the tubes are shaken vigorously to mix. They are left at room temp for 5 minutes before being centrifuged at 21098 × g for 20 minutes. The clear fraction is carefully removed into a new tube. The old fraction is returned to long term storage to enable DNA or protein to be extracted at a later date if wanted. The volume of the aqueous clear colourless fraction (containing RNA) is matched with an equal volume of isopropanol (BP2618-1, Fisher Bioreagents). 1.2 µl of GlycoBlue™ Coprecipitant (AM9516, Invitrogen™) is added to aid in visualisation of the pellet. The mixture is left at room temperature for ten minutes before being spun at 21098 × g for ten minutes. The supernatant is pipetted off before 1 ml of 75% Ethanol (per ml of TRI reagent) is added. The pellet is floated using a vortex machine before being spun again at 21098 × g for 30 minutes. This wash step is repeated using 500 µl of 75% Ethanol (per ml of TRI reagent used) and is extended to a 40-minute spin if the pellet is very small. After removal of the final wash supernatant, the pellet is left to air dry briefly for approximately 10 - 15 minutes before resuspension in either RNase free water or 1 × TE buffer pH 8 (BP2473-500, Fisher Bioreagents). RNA quality and quantity are assessed using a Thermo Scientific™ Nanodrop 8000 Spectrophotometer (Thermo Fisher Scientific, Waltham, Massachusetts, USA).

For the drug screen in chapter five, I used an RNA extraction kit because it was more suitable as a medium-throughput method than the classical

phenol-chloroform extraction. The kit uses a lysis buffer to lyse cells and stabilise RNA, then a silica-based membrane in each well binds the RNA. The plate is washed repeatedly while the RNA is confined to the membrane, until it is eventually eluted into a collection plate. Phenol-chloroform extractions tend to have higher yield and arguably better quality, but are unsuitable for more than 24 simultaneous RNA extractions. Therefore, the PureLink™ Pro 96 RNA Purification Kit was used. This was used according to manufacturers' instructions with elution into 45 µl of RNase free water. A small sample of wells was assessed for RNA quality and quantity on the Thermo Scientific™ Nanodrop 8000 Spectrophotometer.

Reverse transcription

Once RNA is extracted for use in real time quantitative PCR (RTq-PCR), it must first be converted into complementary DNA (cDNA) using reverse transcriptase. For all reverse transcription assays in this thesis, I used Applied Biosystem's High-Capacity cDNA Reverse Transcription Kit (4368813, Applied Biosystems™) in 20 µl reactions (according to their instructions) on a Veriti™ 96-Well Fast Thermal Cycler. Cycling conditions were: 25°C for 10 minutes, 37°C for 120 minutes and 85°C for 5 minutes followed by a 4°C hold step. For all experiments except the senescence screen, RNA concentration was adjusted to be equal before the reverse transcription took place. The method for eventual analysis of RT-qPCR results controls for any concentration differences introduced at this stage, but it is best practice to equalise all RNA concentrations going into a reverse transcription reaction. For the senescence screen, measuring and

adjusting all samples would have meant risking RNA degradation during the time taken to do so. When sampled, the screen's RNA concentrations fell within a narrow range. The range was low enough that typical instrument error in measuring the RNA concentration would probably give a similar range of true RNA concentrations even if the measured RNA concentrations were equalised. We therefore decided to use the RNA without adjusting for concentration differences for these reasons.

Pre-amplification of cDNA

RT-qPCR needs sufficiently concentrated cDNA to be able to detect differences in gene expression, but this cannot always be produced from a single reverse transcription reaction. One option is to perform several reverse transcription reactions, but this makes it difficult to compare gene expression across the entire dataset as extra controls are needed. Another option is to use a pre-amplification PCR reaction step. Pre-amplification is performed by running rounds of PCR on the cDNA using the same primers and probes that will be used in the RT-qPCR. This increases the concentration exponentially in a pre-amplified product and enables RT-qPCR to give results from low concentrations of cDNA. In chapter four, the progeroid cells treated with trametinib had low yield, so I used a pre-amplification step. In chapter six, we required expression analysis on many different genes, so a pre-amplification reaction was used to enable more genes to be analysed from the same reverse transcription reaction. For all pre-amplification reactions, TaqMan™ PreAmp Master Mix (4384266, Applied Biosystems™) and pooled TaqMan™ Gene Expression Assays (FAM) (4331182,

TaqMan®) (see Table 1) were used following manufacturer's instructions on a Veriti™ 96-Well Fast Thermal Cycler. Cycling conditions were: 95°C for 10 minutes, 14 cycles [of 95°C for 15 seconds, 60°C for 4 minutes], 99°C for 10 minutes, followed by a 4°C hold step.

Table 1: List of Taqman Assay IDs. Taqman Assays were used to perform gene expression analysis of the following genes based on their functions.

Gene name	Taqman Assay ID	Role
BCL2	Hs04986394_s1	Ageing pathway/apoptosis marker
ATM	Hs00175892_m1	Ageing pathway/cell cycle
CASP1	Hs00354836_m1	Apoptosis marker
CASP3	Hs00234387_m1	Apoptosis marker
CASP7	Hs00169152_m1	Apoptosis marker
CASP8	Hs06630780_s1	Apoptosis marker
CASP9	Hs00962278_m1	Apoptosis marker
GUSB	Hs00939627_m1	Housekeeping gene
IDH3B	Hs00199382_m1	Housekeeping gene
PGK1	HS99999906_m1	Housekeeping gene
PPIA	Hs04194521_s1	Housekeeping gene
UBC	Hs01871556_s1	Housekeeping gene
UBC	Hs05002522_g1	Housekeeping gene
LMNB1	Hs01059205_m1	Senescence marker/nuclear structure
MYC	Hs00153408_m1	Proto-oncogene/ageing pathway
CXCL1	Hs00236937_m1	SASP marker
CXCL10	Hs00171042_m1	SASP marker
CXCL8 (IL-8)	Hs00174103_m1	SASP marker
IL-10	Hs00961622_m1	SASP marker
IL12A	Hs01073447_m1	SASP marker
IL12B	Hs01011518_m1	SASP marker
IL-1B	Hs01555410_m1	SASP marker
IL-2	Hs00174114_m1	SASP marker
IL-6	Hs00174131_m1	SASP marker
INFy	Hs00989291_m1	SASP marker
LTA (TNFß)	Hs99999086_m1	SASP marker
MMP1	Hs00899658_m1	SASP marker
MMP3	Hs00968305_m1	SASP marker
MMP9	Hs00957562_m1	SASP marker
TNFα	Hs00174128_m1	SASP marker
CDKN1A	Hs00355782_m1	Senescence marker/cell cycle
CDKN2A	Hs00923894_m1	Senescence marker/cell cycle
NOVA1	Hs00359592_m1	Spliceosome component
AKAP17A	Hs00946624_m1	Splicing factor
HNRNPA0	Hs00246543_s1	Splicing factor
HNRNPA1	Hs01656228_s1	Splicing factor
HNRNPA2B1	Hs00242600_m1	Splicing factor
HNRNPD	Hs01086912_m1	Splicing factor
HNRNPH3	Hs01032113_g1	Splicing factor
HNRNPK	Hs00829140_s1	Splicing factor
HNRNPM	Hs00246018_m1	Splicing factor

HNRNPUL2	Hs00859848_m1	Splicing factor
PNISR	Hs00369090_m1	Splicing factor
SRSF1	Hs00199471_m1	Splicing factor
SRSF2	Hs00427515_g1	Splicing factor
SRSF3	Hs00751507_s1	Splicing factor
SRSF6	Hs00607200_g1	Splicing factor
SRSF7	Hs00196708_m1	Splicing factor
TRA2B	Hs00907493_m1	Splicing factor

RT-qPCR

RT-qPCR enables relative gene expression to be measured by the use of gene expression assays. For all chapters, TaqMan™ Gene Expression Assays (FAM) were used. Table 1 shows the genes assayed in this thesis, their assay IDs, and the corresponding function of the gene in the context of this thesis. Gene expression assays use short oligonucleotides that are specific to the 5' and 3' sections of the gene that it is assaying (primers) as well as another short oligonucleotide with an attached fluorophore (probe) that fluoresces when it binds specifically to the section of cDNA within that gene. Taq polymerase enables extension of the template cDNA only when in proximity of the primers, meaning only the particular gene is amplified per round of PCR. Measurement of fluorescence after each cycle of PCR enables detection of cDNA from the gene of interest. A fluorescent dye at a consistent concentration in the reaction mastermix enables normalisation to baseline levels of fluorescence for each well. Given that the cDNA was originally formed from the RNA, the cDNA of the gene of interest will be present in differing amounts depending on the level of gene expression in the cells. The number of cycles of PCR that it takes for the level of fluorescence to meet a threshold (C_T) therefore offers a way to quantify in

real-time the level of gene expression through comparison of the C_T values. This is discussed further in the following section on RT-qPCR analysis.

For all RT-qPCR experiments, 5 µl reactions on 384-well plates were used on the Quantstudio 12K platform from Applied Biosystems™. 1 µl of template and 2.5 µl of Applied Biosystems'™ TaqMan™ Universal Mastermix II were used in combination with the aforementioned gene expression assays (concentrations of which corresponded to 900 nM primer and 250 nM probe). Three technical replicates were performed for every cDNA sample and were mixed prior to loading the plate in order to reduce technical variability. Cycling conditions are: 50°C for 2 minutes, 95°C for 10 minutes, followed by 40-50 cycles of 95°C for 15 seconds and 60°C for 1 minute. Fluorescence intensity was captured at the end of each cycle. Ramp speeds were 1.6°C per second for all transitions.

Analysis of RT-qPCR data

C_T values provide a measurement from which relative gene expression may be calculated using a comparative C_T technique [176]. The Quantstudio 12K platform software automatically assigns a threshold, but it can be adjusted manually (if appropriate) to ensure the threshold crosses all of the fluorescence intensity curves in their exponential phase. After ensuring an appropriate threshold, the median and standard deviation of the C_T values for the three technical replicates were calculated. When the standard deviation exceeded 0.5 cycles, a maximum of one technical replicate was removed to reduce the effects of outliers. After this data cleaning step, the median C_T value was normalised to the expression of

housekeeping genes. Several endogenous housekeeping genes (listed in Table 1) were used for the normalisation. The proposed housekeeping genes, the genes of interest and statistics based on the housekeeping genes (mean, geomean and median) were assessed for stability using the online RefFinder tool [177]. The most stable metric across the dataset was then used for normalising all of the genes. For example, the geomean for the housekeeping genes of a biological sample would be subtracted from the gene of interest for that biological sample. An average is taken of the resulting ΔC_T values for an appropriate control group for each gene of interest. The average ΔC_T of the control group is subtracted from each gene of interest resulting in the $\Delta\Delta C_T$ value. $2^{-\Delta\Delta CT}$ is used to calculate a ratio for comparison. The natural log of the data can be taken to aid with any skew, this is noted in the methods sections of each chapter. Each biological group is used for further statistical analysis and interpretation of results. Several quality control steps are also included throughout the analysis to mitigate for any potential error introduced via data handling. This technique is used in chapters four, five and six before the data can be analysed statistically.

Bioinformatic analysis of structure-function

The development of a bioinformatic structure-function association test is well described in the methods section of chapter five. SMILES (simplified molecular input line entry system) is a way of storing structural information of a chemical within an alphanumeric code. It must be converted into another similar format, SDF (structure-data file), before it can be used in this particular bioinformatic pipeline. This bioinformatics pipeline uses the ChemmineR and fmcsR packages

in Rstudio to compare a compound's structure with that of another [178–180]. A series of comparisons between each compound in a group will result in a matrix of Tanimoto coefficients. The Tanimoto coefficient is a measure of how similar a structure is to another. The contents of a Tanimoto coefficient matrix can be compared against the contents of another matrix in order to compare the overall structural similarity within each group with the other. The data in each matrix is taken forward for statistical analysis (discussed below and detailed in the methods of chapter five).

Statistical analysis and image production

Information on software versions and source are provided in each data chapter. IBM SPSS, Graphpad prism and Matlab software were used to compute statistics where appropriate as detailed in each chapter's methods. Statistical test choice depended on the data format, proposed comparisons and the hypothesis. Generally, a student's t test was used to compare two means, and an ANOVA with a post hoc test was used to compare multiple means. The risk of type one error can be mitigated by controlling for multiple comparisons, however the risk of a type two error can increase. Where appropriate, we corrected for multiple comparisons when our results weren't informed by preliminary results. Where the risk of a type two error was great, and the risk of a type one error would be mitigated by further studies and validation, we opted not to correct for multiple testing.

Graphs were produced using Graphpad Prism, with the exception of graphs for the section regarding the FINS algorithm, which were created using Matlab software version R2017b, and in the senescence chapter regarding the drug panel design, which were created using Microsoft Office Excel. Diagrams were mostly produced using Microsoft Office Powerpoint. Although, where appropriate, diagrams were drawn freehand and/or adjusted using GNU Image Manipulation software.

Chapter 3: Development of methods for assessment of senescence in human-relevant cell culture

Many experimental methods require optimisation before their use. Previous work in our laboratory has worked up several methods for modelling ageing *in vitro* and for assessing senescence characteristics. These include tissue culture techniques, the use of a staining kit for senescence-associated beta galactosidase (SAB) activity, fluorescence staining for Ki67, γH2AX, and TUNEL, as well as PCR-based assays for a wide range of genes [56,60,70,181]. Several of these methods have inherent flaws as discussed below.

In the course of my research, the first aim was to ensure the human-relevance of the model by making all methods animal component-free. Here, I present a draft of a journal article prepared for submission to Cytotechnology in collaboration with my co-authors. The contributions of all co-authors are described within the article structure, however, for its inclusion in my thesis, I provide further detail here on my exact involvement. I had oversight of the article's structure, oversight of the experimental designs for all cell types, conducted the laboratory experiments for the fibroblast cell lines (nHDF types A-C and HUFs), conducted the presentation and analysis of the fibroblast cells, aided in the presentation and analysis of all other cells' data, oversaw the project management, and wrote the majority of the manuscript.

As a staining method itself, the traditional SAB assay was suited to small-scale experiments. I present a short report within this chapter on the trial of an alternative method for analysing SAB.

The methods used by our team for counting stained cells were very time-consuming, inefficient and varied between individual researchers. I recognised an issue with easy access to any automation of counting within our team and began working with a team collaborator and image analysis expert, Dr Jack Spencer, to come up with a simple solution. We briefly investigated the options available for image analysis of SAB-stained cells, however we were unable to identify any initial direction for this particular avenue of research within the time-constraints of this thesis.

We were more successful at developing methods for the other type of staining method used in our group. We were able to create and optimise an automated image analysis program for immunocytochemically-stained cells imaged on a fluorescence microscope. In this chapter, I present a draft journal article prepared for submission to IEEE Transactions on Medical Imaging in collaboration with my co-authors. Within the bounds of the article, the contributions of the co-authors are discussed, but I will elaborate here on my personal contribution for the purposes of the article's inclusion in my thesis. I outlined the problem, conceptualised and managed the project, conducted the majority of the experimental laboratory work that fed into the data for the program's optimisation and testing, had oversight of the experimental approaches used to analyse and test the program, aided in the presentation of data, wrote sections of the manuscript pertaining to the laboratory methods, and the biological applications of the program, and revised the manuscript critically. Sadly, the program was not finalised early enough to be able to use it to analyse image data for the other chapters of this thesis.

Considerations for the replacement of foetal bovine serum with human serum and other alternative supplements in cell culture

Laura R Bramwell[1†], Samantha Gould[1†], Merlin Davies[1], Conor McMullan[2] &

Lorna W Harries[1*]

[1]RNA-Mediated Mechanisms of Disease group, College of Medicine and Health, Institute of Biomedical and Clinical Science, University of Exeter

[2]Technical Services, College of Medicine and Health, Institute of Biomedical and Clinical Science, University of Exeter

[†]these authors contributed equally

*corresponding author

Correspondence address:

Professor Lorna W Harries
Institute of Biomedical and Clinical Sciences
University of Exeter College of Medicine and Health
RILD Building
Royal Devon and Exeter Hospital
Barrack Road
Exeter
Devon
EX2 5DW
United Kingdom

Correspondence email: L.W.Harries@exeter.ac.uk

ORCID numbers: LRB - 0000-0003-4069-3959, SG - 0000-0001-9634-5772, MD - 0000-0002-6951-9762, LWH - 0000-0001-7791-8061

Twitter: @miRNAgirl, @LauraBramwell1, @TeamRNA, @Merlin_Davies

Abstract

Clinical trial failure rates are substantially influenced by poor translation between pre-clinical human *in vitro,* non-human *in vivo,* and human clinical research. Difficulties are often faced when transitioning away from animals into human *in vivo* clinical trials, and there is much reliance in basic science research on traditional methods which often use animal-based products in *in vitro* models. Improving the human-relevance of early models may help, especially when targeting more nuanced species-specific cell processes. Foetal bovine serum (FBS) is the most commonly used media supplement in cell culture, but it can introduce issues with human-relevance. We aimed to derive a process that may inform the transition of any human cell type into animal free culture conditions. We successfully eliminated animal-derived biomaterial from primary fibroblast, endothelial, and mononuclear cell culture. Serum-free alternatives were considered for the culture of fibroblasts and mononuclear cells. However, synthetic supplements, as with traditional growth factors and basal media, are not a one-size-fits-all approach. Human serum tends to be more physiologically relevant to human biology than FBS but suffers from issues regarding supply and batch-to-batch variation. Xeno-free alternatives provide an attractive replacement opportunity due to their consistency, but we found that the synthetic supplement was not always enough to support effective cell culture. We discuss considerations and how the individual requirements of each cell type may vary when transitioning from established culture media. We provide a suggested process for researchers to transition primary cells into a more physiologically relevant, translatable culture environment.

Keywords:

Animal-free, human serum, foetal bovine serum (FBS), cell culture, bovine pituitary extract (BPE), xeno-free, humanise, humanisation,

Animal and human diseases are often not synonymous. The underpinning biology of disease may also differ between animals and humans, making it difficult to translate findings into humans from medical research models that involve animals, animal cells or models that are exposed to animal-derived biomaterials [133,182–184]. For example, in respiratory medical research, "non-humanised" models are almost exclusively used and have poor translational efficiency, with compounds having only a 15% chance of success when entering clinical trials [185]. More generally, this issue contributes to the low number of drugs (10-20%) that successfully pass through all stages of clinical trials and receive marketing approval [186]. The issue of translatability is exemplified by the murine models which are frequently used to inform on human disease. Not only do genetics, physiology, and immunology vary between murine models and humans, but many diseases are also not naturally exhibited in mice at all [182,187]. Due to this disparity, a variety of methods are used to induce human-like disease in murine models including genetic modification and exposure to biological or chemical agents [188–190]. However, due to varying pathogeneses, there may be substantial disparity between the onset, presentation, treatment, and resolution of disease in pre-clinical animal models and clinical disease. This leaves significant room for failure when moving from pre-clinical to clinical trials.

While the translational issues of animal *in vivo* and animal *in vitro* models are often highlighted, any issues resulting from the presence of animal-derived biomaterial in a cell culture model can often be dismissed as one of the inherent

limitations of tissue culture models. However, there is evidence to support that tissue culture methods may be improved by the reduction and replacement of animal-derived biomaterials [136,191]. Altering established cell culture practices to remove animal-derived biomaterials may seem like much effort for little gain, especially with technologies emerging that may potentially outcompete basic two-dimensional cell culture, such as organoids and organ-on-a-chip models. However, cell culture models are still used daily and will continue to be used long-term in many areas of basic research. If a model can be improved quickly and easily, then this may help to bridge the gap in translation before emerging technologies can change the paradigm.

Since the first cells were successfully cultured, balanced salt solutions have been used to enable their survival, and animal proteins, including sera, or fractions thereof, have enabled their further maintenance and expansion [192]. Cell culture media was initially developed for amphibious and avian animal cells in the late 19th century, only moving onto mammalian cells in the early 20th century. In 1951, owing to the isolation of the HeLa cell line from the cervical carcinoma of Henrietta Lacks, human cells could be consistently cultured for the first time [193]. Due to the widespread availability of this first immortalised human cell line, it was possible to further explore, optimise, and better define culture media.

Whilst basal media has become better defined and is often now entirely synthetic, serum is still a common nutrient source in basic cell culture. This is as a result of its rich, but variable, cocktail of hormones, growth factors, amino acids, vitamins, salts, carbohydrates, lipids and proteins that are conducive to cellular

metabolism, viability and proliferation [194]. Foetal bovine serum (FBS, also known as foetal calf serum or FCS) is commonly used for its accessibility and success in supporting a wide range of cell types. Due to the variation of individual animals, batch-to-batch variation of FBS is a well acknowledged issue [195–197]. Batch-testing and maintaining batch consistency mitigates this issue within individual experiments for the most part; however, reproducibility on a wider scale is often still hindered [196]. Additionally, the use of FBS poses concerns surrounding viral contaminants and supply availability [198].

The problem is more pronounced when growing “difficult-to-culture” cell types or when investigating nuanced and highly species-specific processes. As well as for improving reproducibility, there is a call for entirely synthetic media for the culture of more specialised cell types. For example, depending on their origin, primary cells can be highly variable in their growth rates, and an imbalance of growth factors could alter cellular proliferation, viability and phenotype. Serum-free or low serum media is often used for such cell types. However, in the absence of sera, animal-derived constituents such as bovine pituitary extract (BPE) are often used instead to encourage proliferation. These media are frequently proprietary and costly due to their specialised nature. Additionally, whilst BPE is less variable than FBS, its active components are not well-reported. When considering alternatives to FBS for the purposes of improving the human-relevance of a model, we must also consider if its replacement is susceptible to the same problem.

“Xeno-free” alternatives are reliant upon sufficient characterisation of the mitogenic components in traditional sera, in order to identify and include the necessary components required to support the cells. Depending on the origin of the cells, different growth factors are required, not only to promote mitogenic activity, but also to maintain cellular phenotype. In addition to FBS or BPE, specialised culture media will typically contain a cocktail of growth factors that are specific to the maintenance of a particular cell type. Due to the growing market of recombinant growth factors, it is now very possible to replace growth factors with animal-free alternatives. Purchasing lyophilised or “carrier-free” growth factors is often necessary as, when purchased in solution, even recombinant human growth factors are still commonly stabilised with bovine serum albumin (BSA), unless specifically stated otherwise [199].

Whether for translatability, reproducibility or ethical purposes, there are many reasons why it may be desirable to omit FBS and BPE from cell culture entirely. Products derived from human sera may be suitable to permit the growth of human cells in culture, but synthetic serum alternatives may be a better solution [200]. Databases such as the FCS-free database and Cellosaurus can provide resources on cell lines and media [201,202]. Geraghty *et al.* list a selection of vendors for serum-free and xeno-free media [184]. Vendors such as Merck and Fisher Scientific often have information on alternative cell culture supplements. Several approaches exist for transitioning a cell culture model into serum-free media, however the decision-making process involved in choice of medium can often be unclear. Resources, such as those mentioned above, often have guidance on

methods for switching from one medium to another, but they often lack effective advice on the selection of an initial approach and troubleshooting.

Whilst physiological relevance in research is strongly desirable, the very nature of *in vitro* research brings inherent limitations. Cells normally exist in a complex network in a three-dimensional structure within a tissue. Their *in vivo* growth rate may be slower than *in vitro,* and their cell size and shape may also change when put into an *in vitro* model. In many cases, a cell culture model must be able to support enough expansion for experiments, but a growth rate that was the same *in vitro* as *in vivo* would likely be too slow for a useful model. The microenvironment surrounding a cell can cause changes in its size and shape as can the species of origin. It follows that different culture media, particularly when changing from a media containing animal-derived biomaterial, might cause cells to change the speed of their growth and/or their shape or size. Whether the alterations to cell properties in a model becomes an issue depends on the downstream use of the model. Bioreactors, hydrogels and mechanical stress systems have enabled cells to be subjected to gas exchange, space and mechanical pressures that are more akin to the *in vivo* environment [203,204]. It is the cell type and the desired outcome measures that determine the utility of these technologies. Cost and availability are other factors that may influence the ability to culture cells under physiologically relevant conditions. However, it may be argued that tradition is the main reason that the use of animal-derived biomaterials is seen as a “gold standard” in human cell-culture, but moving away from this practice may provide a very simple, yet often overlooked step towards physiological relevance, and hence the translatability of cell culture.

With this in mind, we aimed to determine whether it was possible to “humanise” the cell culture process by transitioning multiple human primary cell types from traditional media into animal component-free cell culture conditions. We demonstrate the suitability of animal-free alternatives to support normal human dermal fibroblasts (nHDF), human uterine fibroblasts (HUF), retinal endothelial cells (RECs), and peripheral blood mononuclear cells (PBMCs) by producing a side-by-side comparison of the cell size and proliferative capacity of cells cultured in their original and trial animal component-free (ACF) media. We acknowledge that there is not a one-size-fits-all approach and discuss the current limitations of the field including the effectiveness and availability of ACF alternatives. We also discuss elements of the “humanisation” process that must be considered by any researcher looking to use ACF alternatives in the future. As such, we derived a flowchart that encompasses the decision-making and troubleshooting process that informed the transition of multiple cell types in order to share these experiences with the wider research community and demonstrate the possibility of animal-free cell culture.

The overall process for the “humanisation” of a new cell type is illustrated in Figure 4. It shows a flowchart that falls into five main steps: reviewing literature, planning, preparing stocks, transitioning and validating. The first step is to assess if the recommended medium is ACF by reviewing product information and contacting suppliers. If it is not ACF, then associated literature and information must be reviewed in order to make a plan to trial an alternative. Following planning, stocks of cells must be prepared according to the vendors’ recommendations in case the new ACF medium does not support the cells appropriately. After a suitable amount of cells are grown, the transition experiment may take place as a side-by-side comparison. We used three passages of cells to enable statistical analysis of population doubling (PD) time and other measures. Monitoring cells using a microscope is important at this stage; cells may show visual signs of struggling in the new medium, such as morphological changes, signs of apoptosis etc. Depending on the outcome of this experiment, the transition step may be repeated to enable troubleshooting of the process. The application of the model determines the criteria that the new medium must meet in order to be used further. Therefore, the final step is to validate according to these planned criteria, e.g. comparison of proliferation, longevity in vitro, morphology, and/or retention of specific cell biomarkers.

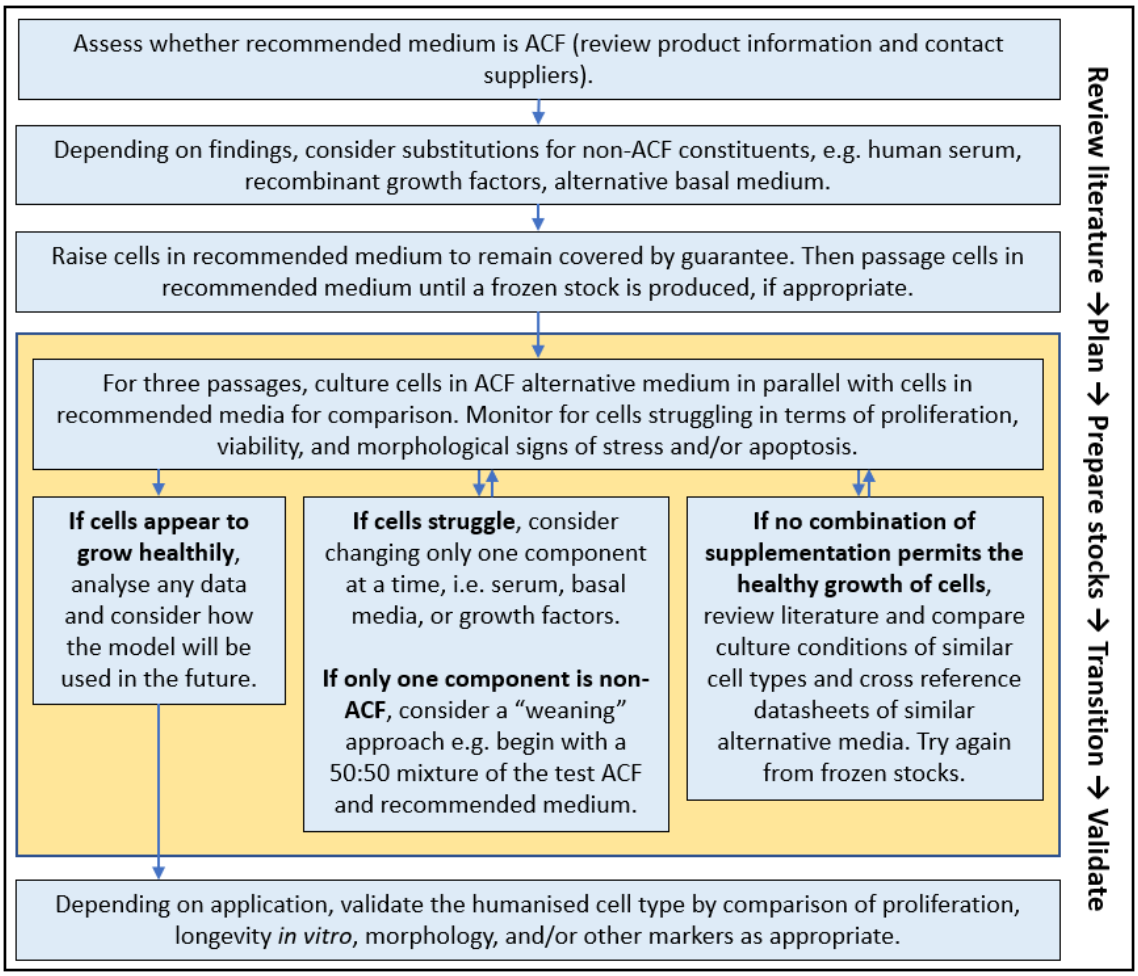

Figure 4: A flowchart outlining the process of transitioning human cells from a recommended media containing animal-derived components to an animal component-free (ACF) media.

Assessment of the ACF status of current methods

In this study, we confirmed that the recommended medium was not already ACF for any cell type studied here. We confirmed this by looking at the product information available online and/or via personal correspondence with company representatives. In this study, we were able to obtain confirmation of ACF status for all basal media, but we were unable to access information on which particular component(s) contained animal-derived biomaterial(s) for every medium investigated.

After assessing that a medium was not ACF and that the vendors did not have a recommended ACF alternative, we searched literature databases (NCBI PubMed, FCS-free Database, Cellosaurus etc.) as well as looking at information on alternative vendors' websites to assess suitability of any other medium on sale. Following this search, we decided on initial approaches for each cell type and proceeded to experimental testing.

General tissue culture

Four main cell types were used in this study: normal human dermal fibroblasts (nHDFs), human uterine fibroblasts (HUFs), retinal endothelial cells (RECs), and peripheral blood mononuclear cells (PBMCs). All cells were raised using the vendor's recommended medium and instructions to ensure the cells were covered by any manufacturer's guarantee. Cells were passaged as per the recommended conditions until a frozen stock could be created.

On occasion, a quick preliminary first-pass assessment of growth was conducted: the ACF medium was applied to cells for a few days while checking for morphological changes in properties such as shape, cell size and cytoplasmic content using a light microscope (Zeiss AxioCam ERC55 PrimoVert). This enabled a quick and easy assessment of any obvious stress and cell death responses. This experiment took advantage of a situation when cells cultured for the main stock were being grown ready for the main side-by-side comparison, but a small amount of excess cells were available and could be used for other experimentation. For most cell types, we had enough cells to run the side-by-side

comparison without this preliminary step. If this preliminary experiment showed promise, we continued to run the side-by-side comparison of media types as planned. If it did not, then we looked back at our research and changed our plan accordingly.

For adherent cells, we looked at cell PD time and cell size over the course of three passages. Figure 5 illustrates this experimental design. A T25 flask of cells was grown in non-ACF media before being split equally into two T25 flasks. A “trial” ACF medium was applied to one flask, while the other flask was kept growing in the “control” non-ACF medium. The two flasks were grown in parallel and were passaged three times using 50% of cells at each split. Cells were counted to enable the calculation of PD time and assessed for cell size at every passage (including the initial split).

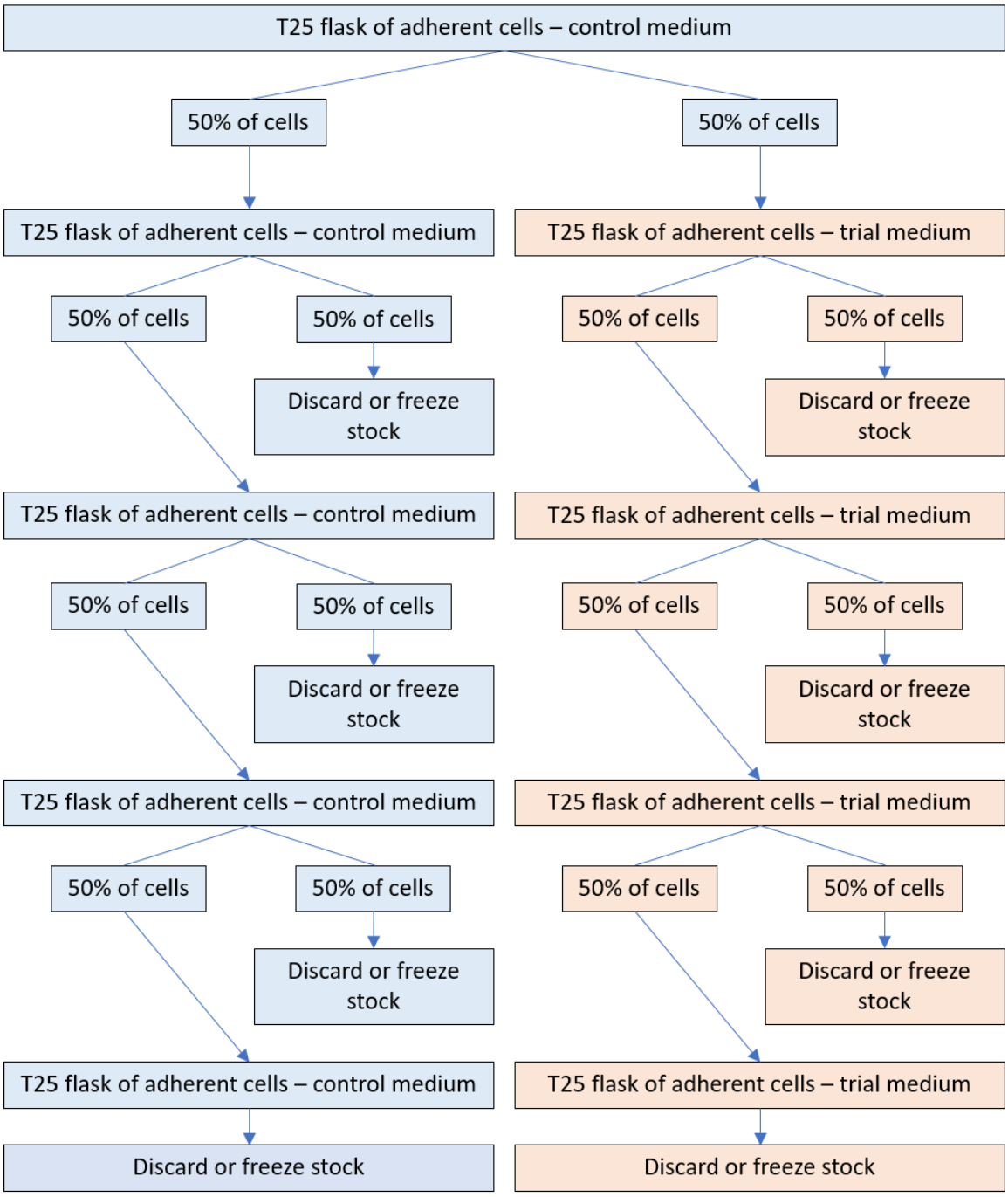

Figure 5: A flowchart outlining a basic side-by-side comparison experiment of adherent cells in an animal component-free (ACF) "trial" medium and a non-ACF "control" medium. Cells are counted and measured for cell size before cells are placed into each new flask.

Dermal fibroblasts

Normal human dermal fibroblasts (nHDFs) from three different donors were sourced from Promocell, Heidelberg, with ethical approval at source (catalogue number C-12302). nHDF A cells were taken from the thigh of a male donor (lot number unavailable). nHDF B cells were from a 28-year-old Caucasian female donor's breast (lot number 467Z026.3). nHDF C cells were from a 36-year-old Caucasian male donor's abdomen (lot number 445Z026.3).

nHDF A cells' cumulative population doublings (cPDL) at the time of this experiment was unknown as they had been cultured previously without record of population doublings. The cPDL at the beginning of this experiment was 17.50 for nHDF B cells and approximately 33.71 for the nHDF C cells.

The control medium for nHDF A cells was Promocell Fibroblast medium (Promocell, Germany) supplemented with 2% foetal bovine serum (FBS, 10270106, Gibco™) and 1% 10,000 units/ml penicillin - 10,000 µg/ml streptomycin (15140122, Gibco™). The control medium for both nHDF B and nHDF C cells was Dulbecco's Modified Eagle Medium (DMEM) 1 g/l glucose + phenol red (31885023, Gibco™), 10% FBS (10270106, Gibco™) and 1% 10,000 units/ml penicillin - 10,000 µg/ml streptomycin (15140122, Gibco™).

The trial medium for both nHDF A and nHDF B cells was DMEM 1 g/l glucose + phenol red (31885023, Gibco™), 10% human serum (HS, H3667, Sigma Aldrich) and 1% 10,000 units/ml penicillin - 10,000 µg/ml streptomycin (15140122,

Gibco™). The trial medium for nHDF C cells was DMEM 1 g/l glucose + phenol red (31885023, Gibco™), 10% GroPro Cell Culture Growth Supplement (SER-HPL-GROPRO, ZenBio) and 1% 10,000 units/ml penicillin - 10,000 µg/ml streptomycin (15140122, Gibco™).

For passaging, nHDF cells were washed twice in Dulbecco's phosphate buffered saline (DPBS) (14190136, Gibco™) before detachment with TryPLE™ Express (12604013, Gibco™). The TryPLE™ Express activity was neutralised using either the control or trial medium. Cells were spun at 700 × g, the supernatant was removed and cells were resuspended in the appropriate media. If needed, following resuspension, cells were frozen in media with 10% dimethylsulfoxide (DMSO) (J66650.AD, Thermo Scientific Alfa Aesar) and 70% serum. FBS (10270106, Gibco™) was used for freezing of control and initial stocks, whereas human serum (H3667, Sigma Aldrich) was used for freezing of trial stocks and for lines after their successful transfer to ACF media.

Uterine fibroblasts

Human uterine fibroblasts (HUFs) were commercially sourced from Promocell, Heidelberg, with ethical approval granted at source (catalogue number C-12385). Cells were derived from the myometrium of an 85-year-old Caucasian female. Cells were at 14.96 cPDLs at the beginning of the experiment for which we present data in this study. The control medium was DMEM 1 g/l glucose + phenol red (31885023, Gibco™), 10% FBS (10270106, Gibco™) and 1% 10,000 units/ml penicillin - 10,000 µg/ml streptomycin (15140122, Gibco™). The trial medium was

DMEM 1 g/l glucose + phenol red (31885023, Gibco™), 10% HS (H3667, Sigma Aldrich) and 1% 10,000 units/ml penicillin - 10,000 µg/ml streptomycin (15140122, Gibco™). HUFs were passaged and frozen following the same protocol and reagents as for the nHDF cells.

Mononuclear cells

Peripheral blood mononuclear cells (PBMCs) were obtained from donors with University of Exeter CMH Ethics Approval (CMH Ethics ID Number 511048). PBMCs were extracted from blood samples using Sepmate-50 IVD separation technology as per the manufacturer's instructions (Stemcell Technologies, Vancouver). Cells were cryogenically preserved after extraction. When thawed, cells were suspended in control or trial media. All media contained RPMI-1640 medium (21875034, Gibco™) with 1% 10,000 units/ml penicillin - 10,000 µg/ml streptomycin (15140122, Gibco™). The media was supplemented by either 10% FBS (10270106, Gibco™), 10% HS (H3667, Sigma Aldrich) or 10% GroPro Cell Culture Growth Supplement (SER-HPL-GROPRO, ZenBio). Cells were spun at 240 × g before resuspension in fresh media. Cells were seeded into a 24-well plate at a cell density of 1×10^6 cells/ml. The diverse repertoire of lymphocytes and other PBMCs in this cell type is not used for long term growth due to the naturally short-term viability. As passaging cells only needs to be carried out when media is nutritionally depleted or when cells exceed maximal seeding density within the culture vessel, passaging was not performed during this study. Cells were sampled for cell size and number periodically during the experiment.

Retinal endothelial cells

Human primary retinal microvascular endothelial cells (RECs) were purchased from Cell Biologics (IL, USA) with ethical approval granted at source (catalogue number H-6065, lot number 122118U), no donor information was available. Cells were initially raised in complete human endothelial cell medium (H1168, Cell Biologics) as recommended by the cell manufacturer, which consisted of a basal medium, 5% FBS, and unstated concentrations of L-Glutamine, vascular endothelial growth factor (VEGF), fibroblast growth factor (FGF), heparin, epidermal growth factor (EGF), hydrocortisone, and an antibiotic/antimycotic. This media contained animal components, and from this point was solely used as the control medium in the subsequent humanisation process.

Endothelial cell medium, MV2 (C-22221, Promocell, Heidelberg) was used as the basal medium for the ACF trial medium, as it was confirmed to be animal-free by the supplier. However, the associated supplement mix (C-39226, Promocell, Heidelberg, containing 5% FBS, 5 ng/ml EGF, 10 ng/ml bFGF, 0.5 ng/ml VEGF, 20 ng/ml IGF, 0.2 µg/ml hydrocortisone and 1 ug/ml ascorbic acid) was not ACF due to the inclusion of FBS and growth factors reconstituted in BSA. RECs were trialled in completed MV2 medium and, as successful, this served as a good starting point for humanisation.

Whilst MV2 basal media and the concentrations of the supplementary growth factors were indicated as suitable for the culture of RECs, alternative animal-free growth factors had to be sourced. The role of each growth factor was considered

when selecting the key components to support RECs. To inform this, multiple commercially available endothelial cell media were compared to determine which growth factors are frequently used and therefore likely necessary for their successful culture as shown in Table 2. ACF growth factors (EGF, FGF, hydrocortisone and serum) that were incorporated into most endothelial cell media were automatically included in the trial medium. The trial medium used Promocell MV2 endothelial growth basal medium supplemented with the aforementioned growth factors. Initially, the growth factors (insulin-like growth factor (IGF) and heparin) were also included as they were present in the supplements of both the recommended medium and MV2. Cellular proliferation and morphology were observed over multiple passages. On this occasion, there was no visible difference in REC morphology or growth between the media containing IGF and heparin and the media without them. Therefore, these components were excluded from the final trial medium.

The final ACF REC trial media consisted of MV2 endothelial growth basal medium (C-22221, Promocell) supplemented with 5% HS (H3667, Sigma Aldrich), 5 ng/ml EGF (236-EG-200, Bio-techne), 10 ng/ml bFGF (HZ-1285, Proteintech), 0.5 ng/ml VEGF (HZ-1038, Proteintech), 0.2 µg/ml Hydrocortisone (1918-FN-02M, Bio-Techne), and 1 µg/ml ascorbic acid (105021000, Acros Organics).

Table 2: Presence of growth factors (Yes/No) in commercial media supplements for retinal endothelial cell (REC) culture.

Growth factor	Cell Biologics (Human endothelial cell)	R&D Systems (Endothelial cell growth)	Lonza (Endothelial cell growth medium-2)	Thermofisher (Primary microvascular endothelial)	Promocell MV (Endothelial growth medium)	Promocell MV2 (Endothelial growth medium)
EGF	Y	Y	Y	Y	Y	Y
FGF	Y	Y	Y	Y	N	Y
IGF	N	Y	Y	N	N	Y
Heparin	Y	Y	Y	Y	Y	N
Hydrocortisone	Y	Y	Y	Y	Y	Y
VEGF	Y	Y	Y	N	N	Y
Ascorbic acid	N	Y	Y	N	Y	Y
Dibutyryl cyclic AMP	N	N	N	Y	N	N
Endothelial cell growth supplement	N	N	N	N	Y	N

RECs were raised in control medium and then expanded for three passages prior to experimentation. Cells were estimated to be at approximately 13 cPDLs at the beginning of this study. Throughout, cell culture flasks were coated with human fibronectin (1918-FN-02M, Bio-Techne) as an alternative to gelatin, to promote attachment. For passaging, REC cells were washed once in DPBS (14190136, Gibco™) before detachment with TryPLE™ Express (12604013, Gibco™). The TryPLE™ Express activity was neutralised using PBS containing 10% FBS or HS depending on whether the cells were in media containing FBS or HS. Cells were

spun at 500 × g for 5 minutes, the supernatant was removed, and cells were resuspended in the appropriate media. Cells were frozen in 40% media with 10% DMSO (J66650.AD, Thermo Scientific Alfa Aesar) and 50% serum. FBS (10270106, Gibco™) was used for freezing of control and initial stocks, whereas human serum (H3667, Sigma Aldrich) was used for freezing of trial stocks and for RECs after their successful transfer to ACF media.

Cell counting and assessment of cell size

Unless otherwise stated, for experiments in this study we used a DeNovix CellDrop™ machine with Acridine Orange - Propidium Iodide (AO/PI) viability stain (BT40039 and BT40017, Cambridge Bioscience) to count cells for PD time calculations and to measure average cell diameter. Primary human fibroblast cells were counted using the Celldrop™ machine, but were also counted using a Hirschmann haemocytometer because their inherent uneven morphology renders automatic counting less accurate. Cell counts from the haemocytometer were therefore used for the calculation of PD time in all fibroblast cell types. One early experiment for nHDF A pre-dates the acquisition of the Celldrop machine in our laboratory. For this particular experiment, we used GNU Image Manipulation Program version 2.10.14 to sample cell size by measuring ten cells per image for ten images per medium type [205]. For the PD time for nHDF A, cell counts were measured manually using a haemocytometer as described above.

Statistics

Independent t tests were used to compare means for all experiments except the comparisons of PBMCs grown in parallel in three different experimental media, which used a one-way ANOVA with Tukey's post hoc test. Statistical tests and graphs were produced using Graphpad Prism version 9.4.1 for Windows (GraphPad Software, San Diego, California USA, www.graphpad.com). Error bars on the graphs represent the standard error of the mean (SEM).

Results

PD time was not affected by transition to ACF conditions

In this study, we present data for side-by-side comparisons of cells grown in control media or trial ACF media. The ACF media contained either human serum or a synthetic growth supplement (GroPro). The PD time did not change significantly for any of four adherent cell types (nHDF A, nHDF B, HUF and REC). Figure 6 shows the results for experiments growing adherent cells in trial media containing human serum, with accompanying data in Table 3 and Table 5.

Only the size of one cell type was affected by a transition to ACF conditions

As shown in Table 5, Figure 6 and Figure 7 the cell size was only altered significantly in one cell type. nHDF B cells were 12% smaller in the trial medium, with a mean diameter of 12.34 ± 0.3466 µm, compared to cells grown in the control medium's mean diameter of 14.14 ± 0.3830 µm ($p = 0.0129$). It is worth noting that the average cell size of nHDF A cells was larger than other types because it was measured when the cells were adherent rather than when in suspension.

Mononuclear cell survival was unchanged when using human serum or a synthetic supplement

PBMC survival did not appear to differ when subjected to different serum supplementation in short-term culture (Table 4 and Figure 7A). No significant statistical difference was detected using a one-way ANOVA ($p = 0.9268$). The survival of cells in media containing FBS decreased slightly by day 5 (Day 3 = 104% of original cell seeding density, Day 5 = 92%). The survival of cells in media containing human serum decreased through both time points (Day 3 = 94%, Day 5 = 98%). Similarly, the survival of cells in media containing GroPro decreased slightly from the original culture (Day 3 = 100%, Day 5 = 95%).

A synthetic supplement was insufficient as a direct substitution for serum in dermal fibroblast culture

GroPro was not sufficient alone as a supplement to support the growth of the nHDF C cells. For this experiment, cells were seeded at the same density for the experimental process as described in Figure 5. At the first passage of cells in control or trial media, the control flask contained 1.65×10^5 cells with a mean diameter of 11.42 µm and the trial flask contained 1.3×10^5 cells with a mean diameter of 14.75 µm. A few days later, the experiment ended when cells in the medium containing GroPro died off. It is worth noting the cells in the medium containing 10% human serum were still growing at the end of the experiment.

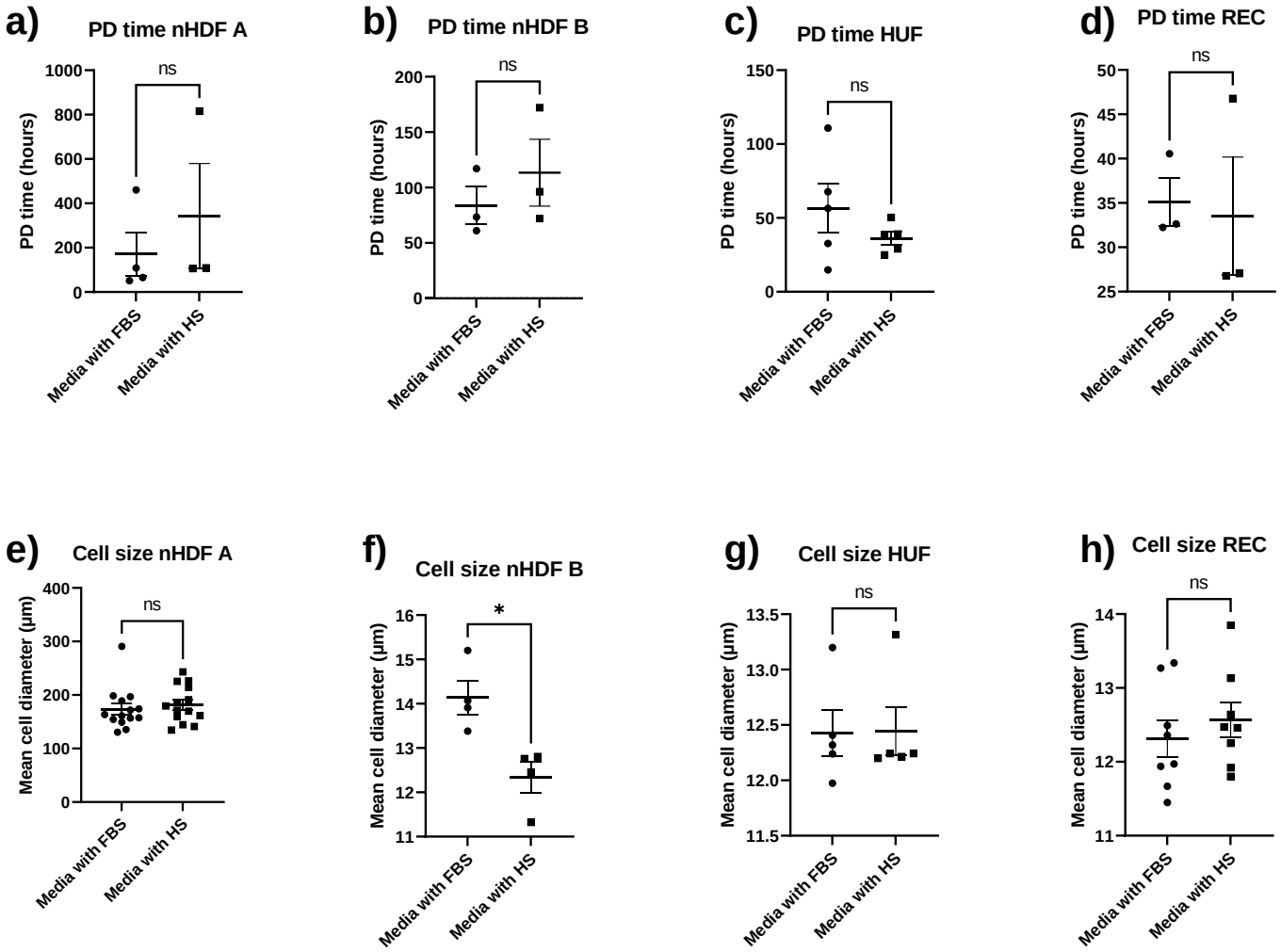

Figure 6: Population doubling (PD) time was unaffected by media supplement (either 10% foetal bovine serum (FBS) or 10% human serum (HS)), but cell size was affected in one cell type. A) and E) normal human dermal fibroblasts (nHDF) type A. Please note nHDF A cell size was measured when cells were adhering to a flask whereas other cell types are measured in suspension. B) and F) nHDF type B, C) and G) human uterine fibroblasts (HUF), D) and H) retinal endothelial cells (REC).

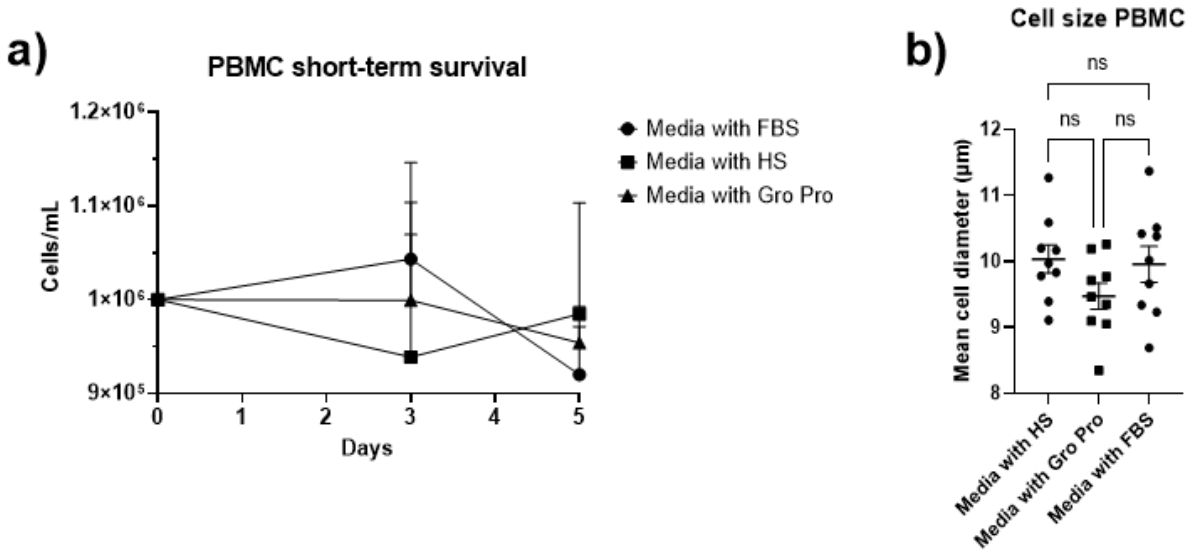

Figure 7: No differences were observed in the survival and size of peripheral blood mononuclear cells (PBMCs) grown in media with different supplementation in parallel. A) Short-term survival. B) Mean cell size.

Table 3: Population doubling (PD) time by cell type. p values computed from an independent t test. SEM denotes standard error of the mean.

Cell type	Control medium			Trial medium			p value
	Mean	SEM	N	Mean	SEM	N	
nHDF A	171.3	97.02	4	343.4	235.8	3	0.4847
nHDF B	83.85	16.96	3	113.4	30.11	3	0.4401
HUF	56.5	16.4	5	36.24	4.404	5	0.2672
REC	35.14	2.706	3	33.54	6.625	3	0.8341

Table 4: Total cell counts of the mononuclear cells by day with different media supplements.

Days	Media with foetal bovine serum			Media with human serum			Media with GroPro supplement		
0	1.00E+06	1.00E+06	1.00E+06	1.00E+06	1.00E+06	1.00E+06	1.00E+06	1.00E+06	1.00E+06
3	9.72E+05	1.25E+06	9.12E+05	7.34E+05	1.18E+06	9.00E+05	1.20E+06	9.56E+05	8.44E+05
5	1.02E+06	8.74E+05	8.64E+05	9.54E+05	1.20E+06	7.96E+05	1.03E+06	9.24E+05	9.08E+05

Table 5: Cell size (µm) by cell type. p values computed from an independent t test or a one-way ANOVA with Tukey's post hoc test in the case of the PBMCs. SEM denotes standard error of the mean. Note that cells were sized when in suspension for all cell types except nHDF A which were sized using a different method while adherent.

Cell type	Control medium			Trial medium 1			Trial medium 2			p value
	Mean	SEM	N	Mean	SEM	N	Mean	SEM	N	
nHDF A	173.5	10.55	4	182.1	235.8	3	-	-	-	0.5457
nHDF B	14.14	0.383	4	12.34	0.3466	4	-	-	-	0.0129
nHDF C	11.42	0.7202	2	14.75	2.25	2	-	-	-	0.2941
HUF	12.43	0.2061	5	12.44	0.2185	5	-	-	-	0.9615
REC	12.31	0.2471	8	12.57	0.2352	8	-	-	-	0.4692
PBMC	9.958	0.2714	9	10.03	0.2128	9	9.471	0.1997	9	0.193

Discussion

Adjusting cell culture medium can improve the physiological relevance of a model to human disease. However, it is not always straightforward to transition to a different medium, and many considerations need to be taken into account during the process. FBS is predominantly used in tissue culture for its availability and because it is traditional, but not due to its specificity nor physiological relevance; it is likely that there are more suitable alternatives for the culture of human cells [197]. In this study, we have formulated ACF alternatives to the medium traditionally used for several different types of primary human cells. We were able to substitute human serum in place of FBS in the medium for dermal fibroblasts, uterine fibroblasts, retinal endothelial cells and peripheral blood mononuclear cells. A synthetic alternative, GroPro, was able to act as a substitute in PBMC culture, but not in the culture of dermal fibroblasts. We illustrate the process we used to transition cells, and the considerations that may need taking into account when trialling alternatives to non-ACF media and animal-derived sera.

A successful cell culture model is defined by its uses, so the main consideration for changing to non-ACF media is the downstream applications of the model itself. In this paper, the cell types were to be used for medical research into the basic science behind ageing, diabetes and immunological responses in humans. These diseases have nuances in humans that are not replicated in animal studies, so it was in our interest to ensure these models were human-relevant [136]. The risk of a model not reflecting human physiology was more important to us than the risks of not identifying a change in the cell properties in the culture model. We must

ensure cells in our models grow enough to be used in experiments and do not show any morphological signs of stress or other obvious morphological changes. Therefore, we monitored cells for changes in PD time, cell size and any obvious visual morphological changes. Cells were grown in the ACF media for experiments once cells grown in trial media had satisfied these criteria.

Therefore, the cell type and the model's future use determines the criteria that a trial medium must meet in order to be used for research. For example, the HUFs described here were to be used in studies involving replicative senescence. In preparation for comparisons between low and high levels of replicative senescence, we continuously grew cells to a point where the culture began to slow in terms of PD time and the tissue accumulated senescent cells. The HUFs were grown in ACF medium for a further 38 population doublings after transitioning from non-ACF medium. The culture did not have any obvious morphological changes compared to cells grown in non-ACF conditions when visually inspected every 2-3 days. The vendor guarantees the cells will grow for more than 15 population doublings in their recommended conditions: the HUFs in ACF media were able to meet this number of population doublings. Other applications may need more stringent criteria to be met before a non-ACF model may be used for research. For example, a model may need to be carefully checked for differences in epithelial to mesenchymal transition, or certain biomarkers to ensure a particular cell retains its original identity that it needs to provide the correct model for the experiment.

The only significant difference in cell size was in the population of nHDF B cells, but this difference does not indicate that the ACF media is unsuitable in this instance. Cell size may be different for several reasons. The mostly likely reason is due to seeding density because nHDFs may get smaller if they are at a high density. We often see dermal fibroblasts change in size in non-ACF media depending on their seeding density. Although both cultures were seeded at the exact same density initially, the cells in the trial medium had a higher seeding density throughout the rest of the experiment. The differing seeding densities and PD times over the course of the experiment were not significantly different overall, so it is difficult to assess if the seeding density was the reason behind the smaller size. It is possible that cells in media containing FBS are larger. Whether this is an issue for us depends on the morphology of the cells. In this case, the cells did not display any signs of stress or morphological changes during routine visual inspection, so we assessed the media as being sufficient for use in our future experiments.

Suspension cultures of non-adherent cells require some minor considerations that differ to adherent cultures. Adequate gas exchange must be simulated by daily gentle shaking/stirring, with growth easily tracked using samples of the suspension counted at regular intervals. Without cell adhesion, enzymatic or chemical dissociation is not required when passaging. It is also worth noting that suspension culture cells such as primary peripheral blood mononuclear cells are not suitable for long term culture expansion – which places a different emphasis on utilisation of growth supplementation used for humanisation. That is to say,

culture medium for these cells needs to support short term survival, but does not need to allow for long term expansion.

The assessment of the ACF status of the current cell culture reagents was usually straightforward. However, whilst some suppliers were very forthcoming with information regarding their products, other suppliers could only provide a little information on proprietary media/products. In some cases, a vendor would refuse to even offer yes or no in answer to whether a product contained any animal-derived biomaterial meaning that we had to assume the product was not ACF.

Many growth factors, supplements and media contain small amounts of Bovine Serum Albumin (BSA) to act as a stabilising agent for proteins [199]. During personal correspondence with company representatives, 50% of the Promocell basal media that we enquired about contained animal-derived biomaterial. It is likely that many serum-free basal media contain BSA as a stabilising agent for certain components of the medium. We also have found that sometimes company representatives misunderstand our queries about a product's ACF status, and only identify the presence of serum and don't always identify that BSA "counts" when we enquire about a product being ACF. It would be good if a standard could be set for naming a product "animal-free", and similarly it would be beneficial if it became mainstream to use human and/or ideally synthetic versions of serum albumins in place of animal-derived serum albumins.

Although several invaluable literature banks exist, such as the FCS-free database, they can be difficult to search, often have many similar entries to search through, and often don't contain the information you are searching for about media and/or growth factors. Although a medium may be free from FBS, it does not mean that it is ACF and the databases do not adequately make the distinction. Similarly, information about individual growth factors can be difficult to find. Clearer, more coherent and more comprehensive information on the components of media, the role of cell culture supplements, and data surrounding their inclusion and/or exclusion in the culture of specific cell types would be very useful to researchers in the future.

For most cell types, the initial approach for transitioning away from medium containing FBS and other animal-derived biomaterial was a simple direct swap for an ACF supplement. This approach worked for several straightforward cell types. However, we found in cells such as Human Aortic Endothelial Cells (HAoECs) that a direct swap of human serum in place of FBS did not always support growth or even caused cell death. For certain cell types, a transition experiment is not possible due to limited lifespan of the cells. In these cases, it is advantageous to develop the trial medium using a similar cell type. For example, we have used the medium worked up for normal human dermal fibroblasts successfully on diseased dermal fibroblasts. The diseased cells do not grow enough in normal conditions to permit a side-by-side comparison, so the medium used in normal cells was simply trialled from the start of the culture of diseased cells. In spite of the disease state, the cells grew successfully and as expected in the ACF medium. For other difficult cell types, a "weaning" approach may work.

Guidance on this type of approach can be found on vendor websites or resources mentioned in the introduction.

FBS has been traditionally used in cell culture since the technique was first developed, and consequently its use is omnipresent in most tissue culture facilities. Tissue culture models are artificial by their very nature and may not react similarly to a tissue *in vivo*; however, human *in vivo* studies are often neither feasible nor ethical for answering a specific research question. Animal *in vivo* studies have their own well-described drawbacks, and the species-specific nature of certain biological processes could mean that a human cell culture model may actually be more representative of what happens *in vivo* in humans [196,197,206,207]. Although any tissue culture experiment will have control groups, the presence of animal-derived biomaterials represents an unknown in cell culture medium which can alter the microenvironment and could mask or change a response. Similarly, human serum could represent an unknown factor, but, arguably, putting a human-derived biomaterial into a human cell model of human disease may represent a better approach than animal-derived biomaterial.

Human-derived alternatives to FBS, such as the human serum used throughout this paper, are derived from pooled human donors. Human serum is obtained in small volumes, pooled, and filtered/treated before sale. Another important thing to note is that the serum is from adult donors. Consent is given at the point of donation, but there are ethical worries surrounding the sale of a person's biomaterial. When we consider that human serum is from an adult rather than a foetus, we identify that the serum is likely to be less mitogenic than FBS. This

alternative may be more representative of the human tissue's *in vivo* physiological environment, but it could also limit the rate and capacity of proliferation. Depending on the level of cellular expansion required, this may be considered disadvantageous for a particular model. This may also be a moot point given that in our study, human serum did not affect the PD time of any cell type.

Another consideration is the fact that because human serum products are typically from pooled donors, they can exhibit batch-to-batch variability. Donor pools of human serum may also include confounding quantities of some element that is key to detection or culture evaluation, and as such may not be appropriate to specific experimental designs. For example, pooled human serum may not be ideal in the context of immune cell-based experiments as any immune system components in the serum could interfere with the detection of human-specific antibodies or receptor binding. Conversely, a baseline level of antibodies and growth hormones, which may be achieved using pooled donor serum, could be beneficial to certain experimental designs where long term proliferation is desired.

Human serum itself can be difficult to work with. We found that batches often vary in the amount of lipids present. The lipids and large debris in the serum can mean that some cells do not respond well to unfiltered human serum in the medium. It also makes it difficult to determine morphological changes when debris is present. We used vacuum filter units to remove the debris. Due to the lipid content, the units could clog quickly so this method isn't without its flaws. We tried centrifuging the serum to remove the lipid fraction, but we were unable to do so.

Serum-free media could be a viable alternative to both FBS and human serum, however many serum-free culture media are not xeno-free and contain BPE as a growth factor source. BPE promotes the survival and mitogenic activity of mammalian cells to a greater degree and in a more potent capacity than those cultured using FBS, but it can influence the culture in other ways, e.g. BPE is known to possess proteins that provide antioxidant activity [208]. Whilst exchanging FBS for BPE may reduce the overall volume of animal components used within cell culture media, it is unlikely to reduce batch-to-batch variability entirely. Although certain factors must remain consistent to enable the proliferation of any cell type, the exact composition of growth factors and hormones present in BPE may vary. Many researchers in the 1980-1990s attempted to determine which components of BPE were required to reproduce its mitogenic activity in a variety of cell types. From inhibiting growth factors, to blocking receptors, to introducing growth factors individually, candidates such as fibroblastic growth factor (FGF) and certain hormones were proposed as the predominant mitogenic factors in BPE. However, results appeared to be cell type dependent, and it was often concluded that additional unknown components contained within the BPE also contributed to cellular proliferation [209–212]. From this early exploratory work, it is clear that no singular component of BPE harnesses its full mitogenic potential.

Fully synthetic xeno-free media and supplements are fully characterised and so this removes the factor of the unknown. Xeno-free medium/supplements also do not suffer from batch-to-batch variation in the same way as biological products and so can make for a more reliable medium. However, these synthetic

substitutes have their own issues to overcome. The supplements are not always a direct replacement for serum. In this study, the GroPro synthetic supplement did not work alone for the dermal fibroblasts tested, but was able to sustain the survival of mononuclear cells sufficiently. The fibroblast cells likely needed more growth signals than the mononuclear cells. A next step for optimising this supplement for fibroblasts would be to add synthetic growth factors to the mix. It is also worthwhile noting here that unless they are specifically ACF, synthetic growth factors often contain small amounts of BSA in the same way that any medium (unless specified as ACF) may contain some animal-derived biomaterial. In addition to culture media and sera, other reagents commonly used in cell culture (and in downstream characterisation, experimentation and analyses) often contain animal-derived biomaterial. More recently, recombinant and synthetic alternatives are becoming more widely available and cheaper as demand increases. In tissue culture, trypsin is commonly used to disassociate adherent cells for passaging. Trypsin is commonly derived from the pancreas of livestock, but alternatives to this now include recombinant trypsin and synthetic alternatives such as TrypLE™ and CTS™Versene™. Recombinant proteins are widely available, but are often reconstituted in BSA. Human serum albumin (HSA) may be substituted in place of BSA to enhance stability, and can also serve as an appropriate blocking buffer for many protein assays. Certain primary cells may require coated culture dishes to promote cellular attachment during culture. Gelatin and animal-derived fibronectin are commonly used reagents for this purpose, however human cell-derived alternatives are available and are ACF. With each new cell line and assay performed, it takes consideration of each component to ensure research can be ACF. Such alternatives are increasing in

popularity, and if an ACF alternative is not available it is beneficial to report this to suppliers that provide similar products and discuss future research needs.

Ultimately all tissue culture models have inherent limitations, meaning it can be difficult to determine what is physiologically relevant enough for a model. Whether a model is suitable enough and relevant enough depends on how the model will be experimented on and its downstream uses. Will a difference in morphology change the outcome of an experiment? Could it improve the human-relevance of an experiment? Or would it cause the cell to become de-differentiated and thus cause the loss of a model of the differentiated cells? The answers will inevitably vary, but the answers are often either neutral or in favour of adopting a more human-relevant model.

Conclusion

The route to the clinic for any new therapy often has issues that are rooted in problems with physiological relevance and translation into human pathologies from animal models and/or models that use animal-components. Making research models more human-relevant at every stage is worth considering. Early tissue culture models used in basic science research may be relatively easy to "humanise" compared to later stage research. The removal of animal-derived biomaterial from the tissue culture process has been successfully performed for four cell types (dermal fibroblasts, uterine fibroblasts, retinal endothelial cells and mononuclear cells). This process highlights how common animal-derived biomaterial is in research that uses *in vitro* models. Human serum is more physiologically relevant to human biology than FBS by nature, and so represents an improvement in several cases. Although, xeno-free alternatives may be better, they are not yet suitable for all cell types. The approaches used in this paper highlight some of the key aspects that researchers must consider when looking to remove FBS and other animal-derived biomaterial in their tissue culture models.

Optimisation of senescence assays

Introduction

Senescence can be difficult to quantify when it represents such a heterogeneous phenotype [68,167,213]. Currently the “gold standard” method for detecting cellular senescence is the measurement of senescence-associated beta galactosidase (SAB) activity, however staining fixed cells, imaging and manually counting them is a laborious process and is subjective between observers [166]. Other biomarkers associated with senescence often change depending on the reason they have entered a senescent state. For example, γH2AX (a phosphorylated histone protein present in areas of DNA damage) and the senescence-associated secretory phenotype (SASP; a collection of inflammatory markers that promote paracrine senescence) are increased in stress-induced senescence.

Beta galactosidase activity is a simple assay which involves the use of a colour change reaction to quantify the activity of the enzyme. At pH 6.5, the activity of beta galactosidase in lysosomes correlates strongly with senescence. Therefore, SAB assays usually consist of a buffered version of a standard beta galactosidase activity assay performed on fixed cells. While SAB is better correlated with all forms of senescence than other biomarkers, the traditional assay is not perfect and has inherent issues with measurement accuracy and subjectivity, as well as the practicalities of the assay itself. The altered morphology of senescent cells is a key confounding factor in terms of the

accuracy and subjectivity. The variability and inconsistency in senescent cell morphology makes automation via current image analysis tools inaccurate, meaning manual counting is still required. New deep machine learning technologies are showing promise in image analysis, but the technology is yet to be tried with SAB images [214]. Subjectivity is introduced when we measure with manual counting due to the nature of counting by eye. The morphology of senescent cells can also mean that the cell has a larger volume of cytoplasm. This makes the staining appear more diffuse in the larger cells and can make it harder to distinguish a truly senescent cell in both an objective and consistent manner.

The SAB staining is performed after fixation and often requires a long incubation before imaging. The colouration develops over time and so the imaging is best done using the same duration of time between the application of the stain and the imaging. The stain can be removed, and glycerol or PBS used to store the stained cells for later imaging, but crystals from the stain can form, compromising the quality of the images. While the assay itself is relatively simple, its timings coupled with the imaging required make it difficult to perform to a high standard in the context of a high or medium-throughput experiment.

There are alternative commercial products for measuring SAB by chemiluminescence and fluorescence, however these are not yet in widespread use in the senescence community. We sought a technique for measuring SAB in order to perform a high to medium-throughput drug screen for senescence. As the traditional assay is not very well suited to this type of screen, we aimed to

optimise a different commercial product for measurement of SAB in the drug screen.

Methods

Tissue culture

Primary normal human dermal fibroblasts (nHDFs) derived from a male donor's thigh were commercially sourced (Promocell, Heidelberg). Cell culture conditions and methods are discussed in Chapter 2: Tissue Culture and Chapter 3: Considerations for the replacement of foetal bovine serum with human serum and other alternative supplements in cell culture. nHDFs were seeded into 96-well plates at a density of 6000 cells/well for each experiment. Several experiments were run with cells at early versus late passages. Cells at P11 were compared with P17 during optimisation of SAB kit volumes (data not shown) and then cells at P5 were compared against P21 (cumulated population doublings are not recorded for this legacy cell type). Cells were treated with 0 µM, 1 µM or 10 µM resveratrol (R5010, Merck) for 24 hours prior to the senescence assays.

SAB fluorescence assay

The Cellular Senescence Activity Kit (ENZ-KIT129-0120, Enzo Life Sciences) was performed according to the manufacturer's instructions. Fluorescence was quantified from the cell lysates using a PHERAstar FSX machine (BMG Labtech). Remaining cell lysates were frozen overnight before using Bradford reagent (B6916, Merck) following manufacturer's instructions to determine protein concentration. Protein standards using human serum albumin (12668, Merck) were made in DPBS. Absorption at 595 nm was measured using a PHERAstar FSX machine (BMG Labtech). The protein concentrations of the lysates were calculated to act as proxies for cell number. Relative fluorescence was then corrected to the blank and normalised to protein concentration.

Traditional SAB staining assay

Cells were stained for SAB using the Senescence Cells Histochemical Staining kit (CS0030, Merck). Further detail is available in Chapter 2: Measurement of cellular senescence and Chapter 2: Analysis of staining.

Statistics

IBM SPSS Statistics for Windows version 27.0 program (Released 2020; IBM Corp, Armonk, NY) was used to conduct independent t tests for the following data. The mean ± standard error of the mean (SEM) is reported unless otherwise noted.

Results

The fluorometric SAB kit was clearly able to detect a difference in levels of senescence in young P5 nHDFs versus old P21 nHDFs with the latter exhibiting over three times the relative fluorescence units (RFU). We recorded 24669 ± 357 RFU for the young cells and 77763 ± 4262 RFU for the old cells ($n = 9$ for both groups, $p<0.0001$).

For suitability as a medium-throughput method for screening drugs for senotherapeutic activity, any SAB assay needs to detect smaller differences in senescence in a small number of replicates than the large difference seen in the early versus late passage test with nine replicates. For this experiment, cells were treated with vehicle only, 1 µM resveratrol or 10 µM resveratrol. There were no significant differences between the control group and either dose: control 809645 ± 242819 RFU, $n = 3$, vs 1 µM resveratrol 795011 ± 155389 RFU, $n = 3$, $p = 0.962$. Control: 809645 ± 242819 RFU, $n = 3$, vs 10 µM resveratrol 1386717 ± 369161 RFU, $n = 3$, $p = 0.262$. Protein concentrations routinely came out below the Human Serum Albumin standard curve and below the sensitivity range for the Bradford reagent.

Discussion

The method traditionally used for measuring general senescence was not suitable for a proposed medium-throughput screen, so a fluorometric kit was trialled to assess if it would be suitable. Although the fluorometric kit could detect large differences in SAB activity, it was unable to detect smaller changes caused by a known senomorphic drug, resveratrol. This makes the kit unsuitable for use in a medium-throughput drug screen because it cannot identify the subtle effects on senescence which are characteristic of senomorphic compounds. Given the new kit was unsuitable, an alternative approach was decided upon using a biomarker of senescence, *CDKN2A* gene expression.

The fluorometric kit detects SAB activity in protein lysates, but does not normalise to cell number. Despite seeding cells at the same density, the cells are likely to be uneven in number between each replicate by the time the experiment has run and cell lysates are made from each well. The SAB activity in the lysate is proportional to the fluorescence intensity, however if cell number was uneven between replicates, it follows that the fluorescence intensity may differ, even if the SAB activity was actually the same for the cells in each replicate. If more senescent cells are growing slowly, then effects may be masked if cell number is not taken into account. Small effects may also be masked by the variation between replicates caused by the lack of normalisation to cell number. Other assays for total protein concentration are available, such as the Thermo Scientific™ Pierce™ 660nm Protein Assay, but many are unsuitable and would require further optimisation to ensure the protein in the lysates was within the

sensitivity range, and to ensure any components in the lysate would not disrupt the protein assay. With further optimisation, the kit may have been able to detect small differences in SAB activity. It is worth noting that senescent cells tend to have more cytoplasm and have accumulated more protein within that cytoplasm, so the total protein concentration may be higher naturally in senescent cells. As a result, normalising the relative fluorescence to total protein concentration may still prove inadequate as effects could still be masked.

Although other markers are not as reliable for the assessment of general senescence, they may be more suitable for high to medium-throughput screens for senescence. Given the fluorometric kit's problems with normalisation and a lack of sensitivity to smaller effects, we elected to use gene expression of *CDKN2A* (an alternative marker of senescence) to continue forward with a medium-throughput drug screen.

Image analysis using the Fluorescence Imaging of Nuclear Staining (FINS) algorithm

Laura R Bramwell[1†], Jack Spencer[2†*], Ryan Frankum[1], Emad Manni[1] & Lorna W Harries[1*]

[1]RNA-Mediated Mechanisms of Disease group, College of Medicine and Health, Institute of Biomedical and Clinical Science, University of Exeter

[2]Translational Research Exchange @ Exeter, Living Systems Institute, University of Exeter

*corresponding author

[†]these authors contributed equally

Correspondence address:

Professor Lorna W Harries
Institute of Biomedical and Clinical Sciences
University of Exeter College of Medicine and Health
RILD Building
Royal Devon and Exeter Hospital
Barrack Road
Exeter
Devon
EX2 5DW
United Kingdom

Correspondence email: L.W.Harries@exeter.ac.uk

ORCID numbers: LRB - 0000-0003-4069-3959, JS - 0000-0003-3441-2479, RF - 0000-0002-2665-5625, EM - 0000-0002-2493-0734, LWH - 0000-0001-7791-8061
Twitter: @miRNAgirl, @LauraBramwell1, @TeamRNA

Abstract

Finding appropriate image analysis techniques for a particular job can be difficult. In the context of the analysis of images of immunocytochemically-stained cells, where the key information lies in how many nuclei contain co-localised fluorescent signal from a protein of interest, researchers often opt to use manual counting techniques over any alternatives for many reasons. Here, we present the development and validation of the Fluorescence Imaging of Nuclear Staining (FINS) algorithm. The FINS algorithm is based on a variational segmentation of the nuclear stain's channel and an iterative thresholding procedure to count co-localised fluorescent signal from nuclear proteins in other channels. We present experimental results comparing the FINS algorithm to the manual counts of seven researchers across a dataset of three cell types which are immunocytochemically-stained for a nuclear marker (DAPI), a biomarker of cellular proliferation (Ki67) and a biomarker of DNA damage (γH2AX). The quantitative performance of the algorithm is analysed in terms of consistency with the researchers' data and computation time. The FINS algorithm counts consistently in the same way as a researcher performs manual counts, but improves the process by reducing subjectivity and time. The algorithm is simple to use, in software that is omnipresent in academia, and allows data review with its simple, intuitive user interface. We hope that, as the FINS tool is open source and is simply built for its particular application, researchers will opt to use this method instead of manual counting techniques.

Keywords:

fluorescence imaging, nuclear stain, automated cell counting, Ki67, γH2AX,

Introduction

There are many easy and open-source ways of analysing images of cell nuclei taken on a fluorescence microscope, however there are far fewer options available for the analysis of immunocytochemically-stained proteins that are co-localised specifically to a cell's nucleus. Many software-based options are geared towards analysis of tissue sections which require slightly different considerations compared to cells grown on coverslips, as is the case here with our focus on immunocytochemically-stained cells from tissue culture experiments. Many researchers count cells in this type of image manually because it can be difficult for the typical academic laboratory researcher who wants to analyse this type of image to find, build or adapt a custom solution and/or to justify the resources spent on creating and validating the process. Researchers may not be able to spend time learning how to use complicated open-source customisable image analysis pipelines or to justify the purchase of expensive proprietary software for a small job that is easy to achieve manually. There is a need for a simple, open-source technique to analyse this type of image that is easy enough to find and use that researchers will find it after a quick literature search and use it. An ideal solution would be specialised enough to be effective and enable some form of data review to enable checking of any anomalous data. Here, we describe a new image analysis algorithm: the Fluorescence Imaging of Nuclear Staining (FINS) analysis algorithm. This tool is specialised to differentiate and to count cell nuclei based on any co-localised fluorescent signal appearing within the boundary of the nucleus. It uses a variational

segmentation method with thresholding to define a fitting term. This creates a reliable base for the nuclear segmentation, mirroring the way a researcher would manually count an image.

We validate the FINS algorithm here for two nuclear proteins of interest: Ki67 and γH2AX. Ki67 is a marker of cell proliferation, and γH2AX is a histone protein that is phosphorylated in the presence of DNA damage (specifically indicating a DNA damage repair response) [166,168,173]. When these two proteins are immunocytochemically-stained, they exhibit punctate staining, where multiple foci may be present in the same nucleus. In this context, scientists often want to count proteins that are in the nucleus, and are simply interested in a binary outcome. That is to say, if a cell has any signal for the protein of interest in the nucleus or not. Therefore, we aimed to use datasets of images of three different cell types and compare the FINS algorithm's performance against manual counts performed by researchers.

Current approaches and software alternatives

For images of this type there are currently several methods for obtaining accurate count data. There is the option to count images manually (identifying cells to count by eye with or without the use of a click-counter/annotation tool), or there are image analysis platforms sold as part of expensive software suites, or free customisable image analysis pipelines. Although the nucleus itself can often be visualised using 4′,6-diamidino-2-phenylindole (DAPI) or similar stains, and segmented easily using basic software techniques, it is more difficult to segment an image based on other stains, especially with staining that is only useful when co-localised with the nuclear stain and may have multiple foci.

Images that are manually counted cannot be compared between researchers as there is often inconsistency; each researcher's classification of a cell being stained for the protein of interest, or not, is dependent on several factors. Similarly, direct comparisons between image datasets from previous experiments/studies would be inappropriate. To compare different studies, overall results must be compared rather than the direct counts. Many of the reasons for this level of subjectivity relate to the individual user: decision-making (manual determination of what constitutes a cell/signal and whether or not to count it), experience at immunocytochemistry/manual cell counting, eyesight, tiredness, care and focus.

There are also differences in how researchers perform manual counts: whether they export images to an alternative format or if they use a counting tool. Many researchers use a counting tool or annotation tool to avoid the need to keep mental track of a number, but some prefer speed and do not use these tools. There are also technical factors that can affect the data, e.g. the screen being used or the level of ambient light at the time of the count. Before analysis can begin, there is already variation introduced between images caused by the researcher's choices regarding adjustment of any image capture settings, not to mention the biological and technical variation that comes with any tissue culture and immunocytochemical staining techniques. All manual counting techniques are time consuming and can be tiring for the researcher, but manually counting cells does mean that researchers can check the images for any irregularities that might not be identified with an automated image analysis tool. There is inherent biological and technical variability with this type of staining experiment. For example, irregularities could be present such as an instance of two cells overlaid following mitosis, higher levels of background autofluorescence in an image or cell debris. Although an automated image analysis tool wouldn't necessarily be able to compensate for all irregularities, it would still remove a lot of subjectivity from the image analysis method compared to manual counts. Ideally, any alternative software would have a user interface to enable checking for irregularities such as those mentioned above.

In spite of the problems with manual counting, many researchers still choose to do so for several reasons. Many academic research groups do not perform enough of

this type of analysis to warrant the expensive purchase of software suites such as the HALO® Image Analysis Platform (Indica Labs Inc., Albuquerque, NM, USA) and many do not have the bioinformatic skills necessary to create, perfect and optimise a custom pipeline using software such as QuPath or Cell Profiler™ [215,216]. There are also indications that a fully custom-built algorithm performs better than approaches built using custom pipeline software [217]. Although some algorithms built for another purpose (e.g. for analysis of tissue sections that are immunohistochemically stained) may be easily adaptable to analyse immunocytochemically-stained images for a bioinformatician, they are often difficult to find as they can be quite niche, and it is not very feasible for an end-point researcher to spend time finding, adapting and validating it for their own purpose. Therefore, many academic studies still tend to use manually acquired data despite the approach's severe limitations. Here, we build a simple tool that can be run using Matlab software (MathWorks Inc., Natick, MA, USA) that is mostly installed and omnipresent in academic research. Our tool is designed specifically for the analysis of images of immunocytochemically-stained nuclear proteins. The tool also has the capability to review data (the user interface is shown in Figure 8) and can be adjusted/adapted for other parameters/software if a researcher wants, but its primary aim is simplicity of use. The script is simple, easily accessible and free, so we hope that the barriers stopping people from using other methods do not apply to this algorithm.

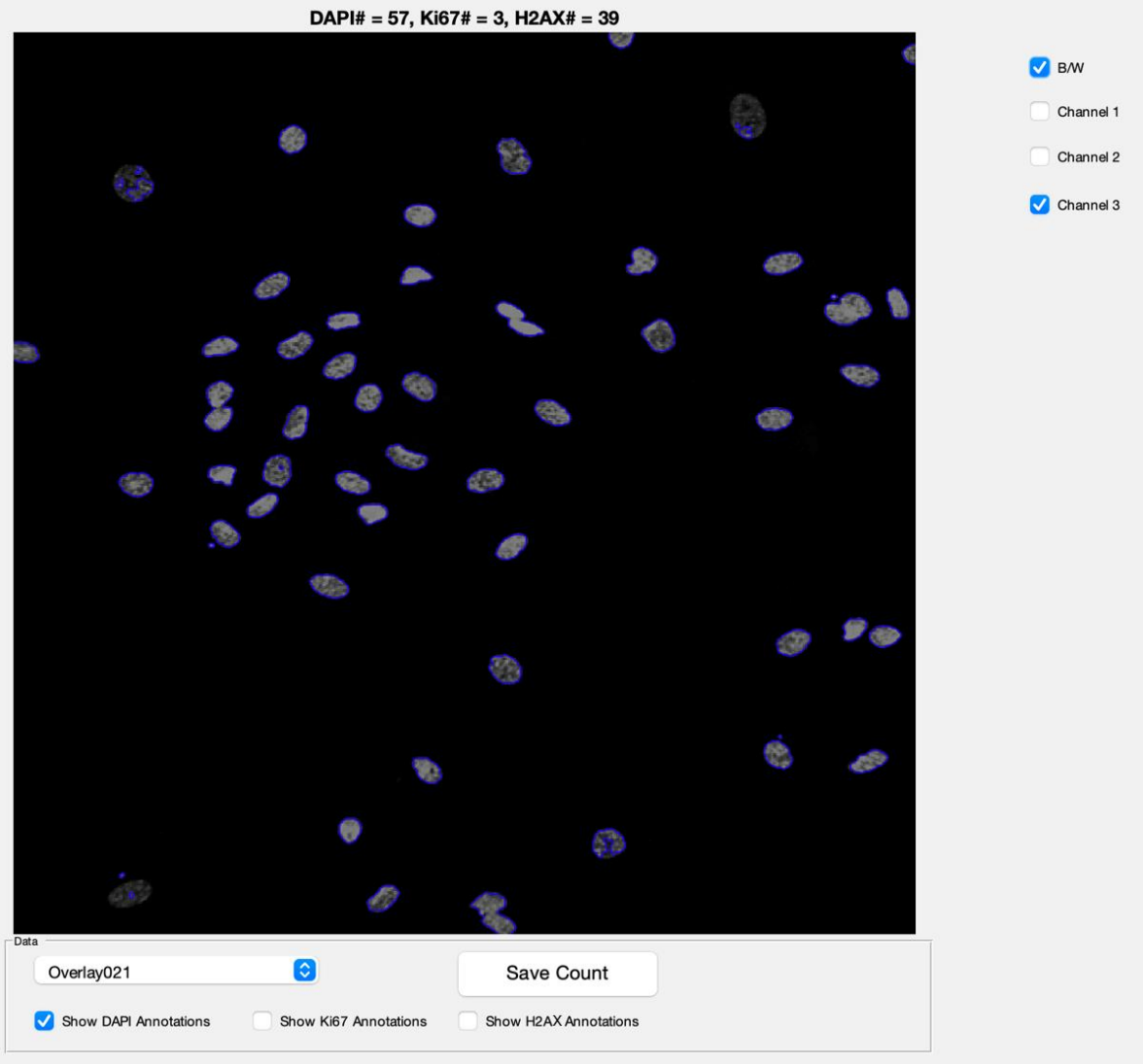

Figure 8: User interface of the FINS algorithm. The computed counts are displayed at the top of the image, and the user may alter the view to show different images in the dataset. The user can also alter the view to overlay different channels, to show the images in false colour or black and white, and to annotate how the algorithm has counted each channel.

Image acquisition and tissue culture

We access images for this study from several populations of cells. Set A (images 1 - 10) are images of human aortic endothelial cells (HAoEC). Set B (images 11 - 20) are images of human dermal fibroblasts (HDF). Set C (images 21 - 30) are human chondrocytes (HCH). HAoECs were cultured in Promocell Endothelial MV2 medium (C-22221, Promocell) supplemented with 2% foetal bovine serum (FBS) (16140071, Gibco™). All human primary dermal fibroblasts were grown in animal component-free conditions. For further detail please see Chapter 2: Tissue culture and Chapter 3: Considerations for the replacement of foetal bovine serum with human serum and other alternative supplements in cell culture. HCHs were cultured in DMEM F12 (21331020, Gibco™), 1% non-essential amino acids (NEAA) (11140035, Gibco™), 10% FBS (10270106, Gibco™) and 1% penicillin streptomycin (15140122, Gibco™). Cells were grown on 13 mm coverslips in 12-well plates at approximately 30,000 cells per well, were fixed using 4% paraformaldehyde and stored in Dulbecco's phosphate buffered saline (DPBS, 14190136, Gibco™). Cells were washed in DPBS, and blocked using ADST [antibody diluent solution - triton: DPBS, 0.1 M L-Lysine (303341000, Thermo Scientific™), 1% w/v albumin (either human serum albumin fraction V (12668-10GM, Sigma-Aldrich) or bovine serum albumin, fraction V, fatty acid-free (10775835001, Roche)), Triton X-100 (A16046.AP, Thermo Scientific Alfa Aesar)] and 5% serum (either human serum (H3667, Sigma Aldrich) or FBS (16140071, Gibco™)) for 30 minutes. Cells were washed and primary antibodies at 2.5 µg/ml (suspended in ADST with 2% human serum or FBS) were

applied overnight. After washing, a solution of secondary antibodies at 5 µg/ml and 4′,6-diamidino-2-phenylindole (DAPI, D1306, Invitrogen™) at 1 µg/ml was applied for 1 hour, before mounting coverslips using Dako mounting medium (S302380-2, Agilent). Information on antibodies is available in Chapter 2: Measurement of protein biomarkers. In Figure 9, we present an example of a dermal fibroblast image (from dataset B), with a grayscale visualisation of the corresponding Ki67, γH2AX, and DAPI channels (FINS denotes these as channels 1, 2 and 3 respectively). There is also an overlay image showing how the nuclear proteins (Ki67 and γH2AX channels) are co-localised with the nucleus (DAPI channel).

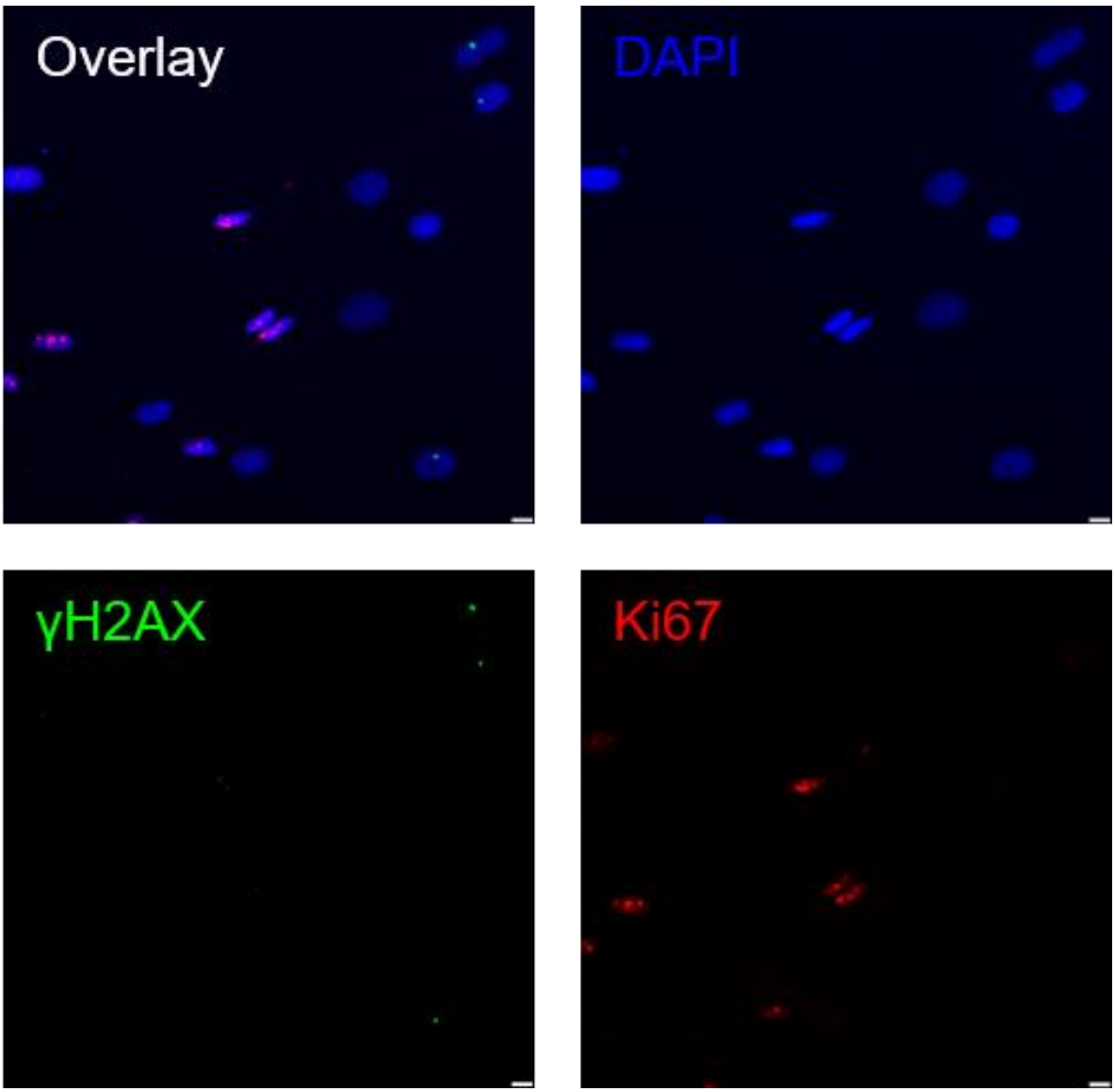

Figure 9: An example of an input image from set B. Note the image is a cropped section and is in false colour to aid visualisation. The four panels show the overlay and the different channels: (top left) Overlaid image, (top right) DAPI staining, (bottom left) γH2AX staining, and (bottom right) Ki67 staining. The scale bars denote 10 µm.

Manual counting techniques

We have access to manual counting data for seven users. However, only five worked on sets A and C, with users 6 and 7 working on set B as well. As expected, there

was a variety of methods used by the different researchers for counting. Five of the researchers did not export any images and stayed using the LASX software and its user interface to visualise the different channels and manually identify co-localised cells. Four of these researchers used the LASX software annotation tool to count and identify cells that had been counted, whilst the other kept mental track of both. One researcher exported images as .tiff files in false colour, opened them in basic image viewing software on a tablet computer, identified the cells with staining for a protein of interest by their false colour, and used a freehand drawing tool to check off cells after counting. They kept track mentally of the ongoing counts. One researcher exported images as .tiff files in false colour and opened them in ImageJ 1.47v software (US National Institute of Health, Bethesda, Maryland, USA) and then used the cell counter plugin to keep count of cells [218]. All researchers recorded their counts by typing them into a spreadsheet. When timing counts, the stopwatch was started when the image in question was open and ready for counting, and stopped after the researcher had finished typing their counts for that image into the spreadsheet.

Proposed Method: FINS algorithm

The FINS algorithm is a script created using Matlab software version R2017b. It is designed to quantify the number of nuclei in the DAPI channel and the number of nuclei containing any signal in the Ki67 and γH2AX channels. A researcher would download the folder containing FINS, move their .lif or .tiff files into the folder for

counting, open the script in Matlab and press “Save count”. After computation has finished, a simple, intuitive user interface enables the researcher to see how FINS has counted any image in the dataset. After reviewing the data if they wish, the researcher saves the count on the user interface which generates a timestamped output .csv file containing image names and all counts for each channel.

The FINS algorithm works by initially computing the nuclear regions and then counting signal within this segment for the protein of interest. To compute the nuclear regions, we use a convex segmentation approach using a fitting term based on a thresholding of the image. It is designed to mimic the manual counting processes currently applied. We then iteratively search these regions in the Ki67 and γH2AX channels based on thresholds calculated from the image data. In the following we refer to the image data from the DAPI, Ki67, and γH2AX channels as: $z_\delta(x)$, $z_\chi(x)$, and $z_\gamma(x)$ respectively and we normalise them such that the intensities are scaled between 0 and 1. This allows for parameters to be defined in a consistent manner.

Nuclear Region Computation

When manually counting nuclei in the DAPI channel the task is essentially a thresholding problem: count any segment where the fluorescence intensity is above a certain threshold. However, for the γH2AX and Ki67 counts, we also need to compute boundaries of the counted DAPI regions. This presents two problems in the context of automating this procedure. The first is how to automatically select the

threshold such that the algorithm can perform consistently across different cell types or multiple image types etc. The second, more challenging issue, is how to account for noise in the image. The process that determines the boundaries of the nuclei in the DAPI channel is crucial as these regions are used to find proteins within the Ki67 and γH2AX channels.

We use a segmentation method, based on a variational approach, to partition the image into two regions: foreground (nuclei) and background. Generally, in the continuous setting, for an image $z(x) \in [0,1]$ in the domain $\Omega \subset R^2$ the task is to compute disjoint subregions Ω_1 and Ω_2, such that $\Omega_1 \cup \Omega_2 = \Omega$, based on some partitioning criteria on the data $z(x)$ [219]. In this setting, we construct a data fitting term using the optimal threshold t_δ based on Otsu thresholding [220]. To select this parameter, we divide the histogram of image intensities into two regions. This approach is an automatic clustering method which determines an optimal threshold value to minimise intra-class variance. This has been implemented efficiently in Matlab with the function 'multithresh'. We utilise the convex relaxation approach of Chan *et al.*, and Goldstein and Osher, where a binary labelling of the foreground and background is determined based on minimising the following energy functional: [221,222].

$$\min_{u \in \{0,1\}} \left\{ \int_\Omega g(x) |\nabla u(x)| \, dx + \lambda \int_\Omega f(x) u(x) \, dx \right\} \quad (1)$$

This involves total variation (TV) regularisation weighted by an edge function, $g(x)$, and some data fidelity term, $f(x)$. Equation (1) is a formulation that is designed to assign zeros ('background') and ones ('foreground') to each part of the image, such that the total value of the terms is minimised. The data term explicitly connects the functional to the image data and the TV term promotes smooth interfaces in the solution. Minimisation of this energy with respect to u is a well understood problem. One possibility is to relax the binary constraint such that intermediate values of $u(x)$ are permitted [221,222]. Given that we are looking to find a regularised version of a thresholding procedure we define an intensity fitting term in (1) as follows:

$$f(x) = f_\delta(x) = t_\delta - z_\delta(x) \tag{2}$$

where $z_\delta(x)$ is the image data in the DAPI channel. Edges are not particularly well defined in this context, such that we can set $g(x) = 1$. According to these choices, the problem then consists of a two-phase variational segmentation problem that we consider in a conventional manner, relaxing the constraint on u, defined by:

$$\min_{u\in[0,1]} \left\{ \int_\Omega |\nabla u(x)|\, dx + \lambda \int_\Omega f_\delta(x) u(x)\, dx \right\} \tag{3}$$

Here, the difference between (1) and (3) is that $g(x)$ and $f(x)$ have been defined, and the problem is now convex. This allows a global minimiser to be found. In this case we use the Split-Bregman approach to compute a minimiser [222,223]. Many

alternative methods are applicable in this case, such as the dual formulation or Chambolle and Pock's algorithm [224–227]. We do not detail them here as the numerical methods are not the focus of this work. We have found that the fastest method to obtain a solution is to define the initialisation, $u_0(x)$, as follows, as this is in close proximity to the global minimiser of (3) by definition.

$$u_0(x) = \begin{cases} 1, & \text{for } x \in f_\delta(x) < 0 \\ 0, & \text{for } x \in f_\delta(x) \geq 0 \end{cases} \quad (4)$$

However, we note that for fixed $f_\delta(x)$ the solution is independent of initialisation. We fix the value of the fitting parameter, $\lambda = 20$, as we have found it to be appropriate for images of this type. We define the solution as $u^*(x)$. Based on the work of Chan *et al.*, Bresson *et al.* and others, this will be approximately binary, such that any thresholding of the function will be a global minimiser of the original problem [221,224]. We define the computed foreground region as follows:

$$\Omega_D = \{x \in \Omega | \, u^*(x) > \beta\} \quad (5)$$

We select $\beta = 0.5$ (although other values, such that $\beta \in (0,1)$, would yield a similar result). In the following we use the binary form of the solution, u^*, denoted Ω_D, to compute the counts of the nuclear proteins. The definition of (5) refers to the areas of the DAPI channel that are considered nuclei.

Nuclear Protein Counts

To simulate the manual counting procedure, we use the region calculated in the previous section, Ω_D. This region will provide a space in which we can search for signal from nuclear proteins. However, unlike DAPI, we do not need to compute the regions of positive Ki67 or γH2AX signals. Instead, we only need to count the nuclei with signal present. We treat the Ki67 and γH2AX channels in an identical way, but describe the method here in general terms using Ki67 as our example. For this channel, we refer to the image data as $z_\chi(x)$. Using Otsu's method, we determine a threshold t_χ on the entire image. For each disconnected region $\Omega_D^i \in \Omega_D$, we determine whether $z_\chi(x) > t_\chi$ for any $x \in \Omega_D^i$. If so, this nucleus is considered to be positive for Ki67. If not, then it is negative for Ki67 (illustrated in Figure 10). This is calculated for $i = 1, \dots, n$, such that the maximum count for Ki67 is n (i.e. the total number of nuclei calculated by the process of determining the nuclear regions in the DAPI channel). For cases where Otsu's method does not provide an adequate threshold, we found it optimal to define a floor on the parameter t_χ such that $t_\chi = t_f = 0.1$. This process is repeated for the γH2AX channel (with $z_\gamma(x)$ and t_γ).

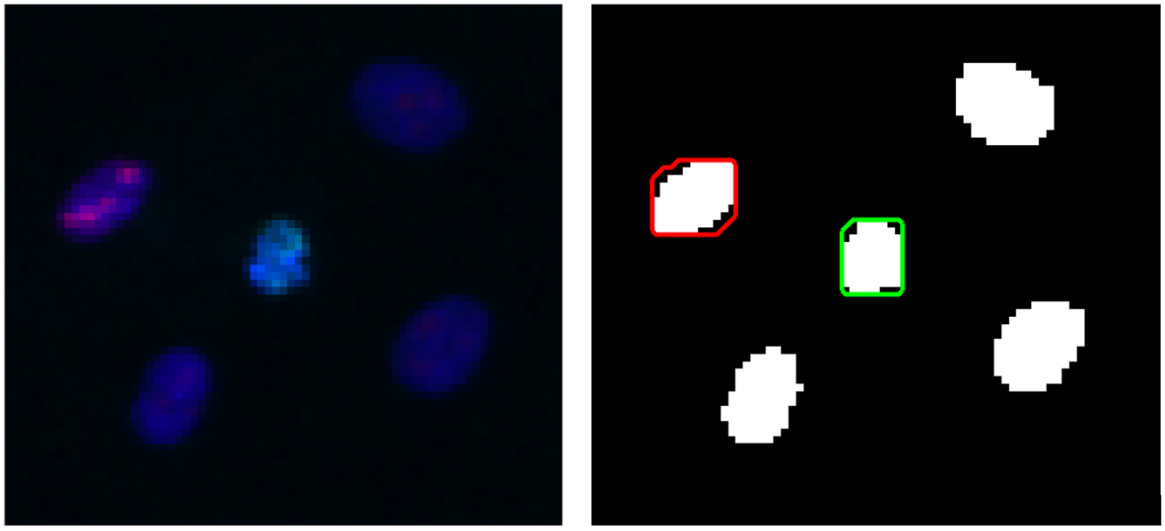

Figure 10: Example of the FINS processing. (Left) cropped overlay image from set B. (Right) corresponding FINS output. Binary regions represent Ω_D indicating five nuclei in this region. Red and green contours indicate Ki67 and γH2AX signal (respectively) which is contained within a nucleus.

Discussion of experimental results

In this section we present results for the proposed algorithm, FINS, compared with the manual counts of researchers 1 - 7 (where available). We are interested in two aspects of the results of the proposed algorithm: the reliability of the counts for each channel in comparison with the manual data, and the improvement in time taken to compute a result. The results consist of three distinct datasets, which we call sets A, B, and C respectively. Set A consists of images 1 - 10 (human primary endothelial cells; HAoECs), Set B consists of images 11 - 20 (human primary dermal fibroblasts; HDFs), and Set C consists of images 21 - 30 (human primary chondrocytes; HCHs). For each image, we have a manual count from the Ki67, γH2AX, and DAPI channels. Researchers 1 - 5 provided counts for all three sets, and researchers 6 and 7 provided additional counts for Set B. We also have data on the time taken to count each image for Set A from researchers 1 - 4. Counts from the FINS algorithm can be reviewed with the user interface, but for more rigorous comparison the counts computed by FINS are not reviewed or adjusted by any researcher.

Count Comparisons

We present a visualisation of the results in Figure 11, Figure 12 and Figure 13. Each figure displays every manual count for each dataset as well as the result achieved by the proposed algorithm. The results are split into Ki67, γH2AX, and DAPI counts. The count computed by the algorithm is connected by a dashed line to distinguish it from the rest of the data.

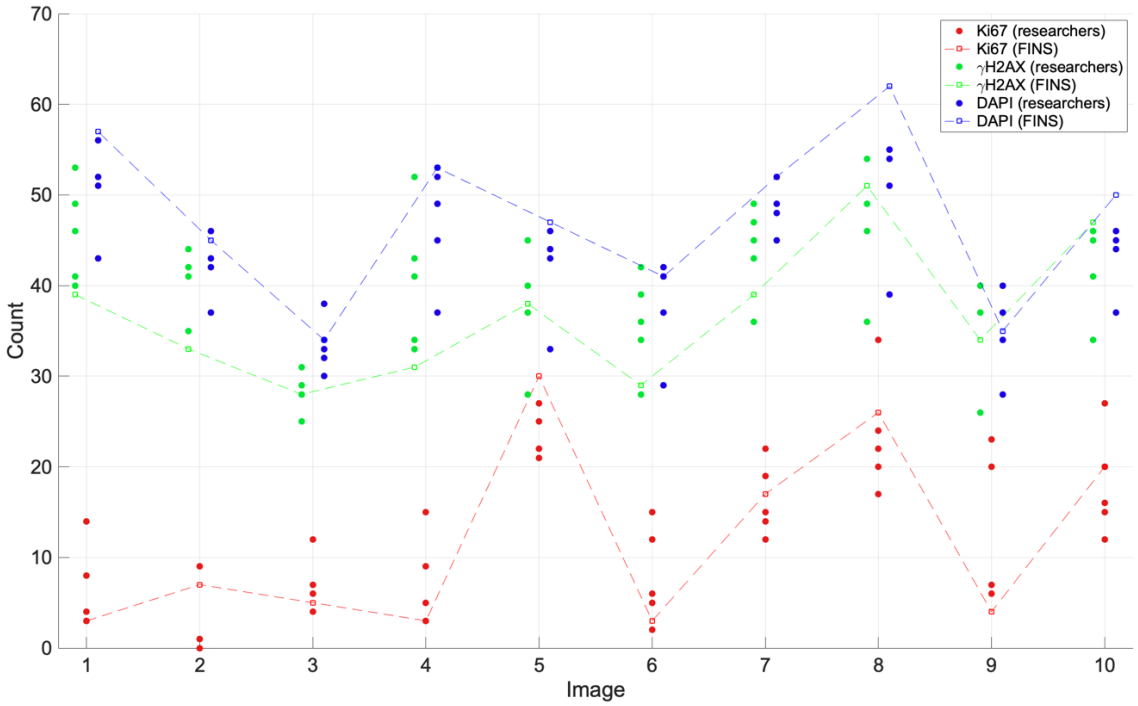

Figure 11: Ki67, γH2AX, and DAPI count results for set A. Algorithm counts are joined by a dashed line for clarity.

Figure 11 concerns set A. It should be noted that the FINS algorithm tends to be at the higher end of the range of the researchers for the DAPI channel, but this appears acceptable and mitigated for in context. For images 1, 5, 8, and 10, the FINS count is higher than the maximum of the researcher counts. For images 1 and 5 this is a small difference, with FINS being 1.79% and 2.17% over the maximum researcher count. However, for image 8 it is 12.7% over, and for image 10 it is 8.7%. For image 8, the researcher counts' range is 39 - 55, with FINS computing 62. The algorithm is closer to the counts of Researchers 1, 2, 3 and 5 (DAPI = 55, 51, 54, and 51 respectively) than Researcher 2 is to the others (DAPI = 39). In this image, there are a lot of borderline cells meaning the researcher counting 39 nuclei is probably using a subjective method, perhaps omitting cells that are at the border of the image. In contrast, FINS is overcounting

likely due to some detritus in this particular image. In this particular biological application within our field of research, nuclear size can often vary considerably within an image of the same cell type. Senescent cells can exhibit polyploidy with very large nuclei as a result, and any cells undergoing mitosis can give condensed small nuclei [68]. Therefore, to enable successful counts of these differently sized nuclei, there is an unavoidable risk of some cell detritus being counted. However, the FINS user interface allows for post-analysis inspection to mitigate this issue. For image 10, FINS is closer (DAPI = 50) to the counts of Researchers 1, 2, 3 and 5 (DAPI = 46, 44, 45, and 46 respectively) than Researcher 2 is (DAPI = 37). In context, this demonstrates that FINS is similar to the manual counts. Ki67 is within the range of the researchers' counts for 80% of images. For γH2AX cells, three images are below the range of researcher counts: image 1 is 2.5% below, image 2 is 5.71%, and image 4 is 6.06% (image 10 is above the range by 2.17%). These are relatively small differences, but we should note that when combined with the minor over-counting for DAPI this could have implications for the conclusions from the data, i.e. the ratio of cells stained for γH2AX to DAPI may be lower than the true percentage due to the γH2AX undercount and DAPI overcount. If this is an unacceptable margin of error to a researcher, then it is easy to mitigate against by using the user interface's review window.

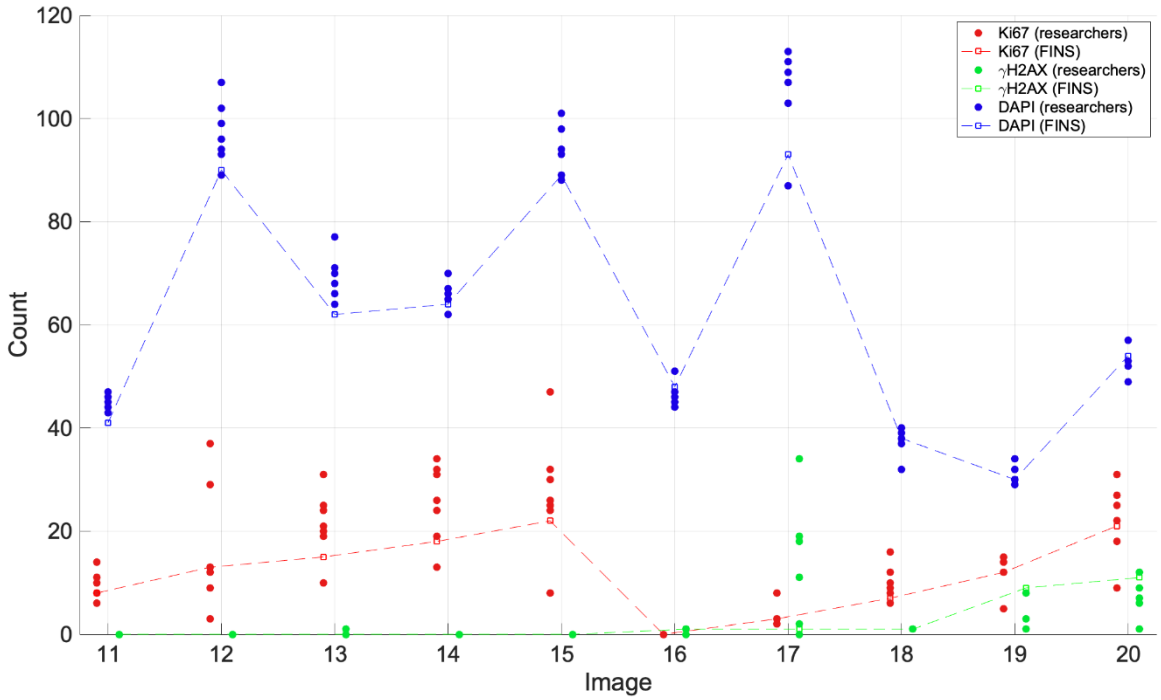

Figure 12: Ki67, γH2AX, and DAPI count results for set B. Algorithm counts are joined by a dashed line for clarity.

Figure 12 shows the results for set B. FINS appears to perform comparably with the manual counts. For Ki67, FINS is within the range of researchers count for all images. For γH2AX, FINS is within the range for 90% of images. The minor trend of over-counting in the DAPI channel in Set A does not seem to have been repeated here in Set B as FINS is within the researcher count range for 80% of images and is under the mean count seven times and over three times. It should be noted that for this data set, we have an additional two users providing manual counts. The Ki67 and γH2AX numbers are very low for set B which creates a large potential for unreliability (even a small amount of over-counting would be very significant here), but FINS appears to be reliable when the number of cells in a channel is low. For the γH2AX data, there are four images (11, 12, 14, 15) where all users agree that there are no cells present, and FINS also computes a zero for these cases which is very encouraging.

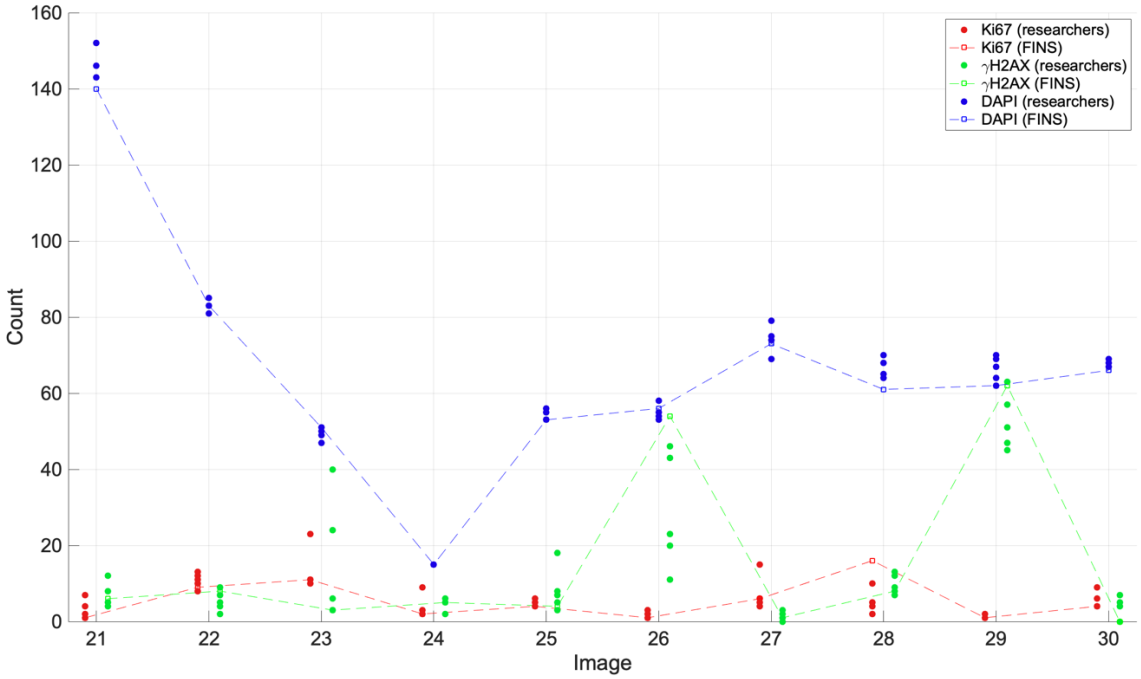

Figure 13: Ki67, γH2AX, and DAPI count results for set C. Algorithm counts are joined by a dashed line for clarity.

We also have encouraging results for set C, shown in Figure 13. For Ki67 and γH2AX, the FINS results are within the researchers' count range for 90% of images. As previously discussed, variation between images can have many reasons such as the image capture settings, so it may be that the minor over-counting trend in the DAPI channel in Set A was as a result of the nature of the images, as this trend is not observed in Set B or Set C. For DAPI, again, there is no trend to over-count (FINS is under the mean count six times, over twice, equal twice), but only 70% are within the researchers' range. However, it is clear that there is broad consensus between the algorithm and the users (image 24 even has all agreeing precisely). Expressed as percentages of the mean, the researcher counts show a range of 6.09% for image 21, 9.04% for image 28, and 2.96% for image 30. For these three cases the FINS results are only slightly below the lowest count (3, 3, and 1 respectively): FINS computes a count which

is 94.7% of the mean count for image 21, 91.9% for image 28, and 97.6% for image 30. On the whole the algorithm is consistently accurate for each channel.

Counts from each channel are not useful in isolation, so we now investigate the performance of the algorithm in the context of these connections. We introduce a quantitative measure of count similarity when Ki67 and γH2AX counts are related back to the DAPI count. In Figure 14 and Figure 16, we plot count data for DAPI versus Ki67 (set B) and γH2AX (set C) respectively. This shows a visual representation of how FINS counts compare against the researcher counts for these datasets. For each image we compute the centroid of the researchers' counts and calculate the distance each researcher's count is from this point. We can then use the maximum of these distances to give a quantitative measure of concordance. The percentage concordance for FINS is then defined as the percentage of instances when the algorithm's count distance from this centroid is below the maximum of the researchers' distances. We can calculate a similar metric for each researcher, e.g. percentage concordance for Researcher 1 would be based on distances from a centroid computed using counts from Researchers 2 - 5. We should note that this does give FINS an inherent slight advantage with this metric as FINS compares against five counts (whereas the researchers compare against four counts) and the maximum distance (hence percentage concordance also) is likely to increase slightly when more counts are present. Nonetheless, it gives us a measure of the extent to which the algorithm counts are similar to the researchers' counts. The results are presented in Table 6, Figure 15 and Figure 17.

Table 6: Percentage concordance comparison between FINS and researcher counts. Percentage concordance is the percentage of instances that the counter's results were outside the range of the other counter's results. The results are based on association with either of the two proteins of interest and the DAPI count.

Counter	Percentage concordance	
	γH2AX and DAPI	Ki67 and DAPI
Researcher 1	73.3	80.0
Researcher 2	70.0	76.7
Researcher 3	83.3	80.0
Researcher 4	20.0	16.7
Researcher 5	83.3	83.3
FINS	80.0	86.7

The results from Table 6 support the idea that FINS count performance is similar to that of the researchers. A percentage concordance of 86.7 for DAPI versus Ki67 counts is higher than any of the researchers. For DAPI versus γH2AX counts the percentage concordance is 80, with only Researchers 3 and 5 higher, at 83.3. Figure 15 and Figure 17 show how these results are calculated for FINS. The blue line here is the distance of the FINS count from the centroid of the researchers' counts. The maximum distance of the researchers' data is indicated by the red line (the range is shaded grey). Here, we can visualise to what extent the count data agree. It is worth stating that the maximum distance tends to be higher for set B due to having additional researcher data. When FINS is above this maximum distance, this is not to say that it is unacceptable in these cases. In the same way a researcher count being furthest away from the centroid doesn't invalidate their data, FINS occasionally (as shown by the percentage concordance) being furthest away is not a negative. In fact, with the algorithm designed to function like a researcher count, we would expect it to be sometimes furthest away from the centroid.

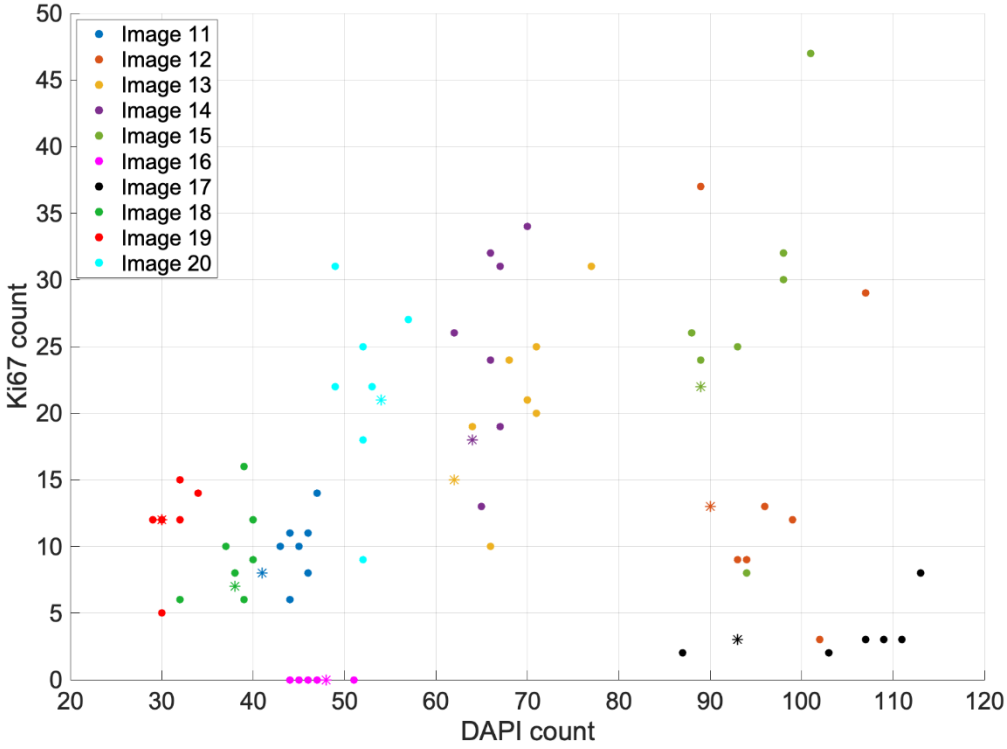

*Figure 14: DAPI versus Ki67 counts for set B. FINS count indicated by a *.*

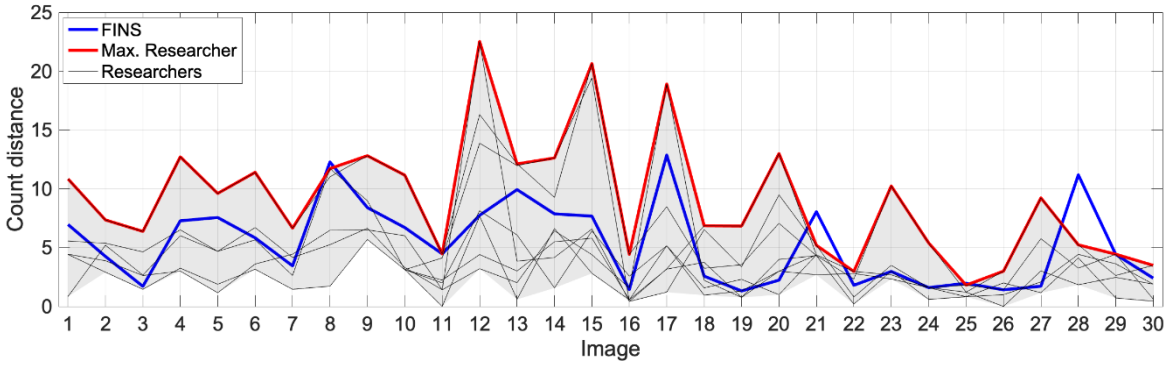

Figure 15: Distance from the centroid of the Ki67 and DAPI results from other counters. The maximum distance from the centroid of all researchers' results is indicated in red. The distance from the centroid for the results from FINS is indicated in blue.

We now include a visualisation of the results that highlight the relationship between DAPI and Ki67 counts; Figure 14 shows the results for set B. It allows us to observe to what extent the results of the algorithm 'cluster' with the manual counts using an important biological metric. Figure 14 shows that images 12, 13,

14, and 15 have data that is quite spread (although it should be noted that there are seven researchers' counts for this data). This demonstrates the inherent variability in the data, highlighting the challenge of counting the cells consistently. We can see that the algorithm performance in these cases is reasonable based on the distances in Figure 15, where FINS is below the maximum distance. For the remaining images, where the data is more clustered, the results are very strong. Over image sets A, B, and C there are four cases where FINS is above the maximum distance. For images 8 and 21 they are over by less than 1. Images 21 and 28 are 2.85 and 5.95 respectively over the maximum distance. For image 28, the researchers' range for DAPI is 64 - 70, and for Ki67 is 2 - 10. The FINS count here is DAPI = 61, Ki67 = 16. This particular image has 11 cells that are cropped by the border of the image. It is subjective as to whether or not to count them and, in this case, it appears most researchers have counted them. However, FINS has not counted them as the signal from them is not likely to have exceeded the threshold in the same way as the other cells in the image. This is arguably preferable because if a full nucleus can't be observed and no nuclear protein staining is seen, we can't be sure if the nuclear protein is stained but is located outside of the image border. Whilst the undercount of DAPI is acceptable, its appearance in tandem with the Ki67 overcount could be of concern. However, the Ki67 overcount appears to be explicable as the result of high levels of autofluorescence. High levels of background autofluorescence are discussed previously, and whilst FINS may not be able to deal with such irregularity in an image as well as a researcher could, it is more likely to be consistent when faced with a difficult image, and the risk of this is mitigated by the ability to review data with the user interface.

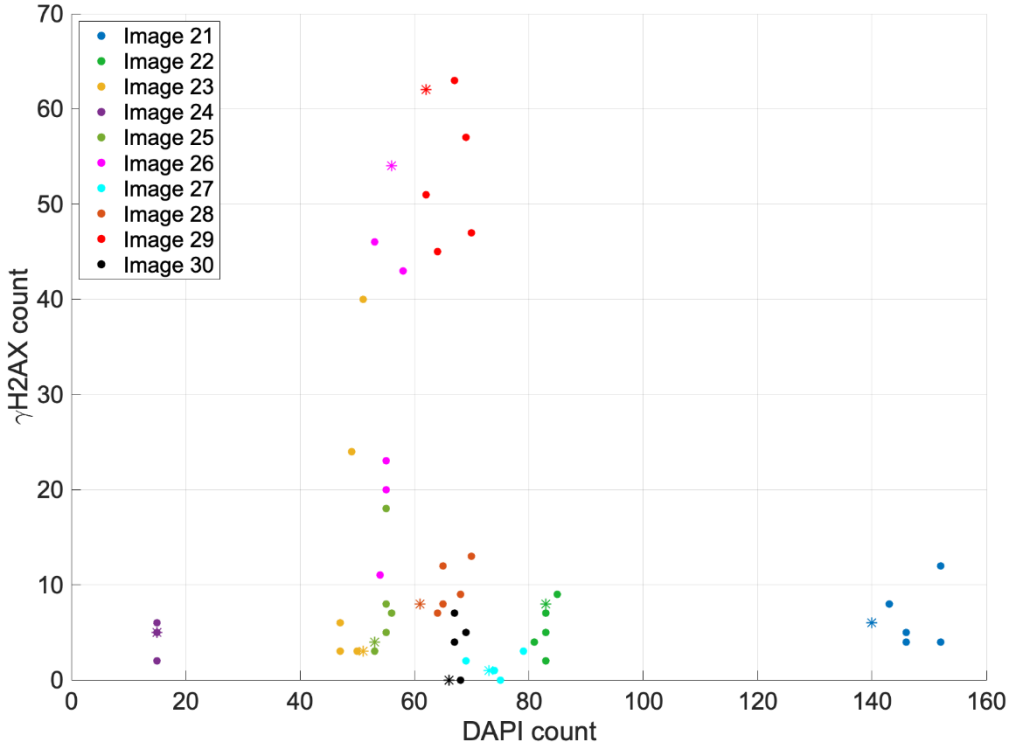

*Figure 16: DAPI versus γH2AX counts for set C. FINS count indicated by a *.*

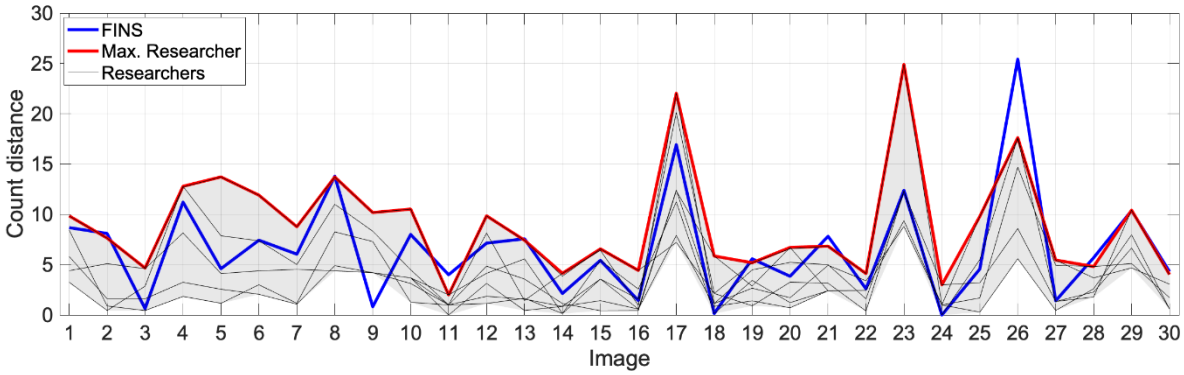

Figure 17: Distance from the centroid of the γH2AX and DAPI results from other counters. The maximum distance from the centroid of all researchers' results is indicated in red. The distance from the centroid for the results from FINS is indicated in blue.

We also have a similar plot for DAPI versus γH2AX counts for set C, shown in Figure 16. Again, this is useful because it allows us to assess the similarity of the counts between manual acquisition and the proposed algorithm. Here, we can see that the FINS count clusters very tightly with the manual counts for the majority of images, confirmed by the distances in Figure 17. These figures allow

us to see clearly that the algorithm is very consistent for DAPI in these cases. Overall, the trend is very similar to the DAPI versus Ki67 comparison above. It is difficult to distinguish the algorithm's performance from the manual data. There are anomalous cases, but this is true for the researchers' data as well. For DAPI versus γH2AX (Figure 16), there are six cases where FINS is above the maximum distance. Images 2, 8, 21, 28, and 30 are less than 1 over the maximum distance, indicating a trivial difference. However, image 26 is 7.79 over the limit. We can see from Figure 17 that there is a near-consensus in the DAPI count (the FINS count is within the range of researchers' counts), indicating that the error is primarily in the γH2AX count which is 54 for this image (the range of the researchers here is 11 - 46). However, FINS is closer to the counts of Researchers 1, 3, 4, and 5 (mean count = 33) than Researcher 2. This particular image has high levels of background autofluorescence meaning that it has inherently more subjectivity over which cell can be identified as being stained for γH2AX. This causes the wide variation in user counts, but arguably proves the need for the algorithm: by its nature it is more likely to behave consistently than researchers when faced with difficult images. Overall, these visualisations provide further support for the reliability of FINS.

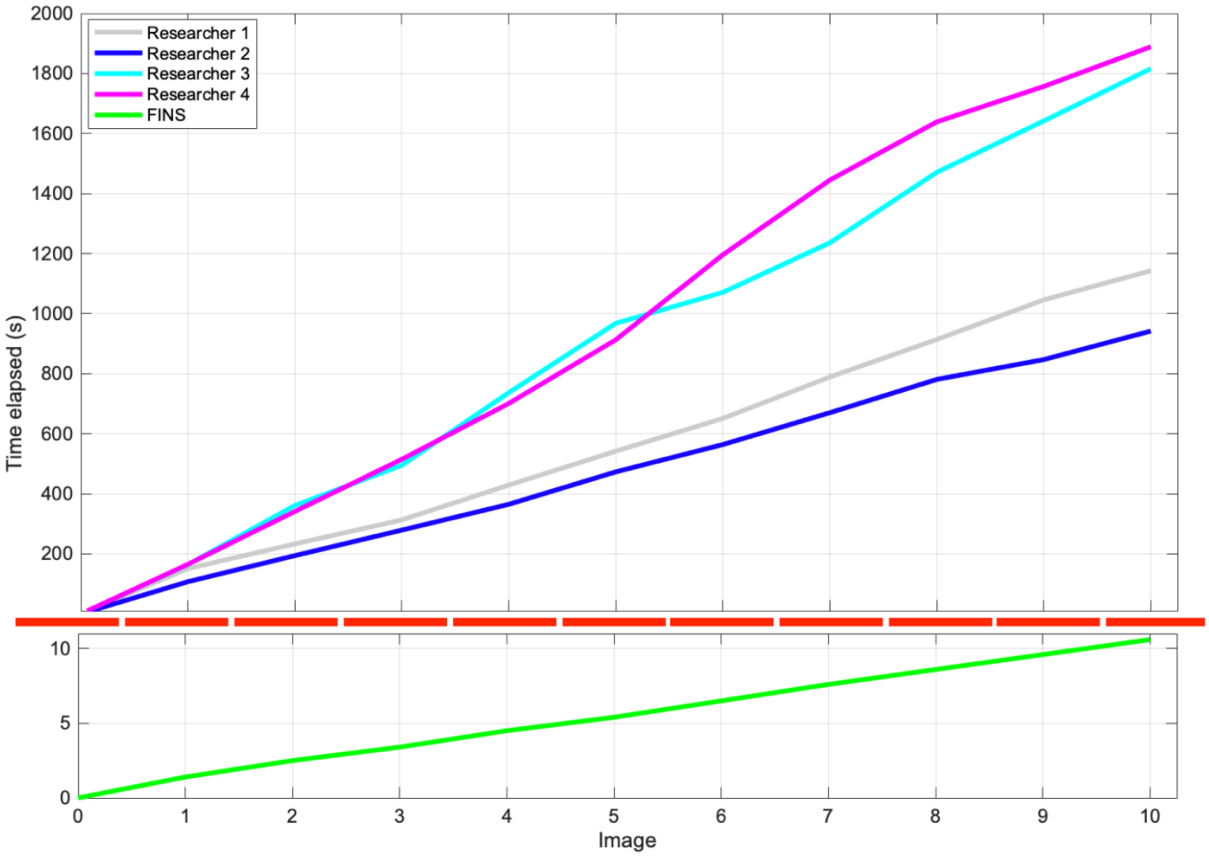

Figure 18: The FINS algorithm is much quicker than the researchers in its time in seconds taken to analyse ten images from set A. Red dashed line indicates a break in the y-axis.

Table 7: Mean cell count and time spent counting per image in seconds for set A. Each researcher counted ten images (n = 10).

Counter	Mean count per image			Mean time per image (s)
	Ki67	γH2AX	DAPI	
Researcher 1	12.1	21.0	60.0	104
Researcher 2	11.1	18.0	57.6	84.7
Researcher 3	9.40	17.9	59.3	164
Researcher 4	16.3	18.3	58.6	189
FINS	9.70	18.1	58.2	1.06

The main advantage of replacing manual counts with an algorithm is the time saved on acquiring the data. In Table 7, we present the mean time taken to manually count an image, which ranges from 84.7 seconds to 189 seconds. This

is a significant drain on time and resources given image datasets in this field are often large and the count data is crucial to drawing meaningful conclusions. Although we present a small dataset here, experimental datasets are often significantly larger. For example, the average number of images per dataset produced by one researcher was 195 images. This would correspond to 4 hours and 35 minutes if the researcher was (unrealistically) able to continuously count non-stop at the fastest researcher's normal speed. A dataset of that size would more realistically take a few working days to complete. All researchers were instructed to follow their normal procedure, whilst timing the duration from beginning to count the cells to inputting the data on a spreadsheet for set A. The counts were taken concurrently, but not necessarily continuously. It is worth noting that the counting time for this dataset was of reasonable duration to allow an individual to retain focus. It is likely that with a larger dataset, the time per image would increase and/or time for a break would have to be included. Despite only having data for set A, it is certainly enough to give an impression of how long manual counts take for this type of data. A key advantage of using an algorithm is to reduce the workload of the users, giving more time for analysis over acquisition. This does imply that the computation time of the algorithm is irrelevant; the user can run the algorithm and return to inspect the results at a later time. However, this is not the ideal approach in this case. Our aim was to create a framework where the results could be supervised in near real time, such that the counts could be efficiently and reliably acquired. There was therefore a requirement to keep the computation time per image as low as possible.

We can see from Table 7 that the mean time per image for the algorithm is 1.06 seconds. Figure 18 shows this in comparison to researchers 1 - 4, with a split axis used because of the scales involved. It shows the variability of the time taken for each user and emphasises the difference between the algorithm and counting cells manually. These results are very positive in the sense that the algorithm takes approximately 1% of the time a manual process takes. Coupled with the accuracy performance discussed above, this is a potentially transformative development. Batches of images that would take hours to process now take minutes to get a result automatically.

Conclusions

The algorithm demonstrates that its accuracy is comparable to that of manual counting. It is more consistent and less subjective than manual counting due to the nature of the algorithm. When examining small biological effects, they can be masked by variability caused by inconsistencies in the method of counting stained cells. The algorithm can reproduce its counts and is able to apply the same parameters to each image, unlike researchers who are inherently more variable in their counting approach. The algorithm also allows for better comparison between datasets; all datasets must be counted by the same researcher in order to make the same comparison, which is often unfeasible. The algorithm's time savings represent a key benefit in themselves. The time savings could also allow researchers to perform more experiments/replicates or image more cells, which could provide greater statistical power for the identification of any small biological differences in an experiment. This algorithm could also be applied to other nuclear fluorescent stains. While other custom pipeline programs, commercial programs or algorithms may exist that could be adapted to produce similar results, we believe this algorithm to be useful as it is quick, easy, simple and free to run, with the ability to review images if needed. These qualities make it attractive for a non-programmer specialist/general laboratory scientist over manual counting and other alternatives.

Acknowledgements

The authors would like to thank the following researchers who aided with image analysis in this study: M Davies, Dr N Jeffery, Dr B P Lee and J M Sinclair.

Sources of Funding

This work was generously supported by the Wellcome Trust Institutional Strategic Support Award (204909/Z/16/Z) and Animal Free Research UK (AFRUK). No reagents containing animal-derived biomaterials were purchased with AFRUK funding.

Author Contributions

LRB designed the experiment, performed laboratory work, data analysis and prepared the manuscript. JS created the algorithm, analysed data and prepared the manuscript. RF and EM performed laboratory work and helped prepare the manuscript. LWH provided overall oversight and helped prepare the manuscript.

Conflicts of Interest

Professor Harries is an inventor on patent PCT/GB2019/052125, and is a founder, chief scientific officer and research and development lead for SENISCA, Ltd. Ms Bramwell, Dr Spencer, Mr Frankum and Mr Manni have no financial interest to declare in relation to the content of this manuscript.

Chapter 4: Senescence, alternative splicing and effects of trametinib treatment in progeroid syndromes.

The hallmarks of cellular ageing are well characterised, but evidence points to splicing factor dysregulation as another such hallmark. Following the trail of evidence in support of splicing factor dysregulation as a hallmark of ageing, we turned to diseases of premature ageing, the progeroid syndromes. Here I present a draft of a journal article prepared for submission to Geroscience in collaboration with Professor Lorna Harries. The author contributions are detailed in the confines of the article. Again, for the purposes of this thesis, I will detail my exact contributions. I conducted literature reviews, designed the experiments, conducted all laboratory work, conducted all data analysis, prepared all figures and tables for the presentation of data, interpreted data, structured the manuscript, and wrote the majority of the manuscript.

Senescence, alternative splicing and effects of trametinib treatment in progeroid syndromes

Laura R Bramwell[1] & Lorna W Harries[1]*

[1]RNA-Mediated Mechanisms of Disease group, College of Medicine and Health, Institute of Biomedical and Clinical Science, University of Exeter

*corresponding author

Correspondence address:

Professor Lorna W Harries
Institute of Biomedical and Clinical Sciences
University of Exeter College of Medicine and Health
RILD Building
Royal Devon and Exeter Hospital
Barrack Road
Exeter
Devon
EX2 5DW
United Kingdom

Correspondence email: L.W.Harries@exeter.ac.uk

ORCID numbers: LRB - 0000-0003-4069-3959, LWH - 0000-0001-7791-8061

Twitter: @miRNAgirl, @LauraBramwell1, @TeamRNA

Abstract

Progeroid syndromes, like Hutchinson-Gilford Progeroid Syndrome (HGPS), Werner syndrome and Cockayne syndrome, result in severely reduced lifespans and premature ageing. Normal senescent cells show splicing factor dysregulation, which has not yet been investigated in syndromic senescent cells. We sought to investigate progeroid syndrome cell cultures' senescence characteristics and their splicing factor expression profiles. Normal cellular senescence can be reversed by application of the senomorphic drug, trametinib, so we also investigated its ability to reverse senescence characteristics in syndromic cells. We found that progeroid cells were significantly more senescent but did not always have differences in levels of proliferation, DNA damage and apoptosis. Splicing factor gene expression appeared dysregulated across the three syndromes. 10 μM trametinib reduced senescence and affected other aspects of the senescence phenotype (including splicing factor expression) in HGPS and Cockayne syndromes. Werner syndrome cells did not decrease in senescence. Splicing factor dysregulation in progeroid cells provides further evidence to support this mechanism as a hallmark of cellular ageing. It also highlights the use of progeroid syndrome cells in the research of ageing and age-related disease. This study suggests that senomorphic drugs such as trametinib could be useful as a therapy for progeroid diseases.

Keywords:

Progeria, human, ageing, dermal fibroblast, senescence, splicing factor

Introduction

The human ageing process is complex and occurs over decades, but insight can be gained by studying the rare monogenic conditions that result in vastly accelerated rates of ageing [228]. These conditions often result from errors in the gene regulatory or DNA damage response machinery and are collectively termed progeroid syndromes. Despite often being extremely rare, the syndromes are life-changing and can be fatal [33,229]. Some of the most studied progeroid syndromes are Hutchinson-Gilford Progeria syndrome (HGPS), Werner syndrome (WS) and Cockayne syndrome (CS). These are rare disorders affecting an estimated 1 in 18 million live births for HGPS and 1 in 200,000 for both WS and CS [229–232].

HPGS is caused by mutations in the Lamin A (*LMNA*) gene that result in a truncated Lamin A protein termed progerin [233]. The genetics of WS is also well defined, with the syndrome caused by mutations in the Werner (*WRN*) gene which encodes the DNA helicase, Werner protein [231]. CS is more genetically and phenotypically diverse, with several subtypes across a spectrum of distinguishing phenotypic features; CS type I (moderate disease/classical phenotype), type II (severe or early-onset), type III (mild), photosensitivity only (adult onset) and cerebraloculofacioskeletal syndrome (COFS; severe, foetal onset) [232,234]. No correlation has yet been found linking the phenotypic subtypes with two known genetic mechanisms of Cockayne syndrome: CS type A and B. The two genetic causes correspond to mutations in excision repair genes *ERCC8* (Cockayne syndrome A) or *ERCC6* (Cockayne syndrome B) [232,234].

All of the three syndromes share common features of accelerated ageing and significantly higher risks of age-related diseases such as cardiovascular disease, cancer, diabetes and chronic kidney disease [33,235,236]. However, the severity of phenotypes between HGPS, WS and CS do demonstrate differences. The defects in *LMNA*, *WRN* and *ERCC6/8* seen in HGPS, WS and CS, respectively, all cause major instability of the nuclear envelope and large scale unrepaired genomic damage, resulting in major curtailment of average lifespan to 14.5 years for HGPS and 54 years for WS [33,231,236,237]. The severity of CS affects the observed mean lifespan across the different phenotypic subtypes. People with CS type I have a mean lifespan of 16.1 years, those with CS type II have a mean lifespan of 5 years, and those with type III have a mean lifespan of 30.3 years [234]. In this study, we examine the mildest subtype, CS type III, which enables a contrast with two more severe syndromes: HGPS and WS. The CS type III subtype is generally milder with patients given an expected lifespan of 10 - 30 years and milder symptoms of accelerated ageing, although they remain abnormally sensitive to UV-induced DNA damage [232,234]. Despite their monogenic cause, the molecular features of ageing observed in progeroid syndromes are similar to those seen during normal ageing. Assessment of potential therapeutics to slow rates of ageing (senotherapeutics) in progeroid syndromes may indicate interventions with efficacy against common, chronic ageing diseases in the wider population.

There are several theories as to how and why we age. Evidence is mounting that the physiological and functional changes that occur during the ageing process arise from the gradual failure of a series of basic health maintenance mechanisms. These mechanisms are termed the hallmarks of ageing, which are also major drivers of

age-related disease [21,22]. Hallmarks include genomic instability, epigenetic alterations, mitochondrial dysfunction, altered intercellular communication, deregulated proteostasis, deregulated nutrient sensing, telomere attrition, stem cell exhaustion, dysregulated RNA splicing, compromised autophagy, altered mechanical properties, disturbances to the microbiome, inflammation and cellular senescence. They are present in normal ageing in multiple species, and underpin many of the common chronic diseases of human ageing [22]. Importantly, the hallmarks of ageing represent promising avenues for therapeutic targeting of the diseases of ageing. This is exemplified by observations that targeted depletion of senescent cells leads to increases in multiple healthspan and lifespan-related parameters in animal ageing/progeria models [73,75,238]. In smaller studies, targeted reduction of senescence can affect the phenotype of idiopathic pulmonary fibrosis and diabetic kidney disease in humans [149,150].

More recently, dysregulation of mRNA splicing has been proposed as a new hallmark of ageing, since it is known to be associated with normal human ageing [21,27,239,240]. mRNA splicing is a carefully controlled mechanism by which our genes can produce many different mRNA transcripts [52]. It is controlled by a portfolio of splicing factors which are themselves regulated by alternative splicing; splicing factors are proteins which act on the gene to influence a change in the splice site of a pre-mRNA transcript. In line with its recent designation as a novel hallmark, splicing factor dysregulation occurs during normal ageing in multiple species, its experimental aggravation induces cellular senescence and ageing phenotypes, and its experimental amelioration alters aspects of cellular and organismal ageing in human cells and in other species [27,56,57,60,61,63,241–244]. Dysregulated splicing factor expression arises from

unresolved and constitutive signalling through ERK and AKT pathways, culminating in altered activity or expression of the *FOXO1* and *ETV6* genes [62]. The fruit fly homologues of these genes (*Foxo* and *Aop*) have also previously been demonstrated to be the genetic effectors of RAS/MEK/ERK and PI3K/AKT signalling in relation to lifespan in *Drosophila melanogaster* [245].

New research into senotherapeutic compounds that modulate senescence-related pathways may be an important avenue for future therapies for progeroid diseases. Compounds with senomorphic (reversal of senescence) or senolytic (lysis of senescent cells) properties may have effects on the premature ageing phenotype seen in the progeroid syndromes. Drugs with senomorphic properties like resveratrol and rapamycin affect several senescence-associated pathways, but can have pleiotropic effects [246]. Some compounds that inhibit p38/MAPK have been suggested to aid in the treatment of WS, however the potential therapeutic effects of inhibiting other senescence pathways have not yet been investigated for WS [247–249]. Only lonafarnib, a farnesyltransferase inhibitor, is approved for HGPS, but several senotherapeutic compounds like rapamycin have been identified as having potential in *in vitro* research [95,250,251]. The action of the farnesyltransferase is able to improve the persistent farnesylation of the aberrant Lamin A protein caused by HGPS [95].

Senotherapeutic compounds can be used to target specific aspects of the senescence phenotype. For example, trametinib is a drug which specifically inhibits both isoforms of MEK (MEK1 and MEK2) and it has been approved by the FDA for the treatment of metastatic melanoma [252–254]. The effects of trametinib on splicing factors have been well-characterised in previous work so we know that with the application of low dose

(1 - 10 µM) trametinib to senescent primary human dermal fibroblasts, we are able to restore splicing factor expression and bring about a reversal of several aspects of the senescent cell phenotype [62]. Drugs like trametinib may help reduce some of the senescent phenotype of progeroid diseases.

Here, we aimed firstly to determine whether disrupted splicing factor expression is a feature of the accelerated ageing phenotypes seen in progeroid syndromes, as it is for normal ageing [241]. Secondly, should splicing factor profiles be disrupted in progeroid cells, we aimed to determine whether trametinib was capable of restoring splicing factor dysregulation and attenuating senescence phenotypes in progeroid cells, as it does in wild-type cells [62]. This study could help identify the mechanisms of senescence further and could identify a future potential therapy for progeroid diseases.

Human primary cells

All cells used in this study were commercially derived, with ethical permission granted at source. Normal human dermal fibroblasts (nHDF) were purchased from Promocell, Heidelberg (catalogue number C-12302, lot number 445Z026.3). The donor was male, Caucasian and 36 years old at donation. Cells were taken from the abdomen. At the time of these experiments, nHDF cells had cumulated population doublings (cPDL) of 29.44. All three progeroid syndrome cell lines were human primary dermal fibroblasts purchased from the Coriell Institute (Camden, New Jersey, United States). Cells from an HGPS donor (catalogue number AG06917) were from a 3-year-old Caucasian male and were taken from the patient's arm. The cells have a normal karyotype (46, XY), but have a *de novo* single point mutation (2036 C>T) in the Lamin A (*LMNA*) gene. The patient displayed reduced subcutaneous tissue, thin skin, a thin beak-like nose characteristic of HGPS, thin underdeveloped nails, narrow clavicles, and growth retardation. HGPS cells had a cPDL of 6.36 for the characterisation of untreated cells, and 36.30 at the time of the trametinib treatment experiments.

Cells from a donor with WS (catalogue number AG05233) were from a 36-year-old male Asian patient. The karyotype of this patient is reported by the Coriell Institute as 46,XY,t(1;9)(1qter>1p32::9q22>9qter;9pter>9q22::1q32>1qter),t(1;2;5)(1pter>1q21::5q11.2>5qter;2pter>2q13::1q21>1qter;5pter>5q11.2::2q13>2qter),t(5;10)(5pter>5q11.2::10p15>10pter;10qter>10p15::5q11.2>5qter),inv(13)(pter>p21::q34>q21::q34>qt

er[43]/46,XY. Data on the exact mutation in the *WRN* gene was not available. Mutations in the *WRN* gene typically cause truncation of the Werner protein [255]. The donor had a short stature, grey hair, skin hyperpigmentation, atrophic skin and subcutaneous tissue, hypogonadism, cataracts and diabetes. Cells were taken from the patient's thigh. 40% of cells show random chromosomal abnormalities, but the remainder have a normal karyotype (46, XY). For both the characterisation of untreated cells and the trametinib treatment experiments, WS cells had a cPDL of 9.00.

Cells from a CS donor (catalogue number AG07076) were donated by an 11-year-old Caucasian female with CS- type A/type III. The patient had the least severe phenotypic type of CS: CS type III. They had a phenotype of dwarfism, mental retardation, cataracts, photophobia, retinopathy and optic atrophy. Being CS type A, the cells have a mutation in the *ERCC8* gene. This donor had a normal karyotype (46XX), but demonstrated compound heterozygosity for two mutations: a 649G-C transversion, and a G-to-T transversion. These mutations result in an ala205-to-pro (A205P) substitution, and a glu13-to-ter (E13X) substitution, respectively [256,257]. CS cells had a cPDL of 11.32 for the characterisation of untreated cells, and 18.63 at the time of the trametinib treatment.

Tissue culture

Cell culture conditions and methods are discussed in Chapter 2: Tissue Culture and Chapter 3: Considerations for the replacement of foetal bovine serum with human serum and other alternative supplements in cell culture. A Hirschmann

haemocytometer was used to perform cell counts, which together with the cPDL numbers given by Promocell and the Coriell Institute, enabled assessment of cPDL at the time of seeding for experiments. Cells were transferred to antibiotic-free media for 48 to 72 hours before seeding. Cells were seeded at approximately 30,000 cells/well in 12-well plates for staining experiments. For harvesting RNA for RT-qPCR analysis, cells were seeded at approximately 50,000 cells/well in 6-well plates. Dosing for trametinib studies was taken from our previous work, where a 10 μM dose suspended in 10% DMSO (HY-10999, MedchemExpress; J66650.AD, Thermo Scientific Alfa Aesar) resulted in attenuation of splicing factor expression and rescue of aspects of the senescent cell phenotype in wild-type human primary dermal fibroblasts.

Senescence-associated beta galactosidase (SAB) experiments and analysis

We used the Senescence Cells Histochemical Staining kit (CS0030, Merck) as per the manufacturer's instructions to stain senescence-associated beta galactosidase (SAB). Further detail is available in Chapter 2: Measurement of cellular senescence and Chapter 2: Analysis of staining.

Immunocytochemical staining experiments and analysis

Further detail is available in Chapter 2: Measurement of protein biomarkers, Chapter 2: Analysis of staining and Chapter 3: Image analysis using the Fluorescence Imaging of Nuclear Staining (FINS) algorithm.

RNA extraction

For further detail on the TRI RNA extraction, please view Chapter 2: Measurement of gene expression. RNA was eluted into 20 µl 1 × TE buffer, pH 8 (BP2473-500, Fisher Bioreagents).

Reverse transcription and pre-amplification

cDNA was produced by reverse transcription using the High-Capacity cDNA Reverse Transcription Kit as detailed in Chapter 2: Measurement of gene expression. Samples for the characterisation of senescence experiments were diluted to 12.5 ng/µl after reverse transcription. Due to low yield for some of the progeroid samples, 50 ng of cDNA for the trametinib versus control experiments was pre-amplified for 14 cycles.

Real-time quantitative PCR (RT-qPCR)

For more details on the RT-qPCR method used, please view Chapter 2: Measurement of gene expression. 40 cycles of RT-qPCR were performed. *CASP3*, *CASP7* and

splicing factors' expression was calculated by the comparative C_T technique, relative to the geometric mean (untreated data) or mean (vehicle/trametinib treated data) expression level of three endogenous housekeeping genes (*GUSB*, *IDH3B* and *PPIA*), which had been empirically demonstrated to provide the most stable baseline for comparison within each dataset using the online Reffinder website [176,177]. For assessment of *CASP3*, *CASP7* and splicing factor expression, transcript levels in progeroid cells were normalised to the mean expression of each gene in wild-type control cells. For the trametinib treatment experiments, the data was normalised to the vehicle-treated controls.

Statistics

The effect size or mean ± standard error of the mean (SEM) is reported in the text, with the full statistics reported in the tables. t test statistics for SAB and immunocytochemical staining were performed using Graphpad Prism version 9.4.1 for Windows (GraphPad Software, San Diego, California USA, www.graphpad.com). IBM SPSS Statistics for Windows version 27.0 programme (Released 2020; IBM Corp, Armonk, NY) was used to perform t tests for the RT-qPCR data. Graphs were produced using GraphPad Prism version 9.4.1. Error bars on the graphs represent the SEM unless otherwise stated.

Results

Senescence phenotypes in HGPS, WS and CS cells

Early passage fibroblasts from all three progeroid syndromes demonstrated higher levels of senescence than similar passage wild-type fibroblasts. SAB staining was 13.5-fold, 1.6-fold and 2-fold higher than nHDFs for HGPS, WS and CS, respectively ($p = < 0.0001$, $p = 0.0129$ and $p = 0.0401$). Senescence phenotypes are shown for HGPS cells in Figure 19, for WS cells in Figure 20, and for CS cells in Figure 21, with full data available in Table 8 and Table 9. Cells from donors with HGPS and WS also demonstrated lower levels of proliferation (80% and 71% lower for HGPS and WS, respectively; $p = 0.0050$ and $p = 0.0082$), whereas cells from the phenotypically less severe CS patient demonstrated no differences in proliferation compared to controls ($p = 0.048$). We did not detect any differences in DNA damage repair (using γH2AX as a biomarker) in cells from progeroid donors compared with wild-type fibroblasts. Levels of apoptosis appeared higher in all three progeroid cell types, with significantly higher levels of relative *CASP3* expression (HGPS: 28% higher, $p = 0.025$. WS: 35% higher, $p = 0.023$. CS: 27% higher, $p = 0.046$). Relative *CASP7* expression was 31% higher in HGPS cells ($p < 0.0001$), but was not significantly different in WS and CS cells (WS: 17% higher, $p = 0.211$. CS: 2% lower, $p = 0.662$).

Table 8: Wild-type nHDFs are compared against HGPS cells, Werner cells, and Cockayne cells for staining for senescence-associated beta galactosidase (SAB), Ki67 or γH2AX. The mean ± standard error of the mean (SEM) and t test p values are reported. Significant p values > 0.05 are emboldened. n = 3 for all experimental groups.

Stain	Wild-type nHDFs		HGPS Untreated			Werner Untreated			Cockayne Untreated		
	Mean (%)	SEM	Mean (%)	SEM	p value	Mean (%)	SEM	p value	Mean (%)	SEM	p value
SAB	4.49	1.472	65.04	2.627	**<0.0001**	11.75	0.8429	**0.0129**	13.35	2.563	**0.0401**
Ki67	41.01	5.473	8.29	2.055	**0.005**	11.83	2.419	**0.0082**	35.51	4.463	0.4796
γH2AX	0.00	0.00	0.18	0.179	0.3715	0.00	0.00	>0.9999	0.12	0.1155	0.3574

Table 9: Wild-type nHDFs are compared against HGPS cells, Werner cells, and Cockayne cells for RT-qPCR analysis. The mean ± standard error of the mean (SEM) and t test p values are reported. Significant p values > 0.05 are emboldened. n = 3 for all experimental groups. All results are logged and normalised to the corresponding natural log of the wild-type nHDFs resulting in a mean of 0.0000 for all nHDFs.

Gene	Wild-type nHDFs		HGPS Untreated			Werner Untreated			Cockayne Untreated		
	Mean	SEM	Mean	SEM	p value	Mean	SEM	p value	Mean	SEM	p value
AKAP17A	0.0000	0.00280	0.1470	0.01363	**0.007**	-0.0546	0.11555	0.683	-0.1459	0.03168	**0.043**
CASP3	0.0000	0.07229	0.2773	0.03158	**0.025**	0.3508	0.06528	**0.023**	0.2650	0.05853	**0.046**
CASP7	0.0000	0.01457	0.3100	0.02392	**0.000**	0.1697	0.09410	0.211	-0.0179	0.03508	0.662
HNRNPA0	0.0000	0.06729	-0.2683	0.19968	0.272	-0.7537	0.26784	0.052	-0.0312	0.12356	0.835
HNRNPA1	0.0000	0.05322	-0.5208	0.01070	**0.001**	-0.4308	0.06006	**0.006**	-0.5611	0.03949	**0.001**
HNRNPA2B1	0.0000	0.07217	-0.2055	0.02496	0.055	-0.0397	0.07462	0.722	-0.9304	0.06115	**0.001**
HNRNPD	0.0000	0.05610	-0.1355	0.00805	0.075	0.2520	0.02337	**0.014**	-0.1257	0.11701	0.387
HNRNPH3	0.0000	0.04276	-0.0759	0.06390	0.379	0.1140	0.10229	0.362	-0.4689	0.03199	**0.001**
HNRNPK	0.0000	0.03673	-0.2728	0.08722	**0.045**	-0.1428	0.03650	0.051	-0.3678	0.02339	**0.001**
HNRNPM	0.0000	0.10042	-0.7215	0.10990	**0.008**	-0.9688	0.21861	**0.016**	-0.7633	0.10946	**0.007**
HNRNPUL2	0.0000	0.13141	0.1405	0.04493	0.369	-0.1551	0.15503	0.488	-0.2533	0.05284	0.148
PNISR	0.0000	0.08904	0.7377	0.11132	**0.007**	0.9260	0.06260	**0.001**	0.5193	0.05651	**0.008**
SRSF1	0.0000	0.03662	-0.3201	0.05212	**0.007**	-0.2801	0.15955	0.217	-0.2279	0.02507	**0.007**
SRSF2	0.0000	0.16357	-1.2819	0.13558	**0.004**	-1.1881	0.33309	**0.033**	-0.3919	0.08658	0.102
SRSF3	0.0000	0.00971	-0.0848	0.06687	0.278	0.1734	0.02958	**0.005**	-0.0263	0.06912	0.741
SRSF6	0.0000	0.04396	0.0396	0.04482	0.563	0.3092	0.08235	**0.030**	0.0416	0.05593	0.590
SRSF7	0.0000	0.04921	-0.2368	0.02322	**0.012**	0.1172	0.01437	0.084	-0.2363	0.02035	**0.011**
TRA2B	0.0000	0.04640	-0.0967	0.03050	0.157	0.0279	0.02613	0.628	0.1031	0.04419	0.183

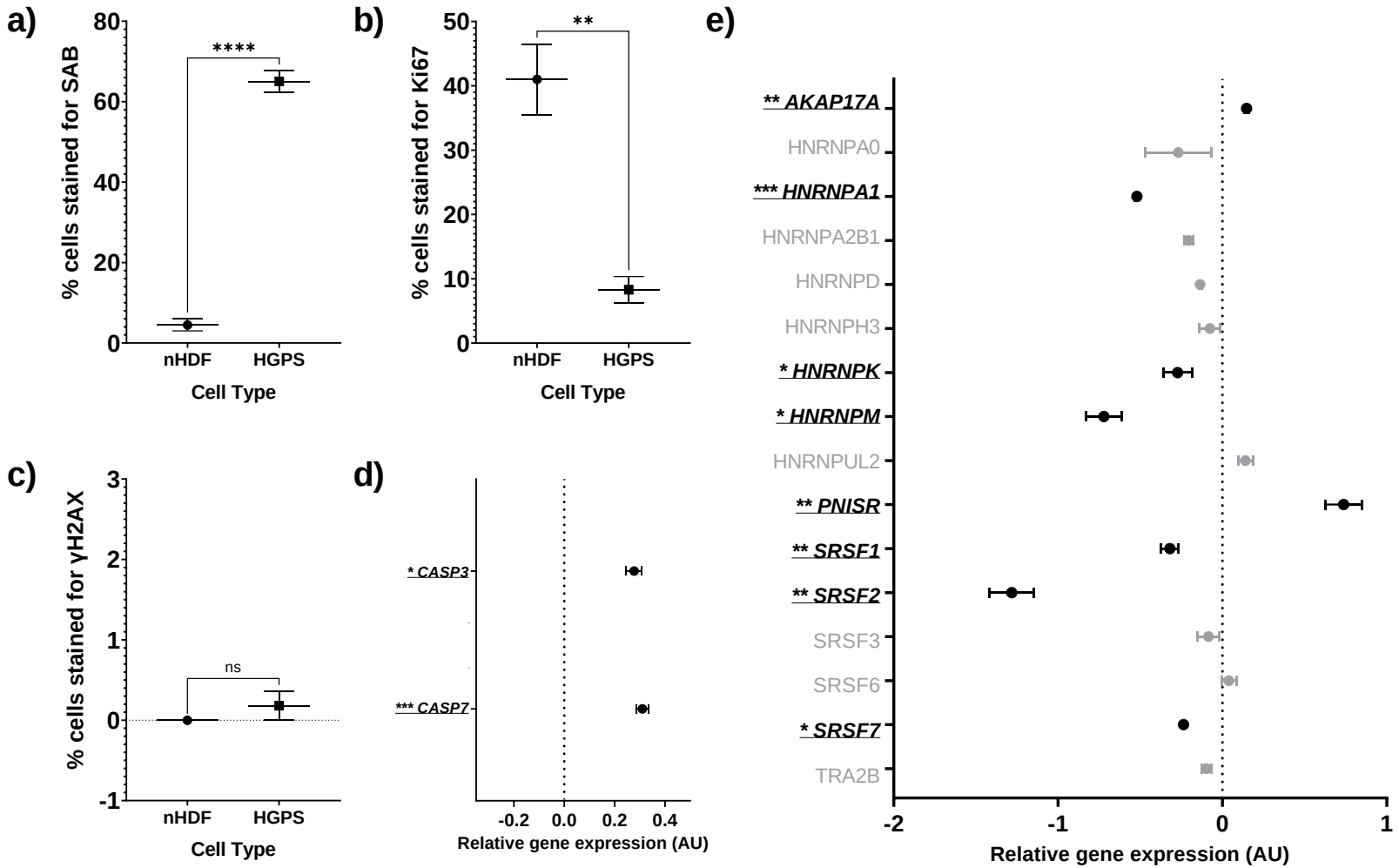

*Figure 19: Senescence characteristics of HGPS cells compared to wild-type nHDFs. The mean ± standard error of the mean (SEM) are graphed. Asterisks denote a significant p value from a t test: * p<0.05, ** p<0.01, *** p<0.001 and **** p<0.0001. n = 3 for all experimental groups. A.) Percentage of SAB positive cells. B.) Percentage of cells stained for Ki67, a marker of proliferation. C.) Percentage of cells stained for γH2AX, a marker of DNA damage repair. D.) Forest plot of relative gene expression (arbitrary units, AU) of CASP3 and CASP7, markers of apoptosis. E.) Forest plot of relative gene expression (AU) of an a priori panel of splicing factors.*

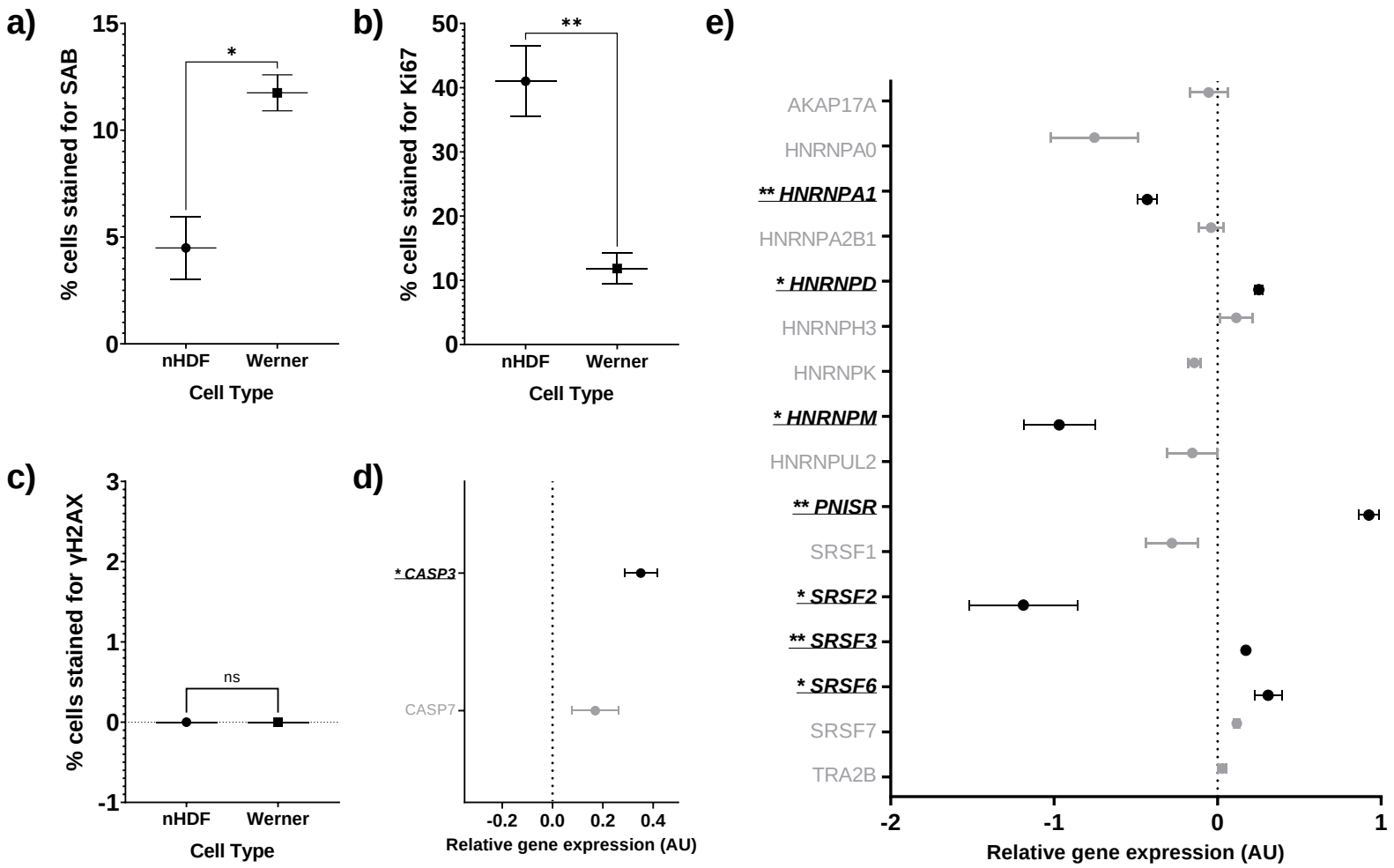

*Figure 20: Senescence characteristics of Werner cells compared to wild-type nHDFs. The mean ± standard error of the mean (SEM) are graphed. Asterisks denote a significant p value from a t test: * p<0.05, ** p<0.01, *** p<0.001 and **** p<0.0001. n = 3 for all experimental groups. A.) Percentage of SAB positive cells. B.) Percentage of cells stained for Ki67, a marker of proliferation. C.) Percentage of cells stained for γH2AX, a marker of DNA damage repair. D.) Forest plot of relative gene expression (arbitrary units, AU) of CASP3 and CASP7, markers of apoptosis. E.) Forest plot of relative gene expression (AU) of an a priori panel of splicing factors.*

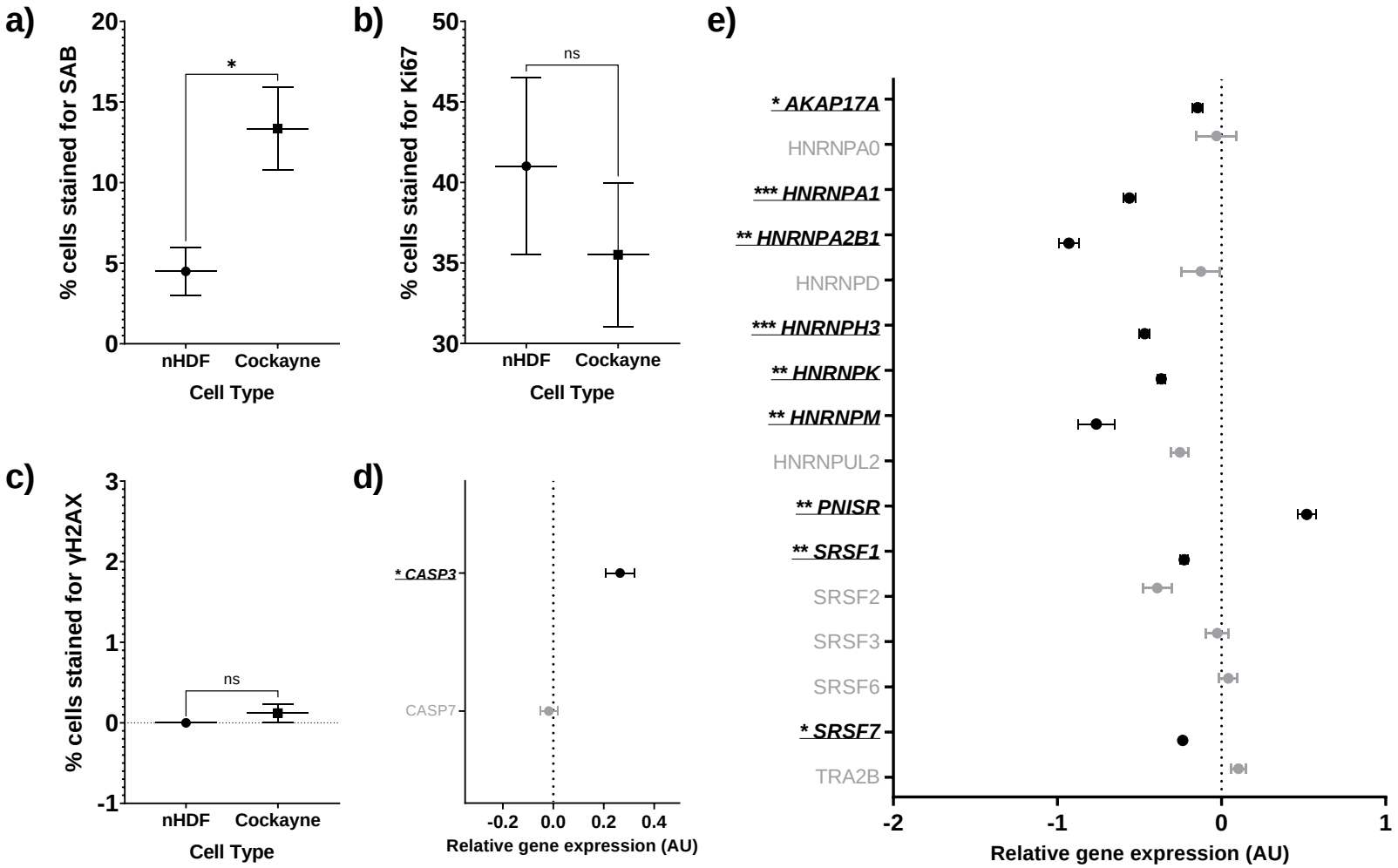

*Figure 21: Senescence characteristics of Cockayne cells compared to wild-type nHDFs. The mean ± standard error of the mean (SEM) are graphed. Asterisks denote a significant p value from a t test: * p<0.05, ** p<0.01, *** p<0.001 and **** p<0.0001. n = 3 for all experimental groups. A.) Percentage of SAB positive cells. B.) Percentage of cells stained for Ki67, a marker of proliferation. C.) Percentage of cells stained for γH2AX, a marker of DNA damage repair. D.) Forest plot of relative gene expression (arbitrary units, AU) of CASP3 and CASP7, markers of apoptosis. E.) Forest plot of relative gene expression (AU) of an a priori panel of splicing factors.*

Splicing factor dysregulation in HGPS, WS and CS cells

Across all three progeroid syndromes, there were differences in the splicing factors affected and directionality, except for *PNISR* which was significantly upregulated in all three types (Table 9, Figure 19, Figure 20 and Figure 21). Overall, most splicing factors were downregulated in progeroid syndromes compared to the wild type. 75% of the significant effects observed in HGPS were a decrease, with 43% and 89% of effects for WS and CS, respectively. In HGPS cells, *AKAP17A* (15%; p = 0.007) and *PNISR* (74%; p = 0.007) gene expression was significantly higher, whereas *HNRNPA1* (-52%; p = 0.001), *HNRNPK* (-27%; p = 0.045), *HNRNPM* (-72%; p = 0.008), *SRSF1* (-32%; p = 0.007), *SRSF2* (-128%; p = 0.004) and *SRSF7* (-24%; p = 0.012) expression was lower. In WS cells, *HNRNPD* (25%; p = 0.014*)*, *PNISR* (93%; p = 0.001), *SRSF3* (17%; p = 0.005) and *SRSF6* (31%; p = 0.030) gene expression was significantly higher, whereas *HNRNPA1* (-43%; p = 0.006), *HNRNPM* (-97%; p = 0.016) and *SRSF2* (-119%; p = 0.033) expression was lower. In CS cells, *PNISR* (52%; p = 0.008) gene expression was significantly higher, however gene expression was lower in *AKAP17A* (-15%; p = 0.043), *HNRNPA1* (-56%; p = 0.001), *HNRNPA2B1* (-93%; p = 0.001), *HNRNPH3* (-47%; p = 0.001), *HNRNPK* (-37%; p = 0.001), *HNRNPM* (-76%; p = 0.007), *SRSF1* (-23%; p = 0.007) and *SRSF7* (-24%; p = 0.011).

Trametinib treatment reduced senescence in HGPS cells

HGPS cells treated with the senomorphic drug, trametinib, are less senescent than vehicle-treated HGPS controls, and have decreased gene expression for three splicing factors (Table 10, Table 11 and Figure 22). SAB levels are 30% lower in the treated

cells (p = 0.0471). Proliferation measured by Ki67 staining was 42% lower in the treated cells, but was not significant (p = 0.0536). DNA damage repair (γH2AX staining) and apoptosis (gene expression of *CASP3* and *CASP7*) did not show any significant changes with treatment. Trametinib treatment affected the gene expression of splicing factors involved with senescence. Gene expression was significantly decreased with treatment in *HNRNPD* (-38%; p = 0.027), *HNRNPM* (-32%; p = 0.048) and *SRSF6* (-54%; p = 0.042).

Table 10: Effects of trametinib treatment on staining for senescence-associated beta galactosidase (SAB), Ki67 or γH2AX in HGPS, Werner and Cockayne syndrome cells. Progeroid cell cultures are treated with a DMSO control or 10 μM trametinib. The mean ± standard error of the mean (SEM) and t test p values are reported. Significant p values > 0.05 are emboldened. n = 3 for all experimental groups.

Stain	DMSO treated HGPS		Trametinib treated HGPS			DMSO treated Werner		Trametinib treated Werner			DMSO treated Cockayne		Trametinib treated Cockayne		
	Mean (%)	SEM	Mean (%)	SEM	p value	Mean (%)	SEM	Mean (%)	SEM	p value	Mean (%)	SEM	Mean (%)	SEM	p value
SAB	42.09	4.1170	29.55	1.6170	**0.0471**	60.19	6.0040	61.00	7.3210	0.9359	4.94	0.4619	2.00	0.4503	**0.0104**
Ki67	33.10	4.8670	19.14	1.6970	0.0536	14.17	5.7450	2.32	0.4561	0.1089	41.39	3.5620	7.41	3.8340	**0.0029**
γH2AX	1.42	1.3110	0.44	0.2483	0.5033	0.27	0.2714	0.27	0.2714	>0.9999	0.10	0.1039	0.07	0.0751	0.8265

Table 11: Gene expression in HGPS cells treated with a DMSO control or 10 μM trametinib. Vehicle-treated cells are compared against treated cells for RT-qPCR analysis. The mean ± standard error of the mean (SEM) and t test p values are reported. Significant p values > 0.05 are emboldened. n = 3 for all experimental groups. All results are logged and normalised to the DMSO treated control resulting in a mean of 0.0000 for these cells.

Gene	DMSO treated HGPS		Trametinib treated HGPS		p value
	Mean	SEM	Mean	SEM	
AKAP17A	0.0000	0.07939	-0.0989	0.04495	0.339
CASP3	0.0000	0.09790	-0.0846	0.12557	0.623
CASP7	0.0000	0.06298	-0.1093	0.11819	0.460
HNRNPA0	0.0000	0.03831	0.1074	0.21222	0.665
HNRNPA1	0.0000	0.04375	-0.4259	0.23231	0.205
HNRNPA2B1	0.0000	0.06580	-0.1838	0.12724	0.269
HNRNPD	0.0000	0.04324	-0.3813	0.10334	**0.027**
HNRNPH3	0.0000	0.12678	-0.1232	0.09660	0.483
HNRNPK	0.0000	0.19698	-0.3700	0.09144	0.164
HNRNPM	0.0000	0.06595	-0.3206	0.09250	**0.048**
HNRNPUL2	0.0000	0.02529	-0.4382	0.41338	0.400
PNISR	0.0000	0.05944	0.1025	0.17489	0.609
SRSF1	0.0000	0.02077	-0.2233	0.11684	0.193
SRSF2	0.0000	0.15928	-1.0493	0.43229	0.085
SRSF3	0.0000	0.14506	-0.2533	0.11203	0.239
SRSF6	0.0000	0.11818	-0.5360	0.13775	**0.042**
SRSF7	0.0000	0.01591	-0.2092	0.12513	0.235
TRA2B	0.0000	0.03686	-0.3055	0.25036	0.294

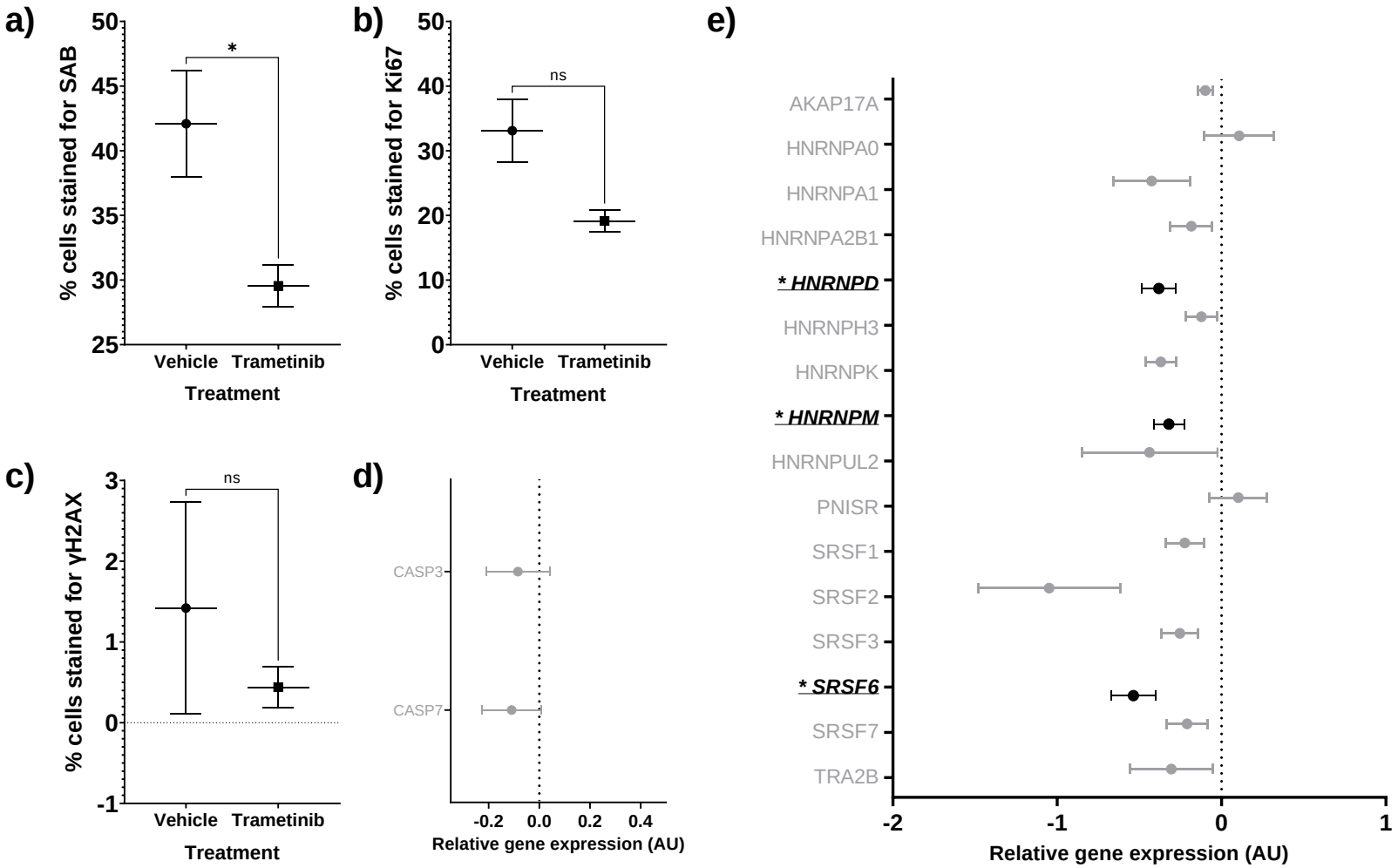

*Figure 22: Senescence characteristics of HGPS cells treated with trametinib 10 μM compared to vehicle controls. The mean ± standard error of the mean (SEM) are graphed. Asterisks denote a significant p value from a t test: * p<0.05, ** p<0.01, *** p<0.001 and **** p<0.0001. n = 3 for all experimental groups. A.) Percentage of SAB positive cells. B.) Percentage of cells stained for Ki67, a marker of proliferation. C.) Percentage of cells stained for γH2AX, a marker of DNA damage repair. D.) Forest plot of relative gene expression (arbitrary units, AU) of CASP3 and CASP7, markers of apoptosis. E.) Forest plot of relative gene expression (AU) of an a priori panel of splicing factors.*

Trametinib had no effect on senescence in Werner syndrome cells

Werner cells did not show any changes in senescence, proliferation or DNA damage repair in response to trametinib treatment, however gene expression of *CASP7* and *SRSF6* were decreased (Table 10, Table 11 and Figure 23). Senescence (SAB staining) did not show any change in response to the treatment. Similarly to the HGPS cells' response, Werner cells had an 83% decrease in Ki67 staining, but this was not significant (p = 0.1089), and γH2AX staining was unchanged. Apoptosis was affected by the treatment: *CASP3* gene expression was not changed, but *CASP7* expression was significantly lower (-16%; p = 0.043). *SRSF6* expression was lower with trametinib treatment (-21%; p = 0.037).

Table 12: Gene expression in Werner cells treated with a DMSO control or 10 μM trametinib. Vehicle-treated cells are compared against treated cells for RT-qPCR analysis. The mean ± standard error of the mean (SEM) and t test p values are reported. Significant p values > 0.05 are emboldened. n = 3 for all experimental groups. All results are logged and normalised to the DMSO treated control resulting in a mean of 0.0000 for these cells.

Gene	DMSO treated Werner		Trametinib treated Werner		p value
	Mean	SEM	Mean	SEM	
AKAP17A	0.0000	0.07775	0.0899	0.13752	0.600
CASP3	0.0000	0.18080	-0.1829	0.06654	0.396
CASP7	0.0000	0.05171	-0.1568	0.01412	**0.043**
HNRNPA0	0.0000	0.17741	-0.0153	0.08047	0.941
HNRNPA1	0.0000	0.20095	-0.4500	0.12193	0.128
HNRNPA2B1	0.0000	0.08419	-0.1348	0.13226	0.439
HNRNPD	0.0000	0.18667	-0.1868	0.08756	0.416
HNRNPH3	0.0000	0.02166	-0.1390	0.05445	0.077
HNRNPK	0.0000	0.24257	-0.1654	0.18525	0.617
HNRNPM	0.0000	0.37251	-0.0475	0.23086	0.919
HNRNPUL2	0.0000	0.56743	0.0817	0.24466	0.901
PNISR	0.0000	0.07420	0.0635	0.13543	0.702
SRSF1	0.0000	0.01980	-0.0463	0.10754	0.694
SRSF2	0.0000	0.57286	-0.4222	0.08741	0.507
SRSF3	0.0000	0.09257	-0.1789	0.07099	0.200
SRSF6	0.0000	0.05241	-0.2093	0.04376	**0.037**
SRSF7	0.0000	0.12667	-0.4149	0.13621	0.090
TRA2B	0.0000	0.02057	-0.1139	0.18060	0.593

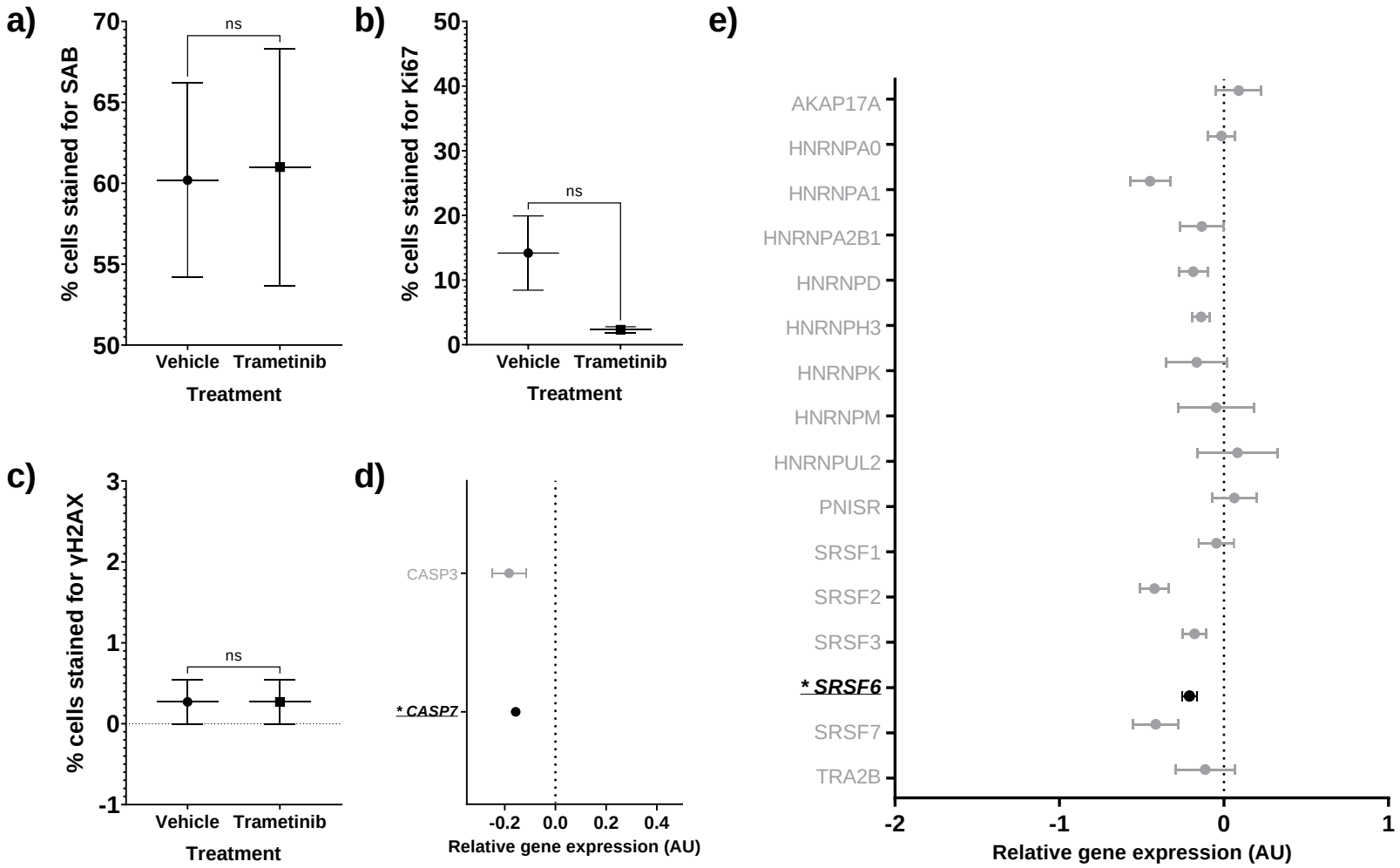

*Figure 23: Senescence characteristics of Werner cells treated with trametinib 10 μM compared to vehicle controls. The mean ± standard error of the mean (SEM) are graphed. Asterisks denote a significant p value from a t test: * p<0.05, ** p<0.01, *** p<0.001 and **** p<0.0001. n = 3 for all experimental groups. A.) Percentage of SAB positive cells. B.) Percentage of cells stained for Ki67, a marker of proliferation. C.) Percentage of cells stained for γH2AX, a marker of DNA damage repair. D.) Forest plot of relative gene expression (arbitrary units, AU) of CASP3 and CASP7, markers of apoptosis. E.) Forest plot of relative gene expression (AU) of an a priori panel of splicing factors.*

Trametinib treatment reduced senescence in Cockayne syndrome cells

Senescence and proliferation are decreased with trametinib treatment in Cockayne cells and six splicing factors have altered gene expression (Table 10, Table 11 and Figure 24). SAB staining is 60% lower ($p = 0.0104$) in treated cells compared to vehicle-treated CS controls. Proliferation is significantly lower in treated Cockayne cells with an 82% reduction in Ki67 staining ($p = 0.0029$). *CASP3* expression is unchanged, but *CASP7* expression indicates a 24% increase in apoptosis with treatment ($p < 0.0005$). DNA damage repair levels (γH2AX staining) remained low and were unchanged with treatment. Trametinib treatment had effects on more splicing factors' gene expression in Cockayne cells compared to HGPS and Werner cells. Gene expression was higher with treatment in *HNRNPA0* (36%; $p = 0.030$), and that gene expression was lower in *HNRNPA1* (-49%; $p = 0.029$), *HNRNPA2B1* (-32%; $p = 0.030$), *HNRNPD* (-44%; $p < 0.0005$), *SRSF3* (-40%; $p = 0.004$) and *SRSF7* (-77%; $p < 0.0005$).

Table 13: Gene expression in Cockayne cells treated with a DMSO control or 10 μM trametinib. Vehicle-treated cells are compared against treated cells for RT-qPCR analysis. The mean ± standard error of the mean (SEM) and t test p values are reported. Significant p values > 0.05 are emboldened. n = 3 for all experimental groups. All results are logged and normalised to the DMSO treated control resulting in a mean of 0.0000 for these cells.

Gene	DMSO treated Cockayne		Trametinib treated Cockayne		p value
	Mean	SEM	Mean	SEM	
AKAP17A	0.0000	0.07884	0.1410	0.12482	0.394
CASP3	0.0000	0.08686	-0.2734	0.04976	0.052
CASP7	0.0000	0.00541	0.2417	0.01002	**0.000**
HNRNPA0	0.0000	0.07020	0.3633	0.08528	**0.030**
HNRNPA1	0.0000	0.13207	-0.4939	0.06731	**0.029**
HNRNPA2B1	0.0000	0.08542	-0.3190	0.04467	**0.030**
HNRNPD	0.0000	0.02346	-0.4350	0.02832	**0.000**
HNRNPH3	0.0000	0.06340	-0.1357	0.02037	0.111
HNRNPK	0.0000	0.09832	0.1883	0.23219	0.497
HNRNPM	0.0000	0.09515	0.1104	0.06560	0.394
HNRNPUL2	0.0000	0.45255	0.2901	0.04871	0.588
PNISR	0.0000	0.08017	0.0710	0.03888	0.470
SRSF1	0.0000	0.06496	-0.3585	0.12077	0.059
SRSF2	0.0000	0.47592	0.1084	0.08712	0.834
SRSF3	0.0000	0.04399	-0.4022	0.05133	**0.004**
SRSF6	0.0000	0.10491	-0.6934	0.29393	0.090
SRSF7	0.0000	0.00882	-0.7748	0.01598	**0.000**
TRA2B	0.0000	0.12949	-0.4098	0.08471	0.057

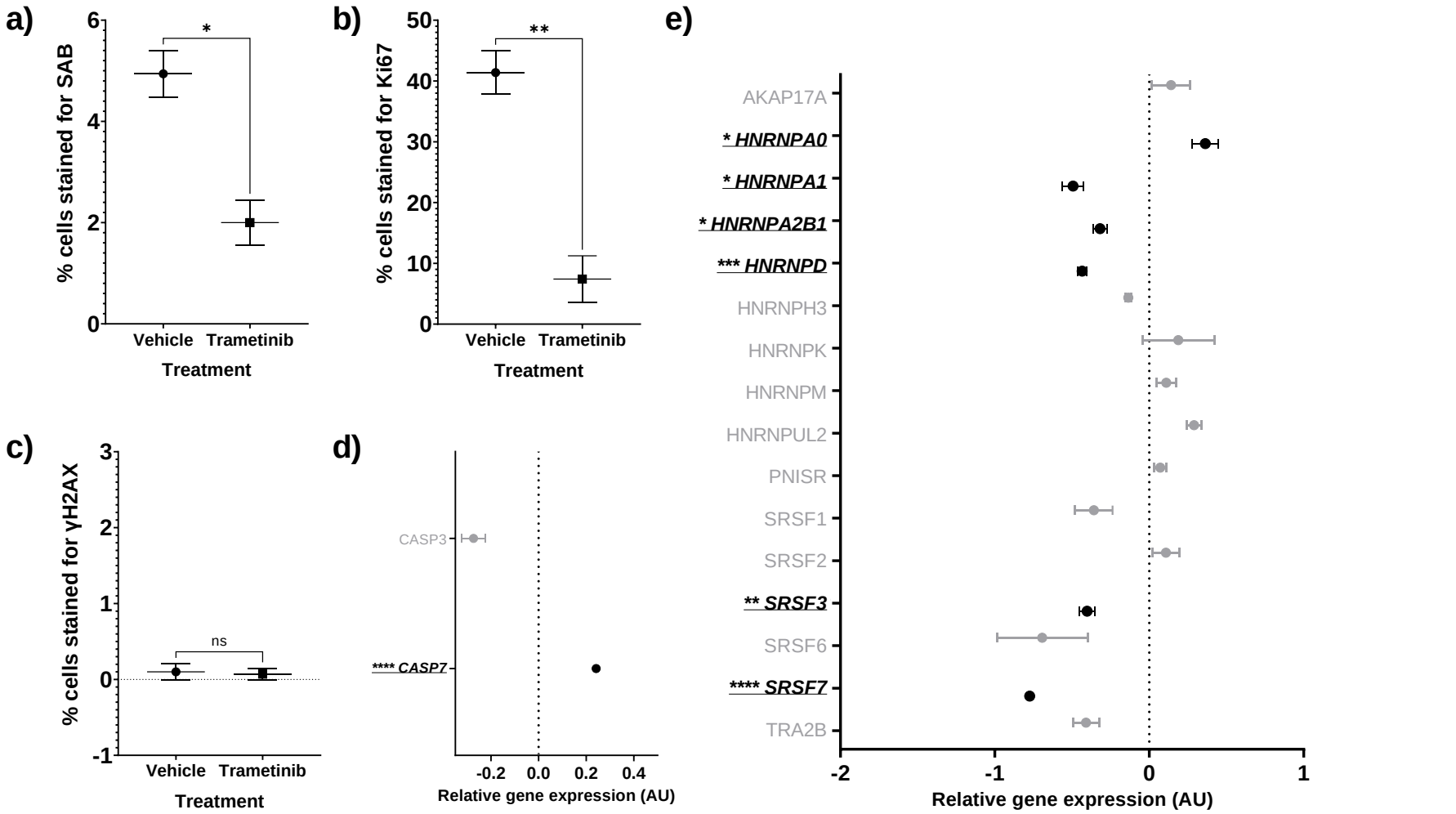

*Figure 24: Senescence characteristics of Cockayne cells treated with trametinib 10 μM compared to vehicle controls. The mean ± standard error of the mean (SEM) are graphed. Asterisks denote a significant p value from a t test: * p<0.05, ** p<0.01, *** p<0.001 and **** p<0.0001. n = 3 for all experimental groups. A.) Percentage of SAB positive cells. B.) Percentage of cells stained for Ki67, a marker of proliferation. C.) Percentage of cells stained for γH2AX, a marker of DNA damage repair. D.) Forest plot of relative gene expression (arbitrary units, AU) of CASP3 and CASP7, markers of apoptosis. E.) Forest plot of relative gene expression (AU) of an a priori panel of splicing factors.*

Discussion

Progeroid syndromes are life-limiting rare diseases that share many similarities with the processes that are involved in normal ageing and age-related diseases. Senotherapeutic compounds can be used to target ageing, age-related disease and premature ageing. With few treatments available for progeroid syndromes, finding new senotherapeutics is important. Some senotherapeutic compounds like trametinib are thought to work by restoring splicing factor regulation. We investigated if splicing factor profile expression was altered in progeroid syndromes, and if a known senomorphic drug, trametinib, could impact the severe senescence phenotype in cells from people with progeroid syndromes. We observed that cultures of early passage primary dermal fibroblast cells from individuals with some progeroid syndromes demonstrated elevated senescent cell load and altered splicing factor expression when compared with early passage wild-type cells. Furthermore, we saw that trametinib was able to influence the levels of some splicing factors and was able to influence some, but not all, aspects of the senescent cell phenotype in these cells.

Senescent cells can show a level of heterogeneity and there is no single definitive marker [166,167]. Senescence can be induced by several means: replication (via telomere attrition), stress (such as the accumulation of mutations due to poor nuclear stability in HGPS) and/or oncogenes [37,68,141]. However, no combination of senescence biomarkers has yet been associated with any particular subtype of senescence. Several studies suggest that senomorphic compounds may target only SASP-induced senescence (a form of stress-induced senescence) [117,258].

It is possible that treatments such as trametinib target only subsets of senescent cells, so that conditions where the balance of subtypes is disturbed may show differential effects on rescue. For example, cells in which senescence has arisen because of catastrophic DNA damage may act differently to those which have arisen because of SASP-induced paracrine senescence. In the former there will be an ongoing signal for senescence, whilst in the latter, once the inflammatory milieu has been normalised, senescence may be more reversible. Our results from this study are consistent with this hypothesis. We noted elevated senescent cell load in the more severe syndromes (HGPS and WS) compared with cells from the more moderately affected CS patient, and disease severity and senescent cell load also correlated with degree of 'rescue' upon trametinib treatment. WS and HGPS cells demonstrated fewer changes to splicing factor expression and a more moderate effect on senescent cell load; upon treatment with trametinib CS cells demonstrated a 71% decrease in senescent cell load (though this effect may be exaggerated as the percentage of SAB stained cells in the vehicle treatment was low) compared with 33% for HGPS and no change for WS (Table 10, Figure 22, Figure 23 and Figure 24). This may suggest that the most severe progerias may have an increased prevalence of terminally and irreversibly senescent cells. Another interesting and surprising observation was the overall low level of damaged cells as measured by γH2AX staining in our progeroid cell cultures. This is counterintuitive given that these are all syndromes of DNA damage. However, it is important to note that γH2AX is more specifically a marker of the initiation of the DNA damage repair response [174,259]. DNA damage repair can be inhibited in progeroid cells and one study found that the intensity of γH2AX foci was low in HGPS cells [33,260]. Another possibility is that DMSO plays

a role in the treated experiments: DMSO was found to affect γH2AX foci in one study [261]. DNA damaged cells with an impaired DNA damage repair response are more likely to undergo apoptosis as a result. Accordingly, we do observe here an elevated degree of apoptosis in cells from progeroid syndromes.

Trametinib as a drug is often used for cancer chemotherapy in combination [262]. The reduction in Ki67 is therefore unsurprising when we consider that trametinib is a known anti-neoplastic therapy [254]. Trametinib commonly has a variety of side effects including gastrointestinal issues, but this is during a high dose daily treatment programme. Single doses have been enough in a senotherapeutic context to give benefit so it may be that future therapies using trametinib for age-related diseases would use a single dose model.

Many senomorphic compounds cause biphasic dose responses in cells. Trametinib has been observed to exert different senotherapeutic effects at the 1 - 10 µM range compared to 20 µM doses in cells [63]. A 10 µM dose was chosen for this study based on this research, but it is possible that with a lower dose in the range the cells may show more restoration of splicing factor expression. A 20 µM dose of trametinib may have no effect on senescence, and, as our results suggest, a 10 µM dose may be sufficient to restore the responsiveness of splicing factor expression, but a 1 µM dose may be the dosage that can produce the best response. This may be as a result of a hormetic effect. A hormetic effect is when a cell responds to a minor stressor and overcompensates to the point that the stressor causes a slight benefit to the cell overall [263]. Several compounds such as resveratrol and metformin show this type of hormetic effect [264,265]. Although

trametinib is more specific in the mechanism that it targets compared to resveratrol or metformin, this type of dose effect is still common in compounds that target tightly controlled and highly autoregulated pathways, such as the networks that control splicing factor expression and cell fate. Autoregulation and cross-regulation have been noted in the MEK/ERK pathway that trametinib targets [62].

One caveat of this work is that the cells studied were dermal fibroblasts, so other cell types from a person with a progeroid syndrome may have different characteristics and responses to trametinib. Other subtypes of Cockayne syndrome, or other progeroid syndromes, such as Bloom syndrome and Xeroderma Pigmentosum, may not be as rescuable as the syndromes examined here. Further research is needed to uncover if these findings are replicated in other progeroid syndromes. Another caveat is that, although progeroid syndromes are widely considered a reasonable model for 'normal' ageing, given that progerias are syndromic in nature, they may not necessarily reflect what happens in normal ageing when used as a model [25]. It is interesting that trametinib is capable of partially rescuing the phenotype of these cells when the phenotypes are so severe. In another study, using a mouse model of HGPS, the senomorphic drug resveratrol was able to alleviate some features of the premature ageing phenotype [244]. This gives more evidence in support of the idea that senomorphic and senotherapeutic drugs may help in the progeroid syndromes [25,250].

Our results are consistent with other studies that show that cells from individuals with progeroid syndromes display characteristics consistent with accelerated cellular and molecular ageing, which may be amenable to future therapeutic targeting [25]. Several senomorphic drugs, such as trametinib and resveratrol show rescue of senescent cell populations in contradiction to Terzi *et al.*'s definition of an "irreversible state of cell cycle arrest" [61,63,64]. Our body of work suggests that the most senescent and most DNA damaged cells are irreversibly senescent, but senomorphic drugs can reverse senescence in cells up to a certain point, giving more weight to the theory of stages of senescence, e.g. a reversible pre-senescent stage [68,266].

Senotherapeutic and senomorphic drugs represent an intriguing way to think about treating progeroid disease as well as age-related disease. As our population ages, we have an increased burden of age-related disease, which means that more therapies will be needed to sustain a healthy population [267]. If compounds are able to help in treating the mechanisms behind several different age-related diseases, then this could have more impact than attempting to treat each age-related disease individually. Our findings suggest that trametinib and other senotherapeutic compounds could be useful in people with progeroid syndromes, and further evidences the notion that mRNA splicing factor dysregulation is a key cellular hallmark of ageing.

Acknowledgements

The authors wish to thank Professor Richard G A Faragher and Professor Elizabeth L Ostler of the University of Brighton for a conversation regarding experimental design prior to the start of the research project.

Sources of Funding

The authors gratefully acknowledge funding from Animal Free Research UK.

Author Contributions

LRB helped design the experiment, performed all laboratory work, data analysis and prepared the manuscript. LWH helped to design the experiment, analyse the data and prepare the manuscript.

Conflicts of Interest

Professor Harries is an inventor on patent PCT/GB2019/052125, and is a founder, chief scientific officer and research and development lead for SENISCA, Ltd. Ms Bramwell has no financial interest to declare in relation to the content of this manuscript.

Chapter 5: A medium-throughput screen of repurposed drugs for senotherapeutic activity and identification of structure-function associations.

Many drugs are tested for efficacy in one particular disease context, however many drugs could offer benefits in other contexts. Looking at compounds that affect ageing at a cellular level may highlight new uses for the compounds in the context of age-related diseases. As the study of senotherapeutic drugs is relatively novel, many drugs available have not been assessed for their effects on cellular ageing. The use of senotherapeutic drugs such as trametinib in our group's previous work and my previous chapter suggests that they may be able to restore cell function [61,63].

Therefore, this chapter details the identification of compounds that may have senotherapeutic activity. The approach is used to identify compounds for further validation and so is not presented as a draft journal article. The subsequent chapter is drafted as an article following the results of a validation of a subset of compounds.

Abstract

Many diseases are age-related and share basic cellular mechanisms that underlie the differing pathologies of each disease, however therapies are normally targeted to each disease's distinct pathology. Repurposing drugs for other diseases represents an opportunity to efficiently identify novel therapies. If the drugs could be screened for impact on basic cellular mechanisms of ageing, then this may lead to identification of novel treatments or therapeutic approaches for a wide range of diseases. We assessed a selection of chemical compounds that are already available in clinics for any effect on a hallmark of cellular ageing: senescence. We selected and screened 240 compounds for effects on gene expression of *CDKN2A*, a marker of senescence. We chose 32 compounds to further validate in a screen for senescence-associated beta galactosidase (SAB) activity, the standard marker of senescence. Using data from these two screens, we performed a bioinformatic association of structure-function. We identified many compounds with senotherapeutic potential and a molecular substructure associated with a decrease in *CDKN2A* expression. We identified three compounds that induced senescence and 11 that decreased senescence. Interestingly, several synthetic female hormones were identified. Further validation is needed to assess if any compounds identified here in the screens could have potential senotherapeutic capabilities in age-related diseases. The substructure identified here provides more evidence for substructures that are associated with a compound's senomorphic or senolytic properties. This approach could be used for other compounds and could inform future studies for novel therapies for age-related disease.

Introduction

People are now living longer than they ever have before thanks to improvements in medicine, technology and public healthcare. A baby girl born in the UK today could reasonably expect to live into her nineties [268]. Despite its associated benefits, this increase in longevity brings with it new challenges and issues; although people may have an increased lifespan, this does not necessarily translate to a long healthspan [3]. As we age, our risk of diseases such as type 2 diabetes, dementia, osteoarthritis and cardiovascular disease increases exponentially [9]. These diseases also represent a huge healthcare and economic burden demonstrated by 41% of hospital admissions being for people over age 65 [4–6]. It is thought that these ageing-related diseases share common underlying mechanisms, therefore finding new therapies targeting these mechanisms would aid in treatment and/or prevention of a variety of different diseases.

Ageing has a molecular basis characterised by fourteen “hallmarks of ageing” often seen in combination [21,22]. These hallmarks are **1. Genome instability** (accumulation of mutations). **2. Telomere attrition** (decrease in telomere length). **3. Epigenetic changes. 4. Dysregulation of alternative splicing** (changes to the regulation of mRNA splicing patterns). **5. Cellular senescence**. **6. A loss of proteostasis** (altered levels of proteins either by dysregulation of functional protein production or degradation). **7. Mitochondrial dysfunction. 8. Altered mechanical properties** (changes in the properties of the extracellular cell matrix and intracellular fibres). **9. Compromised autophagy. 10. Inflammation** (cells secrete a collection of cytokines termed the senescence-associated secretory

phenotype (SASP) which serve to induce senescence in nearby cells). **11. Exhaustion of stem cell supply. 12. Altered cell-cell communication** (changes to the functionality of the immune system as well as disruptions in general endocrine, paracrine and autocrine signalling pathways). **13. Nutrient sensing dysregulation** (impaired function of cellular nutritional pathways, e.g. insulin pathway). **14. Microbiome disturbances** (changes in species diversity of the microbiomes in the body).

Although all of the hallmarks play a role, cellular senescence is particularly important due to its overlap with many of the other hallmarks of molecular ageing. A cell used to be termed senescent when it irreversibly enters into a stable state of cell cycle arrest (new evidence suggests reversal is possible), unlike cellular quiescence which is a reversible non-proliferating state [64]. Cells may become senescent due to reaching their natural replicative limit (termed the “Hayflick” limit), their natural programming during development or can be induced by cellular stress and/or oncogene expression [36,269–271].

Senescent cells have a heterogeneous phenotype, but most will exhibit some of the following: a change in morphology, an increase in expression of anti-proliferative markers, activation of the DNA Damage Response (DDR), and secretion of SASP [69,70]. Senescence can be quantified using biomarkers such as population doubling (PD) times, increased lysosomal activity indicated by senescence-associated beta galactosidase (SAB) activity, incorporation of bromodeoxyuridine into proliferating cells, the proliferation-associated Ki67 protein, the DNA damage-associated recruitment of the γH2AX protein, telomere

length quantification, expression of apoptosis/senescence/age-related genes such as *CDKN2A* which is responsible for the production of the senescence-associated proteins of p16 and p14, caspase activity, expression and activity of SASP proteins, and the expression of age-related genes [166].

Clearance of senescent cells (senolysis) makes a striking difference to ageing phenotypes in animal models. The targeted ablation of $p16^{Ink4a}$-positive senescent cells significantly extends lifespan and improves mobility and fur condition in a mouse model of progeria, and in aged wild-type mice [66,75]. Targeted senolysis (using other methods) has also been seen to confer different health benefits across different species, e.g. fur density and renal output in mice, and improvements in the symptoms of patients who have idiopathic pulmonary fibrosis (IPF) and diabetic kidney disease [149,150,272]. The Harries team and others have previously demonstrated it is possible to uncouple features of senescence (such as reversal of SAB staining and re-entry to cell cycle [61]. An ideal senotherapeutic drug would be able to reverse senescence and attenuate SASP, but would not necessarily elicit re-entry to cell cycle, since rejuvenated cells still have a mutation load (a senomorphic effect).

The discovery of senolysis is now being applied to pharmaceutical development. Currently there are a few senolytic compounds (drugs which induce lysis of senescent cells) in clinical trials for diabetic kidney disease and IPF [149,150]. Both trials are testing a combination of dasatinib and quercetin (two individual senolytics). These senolytic drugs target a variety of cellular pathways, e.g. Bcr-Abl, Src, autophagy and protein tyrosine kinase pathways, but reversing the

senescent state (using a senomorphic drug) may also be useful in addition to identification of more senolytic compounds. Several drugs have been identified as having senomorphic properties. For example, resveratrol and several homologues (termed resveralogues), trametinib, and several mitochondria-targeted hydrogen sulphide donors are classed as senomorphic compounds [61,65,151,181]. Often these compounds exhibit a biphasic dose response affecting senescence differently depending on the dose. In one study, resveratrol at 100 μM decreased senescence, but at 5 mM or above increased senescence. Similarly different effects on adipogenic differentiation were noted for doses in the range of 0.1 μM to 10 μM [273]. This range is relatively low for a dose of small molecules, but has been shown to be effective in many senotherapeutic studies applied to cells for a duration of 24-48 hours [61,181,274].

New therapies for any disease can be difficult to come by, with only 15.3% of drugs in phase 1 clinical trials in the US advancing to gain FDA-approval [133]. Repurposing drugs which are already approved for clinical use represents a tactic which avoids the problems with the leaky pipeline of drug development. Given that senolytic and senomorphic compounds are a relatively new class of drugs and that cell fate pathways are involved in many different diseases, it is likely that some licensed drugs have some senomorphic or senolytic capacity. Panels of small molecules for drug repurposing studies can be bought and customised commercially. Due to the fact that senescence is a collection of features and a very heterogeneous phenotype by its nature, any screen for senotherapeutic ability must take several different approaches. The staining of cells for SAB tends to be the “gold standard” approach for identifying changes in general levels of

senescence, however this approach does not lend itself to quick high-throughput screening [166]. Gene expression of *CDKN2A* is a marker for senescence that can be used in a medium-throughput screen for properties associated with senescence. Here, we use both biomarkers in screens to identify compounds with senotherapeutic potential.

Bioinformatics approaches can also be used to complement wet laboratory screening. For example, artificial intelligence techniques, such as deep neural networking, and structure/ligand-based virtual design and screening, can be used for generalised drug discovery [155]. The rise of new machine learning algorithms can aid in deduction of the molecular signatures associated with different drug activities [155]. Deep neural networks (DNNs) have been used to assess active site structure/ligand binding interactions, and predict a drug's functionality based on its structure [214]. DNNs have also been used successfully to screen databases for similarly structured compounds, for assessing the toxicity of novel compounds, and for the creation of novel compounds with structural similarity to an input molecule and prediction of their properties relevant to drug design (absorption, distribution, metabolism, excretion, and toxicity; ADMET) [214,275,276]. These new approaches give much potential in the realm of drug discovery.

Structure-function associations are of particular interest in the context of a screen for senescence. If a certain structure is associated with a senomorphic or senolytic function, then other compounds could be identified from public drug databases by screening them for the structure. This strategy could offer the discovery of novel drugs in a quicker way than traditional pharmaceutical

discovery processes. Similarly, any structural association with a senescence related function could provide mechanistic insight into the cellular processes at hand. Olascoaga-Del Angel *et al.* recently conducted a large-scale structure-function analysis into senotherapeutic properties using several different bioinformatics approaches [152]. They identified several chemotypes associated with senomorphic or senolytic properties, but found there was much overlap between the two functions. We aimed to use our drug panel's structural information and relate this to functional data from the two screens for *CDKN2A* gene expression and SAB activity to inform a small scale bioinformatic analysis of structure-function.

Drug Panel Design and Preparation

A selection of approximately 240 compounds were chosen from the MedChemExpress FDA-Approved Drug Library Plus (MedChemTronica, Stockholm) panel of 2278 compounds. A variety of drugs that target pathways known to affect senescence/cell fate were chosen. Alongside these compounds, other drugs were chosen to cover a variety of known functions, and a variety of common household medicines. The intention was to perform a wide screen for functionality with a balanced targeting of cell fate-related drugs. The drugs that were tested in the initial senescence screen and their known targets are given in Table 14. Previous studies have used 1 μM or 10 μM doses over 24 hours as a starting point for similar screens, so all drugs were screened for *CDKN2A* gene expression at the two doses [61,181].

Compounds and their doses for the SAB activity screen were selected based on their responses in the initial screen for *CDKN2A* gene expression. Two synthetic female hormones were highlighted in the initial screen so an additional synthetic female hormone was added to the SAB activity screen. Levonorgestrel (also known as D-Norgestrel) targets the progesterone receptor. It was added to compare a synthetic progesterone with two synthetic oestrogen compounds.

Compounds were all supplied at 10 mM concentrations in DMSO. The compounds were diluted appropriately in Gibco™ ultrapure RNase/DNase free

water suitable for preparation of cell culture media and laboratory reagents (A1287301, Gibco™). DMSO (J66650.AD, Thermo Scientific Alfa Aesar) was diluted similarly in the same water to provide vehicle-only control treatments for both doses of drug.

Table 14: Information on compound synonyms, targets and pathways used in a screen for CDKN2A gene expression. Information provided from the MedChemExpress FDA-Approved Drug Library Plus (MedChemTronica, Stockholm).

Product Name	Synonyms	Target	Pathway
5-Aminosalicylic Acid	Mesalamine; 5-ASA;Mesalazine	NF-κB; PAK; PPAR	Cell Cycle/DNA Damage; Cytoskeleton; NF-κB
5-Azacytidine	Ladakamycin; 5-AzaC;Azacitidine	Autophagy; DNA Methyltransferase; Nucleoside Antimetabolite/Analog	Autophagy; Cell Cycle/DNA Damage; Epigenetics
5-Fluorouracil	5-FU	Nucleoside Antimetabolite/Analog	Cell Cycle/DNA Damage
6-Thioguanine	Thioguanine; 2-Amino-6-purinethiol	Autophagy; Deubiquitinase; SARS-CoV	Anti-infection; Autophagy; Cell Cycle/DNA Damage
Abemaciclib (methanesulfonate)	LY2835219 (methanesulfonate)	CDK	Cell Cycle/DNA Damage
Acalabrutinib	ACP-196	Btk	Protein Tyrosine Kinase/RTK
Acamprosate (calcium)	Calcium N-acetylhomotaurinate	GABA Receptor	Membrane Transporter/Ion Channel; Neuronal Signalling
Aceglutamide	α-N-Acetyl-L-glutamine; N2-Acetylglutamine	Autophagy; Endogenous Metabolite	Autophagy; Metabolic Enzyme/Protease
Aclacinomycin A hydrochloride	Aclarubicin hydrochloride	Proteasome; Topoisomerase	Cell Cycle/DNA Damage; Metabolic Enzyme/Protease
Allantoin	5-Ureidohydantoin	Endogenous Metabolite; Imidazoline Receptor	GPCR/G Protein; Metabolic Enzyme/Protease; Neuronal Signalling
Alpelisib	BYL-719	PI3K	PI3K/Akt/mTOR
Altretamine	ENT-50852; RB-1515;WR-95704	DNA Alkylator/Crosslinker	Cell Cycle/DNA Damage
Amlexanox	AA673; Amoxanox; CHX3673	IKK	NF-κB

Amoxapine	CL-67772	Others	Others
Amsacrine	m-AMSA; acridinyl anisidide	Autophagy; Topoisomerase	Autophagy; Cell Cycle/DNA Damage
Anethole (trithione)		Others	Others
Apatinib	YN968D1	Autophagy; c-Kit; RET; Src; VEGFR	Autophagy; Protein Tyrosine Kinase/RTK
Artemisinin	Qinghaosu; NSC 369397	HCV; Parasite	Anti-infection
Artesunate		STAT	JAK/STAT Signalling; Stem Cell/Wnt
Aspirin	ASA; Acetylsalicylic Acid	Autophagy; COX; Mitophagy	Autophagy; Immunology/Inflammation
Atorvastatin (hemicalcium salt)	CI-981; Atorvastatin hemicalcium	Autophagy; HMG-CoA Reductase (HMGCR)	Autophagy; Metabolic Enzyme/Protease
Balsalazide		Interleukin Related; STAT	Immunology/Inflammation; JAK/STAT Signalling; Stem Cell/Wnt
Baricitinib (phosphate)	INCB028050 (phosphate); LY3009104 (phosphate)	JAK	Epigenetics; JAK/STAT Signalling; Stem Cell/Wnt
Belinostat	PXD101; PX105684	Autophagy; HDAC	Autophagy; Cell Cycle/DNA Damage; Epigenetics
Belotecan (hydrochloride)	CKD-602	Topoisomerase	Cell Cycle/DNA Damage
Bendamustine (hydrochloride)	SDX-105; EP-3101	DNA Alkylator/Crosslinker	Cell Cycle/DNA Damage
Bendazol		NO Synthase	Immunology/Inflammation
Berberine (chloride hydrate)	Natural Yellow 18 (chloride hydrate)	Autophagy; Bacterial; ROS; Topoisomerase	Anti-infection; Autophagy; Cell Cycle/DNA Damage; Protein Tyrosine Kinase/RTK
Bexarotene	LGD1069	Autophagy; RAR/RXR	Autophagy; Metabolic Enzyme/Protease
Bezafibrate	BM15075	PPAR	Cell Cycle/DNA Damage
Binimetinib	MEK162; ARRY-162; ARRY-438162	Autophagy; MEK	Autophagy; MAPK/ERK Pathway

Bleomycin (sulfate)		Bacterial; DNA/RNA Synthesis	Anti-infection; Cell Cycle/DNA Damage
Bortezomib	PS-341; Brotezamide; DPBA; LDP 341; MG 341; Radiciol; NSC 681239	Apoptosis; Autophagy; Proteasome	Apoptosis; Autophagy; Metabolic Enzyme/Protease
Bosutinib	SKI-606	Autophagy; Bcr-Abl; Src	Autophagy; Protein Tyrosine Kinase/RTK
Bremelanotide (Acetate)	PT-141 Acetate	Melanocortin Receptor	GPCR/G Protein; Neuronal Signalling
Bromhexine (hydrochloride)		Autophagy; Reactive Oxygen Species	Autophagy; Immunology/Inflammation; Metabolic Enzyme/Protease; NF-κB
Bucladesine (sodium salt)	Dibutyryl-cAMP sodium salt; DC2797; Sodium dibutyryl cAMP	PKA	Protein Tyrosine Kinase/RTK; Stem Cell/Wnt
Bufexamac	Bufexamic acid	HDAC	Cell Cycle/DNA Damage; Epigenetics
Busulfan		DNA Alkylator/Crosslinker	Cell Cycle/DNA Damage
Cabazitaxel	XRP6258; RPR-116258A; taxoid XRP6258	Autophagy; Microtubule/Tubulin	Autophagy; Cell Cycle/DNA Damage; Cytoskeleton
Cabozantinib	XL184; BMS-907351	c-Kit; c-Met/HGFR; FLT3; TAM Receptor; VEGFR	Protein Tyrosine Kinase/RTK
Caffeic acid		5-Lipoxygenase; Endogenous Metabolite; TRP Channel	Membrane Transporter/Ion Channel; Metabolic Enzyme/Protease; Neuronal Signalling
Capecitabine		DNA/RNA Synthesis; Nucleoside Antimetabolite/Analog	Cell Cycle/DNA Damage
Carbamazepine	CBZ; NSC 169864	Autophagy; Mitophagy; Sodium Channel	Autophagy; Membrane Transporter/Ion Channel
Carmofur	HCFU	Nucleoside Antimetabolite/Analog	Cell Cycle/DNA Damage

Carmustine		DNA Alkylator/Crosslinker	Cell Cycle/DNA Damage
Carprofen		Autophagy; COX; FAAH	Autophagy; Immunology/Inflammation; Metabolic Enzyme/Protease; Neuronal Signalling
Ceritinib	LDK378	ALK; IGF-1R; Insulin Receptor	Protein Tyrosine Kinase/RTK
Chlorambucil	CB-1348; WR-139013	DNA Alkylator/Crosslinker	Cell Cycle/DNA Damage
Chloroquine (diphosphate)		Autophagy; Toll-like Receptor (TLR)	Autophagy; Immunology/Inflammation
Chlorpheniramine (maleate)	Chlorphenamine maleate	Histamine Receptor	GPCR/G Protein; Immunology/Inflammation; Neuronal Signalling
Chlorzoxazone		Cytochrome P450	Metabolic Enzyme/Protease
Choline Fenofibrate	ABT-335	Cytochrome P450; PPAR	Cell Cycle/DNA Damage; Metabolic Enzyme/Protease
Chromocarb	Chromone-2-carboxylic acid	Others	Others
Ciprofibrate	Win35833	PPAR	Cell Cycle/DNA Damage
Citalopram (hydrobromide)	(±)-Citalopram hydrobromide; Lu 10-171	Autophagy; Serotonin Transporter	Autophagy; Neuronal Signalling
Citric acid		Apoptosis; Endogenous Metabolite	Apoptosis; Metabolic Enzyme/Protease
Clioquinol	Iodochlorhydroxyquin	Autophagy; Fungal; Mitophagy	Anti-infection; Autophagy
Clofarabine		Autophagy; Nucleoside Antimetabolite/Analog	Autophagy; Cell Cycle/DNA Damage
Clofibrate		PPAR	Cell Cycle/DNA Damage
Cobimetinib	GDC-0973; XL518	MEK	MAPK/ERK Pathway

Colchicine		Autophagy; Microtubule/Tubulin	Autophagy; Cell Cycle/DNA Damage; Cytoskeleton
Conivaptan (hydrochloride)	YM 087	Vasopressin Receptor	GPCR/G Protein
Crizotinib (hydrochloride)	PF-02341066 hydrochloride	ALK; Autophagy; c-Met/HGFR	Autophagy; Protein Tyrosine Kinase/RTK
Cytarabine	Cytosine β-D-arabinofuranoside; Cytosine Arabinoside; Ara-C	Autophagy; DNA/RNA Synthesis; Nucleoside Antimetabolite/Analog	Autophagy; Cell Cycle/DNA Damage
Dabrafenib	GSK2118436A; GSK2118436	Raf	MAPK/ERK Pathway
Dacarbazine	Imidazole Carboxamide	Nucleoside Antimetabolite/Analog	Cell Cycle/DNA Damage
Dacomitinib	PF-00299804; PF-299804	EGFR	JAK/STAT Signalling; Protein Tyrosine Kinase/RTK
Dasatinib (hydrochloride)	BMS 354825 hydrochloride	Autophagy; Bcr-Abl; Src	Autophagy; Protein Tyrosine Kinase/RTK
Daunorubicin (Hydrochloride)	RP 13057 (Hydrochloride); Daunomycin (Hydrochloride); Rubidomycin (Hydrochloride)	ADC Cytotoxin; Autophagy; DNA/RNA Synthesis; Topoisomerase	Antibody-drug Conjugate/ADC Related; Autophagy; Cell Cycle/DNA Damage
Decitabine	NSC 127716; 5-Aza-2'-deoxycytidine	DNA Methyltransferase	Epigenetics
Deferoxamine (mesylate)	Desferrioxamine B mesylate; DFOM	Amyloid-β; Autophagy; Mitophagy	Autophagy; Neuronal Signalling

Dexamethasone	Hexadecadrol; Prednisolone F	Autophagy; Glucocorticoid Receptor; Mitophagy	Autophagy; GPCR/G Protein
Diacerein	Diacerhein; Diacetylrhein	Interleukin Related	Immunology/Inflammation
Diethylstilboestrol	DES; Diethylstilbestrol; Stilbestrol	Estrogen Receptor/ERR	Others
Dimethyl fumarate	DMF	Keap1-Nrf2	NF-κB
Disulfiram	Tetraethylthiuram disulfide; TETD	Aldehyde Dehydrogenase (ALDH); Apoptosis; Interleukin Related	Apoptosis; Immunology/Inflammation; Metabolic Enzyme/Protease
Docetaxel	RP-56976	Microtubule/Tubulin	Cell Cycle/DNA Damage; Cytoskeleton
Doxifluridine	Ro 21-9738; 5-Fluoro-5'-deoxyuridine; 5'-DFUR	Nucleoside Antimetabolite/Analog	Cell Cycle/DNA Damage
Doxorubicin (hydrochloride)	Hydroxydaunorubicin (hydrochloride)	ADC Cytotoxin; AMPK; Autophagy; Mitophagy; Topoisomerase	Antibody-drug Conjugate/ADC Related; Autophagy; Cell Cycle/DNA Damage; Epigenetics; PI3K/Akt/mTOR
Dronedarone	SR 33589	Autophagy; mAChR	Autophagy; GPCR/G Protein; Neuronal Signalling
Duvelisib	IPI-145; INK1197	PI3K	PI3K/Akt/mTOR
Emtricitabine	BW1592	HIV; Reverse Transcriptase	Anti-infection
Enasidenib	AG-221	Isocitrate Dehydrogenase (IDH)	Metabolic Enzyme/Protease
Entacapone		COMT	Metabolic Enzyme/Protease; Neuronal Signalling
Entrectinib	NMS-E628; RXDX-101	ALK; Autophagy; ROS; Trk Receptor	Autophagy; Neuronal Signalling; Protein Tyrosine Kinase/RTK
Epirubicin (hydrochloride)	4'-Epidoxorubicin hydrochloride	Topoisomerase	Cell Cycle/DNA Damage
Erdosteine	RV 144	NF-κB	NF-κB

Erlotinib	CP-358774; NSC 718781; OSI-774	Autophagy; EGFR	Autophagy; JAK/STAT Signalling; Protein Tyrosine Kinase/RTK
Erlotinib (Hydrochloride)	CP-358774 (Hydrochloride); NSC 718781 (Hydrochloride); OSI-774 (Hydrochloride)	Autophagy; EGFR	Autophagy; JAK/STAT Signalling; Protein Tyrosine Kinase/RTK
Estramustine (phosphate sodium)		Microtubule/Tubulin	Cell Cycle/DNA Damage; Cytoskeleton
Ethamsylate		Prostaglandin Receptor	GPCR/G Protein
Ethynyl Estradiol	17α-Ethynylestradiol; Ethynylestradiol	Endogenous Metabolite; Estrogen Receptor/ERR	Metabolic Enzyme/Protease; Others
Etoposide	VP-16; VP-16-213	Apoptosis; Autophagy; Mitophagy; Topoisomerase	Apoptosis; Autophagy; Cell Cycle/DNA Damage
Ezetimibe	SCH 58235	Autophagy; Keap1-Nrf2	Autophagy; NF-κB
Fasudil (Hydrochloride)	HA-1077 (Hydrochloride); AT-877 (Hydrochloride)	Autophagy; Calcium Channel; ROCK	Autophagy; Cell Cycle/DNA Damage; Membrane Transporter/Ion Channel; Neuronal Signalling; Stem Cell/Wnt; TGF-beta/Smad
Favipiravir	T-705	DNA/RNA Synthesis	Cell Cycle/DNA Damage
Fenofibrate		Autophagy; Cytochrome P450; PPAR	Autophagy; Cell Cycle/DNA Damage; Metabolic Enzyme/Protease
Fenofibric acid	FNF acid	COX; PPAR	Cell Cycle/DNA Damage; Immunology/Inflammation
Fingolimod	FTY720 free base	LPL Receptor; PAK	Cell Cycle/DNA Damage; Cytoskeleton; GPCR/G Protein
Floxuridine	5-Fluorouracil 2'-deoxyriboside	Nucleoside Antimetabolite/Analog	Cell Cycle/DNA Damage

Flubendazole		Apoptosis; Microtubule/Tubulin; Parasite	Anti-infection; Apoptosis; Cell Cycle/DNA Damage; Cytoskeleton
Fludarabine	F-ara-A; NSC 118218	DNA/RNA Synthesis; Nucleoside Antimetabolite/Analog; STAT	Cell Cycle/DNA Damage; JAK/STAT Signalling; Stem Cell/Wnt
Fluvastatin (sodium)	XU 62320 sodium	Autophagy; HMG-CoA Reductase (HMGCR)	Autophagy; Metabolic Enzyme/Protease
Folic acid	Vitamin B9; Vitamin M	DNA/RNA Synthesis; Endogenous Metabolite	Cell Cycle/DNA Damage; Metabolic Enzyme/Protease
Forodesine (hydrochloride)	BCX-1777; Immucillin-H hydrochloride	Nucleoside Antimetabolite/Analog	Cell Cycle/DNA Damage
Fostamatinib Disodium	R788(Disodium)	Syk	Protein Tyrosine Kinase/RTK
Gefitinib (hydrochloride)	ZD-1839 hydrochloride	EGFR	JAK/STAT Signalling; Protein Tyrosine Kinase/RTK
Gemcitabine	NSC 613327; LY188011	Autophagy; DNA/RNA Synthesis; Nucleoside Antimetabolite/Analog	Autophagy; Cell Cycle/DNA Damage
Gemfibrozil	CI-719	Cytochrome P450; PPAR	Cell Cycle/DNA Damage; Metabolic Enzyme/Protease
Glasdegib	PF-04449913	Smo	Stem Cell/Wnt
Glycerol phenylbutyrate	HPN-100	Others	Others
Homoharringtonine	Omacetaxine mepesuccinate; HHT	STAT	JAK/STAT Signalling; Stem Cell/Wnt
Hydrocortisone	Cortisol	Endogenous Metabolite; Glucocorticoid Receptor	GPCR/G Protein; Metabolic Enzyme/Protease

Hydroxychloroquine sulfate	HCQ sulfate	Autophagy; Parasite; Toll-like Receptor (TLR)	Anti-infection; Autophagy; Immunology/Inflammation
Hydroxyfasudil	HA-1100	ROCK	Cell Cycle/DNA Damage; Stem Cell/Wnt; TGF-beta/Smad
Hydroxyurea	Hydroxycarbamide	Apoptosis; Autophagy; DNA/RNA Synthesis	Apoptosis; Autophagy; Cell Cycle/DNA Damage
Ibuprofen	(±)-Ibuprofen	COX	Immunology/Inflammation
Idarubicin (hydrochloride)	4-Demethoxydaunorubicin hydrochloride	Autophagy; Topoisomerase	Autophagy; Cell Cycle/DNA Damage
Idelalisib	CAL-101; GS-1101	Autophagy; PI3K	Autophagy; PI3K/Akt/mTOR
Imatinib	STI571; CGP-57148B	Autophagy; Bcr-Abl; c-Kit; PDGFR	Autophagy; Protein Tyrosine Kinase/RTK
Indomethacin	Indometacin	Autophagy; COX	Autophagy; Immunology/Inflammation
Irinotecan (hydrochloride)	CPT-11 hydrochloride; Camptothecin 11 hydrochloride	Autophagy; Topoisomerase	Autophagy; Cell Cycle/DNA Damage
Isotretinoin	13-cis-Retinoic acid	Autophagy; Endogenous Metabolite; RAR/RXR	Autophagy; Metabolic Enzyme/Protease
Ixabepilone	Azaepothilone B; BMS 247550;BMS 247550-1	Apoptosis; Microtubule/Tubulin	Apoptosis; Cell Cycle/DNA Damage; Cytoskeleton
Lamivudine	BCH-189	HIV; Reverse Transcriptase	Anti-infection
Lanatoside C		Autophagy	Autophagy
Lapatinib	GW572016	Autophagy; EGFR	Autophagy; JAK/STAT Signalling; Protein Tyrosine Kinase/RTK
LCZ696	Sacubitril mixture with Valsartan	Angiotensin Receptor; JNK; Neprilysin; NF-κB; p38 MAPK	GPCR/G Protein; MAPK/ERK Pathway; Metabolic Enzyme/Protease; NF-κB

L-Epinephrine (Bitartrate)	(-)-Epinephrine (+)-bitartrate salt; L-Adrenaline (+)-bitartrate salt	Adrenergic Receptor	GPCR/G Protein; Neuronal Signalling
Levoleucovorin (Calcium)	Calcium levofolinate; CL307782	Antifolate	Cell Cycle/DNA Damage
Lidocaine (hydrochloride)	Lignocaine hydrochloride	ERK; MEK; NF-κB; Sodium Channel	MAPK/ERK Pathway; Membrane Transporter/Ion Channel; NF-κB; Stem Cell/Wnt
Loperamide (hydrochloride)	R-18553 (hydrochloride)	Autophagy; Opioid Receptor	Autophagy; GPCR/G Protein; Neuronal Signalling
Lovastatin	Mevinolin	Autophagy; HMG-CoA Reductase (HMGCR)	Autophagy; Metabolic Enzyme/Protease
Melphalan	L-PAM	DNA Alkylator/Crosslinker	Cell Cycle/DNA Damage
Memantine (hydrochloride)	D-145 (hydrochloride)	Autophagy; Cytochrome P450; iGluR	Autophagy; Membrane Transporter/Ion Channel; Metabolic Enzyme/Protease; Neuronal Signalling
Metformin (hydrochloride)	1,1-Dimethylbiguanide hydrochloride	AMPK; Autophagy; Mitophagy	Autophagy; Epigenetics; PI3K/Akt/mTOR
Methotrexate	Amethopterin; CL14377;WR19039	ADC Cytotoxin; Antifolate	Antibody-drug Conjugate/ADC Related; Cell Cycle/DNA Damage
Methylthiouracil	MTU	ERK; Interleukin Related; NF-κB; TNF Receptor	Apoptosis; Immunology/Inflammation; MAPK/ERK Pathway; NF-κB; Stem Cell/Wnt
Metyrapone	Su-4885	Autophagy; Cytochrome P450	Autophagy; Metabolic Enzyme/Protease
Mifepristone	RU486; RU 38486	Autophagy; Glucocorticoid Receptor; Progesterone Receptor	Autophagy; GPCR/G Protein; Others

Miltefosine	HePC; Hexadecyl phosphocholine	Akt; HIV	Anti-infection; PI3K/Akt/mTOR
Mitomycin C	Ametycine	ADC Cytotoxin; Autophagy; DNA Alkylator/Crosslinker; DNA/RNA Synthesis	Antibody-drug Conjugate/ADC Related; Autophagy; Cell Cycle/DNA Damage
Mitoxantrone	Mitozantrone	PKC; Topoisomerase	Cell Cycle/DNA Damage; Epigenetics; TGF-beta/Smad
Mizoribine	NSC 289637; HE 69	HSP	Cell Cycle/DNA Damage; Metabolic Enzyme/Protease
Montelukast (sodium)	MK0476	Autophagy; Leukotriene Receptor	Autophagy; GPCR/G Protein
Mycophenolic acid	Mycophenolate	Others	Others
Nedaplatin	NSC 375101D	DNA/RNA Synthesis	Cell Cycle/DNA Damage
Nefopam (hydrochloride)	Fenazoxine hydrochloride	β-catenin	Stem Cell/Wnt
Nelarabine	506U78; GW 506U78; Nelzarabine	Nucleoside Antimetabolite/Analog	Cell Cycle/DNA Damage
Neratinib	HKI-272	EGFR	JAK/STAT Signalling; Protein Tyrosine Kinase/RTK
Niclosamide	BAY2353	STAT	JAK/STAT Signalling; Stem Cell/Wnt
Nicotinamide	Niacinamide; Nicotinic acid amide; Vitamin B3	Endogenous Metabolite; Sirtuin	Cell Cycle/DNA Damage; Epigenetics; Metabolic Enzyme/Protease
Nifuroxazide		STAT	JAK/STAT Signalling; Stem Cell/Wnt
Niraparib	MK-4827	PARP	Cell Cycle/DNA Damage; Epigenetics
Nitisinone	NTBC; Nitisone;SC0735	Reactive Oxygen Species	Immunology/Inflammation; Metabolic Enzyme/Protease; NF-κB
Olaparib	AZD2281; KU0059436	Autophagy; Mitophagy; PARP	Autophagy; Cell Cycle/DNA Damage; Epigenetics

Opicapone	BIA 9-1067	COMT	Metabolic Enzyme/Protease; Neuronal Signalling
Orotic acid	6-Carboxyuracil; Vitamin B13	Endogenous Metabolite; Nucleoside Antimetabolite/Analog	Cell Cycle/DNA Damage; Metabolic Enzyme/Protease
Osalmid	Oxaphenamide; 4'-Hydroxysalicylanilide	HBV	Anti-infection
Paclitaxel	Taxol	ADC Cytotoxin; Autophagy; Microtubule/Tubulin	Antibody-drug Conjugate/ADC Related; Autophagy; Cell Cycle/DNA Damage; Cytoskeleton
Palbociclib (hydrochloride)	PD 0332991 hydrochloride	CDK	Cell Cycle/DNA Damage
Pamidronic acid		Wnt; β-catenin	Stem Cell/Wnt
Panobinostat	LBH589; NVP-LBH589	Autophagy; HDAC	Autophagy; Cell Cycle/DNA Damage; Epigenetics
Pazopanib	GW786034	Autophagy; c-Kit; FGFR; PDGFR; VEGFR	Autophagy; Protein Tyrosine Kinase/RTK
Pazopanib (Hydrochloride)	GW786034 (Hydrochloride)	Autophagy; c-Fms; c-Kit; FGFR; PDGFR; VEGFR	Autophagy; Protein Tyrosine Kinase/RTK
Peficitinib	ASP015K; JNJ-54781532	JAK	Epigenetics; JAK/STAT Signalling; Stem Cell/Wnt
Pemetrexed (disodium hemipenta hydrate)	LY231514 (disodium hemipenta hydrate)	Antifolate; Autophagy	Autophagy; Cell Cycle/DNA Damage
Penfluridol	R-16341	Autophagy; Calcium Channel	Autophagy; Membrane Transporter/Ion Channel; Neuronal Signalling
Pexidartinib	PLX-3397	c-Fms; c-Kit	Protein Tyrosine Kinase/RTK
Phenindione	Rectadione	Others	Others
Pioglitazone	U 72107	PPAR	Cell Cycle/DNA Damage

Pipobroman		Others	Others
Pirfenidone	AMR69	TGF-beta/Smad	Stem Cell/Wnt; TGF-beta/Smad
Pixantrone (dimaleate)	BBR 2778 dimaleate	Topoisomerase	Cell Cycle/DNA Damage
Podofilox	Podophyllotoxin	Microtubule/Tubulin	Cell Cycle/DNA Damage; Cytoskeleton
Ponatinib	AP24534	Autophagy; Bcr-Abl; FGFR; PDGFR; Src; VEGFR	Autophagy; Protein Tyrosine Kinase/RTK
Pralatrexate		Antifolate	Cell Cycle/DNA Damage
Pranlukast	ONO-1078	Leukotriene Receptor	GPCR/G Protein
Procarbazine (Hydrochloride)		DNA Alkylator/Crosslinker	Cell Cycle/DNA Damage
Propranolol (hydrochloride)		Adrenergic Receptor; Autophagy	Autophagy; GPCR/G Protein; Neuronal Signalling
Pyrimethamine	Pirimecidan; Pirimetamin; RP 4753	Antifolate; Parasite	Anti-infection; Cell Cycle/DNA Damage
Pyrvinium pamoate	Pyrvinium embonate	Wnt	Stem Cell/Wnt
Quinapril (hydrochloride)	CI-906	Angiotensin-converting Enzyme (ACE)	Metabolic Enzyme/Protease
Raloxifene (hydrochloride)	LY156758 hydrochloride; LY139481 hydrochloride	Autophagy; Estrogen Receptor/ERR	Autophagy; Others
Raltitrexed	ZD1694; D1694; ICI-D1694	Nucleoside Antimetabolite/Analog; Thymidylate Synthase	Apoptosis; Cell Cycle/DNA Damage
Rasagiline (mesylate)	AGN1135 (mesylate); TVP1012 (mesylate)	Autophagy; Monoamine Oxidase	Autophagy; Neuronal Signalling
Regorafenib (monohydrate)	BAY 73-4506 monohydrate	Autophagy; PDGFR; Raf; RET; VEGFR	Autophagy; MAPK/ERK Pathway; Protein Tyrosine Kinase/RTK
Resveratrol	SRT 501; trans-Resveratrol	Autophagy; IKK; Mitophagy; Sirtuin	Autophagy; Cell Cycle/DNA Damage; Epigenetics; NF-κB

Retinoic acid	ATRA; Tretinoin; Vitamin A acid; all-trans-Retinoic acid	Autophagy; Endogenous Metabolite; PPAR; RAR/RXR	Autophagy; Cell Cycle/DNA Damage; Metabolic Enzyme/Protease
Ribociclib	LEE011	CDK	Cell Cycle/DNA Damage
Ripasudil	K-115	ROCK	Cell Cycle/DNA Damage; Stem Cell/Wnt; TGF-beta/Smad
Rosiglitazone	BRL 49653	Autophagy; PPAR; TRP Channel	Autophagy; Cell Cycle/DNA Damage; Membrane Transporter/Ion Channel; Neuronal Signalling
Rucaparib (phosphate)	AG-014699 phosphate; PF-01367338 phosphate	PARP	Cell Cycle/DNA Damage; Epigenetics
Ruxolitinib	INCB018424	Autophagy; JAK; Mitophagy	Autophagy; Epigenetics; JAK/STAT Signalling; Stem Cell/Wnt
Salicylic acid	2-Hydroxybenzoic acid	Autophagy; COX; Endogenous Metabolite; Mitophagy	Autophagy; Immunology/Inflammation; Metabolic Enzyme/Protease
Selumetinib	AZD6244; ARRY-142886	MEK	MAPK/ERK Pathway
Sertraline (hydrochloride)		Serotonin Transporter	Neuronal Signalling
Sildenafil	UK-92480	Autophagy; Phosphodiesterase (PDE)	Autophagy; Metabolic Enzyme/Protease
Silibinin	Silybin; Silibinin A; Silymarin I	Autophagy; Reactive Oxygen Species	Autophagy; Immunology/Inflammation; Metabolic Enzyme/Protease; NF-κB
Sitagliptin	MK0431	Autophagy; Dipeptidyl Peptidase	Autophagy; Metabolic Enzyme/Protease
Sodium phenylbutyrate	Sodium 4-phenylbutyrate; TriButyrate	Autophagy; HDAC	Autophagy; Cell Cycle/DNA Damage; Epigenetics
Sorafenib	Bay 43-9006	Autophagy; FLT3; Raf; VEGFR	Autophagy; MAPK/ERK Pathway; Protein Tyrosine Kinase/RTK

Sulfasalazine	NSC 667219	Autophagy; NF-κB	Autophagy; NF-κB
Sunitinib	SU 11248	Autophagy; Mitophagy; PDGFR; VEGFR	Autophagy; Protein Tyrosine Kinase/RTK
Tacrolimus (monohydrate)	FK506 (monohydrate); Fujimycin (monohydrate); FR900506 (monohydrate)	Autophagy; FKBP; Phosphatase	Apoptosis; Autophagy; Immunology/Inflammation; Metabolic Enzyme/Protease
Talazoparib	BMN-673; LT-673	PARP	Cell Cycle/DNA Damage; Epigenetics
Tamoxifen	ICI47699; Z-Tamoxifen; trans-Tamoxifen	Autophagy; Oestrogen Receptor/ERR	Autophagy; Others
Taurodeoxychloic Acid (sodium hydrate)	Sodium taurodeoxycholate monohydrate	Apoptosis; Caspase	Apoptosis
Tegafur	FT 207; NSC 148958	Nucleoside Antimetabolite/Analog	Cell Cycle/DNA Damage
Telmisartan	BIBR 277	Angiotensin Receptor; Autophagy	Autophagy; GPCR/G Protein
Temozolomide	NSC 362856; CCRG 81045; TMZ	Autophagy; DNA Alkylator/Crosslinker	Autophagy; Cell Cycle/DNA Damage
Temsirolimus	CCI-779	Autophagy; mTOR	Autophagy; PI3K/Akt/mTOR
Teniposide	VM26	Topoisomerase	Cell Cycle/DNA Damage
Teprenone	Geranylgeranylacetone	HSP	Cell Cycle/DNA Damage; Metabolic Enzyme/Protease
Terazosin (hydrochloride dihydrate)		Adrenergic Receptor	GPCR/G Protein; Neuronal Signalling
Theophylline	1,3-Dimethylxanthine; Theo-24	Adenosine Receptor; Autophagy; Endogenous	Autophagy; GPCR/G Protein; Metabolic Enzyme/Protease

		Metabolite; Phosphodiesterase (PDE)	
Thio-TEPA		DNA Alkylator/Crosslinker	Cell Cycle/DNA Damage
Tofacitinib (citrate)	Tasocitinib citrate; CP-690550 citrate	JAK	Epigenetics; JAK/STAT Signalling; Stem Cell/Wnt
Topotecan (Hydrochloride)	SKF 104864A (Hydrochloride); NSC 609669 (Hydrochloride)	Autophagy; Topoisomerase	Autophagy; Cell Cycle/DNA Damage
Trametinib (DMSO solvate)	GSK-1120212 (DMSO solvate); JTP-74057 (DMSO solvate)	MEK	MAPK/ERK Pathway
Tranylcypromine (hemisulfate)	dl-Tranylcypromine hemisulfate; trans-2-Phenylcyclopropylamine hemisulfate salt	Histone Demethylase; Monoamine Oxidase	Epigenetics; Neuronal Signalling
Triclabendazole	CGA89317	Microtubule/Tubulin	Cell Cycle/DNA Damage; Cytoskeleton
Trifluridine	Trifluorothymidine; 5-Trifluorothymidine; TFT	HSV; Nucleoside Antimetabolite/Analog; Thymidylate Synthase	Anti-infection; Apoptosis; Cell Cycle/DNA Damage
Trimethoprim		Antifolate	Cell Cycle/DNA Damage
Troglitazone	CS-045	Autophagy; PPAR	Autophagy; Cell Cycle/DNA Damage
Troxipide		Others	Others
Tucidinostat	Chidamide; HBI-8000;CS 055	HDAC	Cell Cycle/DNA Damage; Epigenetics
Upadacitinib	ABT-494	JAK	Epigenetics; JAK/STAT Signalling; Stem Cell/Wnt
VAL-083	Dianhydrodulcitol; Dianhydrogalactitol	DNA Alkylator/Crosslinker	Cell Cycle/DNA Damage

Valproic acid (sodium salt)	Sodium Valproate	Autophagy; HDAC; Mitophagy	Autophagy; Cell Cycle/DNA Damage; Epigenetics
Valpromide		Others	Others
Valrubicin	AD-32	PKC	Epigenetics; TGF-beta/Smad
Vemurafenib	PLX4032; RG7204; RO5185426	Autophagy; Raf	Autophagy; MAPK/ERK Pathway
Venetoclax	ABT-199; GDC-0199	Autophagy; Bcl-2 Family	Apoptosis; Autophagy
Vidarabine	Ara-A; Adenine Arabinoside; 9-β-D-Arabinofuranosyladenine	HSV; Nucleoside Antimetabolite/Analog	Anti-infection; Cell Cycle/DNA Damage
Vinblastine (sulfate)	Vincaleukoblastine sulfate salt	Autophagy; Microtubule/Tubulin	Autophagy; Cell Cycle/DNA Damage; Cytoskeleton
Vinorelbine (ditartrate)	KW-2307; Nor-5'-anhydrovinblastine ditartrate	Autophagy; Microtubule/Tubulin	Autophagy; Cell Cycle/DNA Damage; Cytoskeleton
Vorinostat	SAHA	Autophagy; HDAC; Mitophagy	Autophagy; Cell Cycle/DNA Damage; Epigenetics
Zidovudine	Azidothymidine; AZT; ZDV	CRISPR/Cas9; HIV	Anti-infection; Cell Cycle/DNA Damage

Tissue culture

Normal human dermal fibroblasts (nHDFs) were commercially derived with ethical permission and purchased from Promocell, Heidelberg (catalogue number C-12302, lot number 445Z026.3). For further information including donor details, please view Chapter 2: Tissue culture, Chapter 3: Considerations for the replacement of foetal bovine serum with human serum and other alternative supplements in cell culture, and Chapter 4: Materials & Methods. nHDF cells had cumulated population doublings (cPDL) of an average of 38.91 (range of 34.41 - 40.13 cPDL) at the time of seeding out for the screen of *CDKN2A* gene expression. Cell counts were taken at every passage with a Hirschmann haemocytometer which, together with the cPDL numbers given by Promocell, enabled assessment of cPDL at the time of seeding for experiments. In the SAB activity screen, cells at passage 11 were termed younger (cPDL of 32.69 for all) for investigating the induction of senescence. For investigating the reduction of senescence, cells at passage 21, termed older, were used. These older cells had an average cPDL of 41.92 (range 40.77 - 43.2). PD time is not the most stable of metrics when dealing with primary cells, but nHDF cells at approximately 33.71 cPDL averaged half the PD time of cells at approximately 38.66 cPDL. SAB activity is markedly increased in the latter compared to the former cells (data not shown) meaning these cells are sufficient to model replicative senescence levels in early and late passages. For the *CDKN2A* gene expression screen, cells were seeded out in 96-well plates at 6000 cells per well (a density of 1880 cells/cm^2). For the SAB activity screen, cells were seeded out in 12-well plates at an average seeding density of 6226 cells/cm^2. Cells were grown in antibiotic-free media for

48 to 72 hours before seeding, and all treatments were performed without the presence of antibiotics in the medium.

Treatment for CDKN2A gene expression screen

For the *CDKN2A* screen, cells were grown in their wells for 72 hours before treatment. Dose and incubation times were informed by previous work from our research group and the literature as discussed in the introduction [61,181,274]. On the day of treatment, the medium was removed and replaced with 135 µl of fresh medium and 15 µl of the appropriate stock solution of each drug or control was applied. The drug or control was applied for 24 hours before two washes in DPBS (14190136, Gibco™) and performing the RNA extraction.

Treatment for SAB activity screen

Cells were grown for 24 to 48 hours before treatment following the dose and incubation time rationale as for the prior *CDKN2A* screen. On the day of treatment, the medium was removed and replaced with 1485 µl of fresh medium, and 135 µl of the appropriate stock solution of each drug or control was applied. The drug was applied for 24 hours before being washed twice in DPBS and performing the SAB activity assay.

RNA extraction

The PureLink™ Pro 96 RNA Purification Kit (12173–011A, Fisher Scientific) was used to extra RNA from cells grown in 96-well plates for the *CDKN2A* gene expression screen. The protocol followed the manufacturer's instructions and used 45 µl of RNase-free water for elution. A selection of samples were tested for RNA quality and quantity using the Thermo Scientific™ Nanodrop 8000 Spectrophotometer (Thermo Fisher Scientific, Waltham, Massachusetts, USA). RNA concentration ranged from 5.5 - 9.7 ng/µl across the samples measured.

Reverse transcription

cDNA was produced by reverse transcription using the High-Capacity cDNA Reverse Transcription Kit as detailed in Chapter 2: Measurement of gene expression. Given the very narrow range of RNA concentrations and low yield, the maximum volume possible of RNA was used in the reverse transcription reaction without adjustment to standardise the RNA concentration in each reaction.

Real-time quantitative PCR (RT-qPCR)

For more details on the RT-qPCR method used, please view Chapter 2: Measurement of gene expression. 50 cycles of RT-qPCR were performed. Real-time quantitative PCR (RT-qPCR) was run as two biological and three technical replicates for each compound/control at each dose (1 µM and 10 µM).

Analysis of RT-qPCR data

The relative gene expression was calculated using the comparative C_T technique, relative to the geometric mean expression level of three housekeeping genes (*PGK1*, *PPIA* and *UBC*) [176]. These three genes were shown by Reffinder analysis using the online Reffinder website to be the most stable three genes of a selection of six endogenous housekeeping genes in an earlier preliminary experiment (data not shown) [177]. The geometric mean of the three genes provided the best baseline for comparison across all compounds when analysed again using the Reffinder website. Following normalisation to the housekeeping genes, each biological replicate was normalised to the average of the appropriate dose's vehicle-only control on the plate. The results were expressed as a ratio for comparison and the natural log was used to aid against any skew of data. Due to experimental resource constraints, the experiment could only be performed for two biological replicates. A technical error resulted in poor RNA quality for two experimental plates of the twelve in total. The PCR results from these two plates were subsequently omitted from further analysis due to this error. The mean ± three standard deviations was used to provide upper and lower bounds for determination of effects for informing later validation of results.

Cellular Senescence Staining Assay

The Senescence Cells Histochemical Staining kit (CS0030, Merck) was applied following the manufacturer's instructions to stain for senescence-associated beta

galactosidase (SAB). Further detail is available in Chapter 2: Measurement of cellular senescence and Chapter 2: Analysis of staining.

Bioinformatic analysis using fmcsR

Structural information on each compound (used in the screens for *CDKN2A* gene expression and SAB activity) was given by the supplier (MedChemTronica, Stockholm). The SMILES (simplified molecular input line entry system) data was transformed into SDF (structure data file) data for analysis with ChemmineR and fmcsR packages in Rstudio software version 4.1.0 [178–180,277]. The Tanimoto coefficient was computed for each pair of compounds and used to construct a similarity matrix. The average Tanimoto coefficient within the matrix constructed for a test group of functionally related compounds was compared against the average Tanimoto coefficient within a control group of compounds. All compounds within a group are compared against each other which results in the number of values being the square of the number of compounds. A significant difference indicates that certain structures are more common in the test group suggesting a structure associated with the function. A dendrogram is computed to illustrate the similarities between compounds, and the exact maximum common substructure can be computed for the two least similar compounds to identify the maximum common substructure across the whole test group.

This method was validated using a test group of a selection of compounds that target the oestrogen receptor versus a selection of 30 other compounds as a control group. The test group compounds are known to be structurally and

functionally similar and so this constitutes validation of the methodology. The pipeline was tested with a test group of 30 compounds. The number of oestrogenic compounds and other non-oestrogenic compounds in the test group was varied to assess the sensitivity of the method using 30, 10, 4, 3 and 2 oestrogenic compounds in a group of other compounds totalling 30 for comparison against the control group. Only the test group consisting of 30 oestrogenic compounds versus 30 unknown other compounds was significantly different. Ten oestrogenic compounds compared against ten non-oestrogenic compounds showed significance. This method is not very sensitive. Three experiments were performed using this process. The first two test groups were the compounds that had either increased or decreased *CDKN2A* gene expression the most (averaged across both doses). The third test group was a selection of compounds that had decreased SAB activity in the screen. Control groups for all three tests were selected based on the compounds with the least effect on *CDKN2A* expression and were matched to the number of compounds in each test group. That is to say the compounds were ranked by their effect on *CDKN2A* averaged across both doses, and the compounds with the closest effects on expression to zero were chosen to act as a non-functionally associated control group.

Statistics

Graphs were produced using GraphPad Prism version 9.4.1 for Windows (GraphPad Software, San Diego, California USA, www.graphpad.com) or

Microsoft Office Excel. Error bars on the graphs represent the standard error of the mean (SEM) unless otherwise stated.

Due to resource limitations, the number of biological replicates (n = 2) for the screen of effects on CDKN2A gene expression was insufficient for statistical analysis. Given that this was a first-pass screen for further validation of any observations, we needed to identify the largest effects and use these to inform the selection of compounds for the next screen for SAB activity. The largest effects were measured using the control groups' mean ± several measures of variation (SEM, and one or three standard deviations (SD)) as noted in the results). For most compounds, if the fold change in gene expression exceeded an upper or lower bound which was created from the mean ± three SDs of the appropriate control group, the effect was deemed to be sufficiently large that the compounds may be worthy of further investigation.

Statistical analysis of SAB activity and average structural similarity was performed using Graphpad Prism version 9.4.1. A one-way ANOVA with an uncorrected Fisher's LSD post hoc test was applied to assess significance between each treatment and its associated control for the SAB activity screen. An unpaired t test was used to assess significant differences in the average Tanimoto coefficients in a test group of functionally related compounds and a control group.

Drug panel design

The drug panel for the initial screen was designed to select compounds that target cell fate pathways, as well as a variety of commonly taken medicines. Figure 25 illustrates the variety of compounds screened. Most compounds are FDA-approved with the remainder approved by the EMA or other countries. The compounds are linked with a number of disease research areas. Perhaps unsurprisingly, given the bias towards cell fate pathways, the most frequent research area is for cancer therapies. The compounds are most commonly associated with pathways such as cell fate and autophagy. Similarly, the most frequently reported drug target amongst the compounds was apoptosis, however a wide range of drug targets were reported.

a)

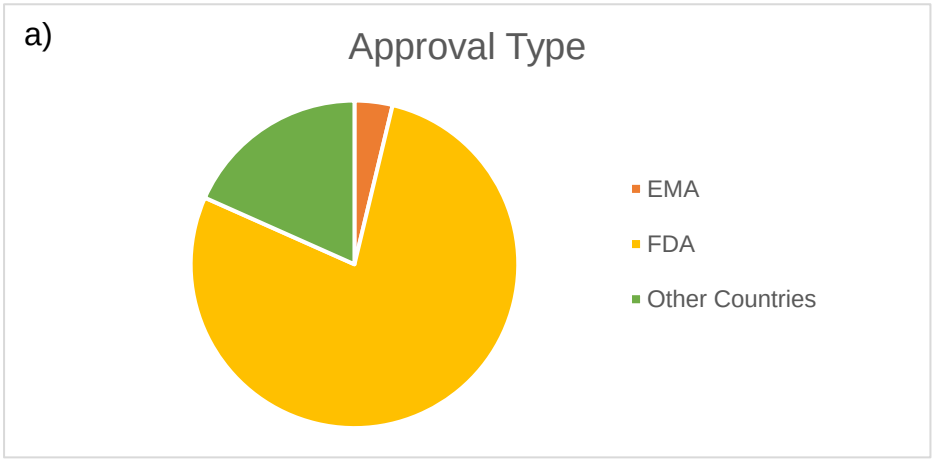
Approval Type
EMA
FDA
Other Countries

b)

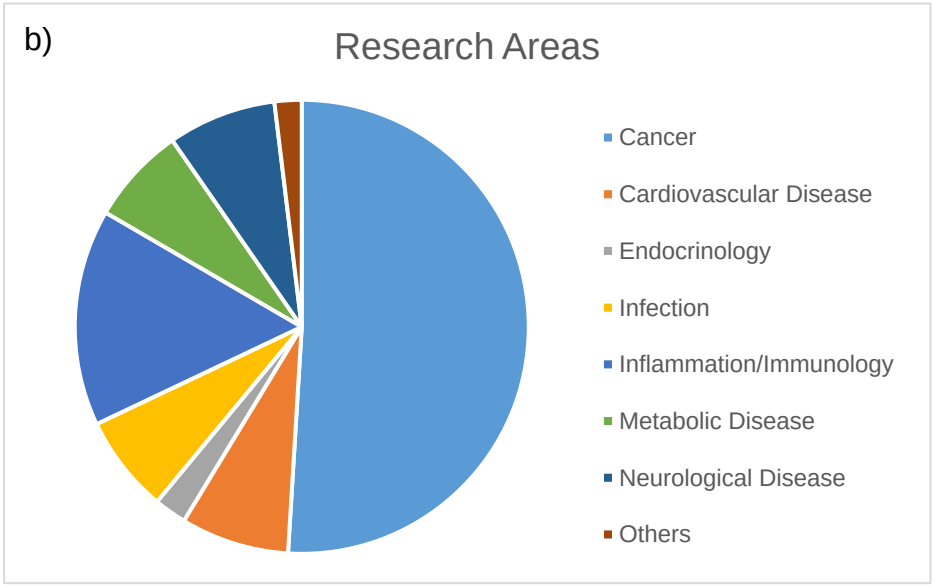
Research Areas
Cancer
Cardiovascular Disease
Endocrinology
Infection
Inflammation/Immunology
Metabolic Disease
Neurological Disease
Others

c)

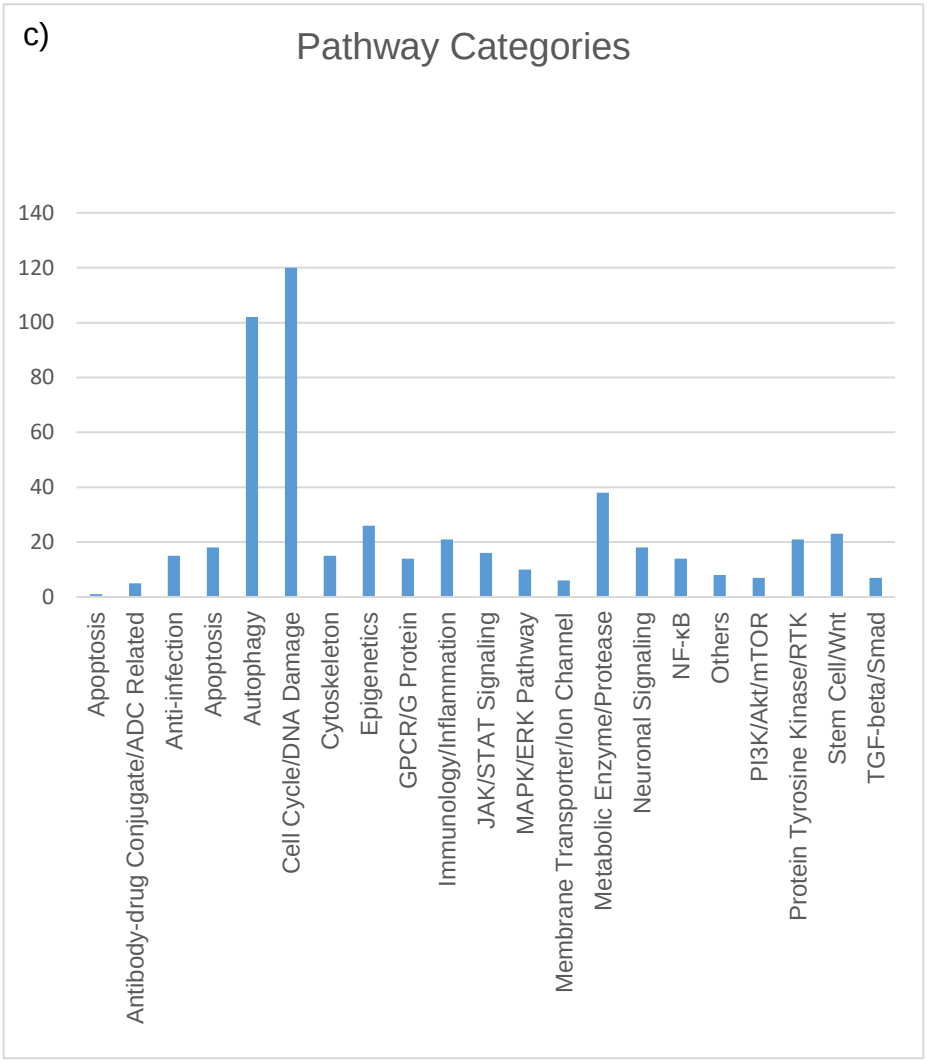
Pathway Categories
140
120
100
80
60
40
20
0
Apoptosis
Antibody-drug Conjugate/ADC Related
Anti-infection
Apoptosis
Autophagy
Cell Cycle/DNA Damage
Cytoskeleton
Epigenetics
GPCR/G Protein
Immunology/Inflammation
JAK/STAT Signaling
MAPK/ERK Pathway
Membrane Transporter/Ion Channel
Metabolic Enzyme/Protease
Neuronal Signaling
NF-κB
Others
PI3K/Akt/mTOR
Protein Tyrosine Kinase/RTK
Stem Cell/Wnt
TGF-beta/Smad

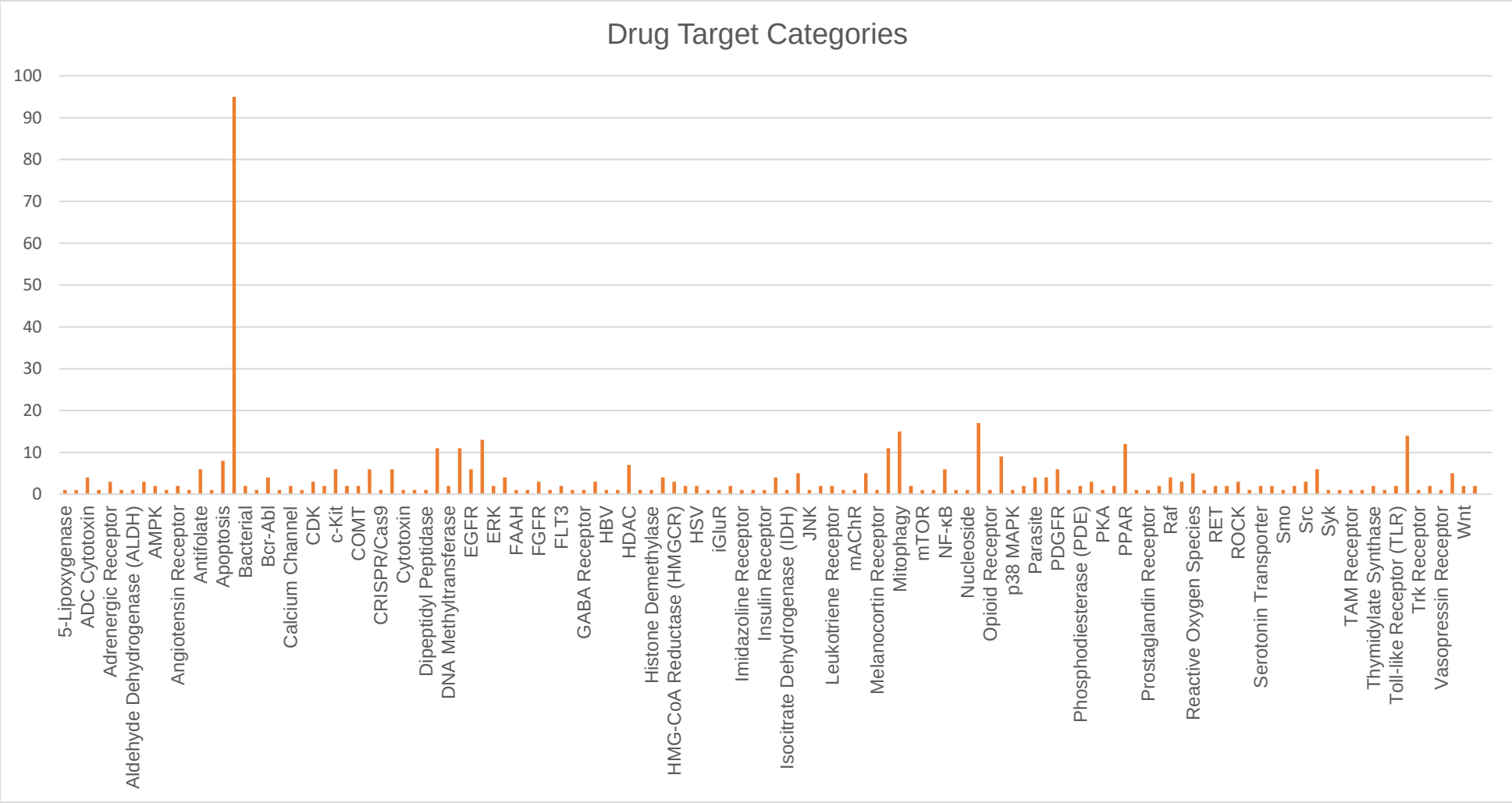

Figure 25: Descriptive data for the drug panel for the senescence screen. A) Type of clinical approval, i.e. compounds approved by the European Medical Association (EMA), the US Food and Drug Administration (FDA) or other countries. B) Research areas linked with each compound. C) Frequency of biological pathways that are targeted by the compounds in the screen. D) Compounds in the panel categorised by target/function.

Many compounds altered CDKN2A gene expression

The fold change in *CDKN2A* gene expression relative to the control was used as a proxy for the impact on cellular senescence. Figure 26 illustrates the change in expression of the compounds in the screen compared to the control group. Out of a possible 480 drug doses (240 individual drugs at 1 or 10 μM), only four drug doses did not have an effect outside of the range of the mean ± SEM of the controls. 233 drug doses increased senescence, and 246 decreased senescence. Using mean ± one SD, 160 drug doses decreased senescence and 111 drug doses increased senescence. Due to the nature of the experiment as a preliminary screen, and the infeasibility of taking so many drugs through to the next phase, more stringency was needed. The mean ± three SDs of the control treatments therefore provided upper and lower bounds. Effects outside of this range were identified as having an effect on senescence that may be worth pursuing. There were 22 drug doses (20 individual drugs) identified that increased senescence, and 98 (70 individual drugs) that decreased senescence out of a possible 480 drug doses (240 drugs). The fold change is recorded in Table 15 for drug doses that had effects that exceeded the mean ± three SDs from the mean of the controls.

We noted the presence of several compounds that have antidepressant and/or anticonvulsant properties in the list of compounds with the largest effects on *CDKN2A* expression, shown in Table 15. Amoxapine, citalopram (hydrobromide), sertraline (hydrochloride) and valpromide were identified in this screen with fold changes in *CDKN2A* of 1.034, -1.094, -1.154, and -1.351 respectively. Most of

these compounds decreased the expression of *CDKN2A*, but amoxapine increased it. Similarly, we noted that two oestrogenic compounds, diethylstilboestrol and ethynyl estradiol, had large effects at both doses in decreasing *CDKN2A* expression. 1 µM diethylstilboestrol had a fold change of -0.753, with a larger effect at 10 µM of -3.068. Diethylstilboestrol at 10 µM was in the top ten compounds/doses to decrease *CDKN2A* expression. Ethynyl estradiol caused a fold change in *CDKN2A* expression of -1.259 at 1 µM and -2.684 at 10 µM.

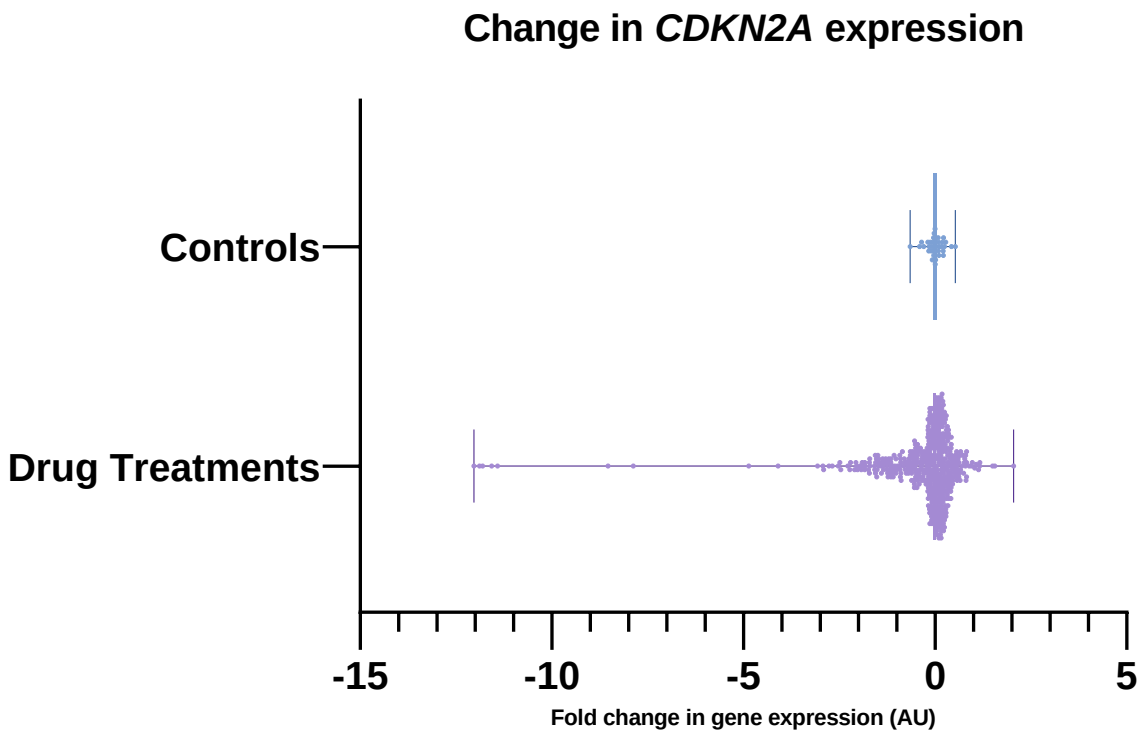

Figure 26: Summary data of all compounds in a screen for effect on CDKN2A gene expression. Many compounds showed indications of being able to reduce and/or increase CDKN2A expression. Each data point represents an individual compound at either 1 µM or 10 µM concentration (average of three technical replicates by two biological replicates). The median and range are plotted.

Table 15: Fold change in CKDN2A (arbitrary units, relative to control) by compound and dose in the initial senescence screen. All effects listed here were more than three standard deviations above or below the mean of control treatments.

Drug Name	Dose (μM)	Fold change in *CDKN2A*
Tucidinostat	10	2.048
Doxifluridine	10	1.559
Doxorubicin (hydrochloride)	10	1.498
Bromhexine (hydrochloride)	10	1.167
Homoharringtonine	10	1.160
Chlorambucil	10	1.133
Aspirin	10	1.072
Amoxapine	10	1.034
Doxorubicin (hydrochloride)	1	0.969
Imatinib	10	0.948
Montelukast (sodium)	10	0.888
Atorvastatin (hemicalcium salt)	10	0.822
Ribociclib	10	0.820
Baricitinib (phosphate)	10	0.820
Irinotecan (hydrochloride)	10	0.804
Levoleucovorin (calcium)	10	0.798
Epirubicin (hydrochloride)	10	0.790
Cobimetinib	10	0.773
Homoharringtonine	1	0.765
Decitabine	10	0.744
Sunitinib	10	0.722
Temozolomide	10	0.700
Silibinin	10	-0.686
Diacerein	10	-0.694
Vinorelbine (ditartrate)	1	-0.713
Alpelisib	10	-0.717
Ethamsylate	10	-0.734
Diethylstilboestrol	1	-0.753
Altretamine	10	-0.782
Panobinostat	1	-0.791
Sertraline (hydrochloride)	1	-0.805
Deferoxamine (mesylate)	10	-0.822
Balsalazide	1	-0.852
Pexidartinib	1	-0.890
Bexarotene	10	-0.894
Clofarabine	10	-0.897
Caffeic acid	10	-0.903
Pazopanib (hydrochloride)	10	-0.909
Aspirin	1	-0.916
Dexamethasone	1	-0.917
Pazopanib	10	-0.921

Rucaparib (phosphate)	10	-0.984
Glasdegib	1	-1.005
Aceglutamide	10	-1.020
Trimethoprim	10	-1.021
Crizotinib (hydrochloride)	10	-1.051
Acalabrutinib	1	-1.069
Zidovudine	10	-1.080
Citalopram (hydrobromide)	10	-1.094
Topotecan (hydrochloride)	10	-1.111
Rucaparib (phosphate)	1	-1.126
Alpelisib	1	-1.153
Sertraline (hydrochloride)	10	-1.154
Erlotinib	1	-1.157
Triclabendazole	10	-1.168
Nefopam (hydrochloride)	10	-1.174
Altretamine	1	-1.184
Bortezomib	1	-1.212
Nefopam (hydrochloride)	1	-1.217
Penfluridol	10	-1.230
Clioquinol	10	-1.241
Ethynyl estradiol	1	-1.259
Panobinostat	10	-1.260
Clofibrate	1	-1.272
Mizoribine	10	-1.291
Belinostat	10	-1.330
Valpromide	10	-1.351
Bosutinib	1	-1.354
Berberine (chloride hydrate)	10	-1.367
Nelarabine	1	-1.403
Acalabrutinib	10	-1.405
Tofacitinib (citrate)	10	-1.412
Erdosteine	1	-1.470
Bortezomib	10	-1.475
Bosutinib	10	-1.478
Osalmid	1	-1.493
Topotecan (hydrochloride)	1	-1.515
Bezafibrate	10	-1.523
Orotic acid	10	-1.532
Methylthiouracil	1	-1.551
Chlorpheniramine (maleate)	10	-1.559
Nitisinone	1	-1.561
Teniposide	10	-1.577
Sulfasalazine	10	-1.584

Pemetrexed (disodium hemipenta hydrate)	1	-1.702
Nifuroxazide	10	-1.705
Osalmid	10	-1.716
Nicotinamide	1	-1.717
Erlotinib	10	-1.741
Bendazol	1	-1.820
Bexarotene	1	-1.835
5-Azacytidine	1	-1.837
Nelarabine	10	-1.893
Clofarabine	1	-1.905
Niraparib	10	-1.927
Mycophenolic acid	10	-1.963
5-Azacytidine	10	-2.022
Chlorzoxazone	1	-2.045
Metyrapone	1	-2.066
Dimethyl fumarate	10	-2.099
Dexamethasone	10	-2.209
Dimethyl fumarate	1	-2.227
Chromocarb	10	-2.277
Penfluridol	1	-2.460
Bendazol	10	-2.486
Methylthiouracil	10	-2.527
Ethynyl estradiol	10	-2.684
Abemaciclib (methanesulfonate)	10	-2.768
Conivaptan (hydrochloride)	10	-2.908
Sunitinib	1	-2.926
Diethylstilbestrol	10	-3.068
Dronedarone	1	-4.099
Sodium 4-phenylbutyrate	10	-4.861
Cabozantinib	10	-7.875
Metyrapone	10	-8.532
Abemaciclib (methanesulfonate)	1	-11.417
Cabozantinib	1	-11.571
Carmofur	10	-11.805
Balsalazide	10	-11.887
Chlorzoxazone	10	-12.035

Effects on CDKN2A expression in known senotherapeutic compounds

Several known senotherapeutic compounds were included in the screen for effects on *CKDN2A* gene expression: dasatinib (hydrochloride), metformin (hydrochloride), resveratrol and trametinib. Table 16 shows the fold change for these compounds. These effects were small, but all compounds and doses were outside of the bounds of the control group's mean ± SEM. Only the fold changes in *CDKN2A* caused by metformin (hydrochloride) at 10 μM and resveratrol at 1 μM were outside the bounds of the control group's mean ± one SD. The criterion for identifying the largest effects was if a fold change was outside the bounds of the control group's mean ± three SDs. Interestingly, none of the known senotherapeutic compounds met this criterion.

Table 16: Fold change in CKDN2A (arbitrary units, relative to control) by compound and dose for known senotherapeutic compounds in the initial senescence screen.

Drug Name	Dose (μM)	Fold change in *CDKN2A*
Dasatinib (hydrochloride)	1	0.158
Dasatinib (hydrochloride)	10	-0.106
Metformin (hydrochloride)	1	-0.181
Metformin (hydrochloride)	10	0.286
Resveratrol	1	-0.143
Resveratrol	10	0.227
Trametinib	1	0.050
Trametinib	10	0.100

Some compounds had opposite effects depending on the dose

90 drugs (of 240) had a difference in the directionality of their effect on *CDKN2A* gene expression between the 1 µM and 10 µM doses. That is to say that one dose decreased and one dose increased *CDKN2A* expression. These effects often did not meet the criterion for identification of the largest effects (an effect outside the bounds of the control group's mean ± three SDs). Excluding those that did not meet the criterion, two compounds had opposing effects: sunitinib and aspirin. Aspirin 10 µM increased *CDKN2A* expression with a fold change of 1.072, whereas the 1 µM dose decreased it with a fold change of -0.916. Conversely, the 1 µM dose of sunitinib decreased *CDKN2A* expression with a fold change of -2.926 compared to the fold change of 0.722 with the 10 µM dose.

SAB activity was increased significantly by three compounds

Treatment with doxorubicin (hydrochloride), homoharringtonine and imatinib at 10 µM concentrations was sufficient to increase SAB staining in younger dermal fibroblasts (cPDL of 32.69 prior to seeding out). Table 17 details the mean percentage of cells stained for SAB with each treatment, and the p values against the appropriate control group. Figure 27 shows the effect size of each treatment. Doxorubicin (hydrochloride) had an average increase in SAB of 197%, homoharringtonine increased SAB by an average of 146%, and imatinib caused an increase of 342%.

11 compounds significantly decreased SAB activity

Dermal fibroblasts at a later passage (average cPDL of 41.92 prior to seeding out) were treated to identify decreases in SAB activity. The effect sizes are shown in Figure 28 and the exact data is described in Table 17. A significant reduction was observed with cells treated with aspirin 10 µM (-17%), cabozantinib 1 µM (-58%), carmofur 10 µM (-39%), chlorpheniramine (maleate) 10 µM (-34%), diethylstilboestrol 10 µM (-30%), ethynyl estradiol 10 µM (-32%), levonorgestrel 10 µM (-51%), metyrapone 10 µM (-44%), penfluridol 10 µM (-45%), sodium-4-phenylbutyrate 10 µM (-41%), and sunitinib 10 µM (-100%).

Investigation of the dose-specific effects of aspirin and sunitinib on senescence

In the screen of early passage cells, neither dose of aspirin caused a significant change in SAB activity. In the screen of later passage cells, aspirin at 1 µM caused no significant change in SAB activity, but the 10 µM dose caused a 40% decrease in SAB activity. Sunitinib at 1 µM appeared not to cause any significant change in SAB activity in either screen of earlier or later passage cells. Sunitinib at 10 µM caused a decrease in SAB activity of 100% in the earlier passage cells, and 93% in the later cells. Sunitinib at 10 µM clearly caused cell death. This was observed during the experiment itself and during image analysis. This is also evidenced clearly by the lack of any SAB activity in the cells at both passages. Details on the exact data can be found in Table 17 and the effect sizes are visualised in Figure 27 and Figure 28.

*Table 17: Results from a screen for senescence-associated beta galactosidase (SAB) activity. The mean percentages of cells stained for SAB were compared against the appropriate experimental control for each batch of the screen. Assays 1-5 were performed on later passage fibroblasts to investigate potential reductions in senescence. Assays 6-7 were performed on earlier passage fibroblasts to investigate potential increases in senescence. The mean ± standard error of the mean (SEM) and p values from one-way ANOVAs with Fisher's post hoc test are reported: (ns) not significant, * p<0.05, ** p<0.01, *** p<0.001 and **** p<0.0001.*

Treatment	Mean	SEM	P	Significance
Assay 1 Control 10µM	44.17	7.506	-	-
5-Azacytidine 10µM	36.99	6.191	0.2496	ns
Caffeic Acid 10µM	31.67	3.34	0.0553	ns
Chlorpheniramine (maleate) 10µM	29.33	3.805	0.0264	*
Diethylstilboestrol 10µM	30.98	1.507	0.0445	*
Ethynyl Estradiol 10µM	30.1	1.317	0.0337	*
Levonorgestrel 10µM	21.54	0.8541	0.002	**
Assay 2 Control 10µM	40.05	9.082	-	-
Amoxapine 10µM	28.92	9.597	0.4353	ns
Bendazol 10µM	23.67	6.348	0.2568	ns
Citalopram (hydrobromide) 10µM	33.56	11.83	0.6466	ns
Methylthiouracil 10µM	33.69	12.09	0.6531	ns
Sertraline (hydrochloride) 10µM	26.81	10.88	0.3556	ns
Valpromide 10µM	23.84	7.242	0.2615	ns
Assay 3 Control 10µM	27.52	3.686	-	-
Balsalazide 10µM	22.99	2.48	0.3251	ns
Carmofur 10µM	16.7	2.985	0.0288	*
Chlorzoxazone 10µM	19.91	2.438	0.109	ns
Conivaptan (hydrochloride) 10µM	22.33	2.988	0.2627	ns
Metyrapone 10µM	15.36	0.7593	0.0161	*
Sodium-4-Phenylbutyrate 10µM	16.16	4.995	0.0228	*
Assay 4 Control 1µM	19.19	4.546	-	-
Abemaciclib (methanesulfonate) 1µM	12.09	1.888	0.1025	ns
Cabozantinib 1µM	8.13	0.2987	0.0159	*
Dronedarone 1µM	14.12	2.768	0.234	ns
Nicotinamide 1µM	12.11	1.795	0.1034	ns
Penfluridol 1µM	10.48	1.586	0.0495	*
Assay 4 Control 10µM	16.11	4.794	-	-
Dexamethasone 10µM	10.26	2.553	0.1728	ns
Assay 5 Control 1µM	39.1	8.275	-	-
Aspirin 1µM	32.61	2.587	0.3269	ns
Sunitinib 1µM	40.42	1.816	0.0396	*
Assay 5 Control 10µM	36.06	3.345	-	-
Aspirin 10µM	21.39	4.997	0.8398	ns
Sunitinib 10µM	2.563	2.563	0.0002	***
Assay 6 Control 1µM	3.163	0.5069	-	-
Aspirin 1µM	4.287	0.5053	0.4963	ns

Sunitinib 1µM	3.493	1.016	0.2333	ns
Assay 6 Control 10µM	4.223	0.6868	-	-
Aspirin 10µM	6.227	1.665	0.8404	ns
Sunitinib 10µM	0	0	0.0199	*
Imatinib 10µM	18.67	2.064	<0.0001	****
Assay 7 Control 10µM	4.07	0.8632	-	-
Bromhexine (hydrochloride) 10µM	5.65	1.818	0.3679	ns
Doxifluridine 10µM	6.04	1.637	0.2654	ns
Doxorubicin (hydrochloride) 10µM	15.84	0.1804	<0.0001	****
Ethynyl Estradiol 10µM	5.33	0.8184	0.4704	ns
Homoharringtonine 10µM	13.11	1.609	0.0001	***
Tucidinostat 10µM	3.13	0.27	0.5886	ns

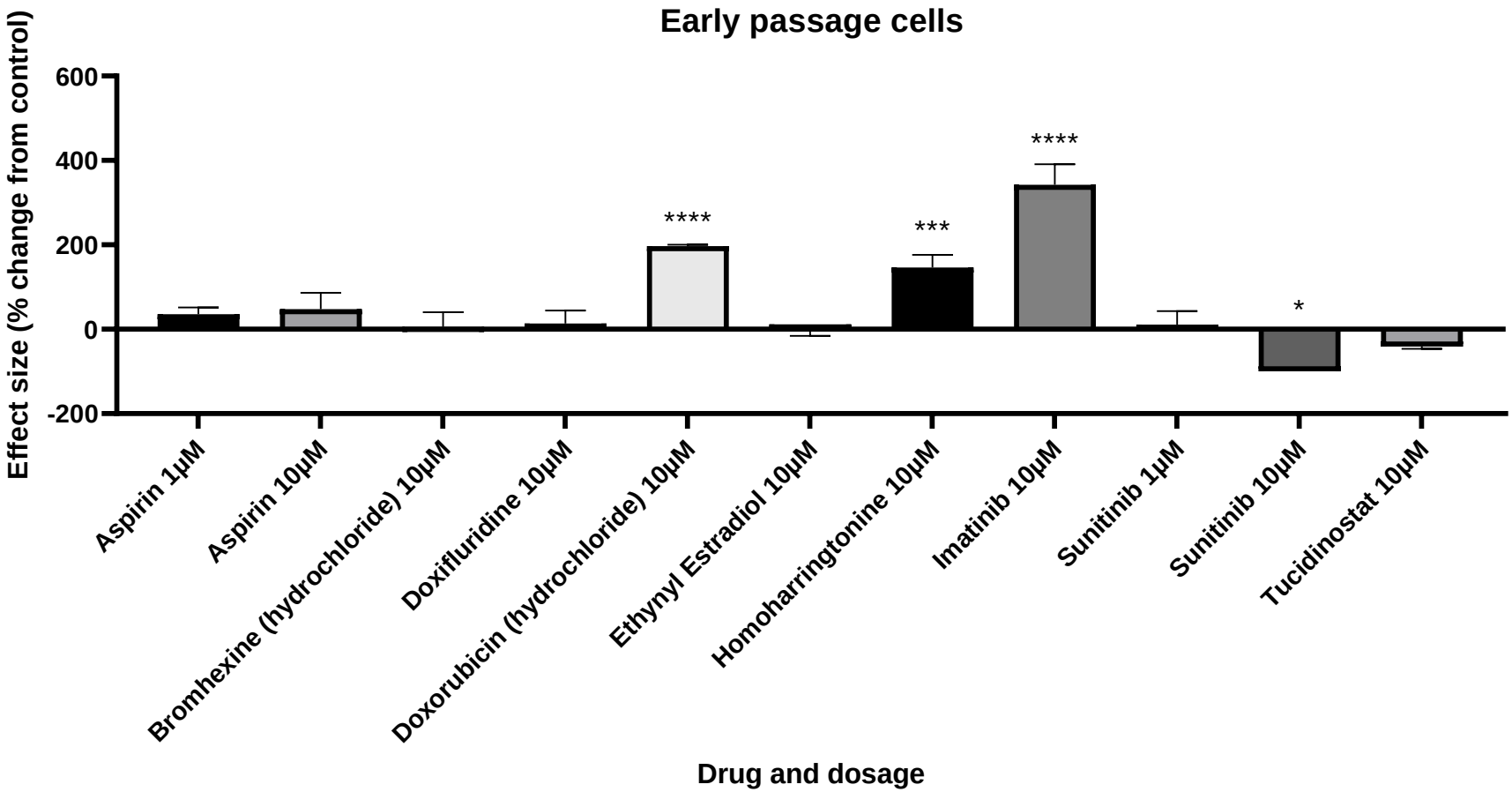

*Figure 27: Three treatments increased and one decreased the level of senescence-associated beta galactosidase (SAB) activity in cells at an early passage with low levels of SAB activity. Error bars show standard error of the mean (SEM), and statistical significance of p values computed using one-way ANOVAs with uncorrected Fisher's LSD post hoc tests (comparing the mean percent of vehicle-treated control cells stained for SAB versus the mean percent of test compound-treated cells stained for SAB) is reported: (ns) not significant, * p<0.05, ** p<0.01, *** p<0.001 and **** p<0.0001.*

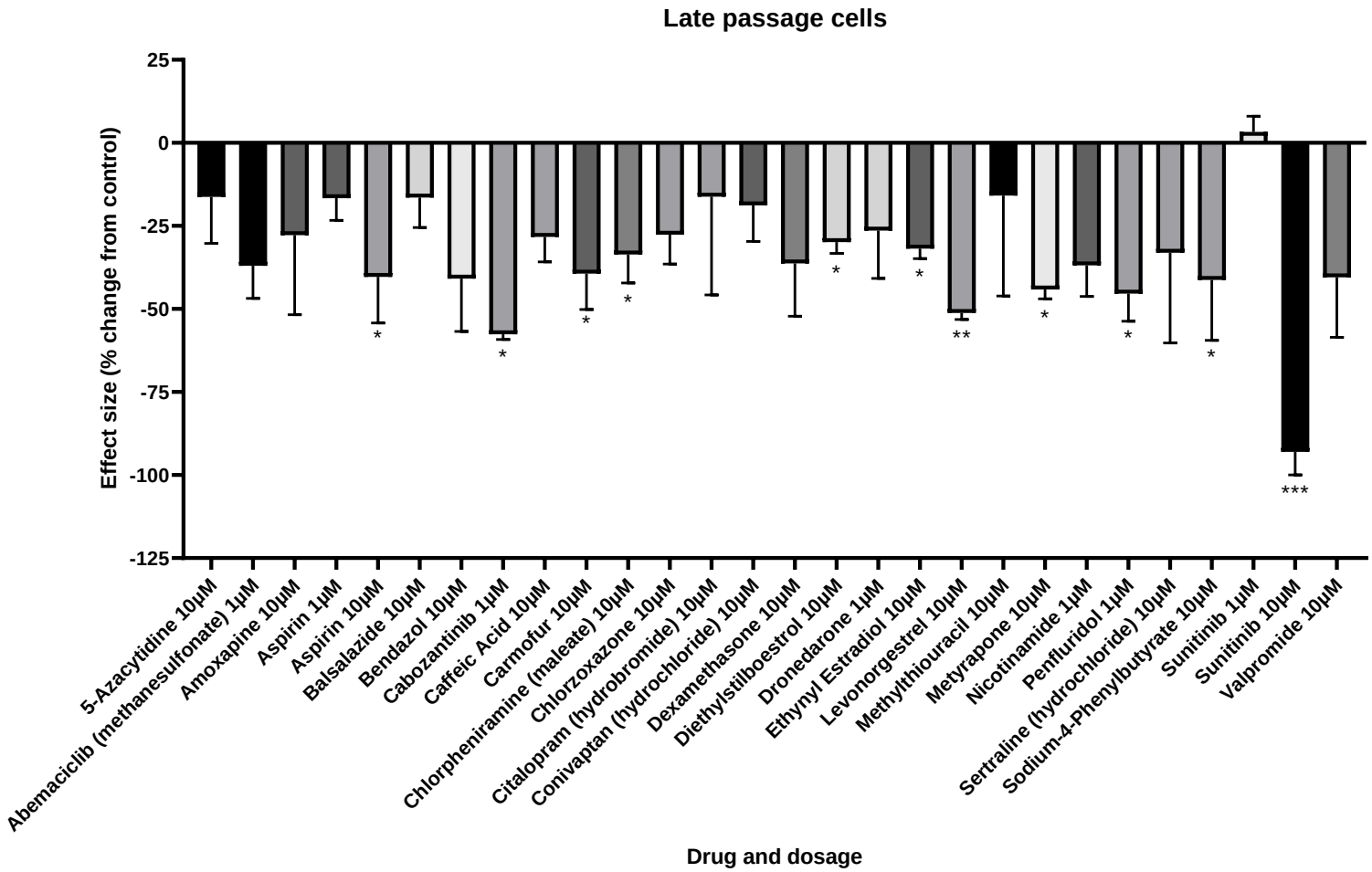

*Figure 28: Several compounds decreased the senescence-associated beta galactosidase (SAB) activity in cells at a late passage with higher levels of SAB activity. Error bars show standard error of the mean (SEM), and statistical significance of p values computed using one-way ANOVAs with uncorrected Fisher's LSD post hoc tests (comparing the mean percent of vehicle-treated control cells stained for SAB versus the mean percent of test compound-treated cells stained for SAB) is reported: (ns) not significant, * p<0.05, ** p<0.01, *** p<0.001 and **** p<0.0001.*

A common substructure was more common in compounds that decreased CKDN2A, but no substructure was detectable in the other functional groups

A structure-function analysis was used to identify any substructure that was associated with compounds split by their functionality from the screens for *CDKN2A* gene expression and SAB activity. Figure 29, Figure 30, and Figure 31 show the three test groups of compounds. Figure 32, Figure 33, and Figure 34 show the structural similarity between the compounds in the three test groups respectively using their Tanimoto coefficients to construct a dendrogram.

The first test group comprised the eight compounds that increased *CDKN2A* expression (above the mean ± 3 SDs criterion) when averaged across both doses. The average Tanimoto coefficient of this group (0.2817 ± 0.03492: mean ± SEM, n = 64) had no significant difference when compared against the average Tanimoto coefficient of eight compounds that had no effect on *CDKN2A* expression (0.2482 ± 0.03798, n = 64, p = 0.5169).

The second test group consisted of the 30 compounds that decreased *CDKN2A* expression the most (averaged across both doses). A maximum of 30 compounds was chosen for this analysis due to computing power limitations. This test group (0.2107 ± 0.005580, n = 900) was significantly structurally different from the control group (0.1755 ± 0.006050, n = 900) with a $p < 0.0001$. The maximum common substructure between the two least similar compounds in the second test group is shown in red in Figure 35.

The number of compounds that increased SAB activity (n = 3) was deemed too small to be suitable for this type of analysis, however the number of compounds that decreased SAB activity was appropriate (n = 11). Sunitinib was omitted from the analysis as it caused cell death rather than acting to reduce senescence. Test group three therefore consisted of a group of ten compounds that decreased SAB activity, and their Tanimoto coefficients were compared against the coefficients of a control group of ten compounds that did not have an effect on *CDKN2A* expression. The average Tanimoto coefficient was not significantly different in the test group (0.2928 ± 0.02544, n = 100) compared to the control group (0.2524 ± 0.02900, n = 100, p = 0.2964).

Atorvastatin (hemicalcium salt)

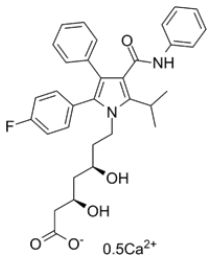

Chlorambucil

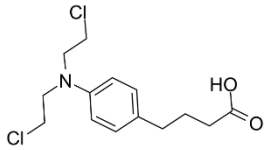

Cobimetinib

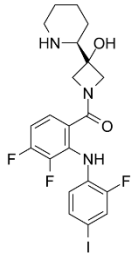

Doxorubicin (hydrochloride)

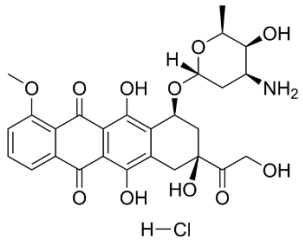

Gemfibrozil

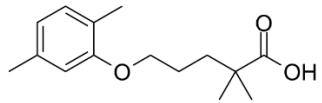

Homoharringtonine

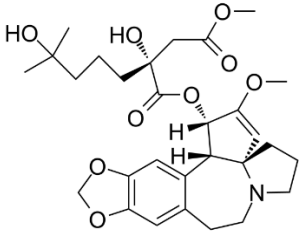

Imatinib

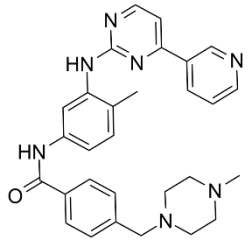

Tucidinostat

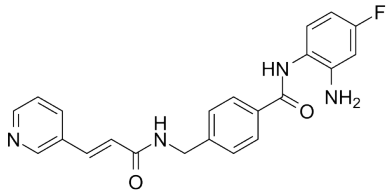

Figure 29: The chemical structures of compounds that increased CDKN2A gene expression and were tested for structure-function association.

5-Azacytidine

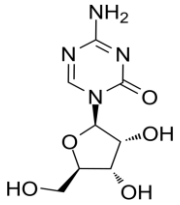

Abemaciclib (methanesulfonate)

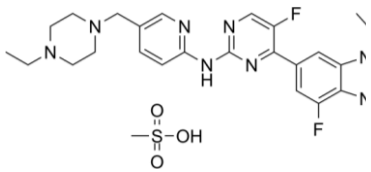

Acalabrutinib

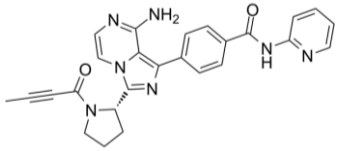

Balsalazide

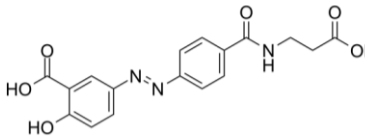

Bendazol

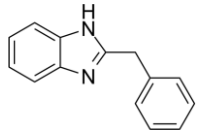

Bexarotene

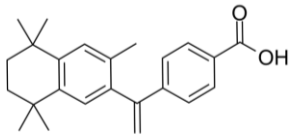

Bortezomib

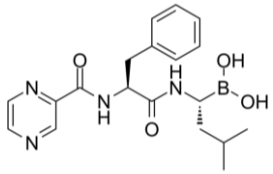

Bosutinib

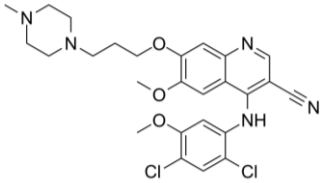

Cabozantinib

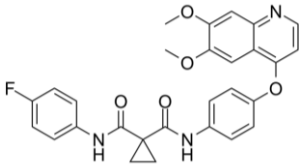

Carmofur

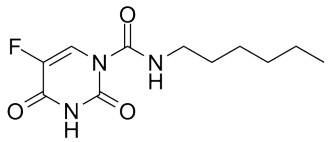

Chlorpheniramine (maleate)

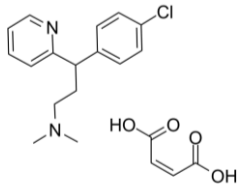

Chlorzoxazone

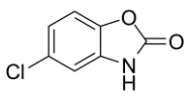

Chromocarb

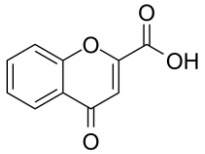

Clofarabine

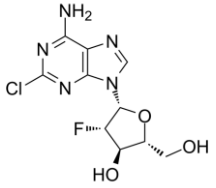

Conivaptan (hydrochloride)

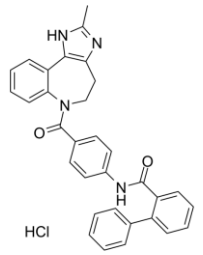

Note this figure continues onto the following page.

Erlotinib

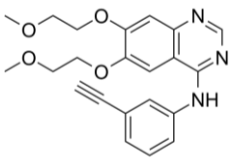

Dexamethasone

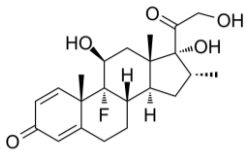

Diethylstilboestrol

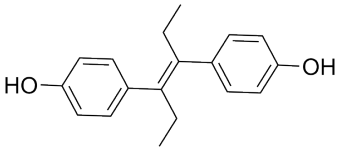

Dimethyl fumarate

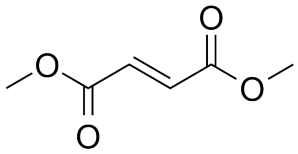

Dronedarone

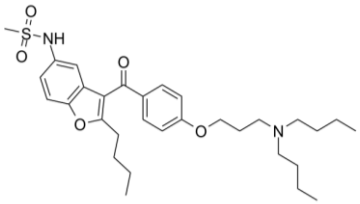

Ethynyl Estradiol

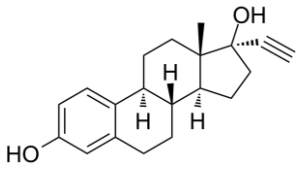

Methylthiouracil

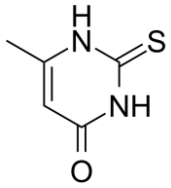

Metyrapone

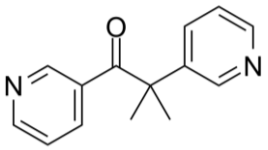

Nefopam (hydrochloride)

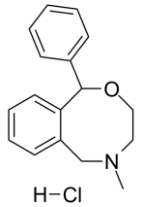

Nelarabine

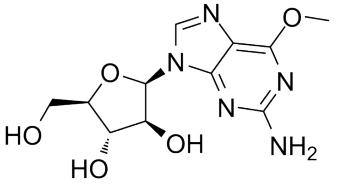

Niraparib

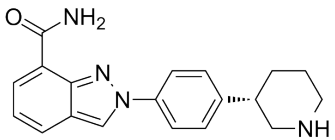

Osalmid

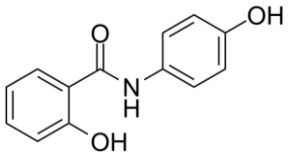

Penfluridol

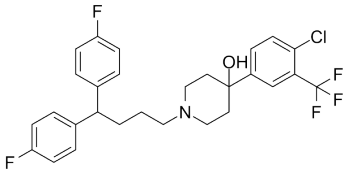

Sodium 4-phenylbutyrate

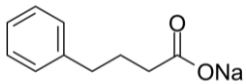

Topotecan (Hydrochloride)

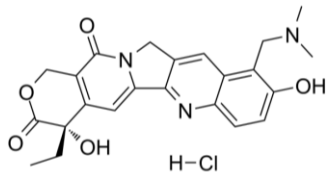

Figure 30: The chemical structures of compounds that decreased CDKN2A gene expression and were tested for structure-function association.

Aspirin

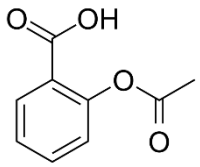

Cabozantinib

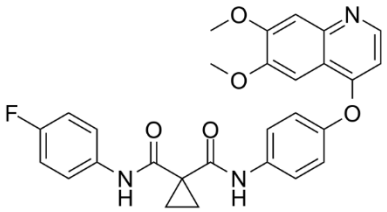

Carmofur

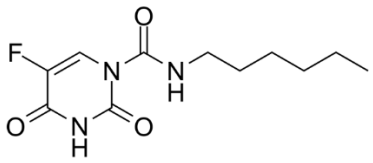

Chlorpheniramine (maleate)

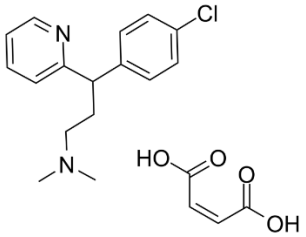

Ethynyl Estradiol

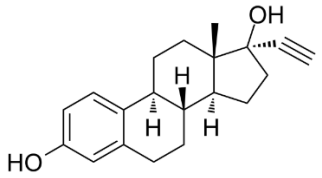

Levonorgestrel

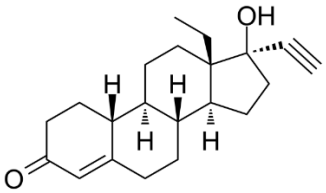

Metyrapone

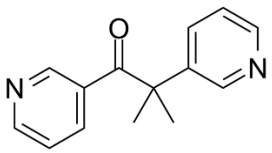

Penfluridol

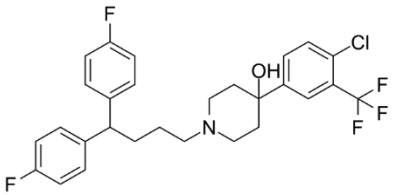

Diethylstilboestrol

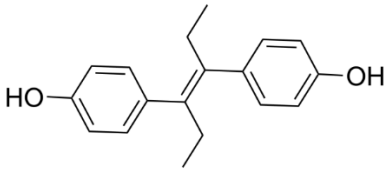

Sodium 4-phenylbutyrate

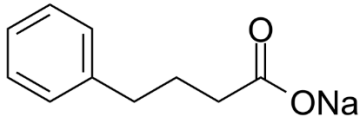

Figure 31: The chemical structures of compounds that decreased SAB activity and were tested for structure-function association.

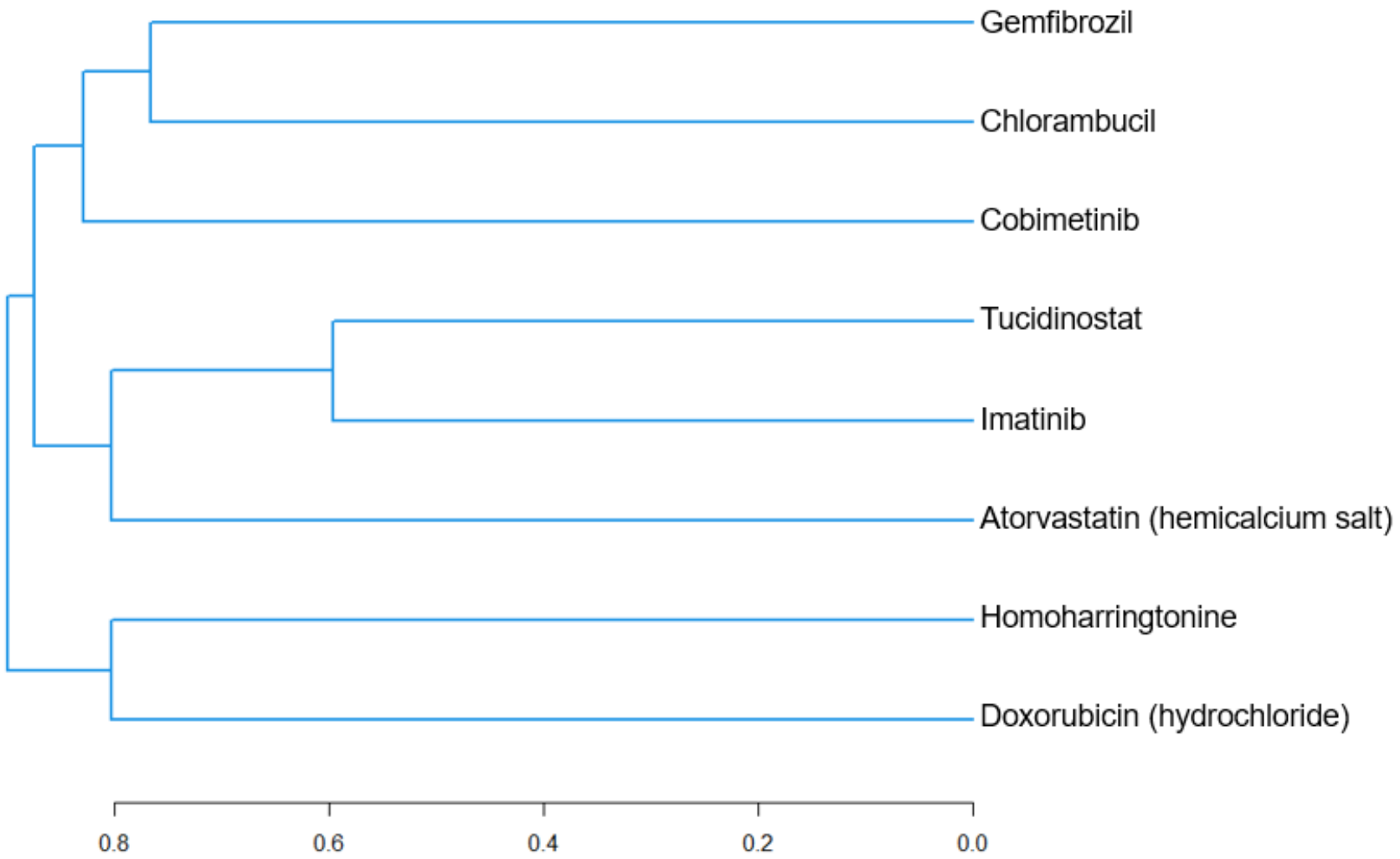

Figure 32: Dendrogram constructed using the Tanimoto coefficient to show structural similarity of compounds tested that increased CDKN2A gene expression.

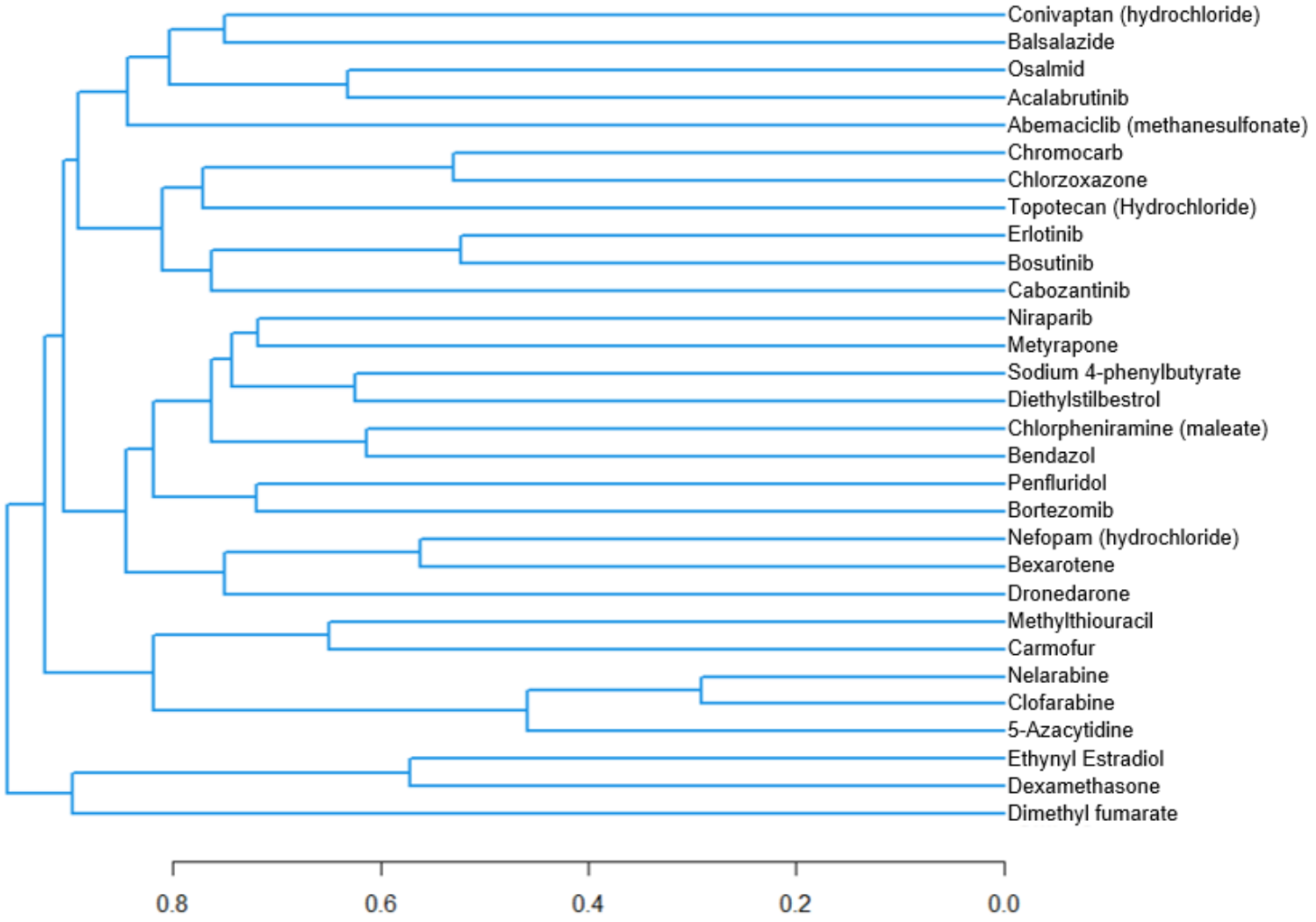

Figure 33: Dendrogram constructed using the Tanimoto coefficient to show structural similarity of compounds tested that decreased CDKN2A gene expression.

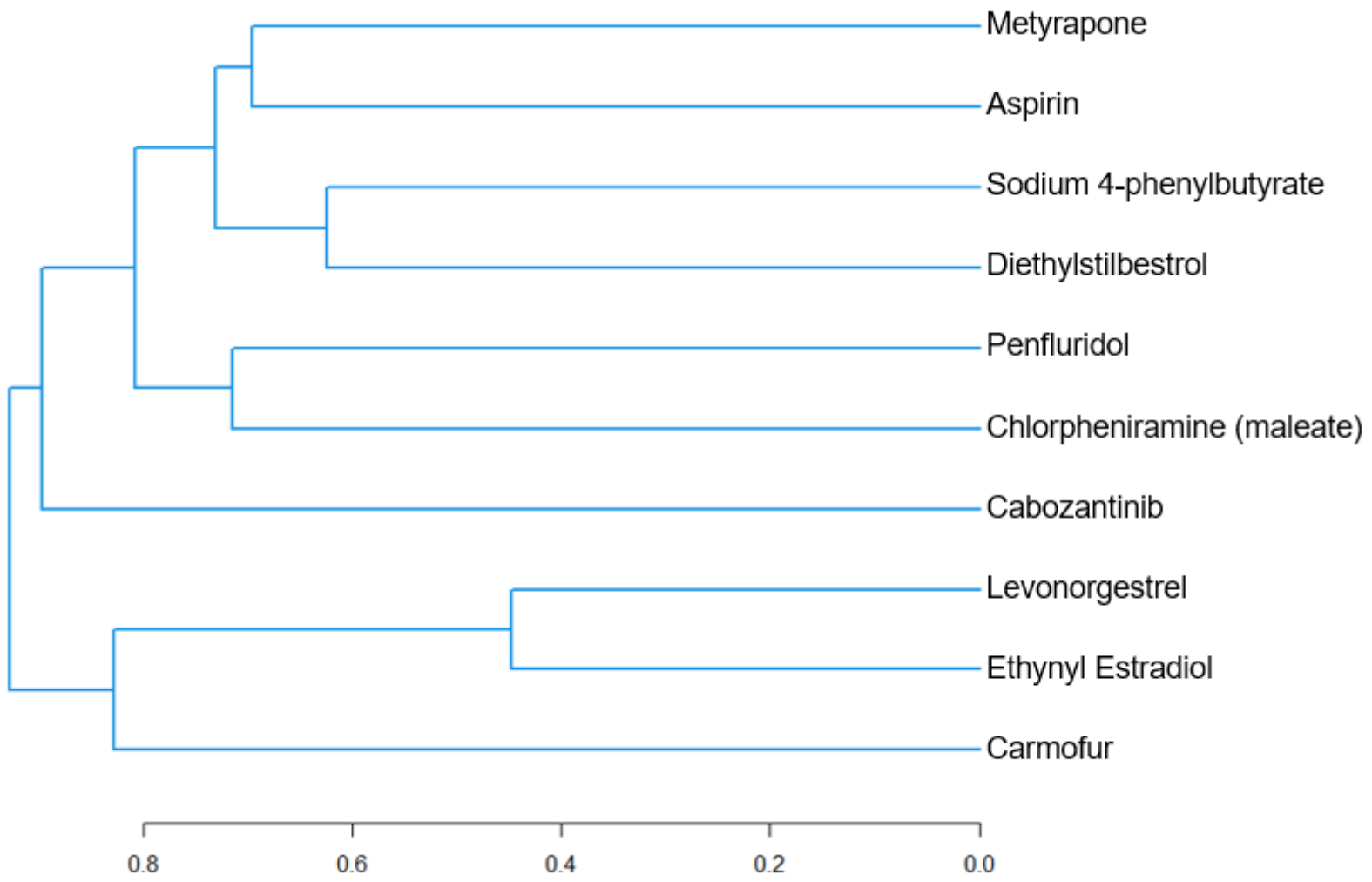

Figure 34: Dendrogram constructed using the Tanimoto coefficient to show structural similarity of compounds tested that decreased SAB activity.

Dimethyl fumarate

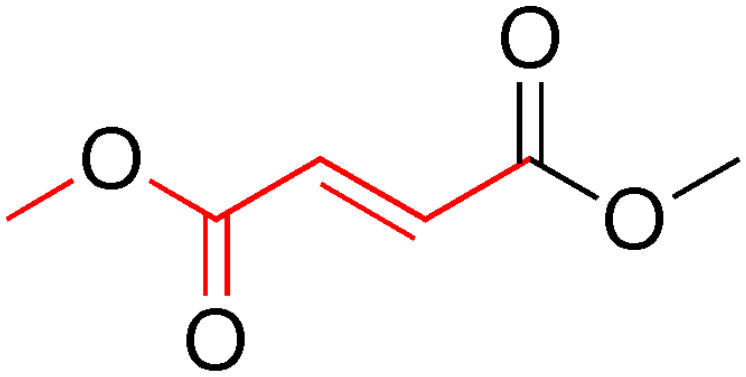

Conivaptan (hydrochloride)

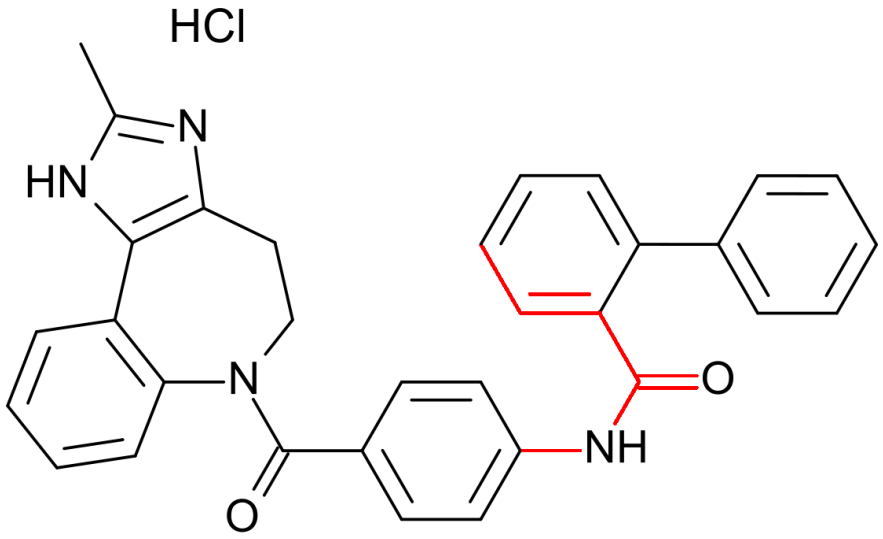

Figure 35: Maximum common substructure of the two least structurally similar compounds that decreased CDKN2A gene expression

Discussion

In this study, we performed a drug repurposing screen for senescence. We assessed compounds based on their effects on gene expression of *CDKN2A* and SAB activity. We identified 90 out of a possible 240 compounds as having an effect on *CDKN2A* (either a decrease or increase). We pursued a screen for SAB activity in 32 compounds and found 11 drugs which decreased SAB activity and three which increased SAB activity. We related the functional information provided by these two screens to the chemical structures of the drugs and found an association with a chemical substructure and a decrease in *CDKN2A* expression.

The *CDKN2A* gene encodes several different transcripts. In particular, the p16 protein, an inhibitor of CDK4, is produced from the *CDKN2A* gene. p16 has been intrinsically linked with senescence and cancer pathways, with its targeted ablation in a progeroid mouse model resulting in astonishing improvements in ageing-related phenotypes [66]. As a biomarker for senescence, *CDKN2A* is useful for identifying compounds for further validation, but it is not the most specific of biomarkers for senescence which is why the SAB activity screen is important. It may therefore come as no surprise that many compounds affected the gene expression of *CDKN2A*. Reassuringly, more compounds decreased *CDKN2A* expression than those that increased it.

Having knowledge of the compounds that increase senescence could be useful in the context of prescribing therapies for age-related diseases or other

non-age-related treatments for elderly patients. Any compounds that are identified as increasing senescence might highlight potential oncotherapies. Forcing cancerous cells to enter a senescent state might be preferable to other therapies, and can give an option to target the cells with senolytic drugs afterwards. Indeed, the three compounds that were identified in both the *CDKN2A* expression and SAB activity screens as increasing senescence were all anti-neoplastic agents in clinical use as oncotherapies. Sunitinib was also identified in the first screen as having contradictory effects at different doses (increasing *CDKN2A* expression at a higher 10 µM dose, while reducing it at 1 µM), but it emerged that this was due to sunitinib's potency at causing cell lysis. It is currently in clinical use as an anti-tumour agent. No substructure was associated with the compounds that increased *CDKN2A* expression. Although these screens did not highlight any novel compounds or structures that increased senescence for further research, they provided evidence of the screening approach's potential uses. For example, in the screen for *CDKN2A* expression, one antidepressant was found to increase *CDKN2A* expression, whereas several others (citalopram and sertraline) decreased it. If these findings had translated in the same way into the SAB activity screen, then (of course, after further validation and testing) this could have been used to inform clinical practice, e.g. prescribing antidepressants that do not increase senescence may be preferable, particularly in elderly patients.

More success was found in the identification of compounds that decreased senescence. As previously discussed, many compounds affected *CDKN2A* gene expression, but the SAB activity screen revealed more robust associations. For

example, it is well-established that resveratrol at the dose range used can decrease senescence, but the compound was not identified amongst the larger effects on *CDKN2A* gene expression. Compounds of a similar nature may well remain unidentified when this screening approach is used, nonetheless, this approach can still identify other compounds for further study. The nature of the senescence assay for SAB activity means that smaller effects, e.g. a 10% decrease, are not likely to meet the significance level required. This means that any effects noted in this screen are likely to be true effects. Interestingly, the common household painkiller, aspirin, was identified as increasing *CKDN2A* expression at 10 µM, but decreasing it at 1 µM. When the two doses of aspirin were tested in the SAB activity screen, only the 10 µM dose was significant, but this time it caused a decrease in the marker for senescence. Aspirin has been shown to extend lifespan in mice [278]. Aspirin is often taken by many patients, and a 17% decrease in senescence could be a good news story, particularly for those with chronic disease who take the medication regularly. However, it is important to note the effect of the dosage.

As discussed in the introduction, senotherapeutic compounds often exhibit biphasic effects with the preliminary findings of studies of senomorphic compounds *in vitro* suggest a low dose is sufficient to provide mid to long term senotherapeutic benefits [181]. These findings need human *in vivo* evidence to support or dismiss the clinical usefulness of the information. Another consideration is that the appropriate doses of any compound will vary between tissue type and person, and will vary according to the bioavailability of the compound at the time. It could be difficult to unravel these mechanisms in

complex biological systems when effects may be small. Nevertheless, identification of any senotherapeutic effect, even if small, may still be useful.

Intriguingly, three compounds that decreased SAB activity were synthetic female hormones. Diethylstilboestrol, ethynyl estradiol and levonorgestrel are commonly used in hormone replacement therapy or contraceptives [279]. The two oestrogenic compounds decreased SAB by about 30%, whereas the synthetic progesterone, levonorgestrel, decreased SAB activity by 51%. This is very interesting given that female hormones are associated with protective benefits in ageing, and there is some evidence of sex differences in senescence-associated phenotypes. However, the effects of exogenous synthetic hormones have not yet been examined in the context of senescence [111,280,281]. This opens an intriguing line of enquiry for future investigation. Could these synthetic female hormones exert protective effects against ageing?

The other compounds that decreased *CDKN2A* gene expression and SAB activity were similarly interesting in their potential for treating age-related disease, for informing clinical practice or for general future study. It would not be feasible for several of these compounds to be used in the clinic for age-related disease, as they may cause severe side effects and, therefore, could be inappropriate for treating milder age-related diseases. Despite this, the information could help patients and clinicians choose treatments, and chemical information on the compounds could still aid in research for similar molecules, e.g. in structure-function research. Evidence from the literature can point towards potential mechanisms for the compounds' senotherapeutic effects, e.g. by selective

induction of apoptosis or increased autophagy. Cabozantinib had the largest effect on SAB activity with a 58% decrease at 1 μM. Cabozantinib is an anti-angiogenic compound that can induce apoptosis in endothelial cells [282]. Carmofur is an anti-neoplastic agent [283]. Chlorpheniramine (maleate) is a histamine H1 receptor antagonist commonly used to treat allergies [284,285]. Metyrapone is an 11β-hydroxylase inhibitor and is known to activate autophagy [286,287]. It is used to treat Cushing's disease and depression [286,288]. Penfluridol is a potent antipsychotic medication used in the treatment of schizophrenia [289]. Sodium-4-phenylbutyrate is used in the treatment of genetic urea cycle disorders, cystic fibrosis and cancers, and has been implicated as a potential therapy for Parkinson's disease in a mouse model of the disease [290,291]. Interestingly it also increased lifespan of *Drosophila melanogaster* [292]. Further validation of the drugs' role in senescence and potential as senotherapeutic drugs will be needed before any clinical utility can be assessed.

The maximum common substructure that was found in compounds that decreased *CDKN2A* expression (shown in Figure 35) was also found in the senotherapeutic-associated substructures identified in a larger-scale analysis. 13 chemical substructures were identified as being associated with senotherapeutic function in the study by Olascoaga-Del Angel *et al.*, and the substructure identified in this thesis is common across 11 of the structures in their study [152]. The compounds they identified often feature ring structures, and this observation holds fast for the compounds that decreased *CDKN2A* expression in this study: many compounds in Figure 30 have similar ring structures. The method used in this thesis identifies the maximum substructure that is common

across all compounds in the test group, however clustering analysis could be used to identify more exact substructures. These more specific substructures could then be used in the future to perform bioinformatic screening of chemical structures in order to select compounds for wet lab screening, and/or to reverse-screen for targets and mechanistic insight into cellular senescence pathways.

Cellular senescence is a collection of molecular features rather than a definitive homogeneous state. It can be induced by different means, such as stress, replication, oncogenes and SASP. The heterogeneity of senescence lends itself to the idea that different types of senescence cannot always be targeted for therapies in the same way. This concept could be useful as it may be preferable to only target a particular type of senescent cell for reversal or for senolysis. For example, it would not be an attractive prospect to reverse senescence and push a DNA damage-induced senescent cell into a proliferative state, but it may be the converse for a SASP-induced senescent cell. Similarly, it could be preferable to use a senolytic compound in oncogene-induced senescence rather than a senomorphic.

This study successfully screened many compounds for potential senotherapeutic effects. Several lines of enquiry for future studies into the senotherapeutic abilities of particular compounds were identified, e.g. the senotherapeutic effects of synthetic female hormones. Other methods for high-throughput analyses may emerge in due course, but the method used here was able to identify candidate compounds and structure-function associations.

Chapter 6: Synthetic female hormones exert sex-specific effects on cellular senescence in human dermal fibroblasts.

This chapter uses preliminary results from the previous chapter's senescence screen of repurposed drugs. This chapter is prepared as a draft journal article for Geroscience in collaboration with my co-authors. Author contributions are mentioned in the confines of the article, but I will elaborate on my exact contribution for its inclusion in this thesis. I conceptualised the experiment, conducted literature reviews, designed the experiment, conducted all laboratory work except for the TUNEL assay, analysed all data, interpreted the data, prepared all figures and tables for presentation, structured the manuscript and wrote the majority of the manuscript.

Synthetic female hormones exert sex-specific effects on cellular senescence in human dermal fibroblasts.

Laura R Bramwell[1], Ryan Frankum[1] & Lorna W Harries[1]*

[1]RNA-Mediated Mechanisms of Disease group, College of Medicine and Health, Institute of Biomedical and Clinical Science, University of Exeter

*corresponding author

Correspondence address:

Professor Lorna W Harries
Institute of Biomedical and Clinical Sciences
University of Exeter College of Medicine and Health
RILD Building
Royal Devon and Exeter Hospital
Barrack Road
Exeter
Devon
EX2 5DW
United Kingdom

Correspondence email: L.W.Harries@exeter.ac.uk

ORCID numbers: LRB - 0000-0003-4069-3959, RF - 0000-0002-2665-5625, LWH - 0000-0001-7791-8061

Twitter: @miRNAgirl, @LauraBramwell1, @TeamRNA

Abstract

Biological sex is known to play a role in ageing and in susceptibility to age-related disease. Cellular senescence is a known ‘hallmark’ and driver of systemic ageing. Evidence is emerging that biological sex can affect cellular senescence, but drug screens for senotherapeutic compounds are rarely carried out in both sexes. Female hormones are beginning to be linked with senescence, but the effects of the synthetic versions of these hormones, which are commonly prescribed to many people, on senescence phenotypes in human cells have yet to be determined. We sought to examine senescence outcomes in male and female normal human dermal fibroblast (nHDF) cells in response to three synthetic female hormones: diethylstilboestrol, ethynyl estradiol and levonorgestrel. All three molecules decreased senescence-associated beta galactosidase (SAB) activity in male nHDF cells, but not in female cells. We also observed some sex-specific differences on measures of apoptosis, DNA damage, senescence-associated secretory phenotype (SASP) and regulation of alternative splicing. Cells from donors of different sexes may respond differently to senotherapeutic compounds, which could provide information on a mechanistic basis for sex-specific responses in the hallmarks of ageing. Furthermore, our work underlines the importance of donor-related characteristics, such as sex, when researching cellular senescence or evaluating senotherapeutic compounds.

Keywords:

Human ageing, dermal fibroblast, senescence, splicing factor, synthetic hormone, female, male, sex differences, sex-specific, senomorphic

Introduction

The average age of a person in our population has continued to increase, with one in five people currently alive set to reach their one hundredth birthday [5]. Unfortunately, “healthspan” (the proportion of life lived without disease), has not increased at the same rate. People now spend proportionally longer in a period of ill health at the end of their lives, due to the impact of age-related disease [3]. This encompasses many common diseases, such as cancer, diabetes and cardiovascular disease, which affect many people in society. For example, one in six people over the age of 80 suffer from dementia, an age-related neurodegenerative disease [6,8]. Although they may have differing pathologies, many of these diseases share similar upstream processes at a molecular level. Targeting these ageing-associated mechanisms may lead to the advent of new and improved treatments for the diseases which commonly affect older people.

It is well-known that biological sex affects ageing, with women tending to live longer than men. Being biologically female is typically associated with a longer lifespan of approximately five years [293]. As of August 2022, of all confirmed living supercentenarians, persons aged 110 years or more, all eleven people are biologically female [294]. Many ageing-related diseases are also affected by biological sex. Differences in disease susceptibility and/or presentation between the sexes have been described across diseases such as Alzheimer’s disease, diabetes, cardiovascular disease and Parkinson’s disease, to name a few [295–298]. It is not yet clear why biological sex can affect susceptibility to age-related disease and why the ageing process differs between the sexes. There are two

main theories as to why this is the case [299]. Firstly, the reproductive-cell cycle theory suggests that female hormones exert a protective effect on ageing in humans due to an antagonistic pleiotropic effect. It is beneficial for the hormones to control cell cycle in early life to push towards biologically-costly reproduction. However, over time, the hormones that regulate reproduction attempt to maintain the reproductive state, which drives ageing processes [18]. Secondly, the genetic differences between the sexes offer an explanation. There are differences in sex-chromosomal and mitochondrial disorders which can account for one sex being more predisposed to particular diseases, but these diseases do not alone account for the overall differences seen in ageing. The most pertinent theory of how genetic sex can affect ageing is the “unguarded-X” theory [299]. This theory suggests that the heterogametic sex is at a disadvantage due to only having one copy of the genes on the X chromosome. This makes it less resilient because there is more opportunity for mutations to alter gene function, whereas in the homogametic sex, each X is “guarded” by the other [300]. These two theories both offer explanations as to how biological sex might drive differences in ageing at a molecular level.

The molecular basis of ageing features fourteen “Hallmarks of Ageing” [21,22]. These hallmarks are present in the normal ageing of multiple species. The experimental amelioration of a hallmark increases lifespan and other ageing-associated parameters. The reverse is also true with experimental aggravation decreasing lifespan. These hallmarks consist of many interrelated processes, but all represent a key mechanism of molecular ageing. Genome instability, telomere attrition, epigenetic changes and dysregulation of alternative

splicing are all hallmarks that ultimately affect genetic processing. Cellular senescence, the loss of proteostasis, mitochondrial dysfunction, changes to cellular mechanical properties and compromised autophagy are hallmarks concerning intracellular processes and functions. In contrast, the remaining hallmarks tend to be exerting effects on many cells: inflammation (via the collection of chemokines and cytokines termed the senescence-associated secretory phenotype (SASP) which can induce senescence in nearby cells), the exhaustion of stem cell supplies, altered cell-cell communication (e.g. disruptions in general endocrine, paracrine and autocrine signalling pathways and impairment of immune system function), altered nutrient sensing pathways and disturbances in the microbiome [21]. As we uncover more information about the hallmarks of ageing, a few examples of potential sex-specific differences in the hallmark processes are beginning to emerge. For example, biological females demonstrate elevated immune responses to stimuli such as vaccines that come at the cost of autoimmunity [301]. Mitochondria in female rats have less oxidative damage, and, in mice, sex-specific mRNA splicing patterns have been demonstrated to exist in cardiac genes involved in mitochondrial function, translation and autophagy [302,303].

Cellular senescence is a particularly key hallmark of ageing as it overlaps with so many of the other hallmarks. There are only a handful of studies investigating sex-specific differences in any aspects of senescence [280,299,304]. Most of these are in murine models and identify sex-specific differences in the onset of senescence. Yousefzadah *et al.* found senescence biomarkers (mRNA expression of the isoforms of *CDKN1A* and *CDKN2A* responsible for p21 and p16

respectively) were elevated in male mouse cells compared to female cells [305]. Overexpression of the senescence protein, p53, in *Drosophila melanogaster,* increased lifespan of male flies but reduced it in female flies [306]. Data is scarce in humans, but alleles encoding p53 proteins with reduced activity have been reported to have lifespan-increasing effects in female humans, but not in males [307]. Sex-specific differences in DNA damage repair mechanisms have been shown in human blood cells [308,309].

Cellular senescence has been described as a stable state of cell cycle arrest and is associated with impaired function [24,64]. Despite this original definition, recent research indicates that the senescence phenotypes can be reversed by so-called senomorphic drugs [143,151]. A drug that targets senescence is termed a senotherapeutic drug. Senotherapeutic compounds can include the aforementioned senomorphic compounds, but can also include drugs that cause preferential lysis of senescent cells (senolysis) or senolytic drugs [71,143,151]. Senescence may appear as part of natural development, but, in the case of ageing, it is often induced by replication, appearing when cells reach their natural replicative limit, or induced by cellular stressors such as DNA damage, oncogenes and other forms of cellular stress [36,37,269–271].

A senescent cell is linked to a collection of phenotypes: while not every aspect will be exhibited in a cell, most senescent cells exhibit one or more characteristic. Most senescent cells have a change in morphology and have altered lysosomal properties which can be indicated by increased activity of senescence-associated beta galactosidase (SAB). SAB activity is typically used as the best measure of

a cell's overall level of senescence [166,167]. Senescent cells may have reduced levels of cellular proliferation which can be measured by staining for Ki67, a nuclear protein and proliferation biomarker. DNA damage is often increased in senescent cells and this can be measured with γH2AX staining (present in the early stages of double-strand break repair) and/or terminal deoxynucleotidyl transferase dUTP nick-end labelling (TUNEL) staining (detects double-strand breaks that are generated in apoptosis) [141,167,310]. Many aspects of the heterogeneous senescent phenotype can be examined by gene expression. Analysis can be performed for genes relating to apoptosis, the cell cycle, matricellular proteins, splicing factors and SASP factors. *CDKN1A* and *CDKN2A* are genes related to proteins that become elevated in senescence (p53 and p16/p14 respectively) [24,75,311]. Together these biomarkers can provide evidence to support observations of senescence in different cells or diseases and to identify if a compound has any impact on senescence.

There is limited evidence to directly identify any sex-specific effects on cellular senescence. It is clear that being biologically female offers protective benefits against ageing, and the two main female hormones, oestrogen and progesterone, are known to be involved in many ageing and senescence-related pathways [304,312–315]. Predictably, the typical nuclear receptors for these two hormones, the oestrogen receptors (ERα and ERβ) and progesterone receptors (PR-A and PR-B) are involved in the same pathways [314,316]. Resveratrol, a compound with known senomorphic properties, is thought to be an ER agonist [317]. Despite much information about the female sex hormones in ageing, there is comparatively very little information about the senotherapeutic properties

of synthetic analogues of the female hormones. Most research is confined to mouse models treated with synthetic oestrogens [315,318–320]. In humans, oestrogen and progesterone are endogenous to both sexes, but understandably differ in their circulating levels [321,322]. Unlike progesterone, there are many forms of oestrogen: estrone (E1), estradiol (E2), estriol (E3) and other minor oestrogens, but the major oestrogen is E2. This has two isoforms: 17α-estradiol and the more potent and biologically-most relevant 17β-estradiol [316,323].

Synthetic oestrogen and progesterone compounds are taken on a daily basis by millions of women for many reasons including perimenopausal hormone replacement therapy (HRT) and for contraceptive purposes. Diethylstilboestrol is a non-steroidal oestrogen analogue that acts on both oestrogen receptors and is commonly prescribed for HRT [324,325]. Ethynyl estradiol is a synthetic analogue of 17β-estradiol, and levonorgestrel is a synthetic progesterone. Often in combination, ethynyl estradiol and levonorgestrel are both commonly prescribed for contraception [279]. Large clinical trials following women taking HRT suggest that the impact on age-related disease risk, such as risks for coronary heart disease and diabetes, is not straightforward. The trials show HRT has a complex effect on chronic disease, and might not be suitable for therapy to prevent chronic diseases. However, the conflicting and complex results demonstrate that the mechanism of action of HRT on ageing and age-related disease is unclear and that the question of whether HRT has any senotherapeutic benefit is as yet unanswered [326].

We aimed to investigate experimentally if synthetic female hormones have any direct senotherapeutic benefit. We sought to identify if any of three compounds, diethylstilboestrol, ethynyl estradiol and levonorgestrel, could have any effect on aspects of the senescence phenotype in an *in vitro* model. We used human dermal fibroblasts from both male and female donors to be able to see any sex-specific effects. We found that female synthetic hormones had a sex-specific senomorphic effect in male cells only. This is important for future research into senotherapeutics as it provides evidence of how female sex hormones can affect the mechanisms of senescence and it highlights the possibility that sex may impact response to a senotherapeutic intervention.

Methods

Tissue culture

Normal human dermal fibroblast (nHDF) cells from a male and a female donor were commercially sourced with full ethical permission granted at source (Promocell, Heidelberg, catalogue number C-12302, lot numbers 445Z026.3 (male) and 467Z026.3 (female)). Both donors were Caucasian. The male donor was 36 years old at the time of donation, and the female donor was 28 years old. The cells were taken from the abdomen of the male donor, whereas the female donor's cells were taken from the breast. For further information on cell culture protocols, please view Chapter 2: Tissue culture and Chapter 3: Considerations for the replacement of foetal bovine serum with human serum and other alternative supplements in cell culture. Cells were grown until their population doubling (PD) time had doubled (approximately passage 17 for both sexes) and then transferred to antibiotic-free medium for a minimum of 48 hours before the experiment. Male cells had cumulated population doublings (cPDL) of 39.46 at the time of seeding out for the experiments. Female cells had a cPDL of 33.68 at the same point. Cells were seeded at approximately 7,200 cells/cm^2 in a 12-well plate for the senescence assay. Cells were seeded at approximately 6,000 cells/cm^2 in a 12-well plate on 13 mm coverslips for immunocytochemical staining for Ki67 and γH2AX. Cells were seeded at approximately 7,000 cells/cm^2 in a 24-well plate on 13 mm coverslips for the TUNEL assay experiments. Cells were seeded at approximately 14,000 cells/cm^2 in a 6-well plate for RNA extraction.

Treatment

Cells were treated with either a DMSO vehicle control (J66650.AD, Thermo Scientific Alfa Aesar), or a 10 μM dose of diethylstilboestrol, ethynyl estradiol or levonorgestrel (Catalogue numbers HY-14598, HY-B0216 or HY-B0257 respectively, MedChemExpress, Stockholm). Fresh medium was added to the plates before the addition of the treatment stock. Cells were treated for 24 hours before being stained for the senescence assay, fixed for immunocytochemistry experiments or harvested for RNA extraction.

Senescence-associated beta galactosidase (SAB) experiments

Senescence-associated beta galactosidase (SAB) was stained for using the Senescence Cells Histochemical Staining kit (CS0030, Merck) following the manufacturer's instructions. Further detail is available in Chapter 2: Measurement of cellular senescence and Chapter 2: Analysis of staining.

Immunocytochemical staining for Ki67 and γH2AX

Further detail is available in Chapter 2: Measurement of protein biomarkers, Chapter 2: Analysis of staining and Chapter 3: Image analysis using the Fluorescence Imaging of Nuclear Staining (FINS) algorithm. The DAPI-stained nuclei that were also stained for Ki67 or γH2AX were expressed as percentages, and the median percentage of the five images was taken forward for each biological replicate for further statistical analysis.

TUNEL assay

Cells were washed in DPBS (14190136, Gibco™), before the cells were fixed with 4% paraformaldehyde, washed again and stored in DPBS. The Click-iT® TUNEL Alexa Fluor® Imaging Assay (C10245, ThermoFisher) was performed according to the manufacturer's instructions using additional DPBS, Bovine serum albumin (BSA) fraction V fatty acid-free (10775835001, Roche), and Triton X-100 (A16046.AP, Thermo Scientific Alfa Aesar. In the same manner as for the other immunofluorescently-stained cells, the Leica DM4 B Upright Microsope at 10 × magnification was used to capture five images per coverslip. The cells in the images were later counted manually using Leica Application Suite X 2019 3.7.1.21655v software (Leica Microsystems, Wetzlar, Germany). For each biological replicate, the median percentage of Hoescht-stained nuclei that also stained for TUNEL was used for further statistical analysis.

RNA extraction

For further detail on the TRI RNA extraction, please view Chapter 2: Measurement of gene expression. RNA was eluted into 20 µl 1 × TE buffer, pH 8 (BP2473-500, Fisher Bioreagents).

Reverse transcription

Reverse transcription was performed on the RNA samples using the High-Capacity cDNA Reverse Transcription Kit following the manufacturer's instructions as detailed in Chapter 2: Measurement of gene expression.

Pre-amplification of cDNA

cDNA was produced by reverse transcription using the High-Capacity cDNA Reverse Transcription Kit as detailed in Chapter 2: Measurement of gene expression. TaqMan™ Gene Expression Assay IDs are listed in Table 1. The pre-amplified products were diluted in 1 × TE buffer, pH 8.0 (BP2473-500, Fisher Bioreagents).

Real-time quantitative PCR (RT-qPCR)

RT-qPCR was performed for 50 cycles as detailed in Chapter 2: Measurement of gene expression.

Analysis of RT-qPCR data

Gene expression was calculated using the comparative C_T technique [176]. Five housekeeping genes (*GUSB*, *IDH3B*, *PGK1*, *PPIA* and *UBC*) were included in the experiment. Using the RefFinder website, the mean of the five genes was shown empirically to be the most stable baseline across the dataset. Gene expression was therefore normalised to the mean of the five endogenous housekeeping genes before being normalised to the respective sex's DMSO

vehicle control [177]. A natural logarithm was taken of the relative ratios to aid with any skew within replicates.

Statistics

The graphs were created using GraphPad Prism version 9.4.1 for Windows (GraphPad Software, San Diego, California USA, www.graphpad.com). Unless otherwise stated, error bars show the standard error of the mean (SEM). The effect sizes and/or means ± SEM are reported in the text, with tabulated full data. One-way ANOVAs with uncorrected Fisher's LSD post hoc tests were used to assess statistical significance.

SAB activity was decreased by synthetic female hormones in male cells, but not in female cells.

SAB activity is the best marker of general senescence and for identifying a senotherapeutic effect. All three synthetic female hormones caused a decrease in SAB activity in male cells, but did not cause any significant effect in female cells. Figure 36 shows a graph of the percentage of cells stained for SAB with data and statistics presented in Table 18. The two synthetic oestrogens exhibited similar effects; a significant 30% (p = 0.0122) and 32% (p = 0.0083) decrease in SAB activity in male cells for diethylstilboestrol and ethynyl estradiol respectively. The male cells were most affected by levonorgestrel which caused a significant 51% (p = 0.0002) decrease in SAB activity.

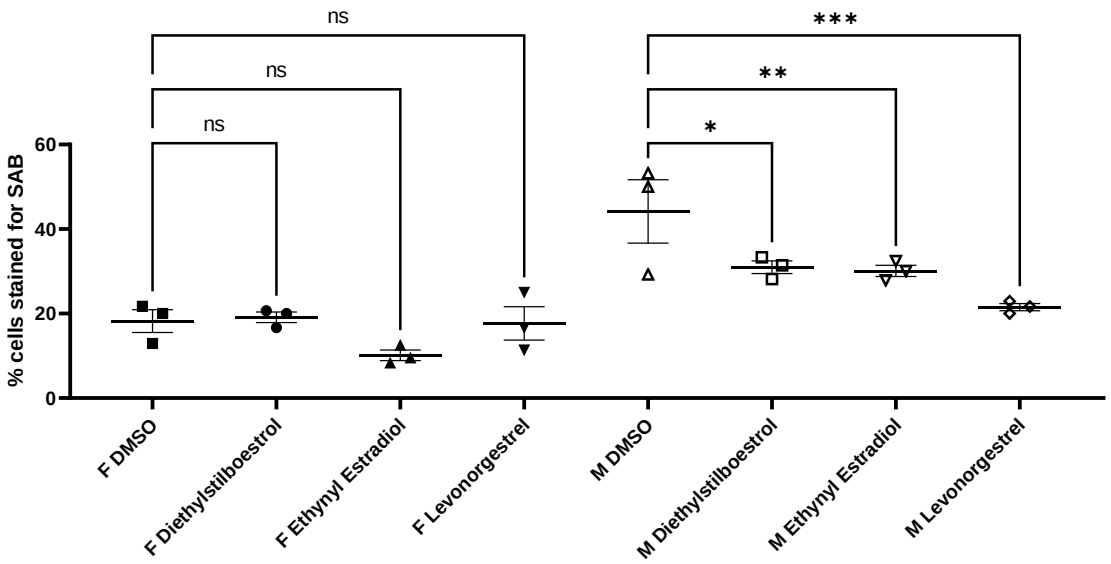

*Figure 36: Male cells had a lower percentage of cells stained for senescence-associated beta galactosidase (SAB), a marker of cellular senescence, in female (F) and male (M) dermal fibroblast cells treated with synthetic female hormones at 10 μM or a DMSO-only control. n = 3 for all groups. Error bars show standard error of the mean (SEM), and statistical significance of p values computed using one-way ANOVAs with uncorrected Fisher's LSD post hoc tests is reported: (ns) not significant, * p<0.05, ** p<0.01, *** p<0.001 and **** p<0.0001.*

Table 18: Statistics of the percentage of cells stained for biomarkers in female (F) and male (M) dermal fibroblast cells treated with synthetic female hormones at 10 μM or a DMSO-only control. Biomarkers for senescence (senescence-associated beta galactosidase (SAB)), proliferation (Ki67) and DNA damage (γH2AX and TUNEL) are assessed. Although some cells stained for it, γH2AX staining was negligible across all experimental groups. The mean ± standard error of the mean (SEM) and p values from one-way ANOVAs with Fisher's post hoc test are reported. Significant p values > 0.05 are emboldened. n = 3 for all groups.

Biomarker	F DSMO		F Diethylstilboestrol			F Ethynyl Estradiol			F Levonorgestrel		
	Mean	SEM	Mean	SEM	p value	Mean	SEM	p value	Mean	SEM	p value
SAB	18.21	2.7040	19.12	1.2410	0.8485	10.12	1.2400	0.1022	17.68	3.9700	0.9099
Ki67	22.66	3.7140	18.24	3.0860	0.3822	20.54	4.0410	0.6722	27.66	2.1510	0.3245
γH2AX	0.00	0.0000	0.00	0.0000	1.0000	0.00	0.0000	1.0000	0.00	0.0000	1.0000
TUNEL	0.93	0.7201	1.45	1.4500	0.8140	4.50	2.4830	0.1185	2.93	2.2740	0.3682
Biomarker	M DMSO		M Diethylstilboestrol			M Ethynyl Estradiol			M Levonorgestrel		
	Mean	SEM	Mean	SEM	p value	Mean	SEM	p value	Mean	SEM	p value
SAB	44.17	7.5060	30.98	1.5070	**0.0122**	30.10	1.3170	**0.0083**	21.54	0.8541	**0.0002**
Ki67	26.04	2.7720	14.23	3.5600	**0.0289**	22.80	4.5130	0.5190	26.52	3.4300	0.9235
γH2AX	0.00	0.0000	0.00	0.0000	1.0000	0.00	0.0000	1.0000	0.00	0.0000	1.0000
TUNEL	0.74	0.1738	1.09	0.8579	0.8757	4.30	1.8790	0.1191	1.23	0.6385	0.8246

Gene expression of biomarkers of senescence showed little change in female cells, but no change in males

Testing genes in pathways involved in senescence can offer some insight into the mechanisms of senescence affected by a compound. *CDKN2A* gene expression was only altered in female cells treated with ethynyl estradiol with a significant 54% increase ($p = 0.0038$). *MYC* gene expression was also increased in the same cells with the same treatment. Female cells treated with ethynyl estradiol had a 50% increase ($p = 0.0471$) in *MYC* gene expression. *CDKN1A* and *ATM* are genes associated with senescence and DNA damage response/cell cycle checkpoint pathways respectively, however unlike *CDKN2A* and *MYC* neither showed any significant change with treatments. Nuclear matrix changes are also linked with senescence, but no change in *LMNB1* gene expression was observed with these treatments. Figure 37 illustrates the changes in gene expression in *CDKN2A* and *MYC* with full data and statistics for all genes available in Table 19 and Table 20.

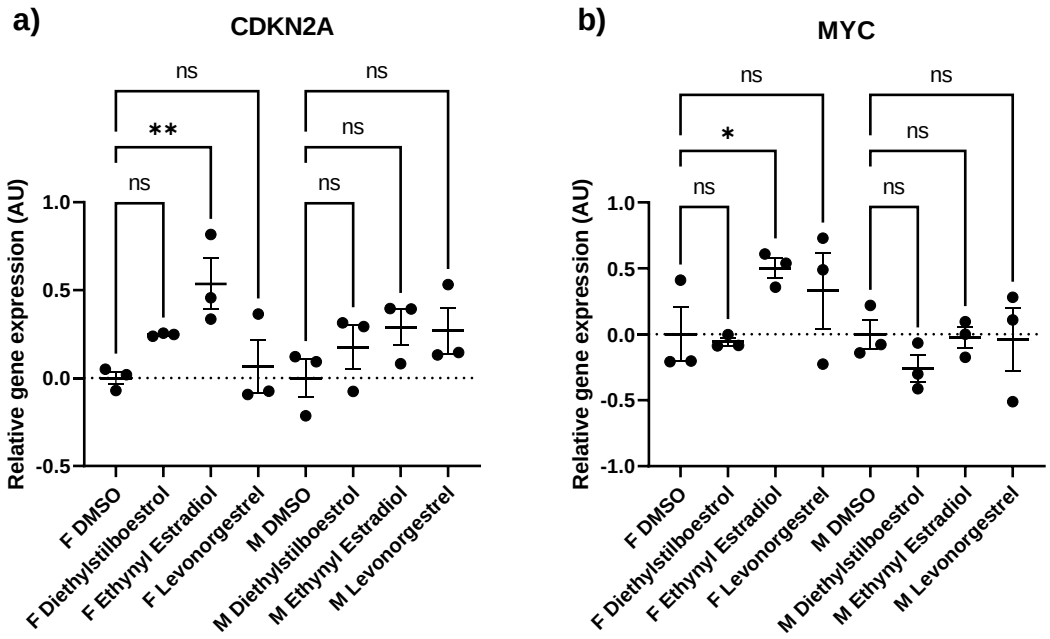

*Figure 37: Gene expression of A) CDKN2A, a biomarker of senescence, and B) MYC, an oncogene, in female (F) and male (M) dermal fibroblast cells treated with synthetic female hormones at 10 µM or a DMSO-only control. n = 3 for all groups. Error bars show standard error of the mean (SEM), and statistical significance of p values computed using one-way ANOVAs with uncorrected Fisher's LSD post hoc tests is reported: (ns) not significant, * p<0.05, ** p<0.01, *** p<0.001 and **** p<0.0001.*

Table 19: Gene expression data in female (F) dermal fibroblast cells treated with synthetic female hormones at 10 μM or a DMSO-only control. Genes relating to apoptosis, senescence, cancer pathways, matrix proteins, senescence-associated secretory phenotype (SASP) factors, splicing factors and spliceosomal components are assessed. The mean ± standard error of the mean (SEM) and p values from one-way ANOVAs with Fisher's post hoc test are reported. Significant p values > 0.05 are emboldened. n = 3 for all groups.

Gene	F DSMO		F Diethylstilboestrol			F Ethynyl Estradiol			F Levonorgestrel		
	Mean	SEM	Mean	SEM	p value	Mean	SEM	p value	Mean	SEM	p value
AKAP17A	0.0000	0.04877	-0.0696	0.06734	0.8157	-0.0861	0.19660	0.7730	-0.6028	0.33060	0.0568
ATM	0.0000	0.09368	0.1328	0.04374	0.5080	0.3512	0.01997	0.0922	0.2723	0.14300	0.1838
BCL2	0.0000	0.29700	-0.1545	0.14940	0.6721	0.8249	0.26470	**0.0351**	0.9137	0.49020	**0.0214**
CASP1	0.0000	0.05322	-0.1025	0.07671	0.5717	0.0087	0.18090	0.9618	-0.0475	0.24950	0.7926
CASP3	0.0000	0.14620	0.0350	0.02214	0.8806	0.2660	0.09735	0.2631	0.2579	0.26520	0.2772
CASP7	0.0000	0.12580	0.2608	0.08696	0.4091	0.4815	0.01044	0.1372	0.2679	0.22760	0.3968
CASP8	0.0000	0.07224	-0.3233	0.06252	**0.0643**	0.1314	0.08837	0.4311	0.0459	0.11180	0.7816
CASP9	0.0000	0.10600	0.0008	0.05213	0.9962	0.0991	0.15160	0.5748	0.1031	0.10360	0.5596
CDKN1A	0.0000	0.07025	0.1623	0.04824	0.3690	0.2715	0.15020	0.1416	0.0000	0.18610	>0.9999
CDKN2A	0.0000	0.03624	0.2474	0.00504	0.1374	0.5361	0.14450	**0.0038**	0.0654	0.14930	0.6848
CXCL1	0.0000	0.02680	-0.1083	0.06449	0.3681	0.3101	0.09798	0.0174	0.4028	0.17070	0.0033
CXCL10	0.0000	0.05642	4.7470	4.55000	0.3820	5.5460	5.34900	0.3092	14.1800	0.28910	**0.0162**
HNRNPA0	0.0000	0.13760	-0.0999	0.16080	0.6152	-0.0924	0.04577	0.6418	-0.1178	0.19000	0.5541
HNRNPA1	0.0000	0.05818	-0.1571	0.07813	0.3730	-0.0338	0.15350	0.8461	0.1071	0.03450	0.5409
HNRNPA2B1	0.0000	0.06352	0.1345	0.04062	0.4240	0.2929	0.11460	0.0931	0.2909	0.18700	0.0951
HNRNPD	0.0000	0.07285	0.0286	0.09641	0.8892	0.3005	0.13140	0.1563	0.2270	0.18050	0.2777
HNRNPH3	0.0000	0.08328	-0.0232	0.26490	0.9271	0.1767	0.32310	0.4884	0.4416	0.17970	0.0955
HNRNPK	0.0000	0.06065	-0.7314	0.07480	**0.0003**	0.1734	0.11820	0.2883	0.2710	0.08945	0.1053
HNRNPM	0.0000	0.46980	-0.0369	0.26360	0.9469	-0.1685	0.37730	0.7610	0.3877	0.18980	0.4867
HNRNPUL2	0.0000	0.03668	0.0272	0.03475	0.8521	0.0702	0.11220	0.6310	0.1518	0.10880	0.3057
IFNy	0.0000	0.05642	0.2689	0.10360	0.2016	0.3659	0.17120	0.0887	0.3534	0.17230	0.0992
IL10	0.0000	4.51400	-0.0561	4.20500	0.9857	-4.0910	0.17120	0.2042	-4.1040	0.17230	0.2028
IL12A	0.0000	0.05474	0.1378	0.02569	0.3868	0.2102	0.05250	0.1935	0.4231	0.07220	**0.0148**
IL12B	0.0000	4.64600	4.9630	4.76200	0.4270	4.8630	4.62700	0.4362	9.6640	0.35930	0.1320

IL1B	0.0000	0.21700	0.0328	0.34880	0.9524	0.2431	0.52080	0.6593	0.6907	0.09538	0.2200
IL2	0.0000	0.05642	0.2689	0.10360	0.2016	0.3659	0.17120	0.0887	0.3534	0.17230	0.0992
IL6	0.0000	0.32160	0.1824	0.14410	0.5236	0.8914	0.36240	**0.0057**	0.4181	0.11000	0.1544
IL8	0.0000	0.13850	0.0514	0.04925	0.8299	0.7404	0.17170	**0.0062**	0.4335	0.27220	0.0841
LMNB1	0.0000	0.17390	-0.0581	0.09258	0.7828	0.1824	0.06735	0.3921	0.0747	0.09352	0.7235
MMP1	0.0000	0.03852	-0.2345	0.13800	0.0792	-0.2480	0.14960	0.0649	0.2607	0.05976	0.0535
MMP3	0.0000	0.12630	0.0219	0.02824	0.9255	0.4238	0.13130	0.0849	0.3824	0.19750	0.1169
MMP9	0.0000	4.71600	0.4995	4.79000	0.9365	-4.2940	0.17120	0.4966	4.9560	4.46200	0.4338
MYC	0.0000	0.20510	-0.0579	0.02788	0.8070	0.5017	0.07474	**0.0471**	0.3308	0.28720	0.1754
NOVA1	0.0000	0.32020	0.4971	0.03800	0.0645	0.7833	0.10840	**0.0065**	0.7211	0.08223	**0.0109**
PNISR	0.0000	0.09611	0.2793	0.03049	0.1691	0.4409	0.18140	**0.0372**	0.4214	0.09260	**0.0452**
SRSF1	0.0000	0.04145	0.0309	0.08961	0.8674	0.0617	0.16330	0.7388	0.0056	0.14670	0.9759
SRSF2	0.0000	0.19890	0.0541	0.19900	0.8910	-0.2066	0.22320	0.6027	0.0718	0.26780	0.8559
SRSF3	0.0000	0.08635	0.1872	0.06322	0.1571	0.1734	0.07024	0.1880	0.1542	0.09125	0.2389
SRSF6	0.0000	0.04241	0.0692	0.02897	0.5374	0.1745	0.06653	0.1317	-0.0079	0.14760	0.9435
SRSF7	0.0000	0.12380	-0.0898	0.27420	0.6773	0.2905	0.07296	0.1891	0.0239	0.21770	0.9116
TNFα	0.0000	4.49500	-0.3955	4.06500	0.9171	-0.1749	4.30400	0.9633	4.6620	0.75530	0.2304
TNFβ	0.0000	0.49780	-4.6310	4.58600	0.3420	-4.0960	4.53000	0.3992	-8.5940	4.85000	0.0879
TRA2B	0.0000	0.07368	0.0641	0.03576	0.6262	0.0000	0.15040	0.9998	-0.0894	0.13670	0.4985

Table 20: Gene expression data in male (M) dermal fibroblast cells treated with synthetic female hormones at 10 μM or a DMSO-only control. Genes relating to apoptosis, senescence, cancer pathways, matrix proteins, senescence-associated secretory phenotype (SASP) factors, splicing factors and spliceosomal components are assessed. The mean ± standard error of the mean (SEM) and p values from one-way ANOVAs with Fisher's post hoc test are reported. Significant p values > 0.05 are emboldened. n = 3 for all groups.

Gene	M DMSO		M Diethylstilboestrol			M Ethynyl Estradiol			M Levonorgestrel		
	Mean	SEM	Mean	SEM	p value	Mean	SEM	p value	Mean	SEM	p value
AKAP17A	0.0000	0.37760	0.0210	0.09971	0.9440	-0.3786	0.04596	0.2155	0.0548	0.18780	0.8543
ATM	0.0000	0.18660	-0.2546	0.25860	0.2124	0.2516	0.11400	0.2176	0.3945	0.08646	0.0613
BCL2	0.0000	0.08764	0.0840	0.05186	0.8177	-0.1902	0.20160	0.6028	0.2631	0.20420	0.4734
CASP1	0.0000	0.05472	-0.2825	0.08580	0.1312	-0.2063	0.09652	0.2625	-0.2590	0.05251	0.1641
CASP3	0.0000	0.15720	0.0125	0.13620	0.9574	0.2428	0.24680	0.3054	0.5133	0.06678	**0.0397**
CASP7	0.0000	0.37070	-0.0541	0.18840	0.8625	-0.3383	0.30450	0.2878	0.1789	0.19410	0.5689
CASP8	0.0000	0.07372	-0.0977	0.17910	0.5567	-0.0275	0.14140	0.8679	0.2294	0.13750	0.1777
CASP9	0.0000	0.09776	-0.0735	0.11170	0.6768	0.0691	0.05622	0.6950	-0.0901	0.21660	0.6099
CDKN1A	0.0000	0.12250	-0.1919	0.13720	0.2907	0.1486	0.08915	0.4100	0.2106	0.13070	0.2478
CDKN2A	0.0000	0.10770	0.1774	0.12650	0.2788	0.2899	0.10420	0.0856	0.2698	0.13110	0.1075
CXCL1	0.0000	0.04399	0.1552	0.05730	0.2029	0.0829	0.07512	0.4884	0.1873	0.01454	0.1288
CXCL10	0.0000	0.26310	4.2230	4.56800	0.4356	4.7290	4.73100	0.3837	4.5990	4.33400	0.3967
HNRNPA0	0.0000	0.23390	0.2974	0.05454	0.1464	0.2161	0.05255	0.2837	-0.0282	0.09186	0.8867
HNRNPA1	0.0000	0.22000	-0.0813	0.09392	0.6417	0.0273	0.06772	0.8755	0.0037	0.14640	0.9832
HNRNPA2B1	0.0000	0.15400	-0.0063	0.09194	0.9698	0.0778	0.02540	0.6415	0.2511	0.14480	0.1452
HNRNPD	0.0000	0.13050	0.0631	0.08105	0.7590	-0.2701	0.23930	0.1999	0.3851	0.13380	0.0747
HNRNPH3	0.0000	0.07911	-0.0558	0.10670	0.8256	-0.0306	0.08842	0.9037	0.3165	0.09597	0.2223
HNRNPK	0.0000	0.18530	0.5549	0.08881	**0.0029**	0.4991	0.04690	**0.0060**	0.6198	0.15490	**0.0012**
HNRNPM	0.0000	0.66730	0.3579	0.03542	0.5204	0.0038	0.48630	0.9945	0.1567	0.18580	0.7773
HNRNPUL2	0.0000	0.15270	-0.1152	0.07064	0.4334	-0.0466	0.15870	0.7493	-0.0581	0.04227	0.6910
IFNy	0.0000	0.26310	-0.2527	0.09234	0.2286	-0.0330	0.03345	0.8722	0.2254	0.10600	0.2806
IL10	0.0000	0.26310	-0.2527	0.09234	0.9358	-0.0330	0.03345	0.9916	0.2254	0.10600	0.9428

IL12A	0.0000	0.24460	0.0120	0.10710	0.9391	0.0624	0.03350	0.6921	0.2606	0.10890	0.1118
IL12B	0.0000	4.41100	4.3260	4.47200	0.4876	0.2934	4.84600	0.9622	0.1350	4.42100	0.9826
IL1B	0.0000	0.49860	0.2727	0.52560	0.6211	0.4637	0.19580	0.4041	1.0400	0.39830	0.0727
IL2	0.0000	0.26310	-0.2527	0.09234	0.2286	-0.0330	0.03345	0.8722	0.2254	0.10600	0.2806
IL6	0.0000	0.08726	-0.0177	0.05395	0.9503	0.0457	0.08289	0.8723	-0.0176	0.16700	0.9507
IL8	0.0000	0.20190	-0.0505	0.16650	0.8329	-0.1289	0.16130	0.5914	0.1584	0.04279	0.5106
LMNB1	0.0000	0.25630	0.1886	0.10950	0.3767	0.2435	0.06835	0.2574	0.2177	0.19370	0.3093
MMP1	0.0000	0.08279	-0.0753	0.08249	0.5556	-0.1072	0.03083	0.4040	-0.0403	0.03862	0.7514
MMP3	0.0000	0.18370	-0.1831	0.14400	0.4390	0.0401	0.07253	0.8643	-0.0985	0.28310	0.6750
MMP9	0.0000	4.82100	4.1040	4.50300	0.5156	0.0306	4.64900	0.9961	0.2664	4.70400	0.9661
MYC	0.0000	0.11100	-0.2597	0.10220	0.2820	-0.0252	0.07915	0.9153	-0.0400	0.24030	0.8661
NOVA1	0.0000	0.03965	-0.2846	0.33680	0.2722	0.0007	0.07166	0.9977	0.1478	0.08962	0.5632
PNISR	0.0000	0.14170	-0.0921	0.09357	0.6413	-0.0557	0.10550	0.7776	0.2480	0.24270	0.2193
SRSF1	0.0000	0.13730	0.1992	0.07704	0.2899	-0.1585	0.13280	0.3967	0.2535	0.17920	0.1827
SRSF2	0.0000	0.48240	0.2587	0.11900	0.5154	-0.0533	0.13000	0.8928	-0.0508	0.37510	0.8977
SRSF3	0.0000	0.08197	0.0421	0.15530	0.7429	0.1169	0.04936	0.3677	0.1806	0.07489	0.1714
SRSF6	0.0000	0.08067	0.1928	0.03623	0.0983	0.2390	0.05504	**0.0449**	-0.0977	0.09249	0.3868
SRSF7	0.0000	0.09516	-0.2363	0.10150	0.2809	-0.1442	0.07144	0.5057	0.1147	0.10790	0.5956
TNFα	0.0000	0.13420	0.1262	0.17540	0.9735	0.2699	0.08071	0.9434	-0.0307	0.20740	0.9936
TNFβ	0.0000	0.33380	0.4300	0.49070	0.9287	0.5454	0.21720	0.9096	-3.8980	4.87100	0.4219
TRA2B	0.0000	0.04219	0.2672	0.07561	0.0550	0.2555	0.02158	0.0653	0.2954	0.10360	**0.0361**

Synthetic female hormones have limited effects on cellular proliferation and apoptosis, and no observable changes in DNA damage repair.

Cellular proliferation, apoptosis and DNA damage are key aspects of the senescence phenotype, but are not present in every senescent cell. However, knowing how a compound affects these aspects can identify if it is a senolytic or a senomorphic compound. Diethylstilboestrol induced a 45% decrease in Ki67 staining (a marker of cellular proliferation) in male cells ($p = 0.0289$). No other effects on proliferation were observed in either male or female cells as shown in Table 18 and Figure 38. As shown in Table 18, the levels of DNA damage repair using the biomarker, γH2AX, were negligible in all cell lines. This was reflected in very low levels of cell death in the culture as measured by TUNEL assay; an average of 2.1% of cells had evidence of double-strand breaks. There was no significant difference in double-strand DNA breaks between any of the experimental groups (Table 18). This was also evident at the molecular level; assessment of apoptosis markers revealed that only two of them, *BCL2* and *CASP3*, had any significant changes (shown in Table 19, Table 20 and Figure 39). *BCL2* expression was increased by 82% ($p = 0.0351$) and 91% ($p = 0.0214$) by ethynyl estradiol and levonorgestrel, respectively, in female cells. There were no significant changes in male cells for *BCL2* expression, but *CASP3* expression was significantly increased by 51% ($p = 0.0397$) when male cells were treated with levonorgestrel. No changes in *CASP3* expression were observed in the treated female cells.

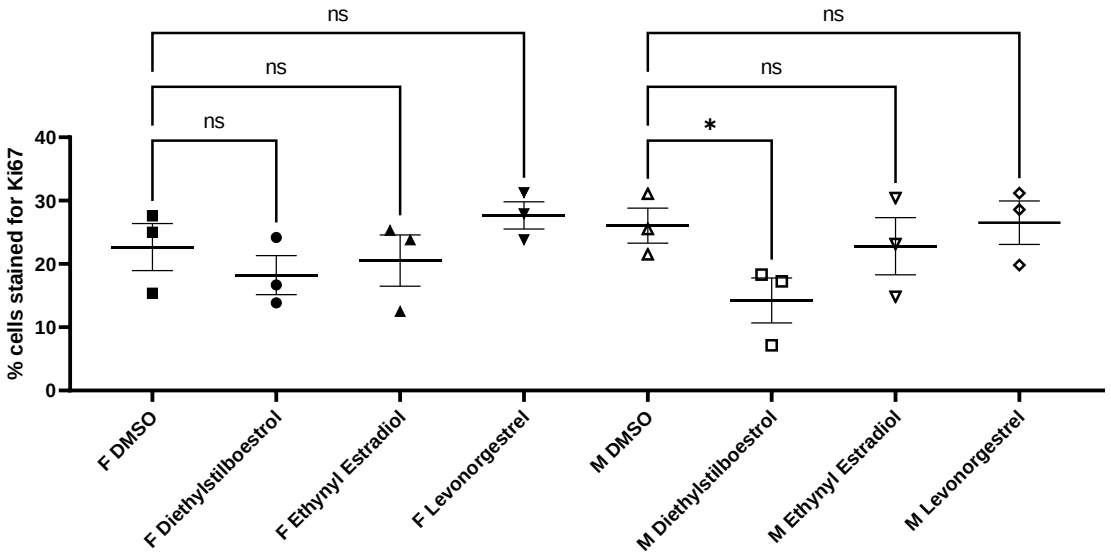

*Figure 38: Ki67 staining was mainly unaffected by the synthetic hormone treatment. Percentage of cells stained for Ki67, a marker of cellular proliferation, in female (F) and male (M) dermal fibroblast cells treated with synthetic female hormones at 10 µM or a DMSO-only control. n = 3 for all groups. Error bars show standard error of the mean (SEM), and statistical significance of p values computed using one-way ANOVAs with uncorrected Fisher's LSD post hoc tests is reported: (ns) not significant, * p<0.05, ** p<0.01, *** p<0.001 and **** p<0.0001.*

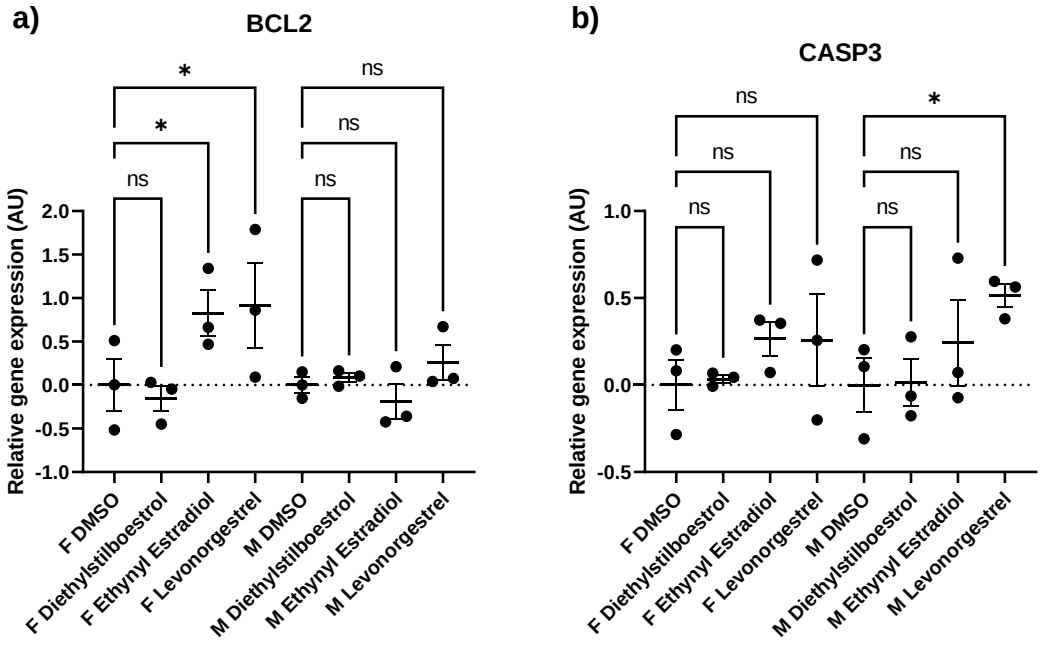

*Figure 39: Gene expression of markers for apoptosis in female (F) and male (M) dermal fibroblast cells treated with synthetic female hormones at 10 µM or a DMSO-only control. A) BCL2 and B) CASP3. n = 3 for all groups. Error bars show standard error of the mean (SEM), and statistical significance of p values computed using one-way ANOVAs with uncorrected Fisher's LSD post hoc tests is reported: (ns) not significant, * p<0.05, ** p<0.01, *** p<0.001 and **** p<0.0001.*

Sex differences in splicing factor expression in response to synthetic female hormones

Splicing factor dysregulation is known to be a driver of senescence, therefore measuring gene expression of a selection of senescence-associated splicing factors or spliceosomal components can help identify the way in which a compound is affecting senescence [56]. There were sex differences in the splicing factor gene expression (Table 19, Table 20 and Figure 40). In female cells, expression of the splicing factor, *PNISR*, was significantly increased by ethynyl estradiol by 44% ($p = 0.0372$). Expression of *NOVA1*, which encodes a spliceosomal component, was increased in female cells by ethynyl estradiol (78%, $p = 0.0065$) and by levonorgestrel (72%, $p = 0.0452$). Whereas in male cells, *SRSF6* expression was increased by ethynyl estradiol by 24% ($p = 0.0449$), and *TRA2B* expression was increased by 30% by levonorgestrel ($p = 0.0361$). Only one splicing factor's gene expression was altered by the treatments in both male and female cells: *HNRNPK*. *HNRNPK* gene expression was significantly increased in male cells by 55% ($p = 0.0029$), 50% ($p = 0.0060$) and 62% ($p = 0.0012$) for diethylstilboestrol, ethynyl estradiol and levonorgestrel respectively. In female cells, only diethylstilboestrol had any effect on *HNRNPK* expression. We observed a decrease of 73% ($p = 0.0003$) in gene expression compared with the increases in *HNRNPK* expression seen in the male cells. No significant change was observed for other splicing factor transcripts.

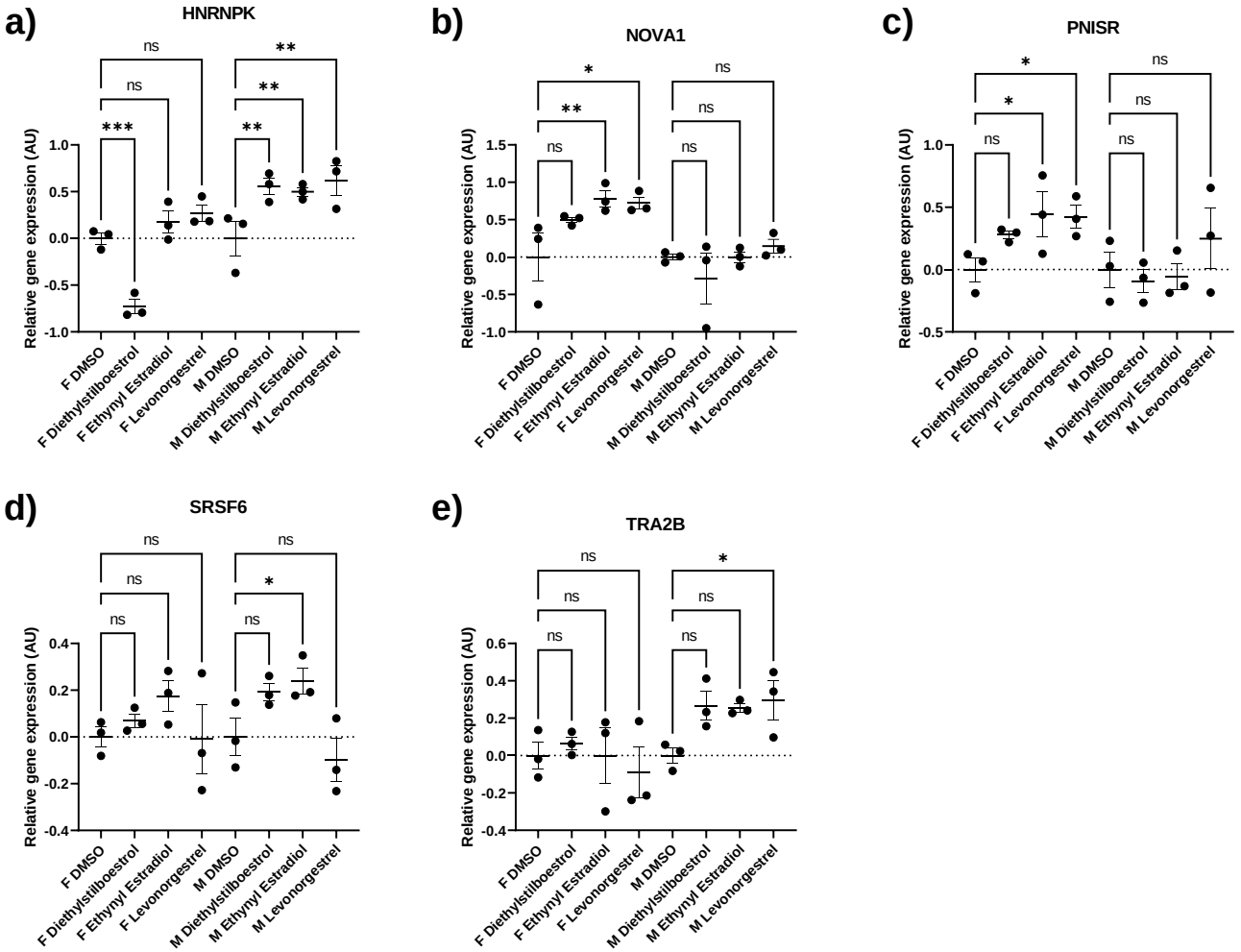

*Figure 40: Gene expression of genes encoding splicing factors or spliceosomal components in female (F) and male (M) dermal fibroblast cells treated with synthetic female hormones at 10 µM or a DMSO-only control. A) HNRNPK, B) NOVA1, C) PNISR, D) SRSF6, and E) TRA2B. n = 3 for all groups. Error bars show standard error of the mean (SEM), and statistical significance of p values computed using one-way ANOVAs with uncorrected Fisher's LSD post hoc tests is reported: (ns) not significant, * p<0.05, ** p<0.01, *** p<0.001 and **** p<0.0001.*

Alterations in the expression of SASP proteins occurred in female, but not male cells, in response to synthetic female hormones

The SASP is another key aspect of the senescence phenotype, and measuring SASP factors can help show how a senotherapeutic compound affects senescence. We found limited evidence of alterations in the expression of SASP markers in response to synthetic female hormones in male or female cells (Table 19, Table 20 and Figure 41). No significant changes were observed in the gene expression of SASP factors in male cells in response to the treatments, but female cells showed several changes in expression of interleukins and CXCLs. In female cells, diethylstilboestrol increased *IL6* expression by 89% ($p = 0.0057$) and *IL8* expression by 74% ($p = 0.0062$). *IL12A* expression was increased by 42% ($p = 0.0148$) in female cells treated with levonorgestrel. *CXCL1* expression in female cells was increased significantly: an increase of 54% ($p = 0.0174$) by ethynyl estradiol and 40% ($p = 0.0033$) by levonorgestrel. *CXCL10* expression in female cells had a 14-fold increase in expression ($p = 0.0162$) caused by levonorgestrel. This is a very large effect, but it is important to say that expression for *CXCL10* was at the edge of detection (average CT of 38 cycles). Thus, this result is likely skewed by low gene expression in the controls, which gives rise to an artificially larger effect. Expression for *IFNy*, *IL2*, *IL10*, *IL12B* and *MMP9* was at the edge of the detectable range for gene expression too, but no significant changes in expression were observed. The remainder of SASP factors examined (*IL1B*, *MMP1*, *MMP3*, *TNFα* and *TNFβ*) were well within the detectable range, but no significant changes were observed in either male or female cells with treatments.

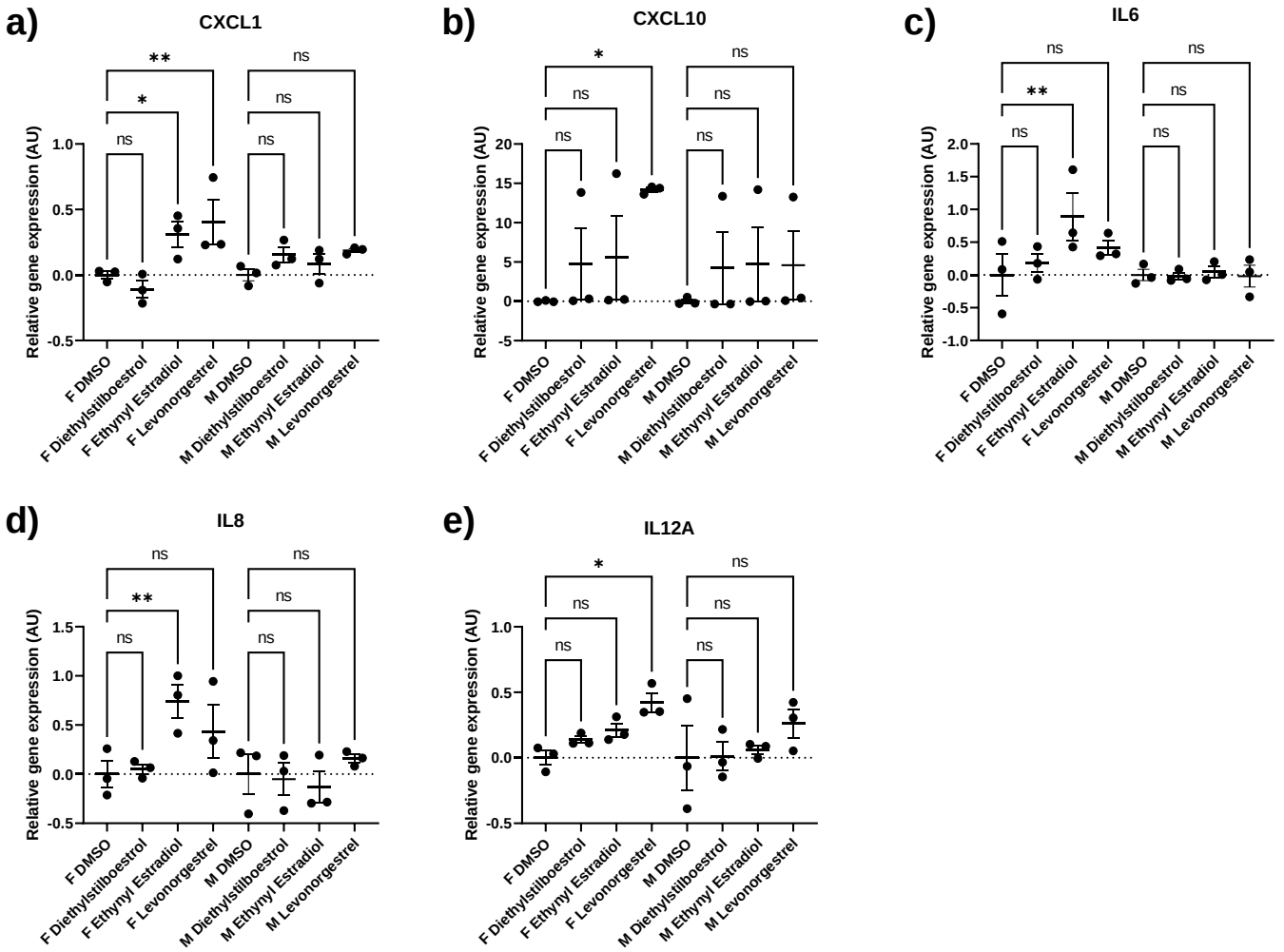

*Figure 41: Gene expression of genes encoding senescence-associated secretory phenotype (SASP) factors in female (F) and male (M) dermal fibroblast cells treated with synthetic female hormones at 10 µM or a DMSO-only control. A) CXCL1, B) CXCL10, C) IL6, D) IL8, and E) IL12A. n = 3 for all groups. Error bars show standard error of the mean (SEM), and statistical significance of p values computed using one-way ANOVAs with uncorrected Fisher's LSD post hoc tests is reported: (ns) not significant, * p<0.05, ** p<0.01, *** p<0.001 and **** p<0.0001.*

Discussion

This study aimed to investigate whether three synthetic female hormones could have an impact on senescence, and identify the type of any senotherapeutic effect observed. The study was repeated in cells from both male and female donors to identify if any of the changes in senescence characteristics were sex-specific. We found that the three compounds were senomorphic, but only in male cells. Other sex-specific patterns were shown across the other aspects of the senescence phenotype.

A key finding is that the three compounds (diethylstilboestrol, ethynyl estradiol and levonorgestrel) do have a senomorphic effect. In males, they lower SAB activity without any major increase of apoptosis. Diethylstilboestrol decreases proliferation in male cells, which is at odds with oestrogen's often growth-inducing effects, e.g. during the female pubertal growth spurt [321]. Reassuringly, there are no changes in DNA damage levels in male cells to accompany the decreases in cellular senescence. Apoptosis is not heavily affected in males, with only *CASP3* gene expression increasing with levonorgestrel treatment. This suggests the three synthetic hormones are not acting in a senolytic manner on the male cells. Therefore, a senomorphic effect is occurring in the cells, or possibly an induction of growth in non-senescent cells in the case of diethylstilboestrol.

The second major takeaway is that the senomorphic effects were only observed in male cells. This suggests a sex-specific response to a senotherapeutic compound. Female cells were affected by the compounds with a minor increase

in the expression of a limited number of genes associated with senescence pathways (*CDKN2A* and *MYC*) and apoptosis (*BCL2*). In the male cells, there were no changes in gene expression of any SASP factors. Whereas in female cells, only the diethylstilboestrol treatment did not affect SASP factor gene expression. The splicing factors/spliceosomal components *NOVA1*, *PNISR*, *SRSF6*, and *TRA2B* were affected by one or two treatments and results appear sex-specific. *HNRNPK* expression was changed with treatment in both sexes, but the directionality of the change is sex-specific.

These results could inform further research as other senotherapeutic compounds may have similarly sex-specific responses. It is worth caveating that, although the two cell donors in this study were matched for ethnicity and age, there was an age gap of 8 years with the male being older. Each cell type will reach replicative senescence at a different number of population doublings, but in this case, there was only 5.78 population doublings between the cells. As far as was reasonable, the cells were matched, but the female cells had lower overall levels of SAB activity. It is possible that the effect of the treatments was the same in both sexes, but, given the lower overall levels of SAB activity in the females, the proportional effects were masked. Arguably, this is more of a relevant comparison than an exact match for SAB activity because females tend to have lower levels of molecular ageing than males; a senomorphic compound may well rescue senescence in male cells, but may not have the same result in female cells.

The reasons for both the senomorphic effect of the three synthetic female hormones and the sex-specificity of the senomorphic effect may well lie with the

pathways involved in senescence and/or bioavailability. The canonical or classical signalling pathways for both oestrogen and progesterone feature the hormone and its respective nuclear receptor(s) acting as ligand-activated transcription factors. The complex binds to hormone responsive elements (HREs) in the genome to control gene expression. There are many HREs across the genome, for example there are over 70,000 oestrogen-responsive-elements identified [327]. Both hormones are able to act via other pathways, including membrane bound GPCRs. Activation of their respective GPCRs can activate cell fate pathways such as Ras/Raf/MEK/ERK and PI3K/Akt, as well as cross-signalling with classical pathways [328,329]. The cell fate pathways are intrinsically linked with senescence, and the involvement of the hormones could provide a potential shared mechanism that may explain why both the oestrogenic compounds and the synthetic progesterone had a similar effect on SAB activity. The altered expression of *CDKN2A* and *MYC* provide evidence of ethynyl estradiol affecting these pathways in the female cells. Differing expression/activity/sensitivity of receptors between the sexes might also be a factor in the sex-specificity of the senotherapeutic effect. The differences in how the synthetic female hormones interact with a male cell versus a female cell could be a reason why splicing factor gene expression is different between the sexes, which could also be driving the difference in the overall effect on senescence. When considering these compounds *in vivo*, the dosage is also a factor. This experiment used a single dose at 10 μM, chosen due to the results from previous experiments with small molecules for senotherapeutic effects, but repeated exposure and/or higher/lower dosage may have different effects. Another consideration is that these cells were donated by a pre-menopausal woman, so

it is possible that cells from women who are undergoing or have gone through the menopause may have differing responses to synthetic female hormones, or indeed they may have a similar effect compared to the effect seen in the male cells. Similarly, the cells are dermal fibroblasts, and results may be tissue specific. Given that the canonical signalling pathways for oestrogen and progesterone can affect the transcription of many genes via HREs, and recently sex-specific splicing factor expression patterns have been identified in the context of ageing, it is perhaps unsurprising that several splicing factors were affected, and that they were not consistent between the sexes [303]. The most affected splicing factor was *HNRNPK*, which is involved in the PI3K/Akt pathway amongst others [330]. This particular splicing factor has been shown to be oestrogen responsive, but the converse effects between the sexes are intriguing: *HNRNPK* expression was increased in all three treatments in male cells, but was decreased in female cells treated with diethylstilboestrol [331]. The same study indicated *HNRNPM* was oestrogen-responsive, however *HNRNPM* expression was not altered in any treatment group. 17β-estradiol is known to regulate *NOVA1*, so one might expect the oestrogenic compounds to affect its expression in both sexes, however it was increased by ethynyl estradiol and levonorgestrel only in female cells [332]. The same two treatments in females caused an upregulation in *PNISR*, a splicing factor, whereas the male cells did not share the same effects. *SRSF6* is inhibited by oestrogen in breast cancer cells, so it is curious that ethynyl estradiol-treated male cells showed an increase in *SRSF6* expression. *TRA2B* is thought to be associated with age at menarche, so given an obvious link with biological sex, it may be expected to be changed more, but only levonorgestrel caused effects in male cells [333].

Similarly, there are sex-specific differences in the expression of the SASP factors. Male cells had no change to the expression of SASP factors in any treatment, whereas female cells showed increased expression of a handful of SASP factors. Female cells treated with ethynyl estradiol had an increase in expression of *CXCL1*, *IL6* and *IL8*. Treating them with levonorgestrel resulted in increases in the expression of *CXCL1*, *CXCL10* and *IL12A* (although *CXCL10* expression levels were so low in the controls that the effect is likely to be exaggerated). The increase in SASP factor expression in response to treatment suggests that female cells may exhibit some inflammation when challenged with female sex hormones.

These findings must be taken into account in future research, in particular when investigating senotherapeutic drug responses. The three synthetic female hormones do not currently offer a potential clinical application as a mainstream senotherapeutic drug. This is because the effect is not observed in females who routinely take the medicines, and males taking the hormones would have feminising side-effects. The side-effects would probably be unwanted and so their risk of side effects would outweigh any benefits offered by the senotherapeutic mechanism. Also, oestrogenic compounds have often been linked with proliferation increases and cancers [326,334]. Despite this, the compounds offer an interesting direction for research. Firstly, the identification of mechanisms - do other senomorphic compounds have sex-specific effects? How are oestrogenic and progesterone-based compounds exerting the same effect? Why does levonorgestrel have the largest effect on SAB activity when oestrogen, rather than progesterone, is more commonly associated with senescence in the literature?

Are splicing factors regulated by sex hormone pathways? Then, clinical applications - are there potential senotherapeutic compounds that have been missed due to studies only using cells from one sex? Are there any similarly-structured polyphenolic and/or steroidogenic compounds that may act via a similar pathway with more targeted effects (as opposed to the widespread endocrine effects of close analogues of female hormones)? Is the effect seen in female cells retained post-menopause? The evidence of sex-specific differences reiterates that sex can affect drug response and any new therapy must consider sex in experimental design as early as the *in vitro* experiments because responses can differ based on the genetic sex of the cells.

Overall, these results indicate that the three compounds have senomorphic effects and that senotherapeutic compounds can show sex-specific effects. Levonorgestrel had the most observed effects on aspects of the senescence phenotype, which may offer a new direction for research that typically focuses on oestrogenic compounds/pathways over progesterone's. These compounds are unlikely to be suitable as widespread therapies for senescence, but open up avenues of research for further exploration of the mechanisms of senescence. Biological sex in *in vitro* experiments can cause dimorphic effects and this should be considered more regularly when designing experiments, particularly in the process of investigating senotherapeutic compounds.

Sources of Funding

The authors gratefully acknowledge funding from Animal Free Research UK. No reagents containing animal-derived biomaterials were purchased with this grant.

Author Contributions

LRB designed the experiment, performed laboratory work, data analysis and prepared the manuscript. RF performed laboratory work and helped prepare the manuscript. LWH provided overall oversight and managed the project.

Conflicts of Interest

Professor Harries is an inventor on patent PCT/GB2019/052125, and is a founder, chief scientific officer and research and development lead for SENISCA, Ltd. Ms Bramwell and Mr Frankum have no financial interest to declare in relation to the content of this manuscript.

Chapter 7: Discussion

Summary of thesis

Ageing-related diseases are set to become more of a problem as our population increases in age. Ageing has a molecular basis and the mechanisms of the hallmarks of ageing underpin many age-related diseases. Therefore, targeting these mechanisms could offer valuable insight and help with future treatments for many different diseases. Cellular senescence and mRNA splicing dysregulation are two hallmarks that are particularly promising in this regard.

Cellular senescence is not a homogeneous state, but rather a collection of characteristics that are typically associated with senescence. Senescence can be targeted with senotherapeutic compounds: senolytic compounds cause selective lysis of senescent cells, whereas senomorphic compounds induce a return to the normal cell cycle. The field of senotherapeutics is relatively novel and many commonly used drugs could have untapped potential.

Our research team uses several techniques for assessing senescence in *in vitro* models, but these required a degree of optimisation for use in this project. I improved the human-relevance of cell culture conditions, developed a method of measuring senescence that was suitable for a medium-throughput application and helped create an algorithm for image analysis of immunocytochemically stained cells to aid in analysis of Ki67 and γH2AX biomarkers.

Aside from being important diseases to study in their own right, premature ageing syndromes or progeroid diseases can offer mechanistic insight into the hallmarks

of ageing. Senescence is known to be increased in progeroid diseases, but as splicing factor dysregulation is a relatively new hallmark of ageing, there was no information on how the progeroid syndromes affected splicing. I assessed splicing factor dysregulation to be present in the progeroid syndromes. I also applied a known senomorphic compound, trametinib, which was able to rescue some aspects of senescence in the progeroid syndromes. Trametinib had more effects in the less severe syndromes meaning that extreme levels of senescence could not be rescued, but lower levels of senescence could. Trametinib and other senomorphic compounds are worthy of investigation as therapies for progeroid syndromes.

As previously mentioned, many commonly used drugs could have untapped senotherapeutic potential. I performed a medium-throughput screen of senescence using *CDKN2A* gene expression and validated a selection of compounds with an SAB activity assay. I performed structure-function analysis and found a substructure to be associated with a decrease in *CDKN2A* expression. Several compounds had potential senotherapeutic effects including some synthetic female hormones.

I investigated this further by conducting an experiment treating male and female cells with three synthetic female hormones. I found a sex-specific senomorphic effect: the compounds decreased SAB activity only in male cells. Further sex-specific effects were seen in other senescence characteristics. This finding of sex-specific senomorphic effects has serious implications in the field of senotherapeutic development.

I developed better techniques for studying senescence, provided further evidence of splicing factor dysregulation, found many potential senotherapeutic compounds and an associated substructure, as well as finding that three synthetic female hormones exert a sex-specific senomorphic effect.

Discussion of thesis

There is much evidence in the literature in support of cellular senescence as a fundamental process involved in ageing and multiple age-related diseases [69,213,335]. The work in this thesis also supports senescence as a fundamental process in ageing, by showing the senescence phenotype again in progeroid diseases and by successfully using senotherapeutic compounds to target the senescence phenotype in both normal and progeroid cells. Cellular senescence is implicated across all of the other hallmarks of ageing; it is possibly the most fundamental hallmark because it overlaps and intersects with so many of the other hallmarks as discussed in the introduction of this thesis [37,44,56,61,63,70,71,104,141,142]. This thesis provides further evidence that the novel hallmark, alternative splicing dysregulation, is also important in ageing and is a part of the senescence phenotype in progeroid cells.

Categorising biological processes as hallmarks of ageing can be beneficial, as the classification draws attention to the biological process itself and can aid in identifying and/or prioritising new and/or key areas for research. This is similar to the way in which ageing can be usefully classed as a disease in certain circumstances [11,12]. However, many of the hallmarks show distinct overlap and/or could be split into further categories. For example, inflammation was recently recognised as a separate hallmark from the original hallmark of altered intercellular communication [21]. Arguably, the evidence presented in the introduction regarding immunosenescence, the SASP and the changes within neuroendocrine pathways is now substantial enough that each aspect also meets

the three criteria and could be considered hallmarks of ageing on their own merit [103,111,122,112–116,119–121]. It is likely that more hallmarks will emerge as time goes on, and they will provide more potential ways in which to target ageing [21].

Cellular senescence is not a homogeneous irreversible state of cell cycle arrest as scientists once thought, but rather a heterogeneous collection of common characteristics which can be reversed in certain circumstances [37,64]. It can be difficult to quantify as a result of its heterogeneous nature, so identifying any unique signatures of different types or stages of senescence could be useful in the future [68,141].

The work in this thesis shows just how difficult senescence can be to quantify. Small effects, which can be a common occurrence with senomorphic compounds, can often fall outside the limit of detection for many methods for measuring general senescence and other aspects of the senescence phenotype. The “gold standard” SAB assay is the most reliable marker of general senescence, but the current methods for quantifying SAB are subjective and difficult to perform in a high or medium-throughput manner [166,167]. The work in this thesis identifies the use of *CDKN2A* gene expression as a suitable first pass screen, but we found it could not replace SAB activity as the “gold standard”. The expression of *CDKN2A* is not as reliable as SAB activity, evidenced by the fact that large effects on *CDKN2A* caused by compounds in the senescence screen in chapter five were not replicated when validated against SAB activity. Unpublished work from within our research team suggests that using gene expression analysis of *CDKN1A*, *CDKN2A* or one of their associated isoforms still has the same issue identified

within this thesis: they are not as reliable as SAB activity as a measure of general senescence. Often the splicing factors that are involved with ageing can regulate large swathes of the genome, meaning it can be difficult to attain a stable baseline as many traditional housekeeping genes are affected by the altered splicing. Absolute quantification of markers of senescence may mitigate against this issue.

The fluorometric kit used in chapter three held promise, but it was not sensitive enough for the small effects on senescence that are caused by many senotherapeutic compounds. Similarly, unpublished work from within our team suggests that senescence assay kits using flow cytometry and/or fluorometric principles are also not appropriate for detecting small senotherapeutic changes. The sensitivity range is a factor again, but the irregular shape of senescent cells and morphology of particular cell types can also cause issues. SAB staining can become diffuse in the cytoplasm in larger cells meaning that although a cell with senescence-associated morphology may have more SAB activity overall, it may appear less stained than a smaller cell that is not showing the senescence-associated morphology. As SAB staining remains the most sensitive and reliable method, it will be worthwhile to further investigate if any improvements can be made because, in spite of it being the most reliable measure, SAB activity is difficult to perform in a high-throughput way and is difficult to analyse in a standard way without subjectivity. Although other options, like fluorometry or flow cytometry, have not been able to replace SAB activity staining, with further optimisation or perhaps used in combination, they may be able to help standardise the measurement of senescence. An automated image analysis technique, perhaps similar to the FINS algorithm created in chapter

three, could eventually be created to analyse images of SAB staining. This could be difficult to achieve as, due to the more complex images involved, it may have to rely on artificial intelligence computing rather than simpler segmentation methods and may need the additions of other stains or measures. For example, ways of measuring nuclear and cell size could be added into the analysis [336]. Recently a study, which uses the artificial intelligence approach of deep neural networking, has been able to link nuclear size and the intensity of DAPI staining to act as a biomarker for senescence [337]. This approach will be tested within our research group.

Other aspects of the senescence phenotype can be difficult to quantify too, due to both the method and the biomarker used. The FINS algorithm should significantly improve upon the manual cell counting techniques used to measure Ki67 and γH2AX within our team. Ki67 is a very reliable marker of cellular proliferation, but γH2AX is less reliable as a biomarker [166–168,174]. γH2AX is often thought to be a biomarker of DNA damage, however it is a little less direct of a biomarker than it is often purported to be. γH2AX is produced following phosphorylation of H2AX by kinases, such as ATM, and is present at the location of double-stranded DNA breaks that are being repaired [173,174,259,338]. In several experiments for this thesis, the level of γH2AX was low or negligible. Low levels of DNA damage could be expected in chapter six as the cells used are from non-diseased donors and aren't subjected to major cell stresses during the course of their treatments, but the observation in chapter four of low levels of a supposed DNA damage biomarker in the progeroid cells was unexpected. It is well reported that progeroid diseases have damaged DNA [33]. However, although

DNA damage is often present in progeroid diseases, the DNA damage repair response is often also affected even in well-characterised disease pathologies like HGPS. Zhang *et al.* find that HGPS cells treated with doxorubicin (to induce DNA damage) have less intense signal than controls at the site of γH2AX foci, and when they attempted to restore part of the ATM activation pathway in these cells, the intensity of the γH2AX signal increased [260]. Similarly, the reason for the low γH2AX levels in the progerias could be due to the lack of repair response rather than lack of DNA damage *per se*. The levels of biomarkers of apoptosis (the gene expression of caspases in this case) are higher in the progeroid cells and could support the notion that the cells are undergoing apoptosis instead of being repaired. Other measures that can assess DNA damage such as a comet assay (or even TUNEL staining, which measures double stranded DNA breaks associated with apoptosis) may perhaps be more appropriate than γH2AX staining for measuring general levels of DNA damage [173,339]. Narrowing down a signature of senescence would be helped by improvements in the way that each characteristic is measured, as well as more research into how each characteristic plays a role in senescence. This could enable further exploration into how senescence could be categorised. Identifying relevant and informative ways of categorising senescence could be useful, particularly if it emerges that different senotherapeutic compounds target specific stages or types of senescence [340].

Although cellular senescence has been shown as a hallmark of ageing across multiple species, as discussed in the introduction, aspects of the senescence phenotype can differ between species. The naked mole-rat's negligible levels of senescence compared with other species exemplifies this statement [60]. Another

hallmark of ageing, the dysregulation of alternative splicing, was also remarkably different in the naked mole-rat compared with other species. The regulatory patterns of RNA splicing are well known to differ between animals, but it is less well known that splicing patterns can be altered by the presence of animal-derived biomaterial within the microenvironment of the cell culture model [136]. To avoid this issue, our team has removed animal-derived biomaterial from the culture of several cell lines. It is worthwhile thinking about all aspects of an *in vitro* cell culture model, as the model can impact experimental results and alter effects. In chapter six, a sex-specific effect is noted. The sex of the cells' donor may play a role in how a cell culture model responds to an intervention, and sex-specific effects could be a contributory factor to the failure at clinical trial of any downstream therapeutic compound. The sex of a cell is particularly important in ageing research because ageing is linked with sex in many regards, including as part of the evolutionary theories of ageing, as discussed in the introduction and chapter six.

There is also overlap between steroid hormone pathways and ageing pathways, so it is possible that some senotherapeutic compounds mimic sex hormones and/or interact via similar mechanisms. For example, the well-known senomorphic compound resveratrol is an agonist for the oestrogen receptor [341]. Despite the unreliability of *CDKN2A* as a biomarker of senescence, the common substructure identified by the bioinformatic structure-function analysis correlates with larger polyphenolic substructures associated with known senomorphic and/or senolytic compounds by other research teams [152]. Future studies might look to identify sex-specific differences of ageing, any senotherapeutic effects of

polyphenolic compounds (including steroidogenic compounds) and any crossover between sex hormone pathways and ageing pathways that could give mechanistic insight into the pathways of senescence.

It is clear that senotherapeutic compounds can have impacts on age-related diseases with clinical trials for several compounds already underway [149,150,153]. Most of these compounds are senolytic drugs, but there are some senomorphic compounds involved. For example, metformin is a drug used to help treat the age-related disease of diabetes, and is currently the focus of a unique clinical trial. Rather than measuring aspects of a specific disease, the TAME trial (targeting ageing with metformin) is following people who are taking the drug to identify any improvements in ageing and age-related diseases [153]. Metformin has senomorphic properties and is known to target many pathways including the IIS and the SASP pathways [153,342,343]. Senomorphic drugs may be only targeting certain aspects of the senescence phenotype, e.g. the SASP [117]. In the work on progeroid syndromes in chapter four, we found the more severely affected cells were less affected by the senomorphic compound, trametinib. This lends support to the notion that senomorphic compounds may not be able to rescue severely damaged cells, as well as to the ideas surrounding different stages or types of senescence as discussed in the introduction [68,141]. Other studies also identify that the phenotype of certain senescent cells cannot be reversed, e.g. senescence induced via p16 was not reversible in Beauséjour *et al.*'s study [266].

Senomorphic compounds, including compounds such as resveratrol and metformin, often show a biphasic dose response which is an example of hormesis

[263–265]. A biphasic dose response is when a drug has two different effects at two different doses, and often can be considered a hormetic response. A hormetic response is when a response to a stressor overcompensates to the extent that it actually provides a benefit overall [263]. This type of response is limited by how much a cell can respond reasonably to ensure a stressor is mitigated against, but without compromising its own survival. The cell may only have a small response overall, and this may be the reason why known senomorphic compounds were not identified within chapter five's senescence screen. In chapter six, female cells exhibited a small amount of inflammation in response to the synthetic female hormones, contrasting with the response of the male cells. The treatments' reduction in senescence in male cells and increase in inflammation in female cells may suggest the synthetic female hormones posed a small amount of cellular stress that induced the male cells to respond (and overcompensate as a hormetic response) more than the female cells. Potentially, future studies seeking repurposed drugs as senomorphic compounds should focus on small changes in the biomarkers of senescence rather than the largest effects. Nonetheless, the approach used in chapter five was sufficient to identify potential senotherapeutic effects, and stratifying a screen by effect size could also help ascertain mechanisms of senescence.

Repurposed drugs can exert senotherapeutic effects, and we have seen that screening for effects on senescence could also identify senescence-inducing compounds that would have potential as anticancer drugs. Further screening studies may be useful to test different compounds to the selection chosen in chapter five. This thesis has revealed some potential senotherapeutic benefit for

drugs prescribed for other indications, e.g. chlorpheniramine maleate. All compounds would need stringent further investigation before the clinical usefulness of each compound as a senotherapeutic could be judged. In chapter four, trametinib was used to successfully ameliorate some aspects of the senescence phenotype in milder progeroid phenotypes, and many compounds were identified in chapter five. On further investigation, some of the compounds may not be feasible as a drug to target ageing and/or age-related diseases as they may have unintended side effects, e.g. chapter six's finding that synthetic female sex hormones can have a senomorphic effect in biologically male cells is highly likely to not be translatable into widespread use as a senomorphic compound. However, several known senomorphic compounds did not come up in the screen and this is likely to be the result of the dosage regimen applied: these compounds often have a biphasic dose response and/or only exhibit a small effect and this method of screening could only identify the largest effects. Further studies that are able to perform a high or medium-throughput screen may expand the premise to use more than two doses, and definitely should have enough resources available to complete multiple repeats enabling proper statistical analysis. These studies can be used in combination with bioinformatic analysis of structure-function, as demonstrated in chapter five, but could also be used for studies to use rational small molecule design to develop compounds from a chemical structure that is associated with the particular function (i.e. a senolytic or senomorphic function).

Conclusion of thesis

This thesis provides further evidence in support of a role for cellular senescence in ageing and age-related disease, and that splicing factor dysregulation is an important contributor to the senescence phenotype. A molecular basis of ageing is formed from the biological processes identified as the hallmarks of ageing. They are interrelated and overlap, but cellular senescence is a particularly key hallmark. Compounds that affect senescence may be useful in treating ageing and age-related disease. Many compounds have senotherapeutic potential, but cellular senescence can be difficult to quantify as a result of both the methods used to assess it and its heterogeneous undefined phenotype.

The work in this thesis improves many methods for assessing senescence, which should help with future ageing and senescence research. We created a pipeline for characterising senotherapeutic effects. We improved methods for assessing senescence/senotherapeutic effects through the creation of more human-relevant tissue culture practices, the optimisation of measuring senescence in a medium-throughput way, the creation of the FINS algorithm, the planning and processing of a drug screen and its subsequent bioinformatic analysis, and the *in vitro* characterisation of senotherapeutic effects in models for both normal ageing and premature ageing. The results from this pipeline also show novel findings.

We found that splicing factor dysregulation occurs in progeroid syndromes, that trametinib can ameliorate some aspects of senescence in progeroid cells, that

several compounds may have senotherapeutic effects and share a molecular substructure, that synthetic female sex hormones can be senomorphic and that senomorphic effects can be sex-specific. These results merit further research and assessment of clinical utility for the potential senotherapeutic compounds identified. The results also contribute to basic knowledge about the mechanisms of senescence. Alternative splicing dysregulation was observed in the progeroid cells, making the case stronger for targeting splicing regulation for senotherapeutic benefit. The literature and this thesis suggest that steroidogenic sex hormone pathways may cross over with pathways that control senescence, and this information can aid in research that seeks to target the pathways of senescence. Polyphenolic compounds appear as steroid sex hormones and many known senotherapeutics. This structure-function association can be helpful in both drug screening and drug design. The association is strengthened by the fact that this thesis finds polyphenolic compounds in its drug screen, bioinformatic analysis and subsequent validation work. This thesis also has evidence supporting the notion that many senomorphic compounds show hormetic or biphasic responses. This is an important consideration for future senotherapeutic research because the benefit may be reliant on a particular dosage.

Overall, this thesis demonstrates that cellular senescence is a fundamental part of the molecular basis of ageing, and that understanding these processes can lead to the identification of new targets for future therapies for ageing and age-related disease. Repurposed drug screens can be used to find novel senotherapeutic effects and repurposed drugs could become promising candidates for the treatment of age-related disease.

References

(1) Fries, J. F. Aging, Natural Death, and the Compression of Morbidity. *N. Engl. J. Med.* **1980**, *303* (3), 130–135.

(2) Seals, D. R.; Justice, J. N.; Larocca, T. J. Physiological Geroscience: Targeting Function to Increase Healthspan and Achieve Optimal Longevity. *J. Physiol.* **2016**, *594* (8), 2001–2024. https://doi.org/10.1113/jphysiol.2014.282665.

(3) Partridge, L.; Deelen, J.; Slagboom, P. E. Facing up to the Global Challenges of Ageing. *Nature* **2018**, *561* (7721), 45–56. https://doi.org/10.1038/s41586-018-0457-8.

(4) Office for Budget Responsibility. *Fiscal Risks and Sustainability Report - July 2022*; 2022.

(5) Storey, A. Living Longer: How Our Population Is Changing and Why It Matters. *Off. Natl. Stat.* **2018**, 1–53.

(6) Age UK. *Later Life in the United Kingdom*; 2019.

(7) Eurostat. *Causes of Death Statistics - People over 65*; 2020.

(8) Wittenberg, R.; Hu, B.; Barraza-Araiza, L.; Rehill, A. *Projections of Older People with Dementia and Costs of Dementia Care in the United Kingdom, 2019–2040*; London, UK, 2019.

(9) National Institute on Aging; World Health Organization. *Global Health and Aging*; 2011. https://doi.org/NIH Publication no. 11-7737.

(10) Kenessary, A.; Zhumadilov, Z.; Nurgozhin, T.; Kipling, D.; Yeoman, M.; Cox, L.; Ostler, E.; Faragher, R. Biomarkers, Interventions and Healthy Ageing. *N. Biotechnol.* **2013**, *30* (4).

https://doi.org/10.1016/j.nbt.2012.11.018.

(11) The Lancet Healthy Longevity. Is Ageing a Disease? *Lancet Heal. Longev.* **2022**, *3* (7), e448. https://doi.org/10.1016/S2666-7568(22)00154-4.

(12) De Winter, G. Aging as Disease. *Med. Heal. Care Philos.* **2015**, *18* (2), 237–243. https://doi.org/10.1007/s11019-014-9600-y.

(13) Viña, J.; Borrás, C.; Miquel, J. Theories of Ageing. *IUBMB Life* **2007**, *59* (4–5), 249–254. https://doi.org/10.1080/15216540601178067.

(14) Johnson, A. A.; Shokhirev, M. N.; Shoshitaishvili, B. Revamping the Evolutionary Theories of Aging. *Ageing Res. Rev.* **2019**, *55*. https://doi.org/10.1016/J.ARR.2019.100947.

(15) Wyld, L.; Bellantuono, I.; Tchkonia, T.; Morgan, J.; Turner, O.; Foss, F.; George, J.; Danson, S.; Kirkland, J. L. Senescence and Cancer: A Review of Clinical Implications of Senescence and Senotherapies. *Cancers (Basel).* **2020**, *12* (8), 1–20. https://doi.org/10.3390/cancers12082134.

(16) Rando, T. A.; Chang, H. Y. Aging, Rejuvenation, and Epigenetic Reprogramming: Resetting the Aging Clock. *Cell* **2012**, *148* (1–2), 46–57. https://doi.org/10.1016/j.cell.2012.01.003.

(17) Horvath, S. DNA Methylation Age of Human Tissues and Cell Types. *Genome Biol.* **2013**, *14* (10), 115. https://doi.org/10.1186/gb-2013-14-10-r115.

(18) Atwood, C. S.; Bowen, R. L. The Reproductive-Cell Cycle Theory of Aging: An Update. *Exp. Gerontol.* **2011**, *46* (2–3), 100–107. https://doi.org/10.1016/J.EXGER.2010.09.007.

(19) Freitas, A. A.; De Magalhães, J. P. A Review and Appraisal of the DNA Damage Theory of Ageing. *Mutat. Res. - Rev. Mutat. Res.* **2011**, *728* (1–

2), 12–22. https://doi.org/10.1016/j.mrrev.2011.05.001.

(20) Jin, K. Modern Biological Theories of Aging. *Aging Dis.* **2010**, *1* (2), 72–74. https://doi.org/10.1093/jn/119.6.952.

(21) Schmauck-Medina, T.; Molière, A.; Lautrup, S.; Zhang, J.; Chlopicki, S.; Madsen, H. B.; Cao, S.; Soendenbroe, C.; Mansell, E.; Vestergaard, M. B.; Li, Z.; Shiloh, Y.; Opresko, P. L.; Egly, J.-M.; Kirkwood, T.; Verdin, E.; Bohr, V. A.; Cox, L. S.; Stevnsner, T.; Rasmussen, L. J.; Fang, E. F. New Hallmarks of Ageing: A 2022 Copenhagen Ageing Meeting Summary. *Aging (Albany. NY).* **2022**, *14* (16). https://doi.org/10.18632/AGING.204248.

(22) López-Otín, C.; Blasco, M. A.; Partridge, L.; Serrano, M.; Kroemer, G. The Hallmarks of Aging. *Cell* **2013**, *153* (6), 1194–1217. https://doi.org/10.1016/j.cell.2013.05.039.

(23) Gems, D.; de Magalhães, J. P. The Hoverfly and the Wasp: A Critique of the Hallmarks of Aging as a Paradigm. *Ageing Res. Rev.* **2021**, *70*, 101407. https://doi.org/10.1016/J.ARR.2021.101407.

(24) Tigges, J.; Krutmann, J.; Fritsche, E.; Haendeler, J.; Schaal, H.; Fischer, J. W.; Kalfalah, F.; Reinke, H.; Reifenberger, G.; Stühler, K.; Ventura, N.; Gundermann, S.; Boukamp, P.; Boege, F. The Hallmarks of Fibroblast Ageing. *Mech. Ageing Dev.* **2014**, *138* (1), 26–44. https://doi.org/10.1016/j.mad.2014.03.004.

(25) Carrero, D.; Soria-Valles, C.; López-Otín, C. Hallmarks of Progeroid Syndromes: Lessons from Mice and Reprogrammed Cells. *Dis. Model. Mech.* **2016**, *9* (7), 719–735. https://doi.org/10.1242/dmm.024711.

(26) Sun, N.; Youle, R. J.; Finkel, T. The Mitochondrial Basis of Aging. *Mol. Cell*

2016, *61* (5), 654–666. https://doi.org/10.1016/j.molcel.2016.01.028.

(27) Bhadra, M.; Howell, P.; Dutta, S.; Heintz, C.; Mair, W. B. Alternative Splicing in Aging and Longevity. *Hum. Genet.* **2020**, *139* (3), 357–369. https://doi.org/10.1007/s00439-019-02094-6.

(28) Kaushik, S.; Cuervo, A. M. Proteostasis and Aging. *Nat. Med.* **2015**, *21* (12), 1406–1415. https://doi.org/10.1038/nm.4001.

(29) Ren, R.; Ocampo, A.; Liu, G.-H.; Carlos, J.; Belmonte, I. Regulation of Stem Cell Aging by Metabolism and Epigenetics. *Cell Metab.* **2017**, *26*, 460–474. https://doi.org/10.1016/j.cmet.2017.07.019.

(30) Mehta, I. S.; Riyahi, K.; Pereira, R. T.; Meaburn, K. J.; Figgitt, M.; Kill, I. R.; Eskiw, C. H.; Bridger, J. M. Interphase Chromosomes in Replicative Senescence: Chromosome Positioning as a Senescence Biomarker and the Lack of Nuclear Motor-Driven Chromosome Repositioning in Senescent Cells. *Front. Cell Dev. Biol.* **2021**, *9* (640200). https://doi.org/10.3389/fcell.2021.640200.

(31) Miller, K. N.; Dasgupta, N.; Liu, T.; Adams, P. D.; Vizioli, M. G. Cytoplasmic Chromatin Fragments-from Mechanisms to Therapeutic Potential. *Elife* **2021**, *10* (e63728), 1–10. https://doi.org/10.7554/eLife.63728.

(32) Vijg, J.; Suh, Y. Genome Instability and Aging. *Annu. Rev. Physiol.* **2013**, *75*, 645–668. https://doi.org/10.1146/annurev-physiol-030212-183715.

(33) Burla, R.; Torre, M. La; Merigliano, C.; Vernì, F.; Saggio, I. Genomic Instability and DNA Replication Defects in Progeroid Syndromes. *Nucleus* **2018**, *9* (1), 368–379. https://doi.org/10.1080/19491034.2018.1476793.

(34) Baker, D. J.; Dawlaty, M. M.; Wijshake, T.; Jeganathan, K. B.; Malureanu, L.; Van Ree, J. H.; Crespo-Diaz, R.; Reyes, S.; Seaburg, L.; Shapiro, V.;

Behfar, A.; Terzic, A.; Van De Sluis, B.; Van Deursen, J. M. Increased Expression of BubR1 Protects against Aneuploidy and Cancer and Extends Healthy Lifespan. *Nat. Cell Biol. 2013 151* **2012**, *15* (1), 96–102. https://doi.org/10.1038/ncb2643.

(35) Blackburn, E. H.; Epel, E. S.; Lin, J. Human Telomere Biology: A Contributory and Interactive Factor in Aging, Disease Risks, and Protection. *Science.* **2015**, *350* (6265), 1193–1198. https://doi.org/10.1126/science.aab3389.

(36) Hayflick, L.; Moorhead, P. S. The Serial Cultivation of Human Diploid Cell Strains. *Exp. Cell Res.* **1961**, *25* (3), 585–621. https://doi.org/10.1016/0014-4827(61)90192-6.

(37) Toussaint, O.; Remacle, J.; Dierick, J. F.; Pascal, T.; Frippiat, C.; Zdanov, S.; Magalhaes, J. P.; Royer, V.; Chainiaux, F. From the Hayflick Mosaic to the Mosaics of Ageing. Role of Stress-Induced Premature Senescence in Human Ageing. *Int. J. Biochem. Cell Biol.* **2002**, *34* (11), 1415–1429. https://doi.org/10.1016/S1357-2725(02)00034-1.

(38) Palm, W.; De Lange, T. How Shelterin Protects Mammalian Telomeres. *Annu. Rev. Genet.* **2008**, *42*, 301–334. https://doi.org/10.1146/annurev.genet.41.110306.130350.

(39) Fumagalli, M.; Rossiello, F.; Clerici, M.; Barozzi, S.; Cittaro, D.; Kaplunov, J. M.; Bucci, G.; Dobreva, M.; Matti, V.; Beausejour, C. M.; Herbig, U.; Longhese, M. P.; Di Fagagna, F. D. A. Telomeric DNA Damage Is Irreparable and Causes Persistent DNA-Damage-Response Activation. *Nat. Cell Biol. 2012 144* **2012**, *14* (4), 355–365. https://doi.org/10.1038/ncb2466.

(40) Turner, K. J.; Vasu, V.; Griffin, D. K. Telomere Biology and Human Phenotype. *Cells* **2019**, *8* (1). https://doi.org/10.3390/cells8010073.

(41) Boonekamp, J. J.; Simons, M. J. P.; Hemerik, L.; Verhulst, S. Telomere Length Behaves as Biomarker of Somatic Redundancy Rather than Biological Age. *Aging Cell* **2013**, *12* (2), 330–332. https://doi.org/10.1111/acel.12050.

(42) Martinez, P.; Blasco, M. A. Role of Shelterin in Cancer and Aging. *Aging Cell* **2010**, *9* (5), 653–666. https://doi.org/10.1111/j.1474-9726.2010.00596.x.

(43) Jaskelioff, M.; Muller, F. L.; Paik, J. H.; Thomas, E.; Jiang, S.; Adams, A. C.; Sahin, E.; Kost-Alimova, M.; Protopopov, A.; Cadiñanos, J.; Horner, J. W.; Maratos-Flier, E.; Depinho, R. A. Telomerase Reactivation Reverses Tissue Degeneration in Aged Telomerase-Deficient Mice. *Nature* **2010**, *469* (7328), 102–106. https://doi.org/10.1038/nature09603.

(44) Kane, A. E.; Sinclair, D. A. Epigenetic Changes during Aging and Their Reprogramming Potential. *Crit. Rev. Biochem. Mol. Biol.* **2019**, *54* (1), 61–83. https://doi.org/10.1080/10409238.2019.1570075.

(45) Guarente, L. Sirtuins in Aging and Disease. *Cold Spring Harb. Symp. Quant. Biol.* **2007**, *72*, 483–488. https://doi.org/10.1101/sqb.2007.72.024.

(46) Imai, S.-I.; Guarente, L. NAD+ and Sirtuins in Aging and Disease. *Trends Cell Biol.* **2014**, *24* (8), 464–471. https://doi.org/10.1016/j.tcb.2014.04.002.

(47) Kawahara, T. L. A.; Michishita, E.; Adler, A. S.; Damian, M.; Berber, E.; Lin, M.; McCord, R. A.; Ongaigui, K. C. L.; Boxer, L. D.; Chang, H. Y.; Chua, K. F. SIRT6 Links Histone H3 Lysine 9 Deacetylation to NF-KB-Dependent Gene Expression and Organismal Life Span. *Cell* **2009**, *136* (1), 62–74.

https://doi.org/10.1016/j.cell.2008.10.052.

(48) Hubbard, B. P.; Sinclair, D. A. Small Molecule SIRT1 Activators for the Treatment of Aging and Age-Related Diseases. *Trends Pharmacol. Sci.* **2014**, *35* (3), 146–154. https://doi.org/10.1016/j.tips.2013.12.004.

(49) Tasselli, L.; Zheng, W.; Chua, K. F. SIRT6: Novel Mechanisms and Links to Aging and Disease. *Trends Endocrinol. Metab.* **2017**, *28* (3), 168. https://doi.org/10.1016/J.TEM.2016.10.002.

(50) Larson, K.; Yan, S. J.; Tsurumi, A.; Liu, J.; Zhou, J.; Gaur, K.; Guo, D.; Eickbush, T. H.; Li, W. X. Heterochromatin Formation Promotes Longevity and Represses Ribosomal RNA Synthesis. *PLoS Genet.* **2012**, *8* (1). https://doi.org/10.1371/JOURNAL.PGEN.1002473.

(51) Peleg, S.; Sananbenesi, F.; Zovoilis, A.; Burkhardt, S.; Bahari-Javan, S.; Agis-Balboa, R. C.; Cota, P.; Wittnam, J. L.; Gogol-Doering, A.; Opitz, L.; Salinas-Riester, G.; Dettenhofer, M.; Kang, H.; Farinelli, L.; Chen, W.; Fischer, A. Altered Histone Acetylation Is Associated with Age-Dependent Memory Impairment in Mice. *Science.* **2010**, *328* (5979), 753–756. https://doi.org/10.1126/science.1186088.

(52) Chen, H. C.; Cheng, S. C. Functional Roles of Protein Splicing Factors. *Biosci. Rep.* **2012**, *32* (4), 345–359. https://doi.org/10.1042/BSR20120007.

(53) Tollervey, J. R.; Wang, Z.; Hortobágyi, T.; Witten, J. T.; Zarnack, K.; Kayikci, M.; Clark, T. A.; Schweitzer, A. C.; Rot, G.; Curk, T.; Zupan, B.; Rogelj, B.; Shaw, C. E.; Ule, J. Analysis of Alternative Splicing Associated with Aging and Neurodegeneration in the Human Brain. *Genome Res.* **2011**, *21* (10), 1572–1582. https://doi.org/10.1101/gr.122226.111.

(54) Ribeiro, M.; Furtado, M.; Martins, S.; Carvalho, T.; Carmo-Fonseca, M.

RNA Splicing Defects in Hypertrophic Cardiomyopathy: Implications for Diagnosis and Therapy. *Int. J. Mol. Sci.* **2020**, *21* (4), 1329. https://doi.org/10.3390/ijms21041329.

(55) Zhu, H.; Ding, Q. Lower Expression Level of Two RAGE Alternative Splicing Isoforms in Alzheimer's Disease. *Neurosci. Lett.* **2015**, *597*, 66–70. https://doi.org/10.1016/j.neulet.2015.04.032.

(56) Holly, A. C.; Melzer, D.; Pilling, L. C.; Fellows, A. C.; Tanaka, T.; Ferrucci, L.; Harries, L. W. Changes in Splicing Factor Expression Are Associated with Advancing Age in Man. *Mech. Ageing Dev.* **2013**, *134* (9), 356–366. https://doi.org/10.1016/j.mad.2013.05.006.

(57) Lee, B. P.; Pilling, L. C.; Emond, F.; Flurkey, K.; Harrison, D. E.; Yuan, R.; Peters, L. L.; Kuchel, G. A.; Ferrucci, L.; Melzer, D.; Harries, L. W. Changes in the Expression of Splicing Factor Transcripts and Variations in Alternative Splicing Are Associated with Lifespan in Mice and Humans. *Aging Cell* **2016**, *15* (5), 903–913. https://doi.org/10.1111/acel.12499.

(58) Lee, B. P.; Pilling, L. C.; Bandinelli, S.; Ferrucci, L.; Melzer, D.; Harries, L. W. The Transcript Expression Levels of HNRNPM, HNRNPA0 and AKAP17A Splicing Factors May Be Predictively Associated with Ageing Phenotypes in Human Peripheral Blood. *Biogerontology* **2019**, 1–15. https://doi.org/10.1007/s10522-019-09819-0.

(59) Balliu, B.; Durrant, M.; Goede, O. De; Abell, N.; Li, X.; Liu, B.; Gloudemans, M. J.; Cook, N. L.; Smith, K. S.; Knowles, D. A.; Pala, M.; Cucca, F.; Schlessinger, D.; Jaiswal, S.; Sabatti, C.; Lind, L.; Ingelsson, E.; Montgomery, S. B. Genetic Regulation of Gene Expression and Splicing during a 10-Year Period of Human Aging. *Genome Biol.* **2019**, *20* (1).

https://doi.org/10.1186/s13059-019-1840-y.

(60) Lee, B. P.; Smith, M.; Buffenstein, R.; Harries, L. W. Negligible Senescence in Naked Mole Rats May Be a Consequence of Well-Maintained Splicing Regulation. *GeroScience* **2020**, *42* (2), 633–651. https://doi.org/10.1007/s11357-019-00150-7.

(61) Latorre, E.; Torregrossa, R.; Wood, M. E.; Whiteman, M.; Harries, L. W. Mitochondria-Targeted Hydrogen Sulfide Attenuates Endothelial Senescence by Selective Induction of Splicing Factors HNRNPD and SRSF2. *Aging (Albany. NY).* **2018**, *10* (7), 1666–1681. https://doi.org/10.18632/aging.101500.

(62) Latorre, E.; Ostler, E. L.; Faragher, R. G. A.; Harries, L. W. FOXO1 and ETV6 Genes May Represent Novel Regulators of Splicing Factor Expression in Cellular Senescence. *FASEB J.* **2019**, *33* (1), 1086–1097. https://doi.org/10.1096/fj.201801154R.

(63) Latorre, E.; Birar, V. C.; Sheerin, A. N.; Jeynes, J. C. C.; Hooper, A.; Dawe, H. R.; Melzer, D.; Cox, L. S.; Faragher, R. G. A. A.; Ostler, E. L.; Harries, L. W. Small Molecule Modulation of Splicing Factor Expression Is Associated with Rescue from Cellular Senescence. *BMC Cell Biol.* **2017**, *18* (1), 1–15. https://doi.org/10.1186/s12860-017-0147-7.

(64) Terzi, M. Y.; Izmirli, M.; Gogebakan, B. The Cell Fate: Senescence or Quiescence. *Mol. Biol. Rep.* **2016**, *43* (11), 1213–1220. https://doi.org/10.1007/s11033-016-4065-0.

(65) Inci, N.; Kamali, D.; Akyildiz, E. O.; Tahir Turanli, E.; Bozaykut, P. Translation of Cellular Senescence to Novel Therapeutics: Insights From Alternative Tools and Models. *Front. Aging* **2022**, *3*.

https://doi.org/10.3389/fragi.2022.828058.

(66) Baker, D. J.; Wijshake, T.; Tchkonia, T.; Lebrasseur, N. K.; Childs, B. G.; Van De Sluis, B.; Kirkland, J. L.; Van Deursen, J. M. Clearance of P16 Ink4a-Positive Senescent Cells Delays Ageing-Associated Disorders. *Nature* **2011**, *479* (7372), 232–236. https://doi.org/10.1038/nature10600.

(67) Gorgoulis, V. G.; Halazonetis, T. D. Oncogene-Induced Senescence: The Bright and Dark Side of the Response. *Curr. Opin. Cell Biol.* **2010**, *22* (6), 816–827. https://doi.org/10.1016/j.ceb.2010.07.013.

(68) Sikora, E.; Bielak-Zmijewska, A.; Mosieniak, G. A Common Signature of Cellular Senescence; Does It Exist? *Ageing Res. Rev.* **2021**, *71* (September), 101458. https://doi.org/10.1016/j.arr.2021.101458.

(69) He, S.; Sharpless, N. E. Senescence in Health and Disease. *Cell* **2017**, *169* (6), 1000–1011. https://doi.org/10.1016/j.cell.2017.05.015.

(70) Bramwell, L. R.; Harries, L. W. Targeting Alternative Splicing for Reversal of Cellular Senescence in the Context of Aesthetic Aging. *Plast. Reconstr. Surg.* **2021**, *147* (1S-2), 25S-32S. https://doi.org/10.1097/PRS.0000000000007618.

(71) Kirkland, J. L.; Tchkonia, T.; Zhu, Y.; Niedernhofer, L. J.; Robbins, P. D. The Clinical Potential of Senolytic Drugs. *J. Am. Geriatr. Soc.* **2017**, *65* (10), 2297–2301. https://doi.org/10.1111/jgs.14969.

(72) Campisi, J.; Kapahi, P.; Lithgow, G. J.; Melov, S.; Newman, J. C.; Verdin, E. From Discoveries in Ageing Research to Therapeutics for Healthy Ageing. *Nature* **2019**, *571* (7764), 183–192. https://doi.org/10.1038/s41586-019-1365-2.

(73) Baker, D. J.; Petersen, R. C. Cellular Senescence in Brain Aging and

Neurodegenerative Diseases: Evidence and Perspectives. *J. Clin. Invest.* **2018**, *128* (4), 1208. https://doi.org/10.1172/JCI95145.

(74) Boquoi, A.; Arora, S.; Chen, T.; Litwin, S.; Koh, J.; Enders, G. H. Reversible Cell Cycle Inhibition and Premature Aging Features Imposed by Conditional Expression of P16Ink4a. *Aging Cell* **2015**, *14* (1), 139–147. https://doi.org/10.1111/acel.12279.

(75) Baker, D. J.; Childs, B. G.; Durik, M.; Wijers, M. E.; Sieben, C. J.; Zhong, J.; A. Saltness, R.; Jeganathan, K. B.; Verzosa, G. C.; Pezeshki, A.; Khazaie, K.; Miller, J. D.; van Deursen, J. M. Naturally Occurring P16Ink4a-Positive Cells Shorten Healthy Lifespan. *Nature* **2016**, *530* (7589), 184–189. https://doi.org/10.1038/nature16932.

(76) Powers, E. T.; Morimoto, R. I.; Dillin, A.; Kelly, J. W.; Balch, W. E. Biological and Chemical Approaches to Diseases of Proteostasis Deficiency. *Annu. Rev. Biochem.* **2009**, *78* (1), 959–991. https://doi.org/10.1146/annurev.biochem.052308.114844.

(77) Calderwood, S. K.; Murshid, A.; Prince, T. The Shock of Aging: Molecular Chaperones and the Heat Shock Response in Longevity and Aging. *Gerontology* **2009**, *55*, 550–558. https://doi.org/10.1159/000225957.

(78) Klaips, C. L.; Jayaraj, G. G.; Hartl, F. U. Pathways of Cellular Proteostasis in Aging and Disease. *J. Cell Biol.* **2018**, *217* (1), 51–63. https://doi.org/10.1083/jcb.201709072.

(79) Rubinsztein, D. C.; Mariño, G.; Kroemer, G. Autophagy and Aging. *Cell* **2011**, *146* (5), 682–695. https://doi.org/10.1016/j.cell.2011.07.030.

(80) Tomaru, U.; Takahashi, S.; Ishizu, A.; Miyatake, Y.; Gohda, A.; Suzuki, S.; Ono, A.; Ohara, J.; Baba, T.; Murata, S.; Tanaka, K.; Kasahara, M.

Decreased Proteasomal Activity Causes Age-Related Phenotypes and Promotes the Development of Metabolic Abnormalities. *AJPA* **2012**, *180* (3), 963–972. https://doi.org/10.1016/j.ajpath.2011.11.012.

(81) Vilchez, D.; Morantte, I.; Liu, Z.; Douglas, P. M.; Merkwirth, C.; Rodrigues, A. P. C.; Manning, G.; Dillin, A. RPN-6 Determines C. Elegans Longevity under Proteotoxic Stress Conditions. *Nature* **2012**, *489* (7415), 263–268. https://doi.org/10.1038/nature11315.

(82) Liu, G.; Rogers, J.; Murphy, C. T.; Rongo, C. EGF Signalling Activates the Ubiquitin Proteasome System to Modulate C. Elegans Lifespan. *EMBO J.* **2011**, *30*, 2990–3003. https://doi.org/10.1038/emboj.2011.195.

(83) Brehme, M.; Voisine, C.; Rolland, T.; Wachi, S.; Soper, J. H.; Zhu, Y.; Orton, K.; Villella, A.; Garza, D.; Vidal, M.; Ge, H.; Morimoto, R. I. A Chaperome Subnetwork Safeguards Proteostasis in Aging and Neurodegenerative Disease. *Cell Rep.* **2014**, *9* (3), 1135–1150. https://doi.org/10.1016/j.celrep.2014.09.042.

(84) Lee, B. H.; Lee, M. J.; Park, S.; Oh, D. C.; Elsasser, S.; Chen, P. C.; Gartner, C.; Dimova, N.; Hanna, J.; Gygi, S. P.; Wilson, S. M.; King, R. W.; Finley, D. Enhancement of Proteasome Activity by a Small-Molecule Inhibitor of USP14. *Nature* **2010**, *467* (7312), 179–184. https://doi.org/10.1038/nature09299.

(85) Kruegel, U.; Robison, B.; Dange, T.; Kahlert, G.; Delaney, J. R.; Kotireddy, S.; Tsuchiya, M.; Tsuchiyama, S.; Murakami, C. J.; Schleit, J.; Sutphin, G.; Carr, D.; Tar, K.; Dittmar, G.; Kaeberlein, M.; Kennedy, B. K.; Schmidt, M. Elevated Proteasome Capacity Extends Replicative Lifespan in Saccharomyces Cerevisiae. *PLoS Genet.* **2011**, *7* (9).

https://doi.org/10.1371/journal.pgen.1002253.

(86) Tauchi, H.; Sato, T. Age Changes in Size and Number of Mitochondria of Human Hepatic Cells. *J. Gerontol.* **1968**, *23* (4), 454–461. https://doi.org/10.1093/geronj/23.4.454.

(87) Mohrin, M.; Shin, J.; Liu, Y.; Brown, K.; Luo, H.; Xi, Y.; Haynes, C. M.; Chen, D. A Mitochondrial UPR-Mediated Metabolic Checkpoint Regulates Hematopoietic Stem Cell Aging. *Science (80-.).* **2015**, *347* (6228), 1374–1377. https://doi.org/10.1126/science.aaa2361.

(88) Kujoth, G. C.; Leeuwenburgh, C.; Prolla, T. A. Mitochondrial DNA Mutations and Apoptosis in Mammalian Aging. *Cancer Res.* **2006**, *66* (15), 7386–7389. https://doi.org/10.1158/0008-5472.CAN-05-4670.

(89) Mansell, E.; Sigurdsson, V.; Soneji, S.; Larsson, J.; Correspondence, T. E.; Deltcheva, E.; Brown, J.; James, C.; Miharada, K.; Enver, T. Mitochondrial Potentiation Ameliorates Age-Related Heterogeneity in Hematopoietic Stem Cell Function. *Stem Cell* **2021**, *28*, 241-256.e6. https://doi.org/10.1016/j.stem.2020.09.018.

(90) Rustin, P.; Von Kleist-Retzow, J.-C.; Vajo, Z.; Rotig, A.; Munnich, A. For Debate: Defective Mitochondria, Free Radicals, Cell Death, Aging-Reality or Myth-Ochondria? *Mech. Ageing Dev.* **2000**, *114*, 201–206.

(91) Proksch, E.; Schunck, M.; Zague, V.; Segger, D.; Degwert, J.; Oesser, S. Oral Intake of Specific Bioactive Collagen Peptides Reduces Skin Wrinkles and Increases Dermal Matrix Synthesis. *Skin Pharmacol. Physiol.* **2014**, *27* (3), 113–119. https://doi.org/10.1159/000355523.

(92) Chen, S. W.; Tung, Y. C.; Jung, S. M.; Chu, Y.; Lin, P. J.; Kao, W. W.-Y.; Chu, P. H. Lumican-Null Mice Are Susceptible to Aging and Isoproterenol-

Induced Myocardial Fibrosis. *Biochem. Biophys. Res. Commun.* **2017**, *482* (4), 1304–1311. https://doi.org/10.1016/j.bbrc.2016.12.033.

(93) Freund, A.; Laberge, R. M.; Demaria, M.; Campisi, J. Lamin B1 Loss Is a Senescence-Associated Biomarker. *Mol. Biol. Cell* **2012**, *23* (11), 2066–2075. https://doi.org/10.1091/mbc.E11-10-0884.

(94) Glynn, M. W.; Glover, T. W. Incomplete Processing of Mutant Lamin A in Hutchinson-Gilford Progeria Leads to Nuclear Abnormalities, Which Are Reversed by Farnesyltransferase Inhibition. *Hum. Mol. Genet.* **2005**, *14* (20), 2959–2969. https://doi.org/10.1093/hmg/ddi326.

(95) Gordon, L. B.; Shappell, H.; Massaro, J.; D'Agostino, R. B.; Brazier, J.; Campbell, S. E.; Kleinman, M. E.; Kieran, M. W. Association of Lonafarnib Treatment vs No Treatment with Mortality Rate in Patients with Hutchinson-Gilford Progeria Syndrome. *JAMA - J. Am. Med. Assoc.* **2018**, *319* (16), 1687–1695. https://doi.org/10.1001/jama.2018.3264.

(96) Yim, W. W. Y.; Mizushima, N. Lysosome Biology in Autophagy. *Cell Discov.* **2020**, *6* (1), 6. https://doi.org/10.1038/s41421-020-0141-7.

(97) Schneider, J. L.; Suh, Y.; Cuervo, A. M. Deficient Chaperone-Mediated Autophagy in Liver Leads to Metabolic Dysregulation. *Cell Metab.* **2014**, *20* (3), 417. https://doi.org/10.1016/J.CMET.2014.06.009.

(98) Kaushik, S.; Cuervo, A. M. The Coming of Age of Chaperone-Mediated Autophagy. *Nat. Rev. Mol. Cell Biol.* **2018**, *19* (6), 365–381. https://doi.org/10.1038/s41580-018-0001-6.

(99) Zhang, C.; Cuervo, A. M. Restoration of Chaperone-Mediated Autophagy in Aging Liver Improves Cellular Maintenance and Hepatic Function. *Nat Med* **2008**, *14* (9), 959–965. https://doi.org/10.1038/nm.1851.

(100) Matsumoto, M.; Kurihara, S.; Kibe, R.; Ashida, H.; Benno, Y. Longevity in Mice Is Promoted by Probiotic-Induced Suppression of Colonic Senescence Dependent on Upregulation of Gut Bacterial Polyamine Production. *PLoS One* **2011**, *6* (8). https://doi.org/10.1371/journal.pone.0023652.

(101) Soda, K.; Dobashi, Y.; Kano, Y.; Tsujinaka, S.; Konishi, F. Polyamine-Rich Food Decreases Age-Associated Pathology and Mortality in Aged Mice. *Exp. Gerontol.* **2009**, *44* (11), 727–732. https://doi.org/10.1016/j.exger.2009.08.013.

(102) Kirkwood, K. L. Inflammaging. *Immunol. Invest.* **2018**, *47* (8), 770–773. https://doi.org/10.1080/08820139.2018.1552392.

(103) Castelo-Branco, C.; Soveral, I. The Immune System and Aging: A Review. *Gynecol. Endocrinol.* **2014**, *30* (1), 16–22. https://doi.org/10.3109/09513590.2013.852531.

(104) Thevaranjan, N.; Puchta, A.; Schulz, C.; Verdú, E. F.; Surette, M. G.; Bowdish, D. M. E.; Naidoo, A.; Szamosi, J. C.; Verschoor, C. P.; Loukov, D.; Schenck, L. P.; Jury, J.; Foley, K. P.; Schertzer, J. D.; Larché, M. J.; Davidson, D. J. Age-Associated Microbial Dysbiosis Promotes Intestinal Permeability, Systemic Inflammation, and Macrophage Dysfunction. *Cell Host Microbe* **2017**, *21*, 455–466. https://doi.org/10.1016/j.chom.2017.03.002.

(105) Tilstra, J. S.; Robinson, A. R.; Wang, J.; Gregg, S. Q.; Clauson, C. L.; Reay, D. P.; Nasto, L. A.; St Croix, C. M.; Usas, A.; Vo, N.; Huard, J.; Clemens, P. R.; Stolz, D. B.; Guttridge, D. C.; Watkins, S. C.; Garinis, G. A.; Wang, Y.; Niedernhofer, L. J.; Robbins, P. D. NF-KB Inhibition Delays DNA

Damage-Induced Senescence and Aging in Mice. *J. Clin. Invest.* **2012**, *122*. https://doi.org/10.1172/JCI45785.

(106) Kolios, G.; Moodley, Y. Introduction to Stem Cells and Regenerative Medicine. *Respiration* **2013**, *85*, 3–10. https://doi.org/10.1159/000345615.

(107) Rossi, D. J.; Bryder, D.; Seita, J.; Nussenzweig, A.; Hoeijmakers, J.; Weissman, I. L. Deficiencies in DNA Damage Repair Limit the Function of Haematopoietic Stem Cells with Age. *Nature* **2007**, *447* (7145), 725–729. https://doi.org/10.1038/nature05862.

(108) Norddahl, G. L.; Pronk, C. J.; Wahlestedt, M.; Sten, G.; Nygren, J. M.; Ugale, A.; Sigvardsson, M.; Bryder, D. Accumulating Mitochondrial DNA Mutations Drive Premature Hematopoietic Aging Phenotypes Distinct from Physiological Stem Cell Aging. *Cell Stem Cell* **2011**, *8* (5), 499–510. https://doi.org/10.1016/j.stem.2011.03.009.

(109) Florian, M. C.; Dörr, K.; Niebel, A.; Daria, D.; Schrezenmeier, H.; Rojewski, M.; Filippi, M. D.; Hasenberg, A.; Gunzer, M.; Scharffetter-Kochanek, K.; Zheng, Y.; Geiger, H. Cdc42 Activity Regulates Hematopoietic Stem Cell Aging and Rejuvenation. *Cell Stem Cell* **2012**, *10* (5), 520–530. https://doi.org/10.1016/j.stem.2012.04.007.

(110) Revuelta, M.; Matheu, A. Autophagy in Stem Cell Aging. *Aging Cell* **2017**, *16* (5), 912–915. https://doi.org/10.1111/acel.12655.

(111) Russell, S. J.; Kahn, C. R. Endocrine Regulation of Ageing. *Nat. Rev. Mol. Cell Biol.* **2007**, *8* (9), 681–691. https://doi.org/10.1038/nrm2234.

(112) Barzilai, N.; Huffman, D. M.; Muzumdar, R. H.; Bartke, A. The Critical Role of Metabolic Pathways in Aging. *Diabetes* **2012**, *61*, 1315–1322. https://doi.org/10.2337/db11-1300.

(113) Fulop, T.; Larbi, A.; Dupuis, G.; Le Page, A.; Frost, E. H.; Cohen, A. A.; Witkowski, J. M.; Franceschi, C. Immunosenescence and Inflamm-Aging as Two Sides of the Same Coin: Friends or Foes? *Front. Immunol.* **2018**, *8* (1960), 1–13. https://doi.org/10.3389/fimmu.2017.01960.

(114) Conboy, I. M.; Conboy, M. J.; Wagers, A. J.; Girma, E. R.; Weismann, I. L.; Rando, T. A. Rejuvenation of Aged Progenitor Cells by Exposure to a Young Systemic Environment. *Nature* **2005**, *433* (7027), 760–764. https://doi.org/10.1038/nature03260.

(115) Hachmo, Y.; Hadanny, A.; Hamed, R. A.; Daniel-kotovsky, M.; Catalogna, M.; Fishlev, G.; Lang, E.; Polak, N.; Doenyas, K.; Friedman, M.; Zemel, Y.; Bechor, Y.; Efrati, S. Hyperbaric Oxygen Therapy Increases Telomere Length and Decreases Immunosenescence in Isolated Blood Cells : A Prospective Trial. *Aging (Albany. NY).* **2020**, *12* (22), 1–12.

(116) Andriani, G. A.; Almeida, V. P.; Faggioli, F.; Mauro, M.; Li Tsai, W.; Santambrogio, L.; Maslov, A.; Gadina, M.; Campisi, J.; Vijg, J.; Montagna, C. Whole Chromosome Instability Induces Senescence and Promotes SASP. *Sci. Rep.* **2016**, *6* (1), 1–17. https://doi.org/10.1038/srep35218.

(117) Birch, J.; Gil, J. Senescence and the SASP: Many Therapeutic Avenues. *Genes Dev.* **2020**, *34* (23–24), 1565–1576. https://doi.org/10.1101/gad.343129.120.

(118) Ohtani, N. Deciphering the Mechanism for Induction of Senescence-Associated Secretory Phenotype (SASP) and Its Role in Ageing and Cancer Development. *J. Biochem.* **2019**, *166* (4), 289–295. https://doi.org/10.1093/jb/mvz055.

(119) Ghosh, K.; Capell, B. C. The Senescence-Associated Secretory

Phenotype: Critical Effector in Skin Cancer and Aging. *J. Invest. Dermatol.* **2016**, *136* (11), 2133–2139. https://doi.org/10.1016/j.jid.2016.06.621.

(120) Basisty, N.; Kale, A.; Jeon, O. H.; Kuehnemann, C.; Payne, T.; Rao, C.; Holtz, A.; Shah, S.; Sharma, V.; Ferrucci, L.; Campisi, J.; Schilling, B. A Proteomic Atlas of Senescence-Associated Secretomes for Aging Biomarker Development. *PLoS Biol.* **2020**, *18* (1), e3000599. https://doi.org/10.1371/journal.pbio.3000599.

(121) Sikka, G.; Miller, K. L.; Steppan, J.; Pandey, D.; Jung, S. M.; Fraser, C. D.; Ellis, C.; Ross, D.; Vandegaer, K.; Bedja, D.; Gabrielson, K.; Walston, J. D.; Berkowitz, D. E.; Barouch, L. A. Interleukin 10 Knockout Frail Mice Develop Cardiac and Vascular Dysfunction with Increased Age. *Exp. Gerontol.* **2013**, *48* (2), 128–135. https://doi.org/10.1016/j.exger.2012.11.001.

(122) Squarzoni, S.; Schena, E.; Sabatelli, P.; Mattioli, E.; Capanni, C.; Cenni, V.; D'Apice, M. R.; Andrenacci, D.; Sarli, G.; Pellegrino, V.; Festa, A.; Baruffaldi, F.; Storci, G.; Bonafè, M.; Barboni, C.; Sanapo, M.; Zaghini, A.; Lattanzi, G. Interleukin-6 Neutralization Ameliorates Symptoms in Prematurely Aged Mice. *Aging Cell* **2021**, *20* (1). https://doi.org/10.1111/acel.13285.

(123) Du, S.; Zheng, H. Role of FoxO Transcription Factors in Aging and Age-Related Metabolic and Neurodegenerative Diseases. *Cell Biosci.* **2021**, *11* (188), 1–17. https://doi.org/10.1186/s13578-021-00700-7.

(124) Duan, H.; Pan, J.; Guo, M.; Li, J.; Yu, L.; Fan, L. Dietary Strategies with Anti-Aging Potential: Dietary Patterns and Supplements. *Food Res. Int.* **2022**, *158* (111501). https://doi.org/10.1016/j.foodres.2022.111501.

(125) Tam, B. T.; Morais, J. A.; Santosa, S. Obesity and Ageing: Two Sides of the Same Coin. *Obes. Rev.* **2020**, *21* (4). https://doi.org/10.1111/obr.12991.

(126) Bonafè, M.; Barbieri, M.; Marchegiani, F.; Olivieri, F.; Ragno, E.; Giampieri, C.; Mugianesi, E.; Centurelli, M.; Franceschi, C.; Paolisso, G. Polymorphic Variants of Insulin-like Growth Factor I (IGF-I) Receptor and Phosphoinositide 3-Kinase Genes Affect IGF-I Plasma Levels and Human Longevity: Cues for an Evolutionarily Conserved Mechanism of Life Span Control. *J. Clin. Endocrinol. Metab.* **2003**, *88* (7), 3299–3304. https://doi.org/10.1210/jc.2002-021810.

(127) Wilkinson, J. E.; Burmeister, L.; Brooks, S. V; Chan, C.-C.; Friedline, S.; Harrison, D. E.; Hejtmancik, J. F.; Nadon, N.; Strong, R.; Wood, L. K.; Woodward, M. A.; Miller, R. A.; Richard Miller, C. A. Rapamycin Slows Aging in Mice. *Aging Cell* **2012**, *11* (4), 675–682. https://doi.org/10.1111/j.1474-9726.2012.00832.x.

(128) Ottaviani, E.; Ventura, N.; Mandrioli, M.; Candela, M.; Franchini, A.; Franceschi, C. Gut Microbiota as a Candidate for Lifespan Extension: An Ecological/Evolutionary Perspective Targeted on Living Organisms as Metaorganisms. *Biogerontology* **2011**, *12* (6), 599–609. https://doi.org/10.1007/s10522-011-9352-5.

(129) Claesson, M. J.; Jeffery, I. B.; Conde, S.; Power, S. E.; O'connor, E. M.; Cusack, S.; Harris, H. M. B.; Coakley, M.; Lakshminarayanan, B.; O'sullivan, O.; Fitzgerald, G. F.; Deane, J.; O'connor, M.; Harnedy, N.; O'connor, K.; O'mahony, D.; Van Sinderen, D.; Wallace, M.; Brennan, L.; Stanton, C.; Marchesi, J. R.; Fitzgerald, A. P.; Shanahan, F.; Hill, C.; Paul

Ross, R.; O'toole, P. W. Gut Microbiota Composition Correlates with Diet and Health in the Elderly. *Nature* **2012**, *488* (7410), 178–184. https://doi.org/10.1038/nature11319.

(130) Wilmanski, T.; Diener, C.; Rappaport, N.; Patwardhan, S.; Wiedrick, J.; Lapidus, J.; Earls, J. C.; Zimmer, A.; Glusman, G.; Robinson, M.; Yurkovich, J. T.; Kado, D. M.; Cauley, J. A.; Zmuda, J.; Lane, N. E.; Magis, A. T.; Lovejoy, J. C.; Hood, L.; Gibbons, S. M.; Orwoll, E. S.; Price, N. D. Gut Microbiome Pattern Reflects Healthy Ageing and Predicts Survival in Humans. *Nat. Metab.* **2021**, *3* (2), 274–286. https://doi.org/10.1038/s42255-021-00348-0.

(131) Franceschi, C.; Garagnani, P.; Parini, P.; Giuliani, C.; Santoro, A. Inflammaging: A New Immune–Metabolic Viewpoint for Age-Related Diseases. *Nat. Rev. Endocrinol.* **2018**, *14* (10), 576–590. https://doi.org/10.1038/s41574-018-0059-4.

(132) Fransen, F.; van Beek, A. A.; Borghuis, T.; El Aidy, S.; Hugenholtz, F.; van der Gaast - de Jongh, C.; Savelkoul, H. F. J.; de Jonge, M. I.; Boekschoten, M. V.; Smidt, H.; Faas, M. M.; de Vos, P. Aged Gut Microbiota Contributes to Systemical Inflammaging after Transfer to Germ-Free Mice. *Front. Immunol.* **2017**, *8* (NOV), 1–12. https://doi.org/10.3389/fimmu.2017.01385.

(133) Hay, M.; Thomas, D. W.; Craighead, J. L.; Economides, C.; Rosenthal, J. Clinical Development Success Rates for Investigational Drugs. *Nat. Biotechnol.* **2014**, *32* (1), 40–51. https://doi.org/10.1038/nbt.2786.

(134) Van Norman, G. A. Limitations of Animal Studies for Predicting Toxicity in Clinical Trials: Is It Time to Rethink Our Current Approach? *JACC Basic to Transl. Sci.* **2019**, *4* (7), 845–854.

https://doi.org/10.1016/j.jacbts.2019.10.008.

(135) Jaroch, K.; Jaroch, A.; Bojko, B. Cell Cultures in Drug Discovery and Development: The Need of Reliable in Vitro-in Vivo Extrapolation for Pharmacodynamics and Pharmacokinetics Assessment. *J. Pharm. Biomed. Anal.* **2018**, *147*, 297–312. https://doi.org/10.1016/j.jpba.2017.07.023.

(136) Jeffery, N.; Richardson, S.; Chambers, D.; Morgan, N. G.; Harries, L. W. Cellular Stressors May Alter Islet Hormone Cell Proportions by Moderation of Alternative Splicing Patterns. *Hum. Mol. Genet.* **2019**, *28* (16), 2763. https://doi.org/10.1093/HMG/DDZ094.

(137) Cagan, A.; Baez-Ortega, A.; Brzozowska, N.; Abascal, F.; H Coorens, T. H.; Sanders, M. A.; J Lawson, A. R.; R Harvey, L. M.; Bhosle, S.; Jones, D.; Alcantara, R. E.; Butler, T. M.; Hooks, Y.; Roberts, K.; Anderson, E.; Lunn, S.; Flach, E.; Spiro, S.; Januszczak, I.; Wrigglesworth, E.; Jenkins, H.; Dallas, T.; Masters, N.; Perkins, M. W.; Deaville, R.; Druce, M.; Bogeska, R.; Milsom, M. D.; Neumann, B.; Gorman, F.; Constantino-Casas, F.; Peachey, L.; Bochynska, D.; St John Smith, E.; Gerstung, M.; Campbell, P. J.; Murchison, E. P.; Stratton, M. R.; Martincorena, I. Somatic Mutation Rates Scale with Lifespan across Mammals. *Nature* **2022**, *604*. https://doi.org/10.1038/s41586-022-04618-z.

(138) Gorelick, A. N.; Naxerova, K. Mutational Clocks Tick Differently across Species. *Nature* **2022**, *604* (7906), 435–436. https://doi.org/10.1038/d41586-022-00976-w.

(139) Cohen, A. A. Aging across the Tree of Life: The Importance of a Comparative Perspective for the Use of Animal Models in Aging. *Biochim.*

Biophys. Acta - Mol. Basis Dis. **2018**, *1864* (9), 2680–2689. https://doi.org/10.1016/j.bbadis.2017.05.028.

(140) Mitchell, S. J.; Scheibye-Knudsen, M.; Longo, D. L.; de Cabo, R. Animal Models of Aging Research: Implications for Human Aging and Age-Related Diseases. *Annu. Rev. Anim. Biosci.* **2015**, *3* (1), 283–303. https://doi.org/10.1146/annurev-animal-022114-110829.

(141) Sharpless, N. E.; Sherr, C. J. Forging a Signature of in Vivo Senescence. *Nat. Rev. Cancer* **2015**, *15* (7), 397–408. https://doi.org/10.1038/nrc3960.

(142) Wiley, C. D.; Campisi, J. The Metabolic Roots of Senescence: Mechanisms and Opportunities for Intervention. *Nat. Metab.* **2021**, *3* (10), 1290–1301. https://doi.org/10.1038/s42255-021-00483-8.

(143) Niedernhofer, L. J.; Robbins, P. D. Senotherapeutics for Healthy Ageing. *Nat. Publ. Gr.* **2018**.

(144) Coppé, J. P.; Rodier, F.; Patil, C. K.; Freund, A.; Desprez, P. Y.; Campisi, J. Tumor Suppressor and Aging Biomarker P16 INK4a Induces Cellular Senescence without the Associated Inflammatory Secretory Phenotype. *J. Biol. Chem.* **2011**, *286* (42), 36396–36403. https://doi.org/10.1074/jbc.M111.257071.

(145) Kosar, M.; Bartkova, J.; Hubackova, S.; Hodny, Z.; Lukas, J.; Bartek, J. Senescence-Associated Heterochromatin Foci Are Dispensable for Cellular Senescence, Occur in a Cell Type- and Insult-Dependent Manner, and Follow Expression of P16ink4a. *Cell Cycle* **2011**, *10* (3), 457–468. https://doi.org/10.4161/cc.10.3.14707.

(146) Rodier, F.; Campisi, J. Four Faces of Cellular Senescence. *J. Cell Biol.* **2011**, *192* (4), 547–556. https://doi.org/10.1083/jcb.201009094.

(147) Kang, C. Senolytics and Senostatics: A Two-Pronged Approach to Target Cellular Senescence for Delaying Aging and Age-Related Diseases. *Mol. Cells* **2019**, *42* (12), 821–827. https://doi.org/10.14348/molcells.2019.0298.

(148) Song, S.; Lam, E. W. F.; Tchkonia, T.; Kirkland, J. L.; Sun, Y. Senescent Cells: Emerging Targets for Human Aging and Age-Related Diseases. *Trends Biochem. Sci.* **2020**. https://doi.org/10.1016/j.tibs.2020.03.008.

(149) Justice, J. N.; Nambiar, A. M.; Tchkonia, T.; Lebrasseur, N. K.; Pascual, R.; Hashmi, S. K.; Prata, L.; Masternak, M. M.; Kritchevsky, S. B.; Musi, N.; Kirkland, J. L. Senolytics in Idiopathic Pulmonary Fibrosis: Results from a First-in-Human, Open-Label, Pilot Study. *EBioMedicine* **2019**, *40*, 554–563. https://doi.org/10.1016/j.ebiom.2018.12.052.

(150) Hickson, L. J.; Langhi Prata, L. G. P.; Bobart, S. A.; Evans, T. K.; Giorgadze, N.; Hashmi, S. K.; Herrmann, S. M.; Jensen, M. D.; Jia, Q.; Jordan, K. L.; Kellogg, T. A.; Khosla, S.; Koerber, D. M.; Lagnado, A. B.; Lawson, D. K.; Lebrasseur, N. K.; Lerman, L. O.; Mcdonald, K. M.; Mckenzie, T. J.; Passos, J. F.; Pignolo, R. J.; Pirtskhalava, T.; Saadiq, I. M.; Schaefer, K. K.; Textor, S. C.; Victorelli, S. G.; Volkman, T. L.; Xue, A.; Wentworth, M. A.; Wissler Gerdes, E. O.; Zhu, Y.; Tchkonia, T.; Kirkland, J. L. Senolytics Decrease Senescent Cells in Humans: Preliminary Report from a Clinical Trial of Dasatinib plus Quercetin in Individuals with Diabetic Kidney Disease. *EBioMedicine* **2019**, *47*, 446–456. https://doi.org/10.1016/j.ebiom.2019.08.069.

(151) Lee, B. P.; Harries, L. W. Senotherapeutic Drugs: A New Avenue for Skincare? *Plast. Reconstr. Surg.* **2021**, *148* (6 S), 21S-26S.

https://doi.org/10.1097/PRS.0000000000008782.

(152) Olascoaga-Del Angel, K. S.; Gutierrez, H.; Königsberg, M.; Pérez-Villanueva, J.; López-Diazguerrero, N. E. Exploring the Fuzzy Border between Senolytics and Senomorphics with Chemoinformatics and Systems Pharmacology. *Biogerontology* **2022**, *23* (4), 453–471. https://doi.org/10.1007/s10522-022-09974-x.

(153) Barzilai, N.; Crandall, J. P.; Kritchevsky, S. B.; Espeland, M. A. Metformin as a Tool to Target Aging. *Cell Metab.* **2016**, *23* (6), 1060–1065. https://doi.org/10.1016/J.CMET.2016.05.011.

(154) Ziehm, M.; Kaur, S.; Ivanov, D. K.; Ballester, P. J.; Marcus, D.; Partridge, L.; Thornton, J. M. Drug Repurposing for Aging Research Using Model Organisms. *Aging Cell* **2017**, *16* (5), 1006–1015. https://doi.org/10.1111/acel.12626.

(155) Yang, X.; Wang, Y.; Byrne, R.; Schneider, G.; Yang, S. Concepts of Artificial Intelligence for Computer-Assisted Drug Discovery. *Chem. Rev.* **2019**, *119* (18), 10520–10594. https://doi.org/10.1021/acs.chemrev.8b00728.

(156) Pun, F. W.; Leung, G. H. D.; Leung, H. W.; Liu, B. H. M.; Long, X.; Ozerov, I. V; Wang, J.; Ren, F.; Aliper, A.; Izumchenko, E.; Moskalev, A.; de Magalhães, J. P.; Zhavoronkov, A. Hallmarks of Aging-Based Dual-Purpose Disease and Age-Associated Targets Predicted Using PandaOmics AI-Powered Discovery Engine. *Aging (Albany. NY).* **2022**, *14* (6), 2475–2506.

(157) Pan, Q.; Shai, O.; Lee, L. J.; Frey, B. J.; Blencowe, B. J. Deep Surveying of Alternative Splicing Complexity in the Human Transcriptome by High-

Throughput Sequencing. *Nat. Genet.* **2008**, *40* (12). https://doi.org/10.1038/ng.259.

(158) Tazi, J.; Bakkour, N.; Stamm, S. Alternative Splicing and Disease. *Biochim. Biophys. Acta - Mol. Basis Dis.* **2009**, *1792* (1), 14–26. https://doi.org/10.1016/j.bbadis.2008.09.017.

(159) Deschênes, M.; Chabot, B. The Emerging Role of Alternative Splicing in Senescence and Aging. *Aging Cell* **2017**, *16* (5), 918–933. https://doi.org/10.1111/acel.12646.

(160) Havens, M. A.; Hastings, M. L. Splice-Switching Antisense Oligonucleotides as Therapeutic Drugs. *Nucleic Acids Res.* **2016**, *44* (14), 6549–6563. https://doi.org/10.1093/nar/gkw533.

(161) Lai, W. F.; Lin, M.; Wong, W. T. Tackling Aging by Using MiRNA as a Target and a Tool. *Trends Mol. Med.* **2019**, *25* (8), 673–684. https://doi.org/10.1016/j.molmed.2019.04.007.

(162) Wang, Z.; Gao, J.; Xu, C. Tackling Cellular Senescence by Targeting MiRNAs. *Biogerontology* **2022**, *23* (4), 387–400. https://doi.org/10.1007/s10522-022-09972-z.

(163) Wilusz, C. J.; Wormington, M.; Peltz, S. W. The Cap-to-Tail Guide to MRNA Turnover. *Nat. Rev. Mol. Cell Biol.* **2001**, *2*, 237–246.

(164) Gomez-Verjan, J. C.; Vazquez-Martinez, E. R.; Rivero-Segura, N. A.; Medina-Campos, R. H. The RNA World of Human Ageing. *Hum. Genet.* **2018**, *137* (11–12), 865–879. https://doi.org/10.1007/s00439-018-1955-3.

(165) Itahana, K.; Campisi, J.; Dimri, G. P. Methods to Detect Biomarkers of Cellular Senescence: The Senescence-Associated β-Galactosidase Assay. *Methods Mol. Biol.* **2007**, *371* (May), 21–31.

https://doi.org/10.1385/1-59745-361-7:21.

(166) Biran, A.; Zada, L.; Abou Karam, P.; Vadai, E.; Roitman, L.; Ovadya, Y.; Porat, Z.; Krizhanovsky, V. Quantitative Identification of Senescent Cells in Aging and Disease. *Aging Cell* **2017**, *16* (4), 661–671. https://doi.org/10.1111/acel.12592.

(167) Noren Hooten, N.; Evans, M. K. Techniques to Induce and Quantify Cellular Senescence. *J. Vis. Exp* **2017**, No. 123, 55533. https://doi.org/10.3791/55533.

(168) Scholzen, T.; Gerdes, J. The Ki-67 Protein : From the Known and the Unknown. *J. Cell.* **2000**, *182*, 311–322.

(169) Sun, X.; Kaufman, P. D. Ki-67: More than a Proliferation Marker. *Chromosoma* **2018**, *127*, 175–186. https://doi.org/10.1007/s00412-018-0659-8.

(170) Remnant, L.; Kochanova, N. Y.; Reid, C.; Cisneros-Soberanis, F.; Earnshaw, W. C. The Intrinsically Disorderly Story of Ki-67. *Open Biol.* **2021**, *11* (210120), 1–15. https://doi.org/10.1098/rsob.210120.

(171) Miller, I.; Min, M.; Yang, C.; Tian, C.; Gookin, S.; Carter, D.; Spencer, S. L. Ki67 Is a Graded Rather than a Binary Marker of Proliferation versus Quiescence. *Cell Rep.* **2018**, *24* (5), 1105–1112. https://doi.org/10.1016/j.celrep.2018.06.110.

(172) Alessio, N.; Aprile, D.; Cappabianca, S.; Peluso, G.; Di Bernardo, G.; Galderisi, U. Different Stages of Quiescence, Senescence, and Cell Stress Identified by Molecular Algorithm Based on the Expression of Ki67, RPS6, and Beta-Galactosidase Activity. *Int. J. Mol. Sci.* **2021**, *22* (6), 1–13. https://doi.org/10.3390/ijms22063102.

(173) Atkinson, J.; Bezak, E.; Kempson, I. Imaging DNA Double-Strand Breaks — Are We There Yet? *Nat. Rev. Mol. Cell Biol.* **2022**, *23* (9), 579–580. https://doi.org/10.1038/s41580-022-00513-7.

(174) Cleaver, J. E.; Feeney, L.; Revet, I. Phosphorylated H2Ax Is Not an Unambiguous Marker for DNA Double Strand Breaks. *Cell Cycle* **2011**, *10* (19), 3223–3224. https://doi.org/10.4161/cc.10.19.17448.

(175) Kim, Y.-K.; Yeo, J.; Kim, B.; Ha, M.; Kim, V. N. Short Structured RNAs with Low GC Content Are Selectively Lost during Extraction from a Small Number of Cells. *Mol. Cell* **2012**, *46* (6), 893–895. https://doi.org/10.1016/j.molcel.2012.05.036.

(176) Pfaffl, M. W. A New Mathematical Model for Relative Quantification in Real-Time RT–PCR. *Nucleic Acids Res.* **2001**, *29* (9), 2002–2007. https://doi.org/10.1093/nar/29.9.e45.

(177) Xie, F.; Xiao, P.; Chen, D.; Xu, L.; Zhang, B. MiRDeepFinder: A MiRNA Analysis Tool for Deep Sequencing of Plant Small RNAs. *Plant Mol. Biol.* **2012**, *80* (1), 75–84. https://doi.org/10.1007/S11103-012-9885-2/FIGURES/3.

(178) Cao, Y.; Charisi, A.; Cheng, L. C.; Jiang, T.; Girke, T. ChemmineR: A Compound Mining Framework for R. *Bioinformatics* **2008**, *24* (15), 1733–1734. https://doi.org/10.1093/BIOINFORMATICS/BTN307.

(179) Wang, Y.; Backman, T. W. H.; Horan, K.; Girke, T. FmcsR: Mismatch Tolerant Maximum Common Substructure Searching in R. *Bioinformatics* **2013**, *29* (21), 2792–2794. https://doi.org/10.1093/bioinformatics/btt475.

(180) RStudio Team. RStudio: Integrated Development Environment for R. RStudio, PBC: Boston, Massachusetts 2020.

(181) Latorre, E.; Birar, V. C.; Sheerin, A. N.; Jeynes, J. C. C.; Hooper, A.; Dawe, H. R.; Melzer, D.; Cox, L. S.; Faragher, R. G. A.; Ostler, E. L.; Harries, L. W. Small Molecule Modulation of Splicing Factor Expression Is Associated with Rescue from Cellular Senescence. *BMC Cell Biol.* **2017**, *18* (1). https://doi.org/10.1186/s12860-017-0147-7.

(182) Perlman, R. L. Mouse Models of Human Disease An Evolutionary Perspective. *Evolution (N. Y).* **2016**, 170–176. https://doi.org/10.1093/emph/eow014.

(183) James, E. L.; Parkinson, E. K. Serum Metabolomics in Animal Models and Human Disease. *Curr. Opin. Clin. Nutr. Metab. Care* **2015**, *18* (5), 478–483. https://doi.org/10.1097/MCO.0000000000000200.

(184) Geraghty, R. J.; Capes-Davis, A.; Davis, J. M.; Downward, J.; Freshney, R. I.; Knezevic, I.; Lovell-Badge, R.; Masters, J. R. W.; Meredith, J.; Stacey, G. N.; Thraves, P.; Vias, M. Guidelines for the Use of Cell Lines in Biomedical Research. *Br. J. Cancer* **2014**, *111* (6), 1021–1046. https://doi.org/10.1038/bjc.2014.166.

(185) Yaqub, N.; Wayne, G.; Birchall, M.; Song, W. Recent Advances in Human Respiratory Epithelium Models for Drug Discovery. *Biotechnol. Adv.* **2022**, *54*. https://doi.org/10.1016/j.biotechadv.2021.107832.

(186) Yamaguchi, S.; Kaneko, M.; Narukawa, M. Approval Success Rates of Drug Candidates Based on Target, Action, Modality, Application, and Their Combinations. *Clin. Transl. Sci.* **2021**, *14* (3), 1113–1122. https://doi.org/10.1111/CTS.12980.

(187) Seok, J.; Shaw Warren, H.; Cuenca, A. G.; Mindrinos, M. N.; Baker, H. V; Xu, W.; Richards, D. R.; Mcdonald-Smith, G. P.; Gao, H.; Hennessy, L.;

Finnerty, C. C.; López, C. M.; Honari, S.; Moore, E. E.; Minei, J. P.; Cuschieri, J.; Bankey, P. E.; Johnson, J. L.; Sperry, J.; Nathens, A. B.; Billiar, T. R.; West, M. A.; Jeschke, M. G.; Klein, M. B.; Gamelli, R. L.; Gibran, N. S.; Brownstein, B. H.; Miller-Graziano, C.; Calvano, S. E.; Mason, P. H.; Cobb, J. P.; Rahme, L. G.; Lowry, S. F.; Maier, R. V; Moldawer, L. L.; Herndon, D. N.; Davis, R. W.; Xiao, W.; Tompkins, R. G. Genomic Responses in Mouse Models Poorly Mimic Human Inflammatory Diseases. *Proc. Natl. Acad. Sci. U. S. A.* **2013**, *110* (9), 3507–3512. https://doi.org/10.1073/pnas.1222878110.

(188) Gurumurthy, C. B.; Kent Lloyd, K. C. Generating Mouse Models for Biomedical Research: Technological Advances. *DMM Dis. Model. Mech.* **2019**, *12* (1). https://doi.org/10.1242/DMM.029462/3039.

(189) Khorramizadeh, M. R.; Saadat, F. Animal Models for Human Disease. In *Animal Biotechnology: Models in Discovery and Translation*; Elsevier, 2020; pp 153–171. https://doi.org/10.1016/B978-0-12-811710-1.00008-2.

(190) Elsea, S. H.; Lucas, R. E. The Mousetrap: What We Can Learn When the Mouse Model Does Not Mimic the Human Disease. *ILAR J.* **2002**, *43* (2), 66–79. https://doi.org/10.1093/ILAR.43.2.66.

(191) Martin, E.-R.; Gandawijaya, J.; Oguro-Ando, A. A Novel Method for Generating Glutamatergic SH-SY5Y Neuron-like Cells Utilizing B-27 Supplement. *Front. Pharmacol.* **2022**, No. October, 1–20. https://doi.org/10.3389/fphar.2022.943627.

(192) Yao, T.; Asayama, Y. Animal-cell Culture Media: History, Characteristics, and Current Issues. *Reprod. Med. Biol.* **2017**, *16* (2), 99. https://doi.org/10.1002/RMB2.12024.

(193) Beskow, L. M. Lessons from HeLa Cells: The Ethics and Policy of Biospecimens. *Annu. Rev. Genomics Hum. Genet.* **2016**, *17*, 395. https://doi.org/10.1146/ANNUREV-GENOM-083115-022536.

(194) Subbiahanadar Chelladurai, K.; Selvan Christyraj, J. D.; Rajagopalan, K.; Yesudhason, B. V.; Venkatachalam, S.; Mohan, M.; Chellathurai Vasantha, N.; Selvan Christyraj, J. R. S. Alternative to FBS in Animal Cell Culture - An Overview and Future Perspective. *Heliyon* **2021**, *7* (8), e07686. https://doi.org/10.1016/J.HELIYON.2021.E07686.

(195) Zheng, X.; Baker, H.; Hancock, W. S.; Fawaz, F.; McCaman, M.; Pungor, E. Proteomic Analysis for the Assessment of Different Lots of Fetal Bovine Serum as a Raw Material for Cell Culture. Part IV. Application of Proteomics to the Manufacture of Biological Drugs. *Biotechnol. Prog.* **2006**, *22* (5), 1294–1300. https://doi.org/10.1021/BP060121O.

(196) Valk, J. van der; Gstraunthaler, G. Fetal Bovine Serum (FBS) — A Pain in the Dish? *ATLA* **2017**, *45* (6), 329–332. https://doi.org/10.1177/026119291704500611.

(197) van der Valk, J.; Bieback, K.; Buta, C.; Cochrane, B.; Dirks, W. G.; Fu, J.; Hickman, J. J.; Hohensee, C.; Kolar, R.; Liebsch, M.; Pistollato, F.; Schulz, M.; Thieme, D.; Weber, T.; Wiest, J.; Winkler, S.; Gstraunthaler, G. Fetal Bovine Serum (FBS): Past - Present - Future. *ALTEX* **2018**, *35* (1), 99–118. https://doi.org/10.14573/altex.1705101.

(198) Gstraunthaler, G.; Lindl, T.; Van Der Valk, J. A Plea to Reduce or Replace Fetal Bovine Serum in Cell Culture Media. *Cytotechnology* **2013**, *65* (5), 791. https://doi.org/10.1007/S10616-013-9633-8.

(199) Chang, B.; Mahoney, R. Enzyme Thermostabilization by Bovine Serum

Albumin and Other Proteins: Evidence for Hydrophobic Interactions. *Biotechnol. Appl. Biochem.* **1995**, *22* (2), 203–214. https://doi.org/10.1111/J.1470-8744.1995.TB00346.X.

(200) Muraglia, A.; Nguyen, V. T.; Nardini, M.; Mogni, M.; Coviello, D.; Dozin, B.; Strada, P.; Baldelli, I.; Formica, M.; Cancedda, R.; Mastrogiacomo, M. Culture Medium Supplements Derived from Human Platelet and Plasma: Cell Commitment and Proliferation Support. *Front. Bioeng. Biotechnol.* **2017**, *5* (NOV). https://doi.org/10.3389/FBIOE.2017.00066.

(201) Fetal Calf Serum Free Database https://fcs-free.org/ (accessed Oct 5, 2022).

(202) Bairoch, A. The Cellosaurus, a Cell-Line Knowledge Resource. *J. Biomol. Tech.* **2018**, *29* (2), 25–38. https://doi.org/10.7171/JBT.18-2902-002.

(203) Stephenson, M.; Grayson, W. L.; Ma, T.; Geris, L.; Leuven, K. U. Recent Advances in Bioreactors for Cell-Based Therapies. *F1000Research 2018 7517* **2018**, *7*, 517. https://doi.org/10.12688/f1000research.12533.1.

(204) Caliari, S. R.; Burdick, J. A. A Practical Guide to Hydrogels for Cell Culture. *Nat. Methods* **2016**, *13* (5), 405. https://doi.org/10.1038/NMETH.3839.

(205) The GIMP Development Team. GIMP. 2002.

(206) Witzeneder, K.; Lindenmair, A.; Gabriel, C.; Höller, K.; Theiß, D.; Redl, H.; Hennerbichler, S. Human-Derived Alternatives to Fetal Bovine Serum in Cell Culture. *Transfus. Med. Hemotherapy* **2013**, *40* (6), 417–423. https://doi.org/10.1159/000356236.

(207) Gstraunthaler, G. Alternatives to the Use of Fetal Bovine Serum: Serum-Free Cell Culture. *ALTEX* **2003**, *20* (4), 275–281. https://doi.org/10.14573/altex.2003.4.257.

(208) Kent, K. D.; Bomser, J. A. Bovine Pituitary Extract Provides Remarkable Protection against Oxidative Stress in Human Prostate Epithelial Cells. *Vitr. Cell. Dev. Biol. - Anim.* **2003**, *39* (8–9), 388–394. https://doi.org/10.1290/0311082.

(209) Galy, A.; Jolivet, M.; Jolivet-Reynaud, C.; Hadden, J. Fibroblast Growth Factor (FGF) and an FGF-like Molecule in Pituitary Extracts Stimulate Thymic Epithelial Cell Proliferation. *Thymus* **1990**, *15* (4), 199–211.

(210) Hadden, M. Factor Induces Proliferation Thymic Epithelial in Vitro. **1989**, *159*, 149–159.

(211) Tanigaki-Obana, N.; Ito, M. Can Fibroblast Growth Factors Substitute for Bovine Pituitary Extracts in Culture Systems for Hair Apparatus Cells? *Arch Dermatol Res* **1994**, *286*, 484–489.

(212) Hammond, S. L.; Ham, R. G.; Stampfert, M. R. Serum-Free Growth of Human Mammary Epithelial Cells: Rapid Clonal Growth in Defined Medium and Extended Serial Passage with Pituitary Extract (Prostaglandin El/Cycic AMP/Ethanolamine/Insulin/Epidermal Growth Factor). *Cell Biol.* **1984**, *81*, 5435–5439.

(213) Campisi, J. Aging, Cellular Senescence, and Cancer. *Annu. Rev. Physiol.* **2013**, *75* (1), 685–705. https://doi.org/10.1146/annurev-physiol-030212-183653.

(214) Chan, H. C. S.; Shan, H.; Dahoun, T.; Vogel, H.; Yuan, S. Advancing Drug Discovery via Artificial Intelligence. *Trends Pharmacol. Sci.* **2019**, *40* (8), 592–604. https://doi.org/10.1016/j.tips.2019.06.004.

(215) Bankhead, P.; Loughrey, M. B.; Fernández, J. A.; Dombrowski, Y.; McArt, D. G.; Dunne, P. D.; McQuaid, S.; Gray, R. T.; Murray, L. J.; Coleman, H.

G.; James, J. A.; Salto-Tellez, M.; Hamilton, P. W. QuPath: Open Source Software for Digital Pathology Image Analysis. *Sci. Rep.* **2017**, *7* (1). https://doi.org/10.1038/s41598-017-17204-5.

(216) Stirling, D. R.; Swain-Bowden, M. J.; Lucas, A. M.; Carpenter, A. E.; Cimini, B. A.; Goodman, A. CellProfiler 4: Improvements in Speed, Utility and Usability. *BMC Bioinformatics* **2021**, *22* (1). https://doi.org/10.1186/s12859-021-04344-9.

(217) Paulik, R.; Micsik, T.; Kiszler, G.; Kaszál, P.; Székely, J.; Paulik, N.; Várhalmi, E.; Prémusz, V.; Krenács, T.; Molnár, B. An Optimized Image Analysis Algorithm for Detecting Nuclear Signals in Digital Whole Slides for Histopathology. *Cytom. Part A* **2017**, *91* (6), 595–608. https://doi.org/10.1002/CYTO.A.23124.

(218) Schneider, C. A.; Rasband, W. S.; Eliceiri, K. W. NIH Image to ImageJ: 25 Years of Image Analysis. *Nat. Methods* **2012**, *9* (7), 671–675. https://doi.org/10.1038/nmeth.2089.

(219) Chambolle, A.; Pock, T. An Introduction to Continuous Optimization for Imaging. *Acta Numer.* **2016**, *25*, 161–319.

(220) Otsu, N. A Threshold Selection Method from Gray-Level Histograms. *IEEE Trans. Syst. Man. Cybern.* **1979**, *9* (1), 62–66.

(221) Chan, T.; Esedoglu, S.; Nikolova, M. Algorithms for Finding Global Minimizers of Image Segmentation and Denoising Models. *SIAM J. Appl. Math.* **2006**, *66* (5), 1632–1648.

(222) Goldstein, T.; Osher, S. The Split Bregman Method for L1-Regularized Problems. *SIAM J. Imaging Sci.* **2009**, *2* (2), 323–343.

(223) Goldstein, T.; Bresson, X.; Osher, S. Geometric Applications of the Split

Bregman Method. *J. Sci. Comput.* **2010**, *45* (1–3), 272–293.

(224) Bresson, X.; Esedoglu, S.; Vandergheynst, P.; Thiran, J. P.; Osher, S. Fast Global Minimization of the Active Contour/Snake Model. *J. Math. Imaging Vis.* **2007**, *28* (2), 151–167.

(225) Chambolle, A. An Algorithm For Total Variation Minimization and Applications. *J. Math. Imaging Vis.* **2004**, *20*, 89–97.

(226) Aujol, J. F.; Gilboa, G.; Chan, T.; Osher, S. Structure-Texture Decomposition - Modeling, Algorithms, and Parameter Selection. *Int. J. Comput. Vis.* **2006**, *67* (1), 111–136.

(227) Chambolle, A.; Pock, T. A First-Order Primal-Dual Algorithm for Convex Problems with Applications to Imaging. *J. Math. Imaging Vis.* **2011**, *40*, 120–145.

(228) Freije, J. M. P.; López-Otín, C. Reprogramming Aging and Progeria. *Curr. Opin. Cell Biol.* **2012**, *24* (6), 757–764. https://doi.org/10.1016/j.ceb.2012.08.009.

(229) Gordon, L. B. PRF by the Numbers. *The Progeria Research Foundation*. Progeria Research Foundation 2022.

(230) Gordon, L. B.; Brown, W. T.; Collins, F. S. Hutchinson-Gilford Progeria Syndrome. In *GeneReviews*®; 2019; pp 1–20.

(231) Oshima, J.; Martin, G. M.; Hisama, F. M. Werner Syndrome. In *GeneReviews*®; 2021; pp 1–16.

(232) Laugel, V. Cockayne Syndrome. In *GeneReviews*®; 2019; pp 1–19. https://doi.org/10.1007/s11825-012-0364-6.

(233) Eriksson, M.; Brown, W. T.; Gordon, L. B.; Glynn, M. W.; Singer, J.; Scott, L.; Erdos, M. R.; Robbins, C. M.; Moses, T. Y.; Berglund, P.; Dutra, A.; Pak,

E.; Durkin, S.; Csoka, A. B.; Boehnke, M.; Glover, T. W.; Collins, F. S. Recurrent de Novo Point Mutations in Lamin A Cause Hutchinson–Gilford Progeria Syndrome. *Nature* **2003**, *423*, 293–298. https://doi.org/10.1177/002199839502901205.

(234) Natale, V. A Comprehensive Description of the Severity Groups in Cockayne Syndrome. *Am. J. Med. Genet. Part A* **2011**, *155* (5), 1081–1095. https://doi.org/10.1002/AJMG.A.33933.

(235) Strandgren, C.; Revêchon, G.; Carvajal, A. S.; Eriksson, M. Emerging Candidate Treatment Strategies for Hutchinson-Gilford Progeria Syndrome. *Biochem. Soc. Trans.* **2017**, *45* (6), 1279–1293. https://doi.org/10.1042/BST20170141.

(236) Kubben, N.; Misteli, T. Shared Molecular and Cellular Mechanisms of Premature Ageing and Ageing-Associated Diseases. *Nat. Rev. Mol. Cell Biol.* **2017**, *18* (10), 595–609. https://doi.org/10.1038/nrm.2017.68.

(237) Kyng, K. J.; May, A.; Stevnsner, T.; Becker, K. G.; Kølvrå, S.; Bohr, V. A. Gene Expression Responses to DNA Damage Are Altered in Human Aging and in Werner Syndrome. *Oncogene* **2005**, *24* (32), 5026–5042. https://doi.org/10.1038/sj.onc.1208692.

(238) Baar, M. P.; Perdiguero, E.; Muñoz-Cánoves, P.; de Keizer, P. L. Musculoskeletal Senescence: A Moving Target Ready to Be Eliminated. *Curr. Opin. Pharmacol.* **2018**, *40*, 147–155. https://doi.org/10.1016/J.COPH.2018.05.007.

(239) Harries, L. W. Messenger RNA Processing and Its Role in Diabetes. *Diabet. Med.* **2011**, *28* (9), 1010–1017. https://doi.org/10.1111/j.1464-5491.2011.03373.x.

(240) Harries, L. W. Dysregulated RNA Processing and Metabolism: A New Hallmark of Ageing and Provocation for Cellular Senescence. *FEBS J.* **2022**. https://doi.org/10.1111/FEBS.16462.

(241) Harries, L. W.; Hernandez, D.; Henley, W.; Wood, A. R.; Holly, A. C.; Bradley-Smith, R. M.; Yaghootkar, H.; Dutta, A.; Murray, A.; Frayling, T. M.; Guralnik, J. M.; Bandinelli, S.; Singleton, A.; Ferrucci, L.; Melzer, D. Human Aging Is Characterized by Focused Changes in Gene Expression and Deregulation of Alternative Splicing. *Aging Cell* **2011**, *10* (5), 868–878. https://doi.org/10.1111/j.1474-9726.2011.00726.x.

(242) Pont, A. R.; Sadri, N.; Hsiao, S. J.; Smith, S.; Schneider, R. J. MRNA Decay Factor AUF1 Maintains Normal Aging, Telomere Maintenance, and Suppression of Senescence by Activation of Telomerase Transcription. *Mol. Cell* **2012**, *47* (1), 5–15. https://doi.org/10.1016/j.molcel.2012.04.019.

(243) Deschênes, M.; Chabot, B. The Emerging Role of Alternative Splicing in Senescence and Aging. *Aging Cell* **2017**, *16* (5), 918–933. https://doi.org/10.1111/acel.12646.

(244) Liu, B.; Ghosh, S.; Yang, X.; Zheng, H.; Liu, X.; Wang, Z.; Jin, G.; Zheng, B.; Kennedy, B. K.; Suh, Y.; Kaeberlein, M.; Tryggvason, K.; Zhou, Z. Resveratrol Rescues SIRT1-Dependent Adult Stem Cell Decline and Alleviates Progeroid Features in Laminopathy-Based Progeria. *Cell Metab.* **2012**, *16* (6), 738–750. https://doi.org/10.1016/j.cmet.2012.11.007.

(245) Slack, C.; Alic, N.; Foley, A.; Cabecinha, M.; Hoddinott, M. P.; Partridge Correspondence, L. The Ras-Erk-ETS-Signaling Pathway Is a Drug Target for Longevity. *Cell* **2015**, *162*, 72–83. https://doi.org/10.1016/j.cell.2015.06.023.

(246) Slack, C. Ras Signaling in Aging and Metabolic Regulation. *Nutr. Heal. Aging* **2017**, *4*, 195–205. https://doi.org/10.3233/NHA-160021.

(247) Bagley, M. C.; Davis, T.; Murziani, P. G. S.; Widdowson, C. S.; Kipling, D. Use of P38 MAPK Inhibitors for the Treatment of Werner Syndrome. *Pharmaceuticals (Basel).* **2010**, *3* (6), 1842–1872. https://doi.org/10.3390/PH3061842.

(248) Davis, T.; Bachler, M. A.; Wyllie, F. S.; Bagley, M. C.; Kipling, D. Evaluating the Role of P38 MAP Kinase in Growth of Werner Syndrome Fibroblasts. *Ann. N. Y. Acad. Sci.* **2010**, *1197*, 45–48. https://doi.org/10.1111/J.1749-6632.2010.05195.X.

(249) Bagley, M. C.; Dwyer, J. E.; Baashen, M.; Dix, M. C.; Murziani, P. G. S.; Rokicki, M. J.; Kipling, D.; Davis, T. The Effect of RO3201195 and a Pyrazolyl Ketone P38 MAPK Inhibitor Library on the Proliferation of Werner Syndrome Cells. *Org. Biomol. Chem.* **2016**, *14* (3), 947–956. https://doi.org/10.1039/C5OB02229K.

(250) Bikkul, M. U.; Clements, C. S.; Godwin, L. S.; Goldberg, M. W.; Kill, I. R.; Bridger, J. M. Farnesyltransferase Inhibitor and Rapamycin Correct Aberrant Genome Organisation and Decrease DNA Damage Respectively, in Hutchinson-Gilford Progeria Syndrome Fibroblasts. *Biogerontology* **2018**, *19* (6), 579–602. https://doi.org/10.1007/s10522-018-9758-4.

(251) Chen, X.; Yao, H.; Andrés, V.; Bergo, M. O.; Kashif, M. Status of Treatment Strategies for Hutchinson–Gilford Progeria Syndrome with a Focus on Prelamin: A Posttranslational Modification. *Basic Clin. Pharmacol. Toxicol.* **2022**, 1–7. https://doi.org/10.1111/BCPT.13770.

(252) Zeiser, R.; Andrlová, H.; Meiss, F. Trametinib (GSK1120212). *Recent*

Results Cancer Res. **2018**, *211*, 91–100. https://doi.org/10.1007/978-3-319-91442-8_7.

(253) Khan, Z. M.; Real, A. M.; Marsiglia, W. M.; Chow, A.; Duffy, M. E.; Yerabolu, J. R.; Scopton, A. P.; Dar, A. C. Structural Basis for the Action of the Drug Trametinib at KSR-Bound MEK. *Nature* **2020**, *588* (7838), 509–514. https://doi.org/10.1038/s41586-020-2760-4.

(254) Thota, R.; Johnson, D. B.; Sosman, J. A. Trametinib in the Treatment of Melanoma. *Expert Opin. Biol. Ther.* **2015**, *15* (5), 735–747. https://doi.org/10.1517/14712598.2015.1026323.

(255) Yokote, K.; Chanprasert, S.; Lee, L.; Eirich, K.; Takemoto, M.; Watanabe, A.; Koizumi, N.; Lessel, D.; Mori, T.; Hisama, F. M.; Ladd, P. D.; Angle, B.; Baris, H.; Cefle, K.; Palanduz, S.; Ozturk, S.; Chateau, A.; Deguchi, K.; Easwar, T. K. M.; Federico, A.; Fox, A.; Grebe, T. A.; Hay, B.; Nampoothiri, S.; Seiter, K.; Streeten, E.; Piña-Aguilar, R. E.; Poke, G.; Poot, M.; Posmyk, R.; Martin, G. M.; Kubisch, C.; Schindler, D.; Oshima, J. WRN Mutation Update: Mutation Spectrum, Patient Registries, and Translational Prospects. *Hum. Mutat.* **2017**, *38* (1), 7–15. https://doi.org/10.1002/humu.23128.

(256) Cao, K.; Blair, C. D.; Faddah, D. A.; Kieckhaefer, J. E.; Olive, M.; Erdos, M. R.; Nabel, E. G.; Collins, F. S. Progerin and Telomere Dysfunction Collaborate to Trigger Cellular Senescence in Normal Human Fibroblasts. *J. Clin. Invest.* **2011**, *121* (7), 2833–2844. https://doi.org/10.1172/JCI43578.

(257) Calmels, N.; Botta, E.; Jia, N.; Fawcett, H.; Nardo, T.; Nakazawa, Y.; Lanzafame, M.; Moriwaki, S.; Sugita, K.; Kubota, M.; Obringer, C.; Spitz,

M. A.; Stefanini, M.; Laugel, V.; Orioli, D.; Ogi, T.; Lehmann, A. R. Functional and Clinical Relevance of Novel Mutations in a Large Cohort of Patients with Cockayne Syndrome. *J. Med. Genet.* **2018**, *55* (5), 329–343. https://doi.org/10.1136/jmedgenet-2017-104877.

(258) Tchkonia, T.; Zhu, Y.; Van Deursen, J.; Campisi, J.; Kirkland, J. L. Cellular Senescence and the Senescent Secretory Phenotype: Therapeutic Opportunities. *J. Clin. Invest.* **2013**, *123* (3), 966–972. https://doi.org/10.1172/JCI64098.

(259) Nakamura, A. J.; Rao, V. A.; Pommier, Y.; Bonner, W. M. The Complexity of Phosphorylated H2AX Foci Formation and DNA Repair Assembly at DNA Double-Strand Breaks. *Cell Cycle* **2010**, *9* (2), 389–397. https://doi.org/10.4161/cc.9.2.10475.

(260) Zhang, H.; Sun, L.; Wang, K.; Wu, D.; Trappio, M.; Witting, C.; Cao, K. Loss of H3K9me3 Correlates with ATM Activation and Histone H2AX Phosphorylation Deficiencies in Hutchinson-Gilford Progeria Syndrome. *PLoS One* **2016**, *11* (12). https://doi.org/10.1371/journal.pone.0167454.

(261) Zwicker, F.; Hauswald, H.; Debus, J.; Huber, P. E.; Weber, K. J. Impact of Dimethyl Sulfoxide on Irradiation-Related DNA Double-Strand-Break Induction, -Repair and Cell Survival. *Radiat. Environ. Biophys.* **2019**, *58* (3), 417–424. https://doi.org/10.1007/s00411-019-00797-y.

(262) Joint Formulary Committee. Trametinib. *British National Formulary (BNF) (online)*. BMJ Group and Pharmaceutical Press: London, UK 2022.

(263) Calabrese, E. J.; Mattson, M. P. How Does Hormesis Impact Biology, Toxicology, and Medicine? *npj Aging Mech. Dis.* **2017**, *3* (13). https://doi.org/10.1038/s41514-017-0013-z.

(264) Calabrese, E. J.; Mattson, M. P.; Calabrese, V. Dose Response Biology: The Case of Resveratrol. *Hum. Exp. Toxicol.* **2010**, *29* (12), 1034–1037. https://doi.org/10.1177/0960327110383641.

(265) Calabrese, E. J.; Agathokleous, E.; Kapoor, ; Rachna; Dhawan, G.; Walter, ; Kozumbo, J.; Calabrese, V. Metformin Enhances Resilience via Hormesis. *Ageing Res. Rev.* **2021**, *71* (101418).

(266) Beauséjour, C. M.; Krtolica, A.; Galimi, F.; Narita, M.; Lowe, S. W.; Yaswen, P.; Campisi, J. Reversal of Human Cellular Senescence: Roles of the P53 and P16 Pathways. *EMBO J.* **2003**, *22* (16), 4212–4222. https://doi.org/10.1093/emboj/cdg417.

(267) Kehler, D. S. Age-Related Disease Burden as a Measure of Population Ageing. *Lancet Public Heal.* **2019**, *4* (3), e123–e124. https://doi.org/10.1016/S2468-2667(19)30026-X.

(268) Morgan, E. Past and Projected Period and Cohort Life Tables, 2018-Based, UK: 1981 to 2068. *United Kingdom Off. Natl. Stat.* **2019**, No. l, 1–14.

(269) Muñoz-Espín, D.; Cañamero, M.; Maraver, A.; Gómez-López, G.; Contreras, J.; Murillo-Cuesta, S.; Rodríguez-Baeza, A.; Varela-Nieto, I.; Ruberte, J.; Collado, M.; Serrano, M. Programmed Cell Senescence during Mammalian Embryonic Development. *Cell* **2013**, *155* (5), 1104. https://doi.org/10.1016/j.cell.2013.10.019.

(270) Storer, M.; Mas, A.; Robert-Moreno, A.; Pecoraro, M.; Ortells, M. C.; Giacomo, V. Di; Yosef, R.; Pilpel, N.; Krizhanovsky, V.; Sharpe, J.; Keyes, W. M. Senescence Is a Developmental Mechanism That Contributes to Embryonic Growth and Patterning. *Cell* **2013**, *155*, 1119–1130. https://doi.org/10.1016/j.cell.2013.10.041.

(271) Serrano, M.; Lin, A. W.; McCurrach, M. E.; Beach, D. Oncogenic Ras Provokes Premature Cell Senescence Associated with Accumulation of P53 and P16 INK4a. *Cell* **1997**, *88*, 593–602.

(272) Baar, M. P.; Brandt, R. M. C.; Putavet, D. A.; Klein, J. D. D.; Derks, K. W. J.; Bourgeois, B. R. M.; Stryeck, S.; Rijksen, Y.; van Willigenburg, H.; Feijtel, D. A.; van der Pluijm, I.; Essers, J.; van Cappellen, W. A.; van IJcken, W. F.; Houtsmuller, A. B.; Pothof, J.; de Bruin, R. W. F.; Madl, T.; Hoeijmakers, J. H. J.; Campisi, J.; de Keizer, P. L. J. Targeted Apoptosis of Senescent Cells Restores Tissue Homeostasis in Response to Chemotoxicity and Aging. *Cell* **2017**, *169* (1), 132-147.e16. https://doi.org/10.1016/j.cell.2017.02.031.

(273) Peltz, L.; Gomez, J.; Marquez, M.; Alencastro, F.; Atashpanjeh, N. Resveratrol Exerts Dosage and Duration Dependent Effect on Human Mesenchymal Stem Cell Development. *PLoS One* **2012**, *7* (5), 37162. https://doi.org/10.1371/journal.pone.0037162.

(274) Barra, V.; Chiavetta, R. F.; Titoli, S.; Provenzano, I. M.; Carollo, P. S.; Di Leonardo, A. Specific Irreversible Cell-Cycle Arrest and Depletion of Cancer Cells Obtained by Combining Curcumin and the Flavonoids Quercetin and Fisetin. *Genes (Basel).* **2022**, *13* (7), 1125. https://doi.org/10.3390/GENES13071125.

(275) Hessler, G.; Baringhaus, K. H. Artificial Intelligence in Drug Design. *Molecules* **2018**, *23* (10). https://doi.org/10.3390/molecules23102520.

(276) Batool, M.; Ahmad, B.; Choi, S. A Structure-Based Drug Discovery Paradigm. *Int. J. Mol. Sci.* **2019**, *20* (11). https://doi.org/10.3390/ijms20112783.

(277) Backman, T. W. H.; Cao, Y.; Girke, T. ChemMine Tools: An Online Service for Analyzing and Clustering Small Molecules. *Nucleic Acids Res.* **2011**, *39*, 486–491. https://doi.org/10.1093/nar/gkr320.

(278) Strong, R.; Miller, R. A.; Astle, C. M.; Floyd, R. A.; Flurkey, K.; Hensley, K. L.; Javors, M. A.; Leeuwenburgh, C.; Nelson, J. F.; Ongini, E.; Nadon, N. L.; Warner, H. R.; Harrison, D. E. Nordihydroguaiaretic Acid and Aspirin Increase Lifespan of Genetically Heterogeneous Male Mice. *Aging Cell* **2008**, *7* (5), 641–650. https://doi.org/10.1111/j.1474-9726.2008.00414.x.

(279) FSRH. *FSRH Clinical Guideline: Combined Hormonal Contraception*; 2020; Vol. 2019.

(280) Ng, M.; Hazrati, L. N. Evidence of Sex Differences in Cellular Senescence. *Neurobiol. Aging* **2022**, *120*, 88–104. https://doi.org/10.1016/j.neurobiolaging.2022.08.014.

(281) van den Beld, A. W.; Kaufman, J. M.; Zillikens, M. C.; Lamberts, S. W. J.; Egan, J. M.; van der Lely, A. J. The Physiology of Endocrine Systems with Ageing. *Lancet Diabetes Endocrinol.* **2018**, *6* (8), 647–658. https://doi.org/10.1016/S2213-8587(18)30026-3.

(282) Yakes, F. M.; Chen, J.; Tan, J.; Yamaguchi, K.; Shi, Y.; Yu, P.; Qian, F.; Chu, F.; Bentzien, F.; Cancilla, B.; Orf, J.; You, A.; Laird, A. D.; Engst, S.; Lee, L.; Lesch, J.; Chou, Y. C.; Joly, A. H. Cabozantinib (XL184), a Novel MET and VEGFR2 Inhibitor, Simultaneously Suppresses Metastasis, Angiogenesis, and Tumor Growth. *Mol. Cancer Ther.* **2011**, *10* (12), 2298–2308. https://doi.org/10.1158/1535-7163.MCT-11-0264.

(283) Islam, M. M.; Mirza, S. P. Versatile Use of Carmofur: A Comprehensive Review of Its Chemistry and Pharmacology. *Drug Dev. Res.* **2022**.

https://doi.org/10.1002/DDR.21984.

(284) Maconochie, J.; Woodings, E.; Richards, D. Effects of H1- and H2-receptor Blocking Agents on Histamine-induced Bronchoconstriction in Non-asthmatic Subjects. *Br. J. Clin. Pharmacol.* **1979**, *7* (3), 231–236. https://doi.org/10.1111/j.1365-2125.1979.tb00927.x.

(285) Joint Formulary Committee. Chlorphenamine Maleate. *British National Formulary (BNF) (online)*. BMJ Group and Pharmaceutical Press: London, UK 2022.

(286) Jahn, H.; Schick, M.; Kiefer, F.; Kellner, M.; Yassouridis, A.; Wiedemann, K. Metyrapone as Additive Treatment in Major Depression: A Double-Blind and Placebo-Controlled Trial. *Arch. Gen. Psychiatry* **2004**, *61* (12), 1235–1244. https://doi.org/10.1001/ARCHPSYC.61.12.1235.

(287) Holczer, M.; Márton, M.; Kurucz, A.; Bánhegyi, G.; Kapuy, O. A Comprehensive Systems Biological Study of Autophagy-Apoptosis Crosstalk during Endoplasmic Reticulum Stress. *Biomed Res. Int.* **2015**, *2015*. https://doi.org/10.1155/2015/319589.

(288) Daniel, E.; Aylwin, S.; Mustafa, O.; Ball, S.; Munir, A.; Boelaert, K.; Chortis, V.; Cuthbertson, D. J.; Daousi, C.; Rajeev, S. P.; Davis, J.; Cheer, K.; Drake, W.; Gunganah, K.; Grossman, A.; Gurnell, M.; Powlson, A. S.; Karavitaki, N.; Huguet, I.; Kearney, T.; Mohit, K.; Meeran, K.; Hill, N.; Rees, A.; Lansdown, A. J.; Trainer, P. J.; Minder, A. E. H.; Newell-Price, J. Effectiveness of Metyrapone in Treating Cushing's Syndrome: A Retrospective Multicenter Study in 195 Patients. *J. Clin. Endocrinol. Metab.* **2015**, *100* (11), 4146–4154. https://doi.org/10.1210/jc.2015-2616.

(289) Soares, B. G.; Silva de Lima, M. Penfluridol for Schizophrenia. *Cochrane*

Database Syst. Rev. **2006**. https://doi.org/10.1002/14651858.cd002923.pub2.

(290) Ono, K.; Ikemoto, M.; Kawarabayashi, T.; Ikeda, M.; Nishinakagawa, T.; Hosokawa, M.; Shoji, M.; Takahashi, M.; Nakashima, M. A Chemical Chaperone, Sodium 4-Phenylbutyric Acid, Attenuates the Pathogenic Potency in Human Alpha-Synuclein A30P + A53T Transgenic Mice. *Parkinsonism Relat. Disord.* **2009**, *15* (9), 649–654. https://doi.org/10.1016/J.PARKRELDIS.2009.03.002.

(291) Singh, O. V; Vij, N.; Mogayzel, P. J.; Jozwik, C.; Pollard, H. B.; Zeitlin, P. L. Pharmacoproteomics of 4-Phenylbutyrate-Treated IB3-1 Cystic Fibrosis Bronchial Epithelial Cells. *J. Proteome Res.* **2006**, *5* (3), 562–571. https://doi.org/10.1021/pr050319o.

(292) Kang, H. L.; Benzer, S.; Min, K. T. Life Extension in Drosophila by Feeding a Drug. *Proc. Natl. Acad. Sci. U. S. A.* **2002**, *99* (2), 838–843. https://doi.org/10.1073/pnas.022631999.

(293) Rochelle, T. L.; Yeung, D. K. Y.; Bond, M. H.; Li, L. M. W. Predictors of the Gender Gap in Life Expectancy across 54 Nations. *Psychol. Heal. Med.* **2015**, *20* (2), 129–138. https://doi.org/10.1080/13548506.2014.936884.

(294) Gerontology Research Group. GRG World Supercentenarian Rankings List https://grg.org/WSRL/TableE.aspx (accessed Oct 23, 2022).

(295) Pike, C. J. Sex and the Development of Alzheimer's Disease. *J. Neurosci. Res.* **2017**, *95* (1–2), 671–680. https://doi.org/10.1002/JNR.23827.

(296) Tramunt, B.; Smati, S.; Grandgeorge, N.; Lenfant, F.; Arnal, J. F.; Montagner, A.; Gourdy, P. Sex Differences in Metabolic Regulation and Diabetes Susceptibility. *Diabetologia* **2020**, *63* (3), 453–461.

https://doi.org/10.1007/S00125-019-05040-3.

(297) Regitz-Zagrosek, V.; Kararigas, G. Mechanistic Pathways of Sex Differences in Cardiovascular Disease. *Physiol. Rev.* **2017**, *97* (1), 1–37. https://doi.org/10.1152/physrev.00021.2015.

(298) Heinzel, S.; Kasten, M.; Behnke, S.; Vollstedt, E. J.; Klein, C.; Hagenah, J.; Pausch, C.; Heilmann, R.; Brockmann, K.; Suenkel, U.; Yilmaz, R.; Liepelt-Scarfone, I.; Walter, U.; Berg, D. Age- and Sex-Related Heterogeneity in Prodromal Parkinson's Disease. *Mov. Disord.* **2018**, *33* (6), 1025–1027. https://doi.org/10.1002/MDS.27349.

(299) Hägg, S.; Jylhävä, J. Sex Differences in Biological Aging with a Focus on Human Studies. *Elife* **2021**, *10* (e63425), 1–27. https://doi.org/10.7554/ELIFE.63425.

(300) Sultanova, Z.; Andic, M.; Carazo, P. The "Unguarded-X" and the Genetic Architecture of Lifespan. *Source Evol.* **2018**, *72* (3), 540–552. https://doi.org/10.2307/48577415.

(301) Ruggierii, A.; Anticoli, S.; D'ambrosio, A.; Giordani, L.; Mora, M. The Influence of Sex and Gender on Immunity, Infection and Vaccination. *Ann. Ist. Super. Sanita* **2016**, *52* (2), 198–204. https://doi.org/10.4415/ANN_16_02_11.

(302) Borrás, C.; Sastre, J.; García-Sala, D.; Lloret, A.; Pallardó, F. V.; Viña, J. Mitochondria from Females Exhibit Higher Antioxidant Gene Expression and Lower Oxidative Damage than Males. *Free Radic. Biol. Med.* **2003**, *34* (5), 546–552. https://doi.org/10.1016/S0891-5849(02)01356-4.

(303) Han, Y.; Wennersten, S. A.; Wright, J. M.; Ludwig, R. W.; Lau, E.; Lam, M. P. Y. Proteogenomics Reveals Sex-Biased Aging Genes and Coordinated

Splicing in Cardiac Aging. *Am. J. Physiol. Hear. Circ. Physiol.* **2022**, *323* (3), H538–H558. https://doi.org/10.1152/ajpheart.00244.2022.

(304) Rubin, J. B.; Lagas, J. S.; Broestl, L.; Sponagel, J.; Rockwell, N.; Rhee, G.; Rosen, S. F.; Chen, S.; Klein, R. S.; Imoukhuede, P.; Luo, J. Sex Differences in Cancer Mechanisms. *Biol. Sex Differ.* **2020**, *11* (1). https://doi.org/10.1186/s13293-020-00291-x.

(305) Yousefzadeh, M. J.; Zhao, J.; Bukata, C.; Wade, E. A.; McGowan, S. J.; Angelini, L. A.; Bank, M. P.; Gurkar, A. U.; McGuckian, C. A.; Calubag, M. F.; Kato, J. I.; Burd, C. E.; Robbins, P. D.; Niedernhofer, L. J.; Laura Niedernhofer, C. J. Tissue Specificity of Senescent Cell Accumulation during Physiologic and Accelerated Aging of Mice. *Aging Cell* **2020**, *19* (e13094).

(306) Waskar, M.; Landis, G. N.; Shen, J.; Curtis, C.; Tozer, K.; Abdueva, D.; Skvortsov, D.; Tavaré, S.; Tower, J. Drosophila Melanogaster P53 Has Developmental Stage-specific and Sex-specific Effects on Adult Life Span Indicative of Sexual Antagonistic Pleiotropy. *Aging (Albany. NY).* **2009**, *1* (11), 903–936. https://doi.org/10.18632/AGING.100099.

(307) Groß, S.; Mmel, U.-D.; Klintschar, M.; Bartel, F. Germline Genetics of the P53 Pathway Affect Longevity in a Gender Specific Manner. *Curr. Aging Sci.* **2014**, *7* (2).

(308) Rall-Scharpf, M.; Friedl, T. W. P.; Biechonski, S.; Denkinger, M.; Milyavsky, M.; Wiesmüller, L. Sex-Specific Differences in DNA Double-Strand Break Repair of Cycling Human Lymphocytes during Aging. *Aging.* **2021**, *13* (17), 21066–21089. https://doi.org/10.18632/AGING.203519.

(309) Trzeciak, A. R.; Barnes, J.; Ejiogu, N.; Foster, K.; Brant, L. J.; Zonderman,

A. B.; Evans, M. K. Age, Sex, and Race Influence Single-Strand Break Repair Capacity in a Human Population NIH Public Access. *Radic Biol Med* **2008**, *45* (12), 1631–1641. https://doi.org/10.1016/j.freeradbiomed.2008.08.031.

(310) Galvis, D.; Walsh, D.; Harries, L. W.; Latorre, E.; Rankin, J. A Dynamical Systems Model for the Measurement of Cellular Senescence. *J. R. Soc. Interface* **2019**, *16* (159). https://doi.org/10.1098/rsif.2019.0311.

(311) Muñoz, D. P.; Yannone, S. M.; Daemen, A.; Sun, Y.; Vakar-Lopez, F.; Kawahara, M.; Freund, A. M.; Rodier, F.; Wu, J. D.; Desprez, P.-Y. Y.; Raulet, D. H.; Nelson, P. S.; van't Veer, L. J.; Campisi, J.; Coppé, J.-P. P.; Van 't Veer, L. J.; Campisi, J.; Coppé, J.-P. P. Targetable Mechanisms Driving Immunoevasion of Persistent Senescent Cells Link Chemotherapy-Resistant Cancer to Aging. *JCI Insight* **2019**, *4* (14). https://doi.org/10.1172/jci.insight.124716.

(312) Sasaki, Y.; Ikeda, Y.; Miyauchi, T.; Uchikado, Y.; Akasaki, Y.; Ohishi, M. Estrogen-Sirt1 Axis Plays a Pivotal Role in Protecting Arteries against Menopause-Induced Senescence and Atherosclerosis. *J. Atheroscler. Thromb.* **2020**, *27* (1), 47–59. https://doi.org/10.5551/jat.47993.

(313) Vernier, M.; Giguère, V. Aging, Senescence and Mitochondria: The PGC-1/ERR Axis. *J. Mol. Endocrinol.* **2021**, *66* (1), R1–R14. https://doi.org/10.1530/JME-20-0196.

(314) Diep, C. H.; Charles, N. J.; Gilks, C. B.; Kalloger, S. E.; Argenta, P. A.; Lange, C. A. Progesterone Receptors Induce FOXO1-Dependent Senescence in Ovarian Cancer Cells. *Cell Cycle* **2013**, *12* (9), 1433–1449. https://doi.org/10.4161/cc.24550.

(315) Harrison, D. E.; Strong, R.; Reifsnyder, P.; Kumar, N.; Fernandez, E.; Flurkey, K.; Javors, M. A.; Lopez-Cruzan, M.; Macchiarini, F.; Nelson, J. F.; Bitto, A.; Sindler, A. L.; Cortopassi, G.; Kavanagh, K.; Leng, L.; Bucala, R.; Rosenthal, N.; Salmon, A.; Stearns, T. M.; Bogue, M.; Miller, R. A. 17-a-Estradiol Late in Life Extends Lifespan in Aging UM-HET3 Male Mice; Nicotinamide Riboside and Three Other Drugs Do Not Affect Lifespan in Either Sex. *Aging Cell* **2021**, *00* (e13328). https://doi.org/10.1111/acel.13328.

(316) Wilkinson, H. N.; Hardman, M. J. The Role of Estrogen in Cutaneous Ageing and Repair. *Maturitas* **2017**, *103*, 60–64. https://doi.org/10.1016/J.MATURITAS.2017.06.026.

(317) Gehm, B. D.; McAndrews, J. M.; Chien, P. Y.; Jameson, J. L. Resveratrol, a Polyphenolic Compound Found in Grapes and Wine, Is an Agonist for the Estrogen Receptor. *Proc. Natl. Acad. Sci. U. S. A.* **1997**, *94* (25), 14138–14143. https://doi.org/10.1073/pnas.94.25.14138.

(318) Dai, X.; Hong, L.; Shen, H.; Du, Q.; Ye, Q.; Chen, X.; Zhang, J. Estradiol-Induced Senescence of Hypothalamic Astrocytes Contributes to Aging-Related Reproductive Function Declines in Female Mice. *Aging.* **2020**, *12* (7), 6089–6108. https://doi.org/10.18632/AGING.103008.

(319) Garratt, M.; Lagerborg, K. A.; Tsai, Y. M.; Galecki, A.; Jain, M.; Miller, R. A. Male Lifespan Extension with 17-α Estradiol Is Linked to a Sex-Specific Metabolomic Response Modulated by Gonadal Hormones in Mice. *Aging Cell* **2018**, *17* (4), e12786. https://doi.org/10.1111/ACEL.12786.

(320) Song, C. H.; Kim, N.; Nam, R. H.; Choi, S. I.; Lee, H. N.; Surh, Y. J. 17β-Estradiol Supplementation Changes Gut Microbiota Diversity in Intact and

Colorectal Cancer-Induced ICR Male Mice. *Sci. Rep.* **2020**, *10* (1), 12283. https://doi.org/10.1038/s41598-020-69112-w.

(321) Institute of Medicine (US) Committee on Understanding the Biology of Sex and Gender; Wizemann, T. M.; Pardue, M.-L. Exploring the Biological Contributions to Human Health: Does Sex Matter?: Sex Begins in the Womb; National Academies Press (US): Washington (DC), 2001.

(322) Oettel, M.; Mukhopadhyay, A. K. Progesterone: The Forgotten Hormone in Men? *Aging Male* **2004**, *7* (3), 236–257. https://doi.org/10.1080/13685530400004199.

(323) Hiller-Sturmhöfel, S.; Bartke, A. The Endocrine System: An Overview. *Alcohol Heal. Res World* **1998**, *22* (3), 153–164.

(324) Coelingh Bennink, H. J. T. Are All Estrogens the Same? *Maturitas* **2004**, *47* (4), 269–275. https://doi.org/10.1016/j.maturitas.2003.11.009.

(325) Bjorkman, S.; Taylor, H. S. Diethylstilbestrol (DES). *Encycl. Reprod.* **2018**, 760–766. https://doi.org/10.1016/B978-0-12-801238-3.64417-3.

(326) Manson, J. A. E.; Chlebowski, R. T.; Stefanick, M. L.; Aragaki, A. K.; Rossouw, J. E.; Prentice, R. L.; Anderson, G.; Howard, B. V.; Thomson, C. A.; LaCroix, A. Z.; Wactawski-Wende, J.; Jackson, R. D.; Limacher, M.; Margolis, K. L.; Wassertheil-Smoller, S.; Beresford, S. A.; Cauley, J. A.; Eaton, C. B.; Gass, M.; Hsia, J.; Johnson, K. C.; Kooperberg, C.; Kuller, L. H.; Lewis, C. E.; Liu, S.; Martin, L. W.; Ockene, J. K.; O'Sullivan, M. J.; Powell, L. H.; Simon, M. S.; Van Horn, L.; Vitolins, M. Z.; Wallace, R. B. Menopausal Hormone Therapy and Health Outcomes during the Intervention and Extended Poststopping Phases of the Women's Health Initiative Randomized Trials. *JAMA* **2013**, *310* (13), 1353–1368.

https://doi.org/10.1001/jama.2013.278040.

(327) Fuentes, N.; Silveyra, P. Estrogen Receptor Signaling Mechanisms. *Adv. Protein Chem. Struct. Biol.* **2019**, *116*, 135. https://doi.org/10.1016/BS.APCSB.2019.01.001.

(328) Ranganathan, P.; Nadig, N.; Nambiar, S. Non-Canonical Estrogen Signaling in Endocrine Resistance. *Front. Endocrinol.* **2019**, *10*, 708. https://doi.org/10.3389/FENDO.2019.00708/BIBTEX.

(329) Thomas, P. Membrane Progesterone Receptors (MPRs, PAQRs): Review of Structural and Signaling Characteristics. *Cells* **2022**, *11* (11). https://doi.org/10.3390/CELLS11111785.

(330) Gallardo, M.; Hornbaker, M. J.; Zhang, X.; Hu, P.; Bueso-Ramos, C.; Post, S. M. Aberrant HnRNP K Expression: All Roads Lead to Cancer. *Cell Cycle*. 2016, pp 1552–1557. https://doi.org/10.1080/15384101.2016.1164372.

(331) Euteneuer, A. M.; Seeger-Nukpezah, T.; Nolte, H.; Henjakovic, M. Estrogen Receptor α (ERα) Indirectly Induces Transcription of Human Renal Organic Anion Transporter 1 (OAT1). *Physiol. Rep.* **2019**, *7* (21), e14229. https://doi.org/10.14814/PHY2.14229.

(332) Shults, C. L.; Dingwall, C. B.; Kim, C. K.; Pinceti, E.; Rao, Y. S.; Pak, T. R. 17β-Estradiol Regulates the RNA-Binding Protein Nova1, Which Then Regulates the Alternative Splicing of Estrogen Receptor β in the Aging Female Rat Brain. *Neurobiol. Aging* **2018**, *61*, 13–22. https://doi.org/10.1016/j.neurobiolaging.2017.09.005.

(333) Elks, C. E.; Perry, J. R. B.; Sulem, P.; Chasman, D. I.; Franceschini, N.; He, C.; Lunetta, K. L.; Visser, J. A.; Byrne, E. M.; Cousminer, D. L.; Gudbjartsson, D. F.; Esko, T.; Feenstra, B.; Hottenga, J. J.; Koller, D. L.;

Kutalik, Z.; Lin, P.; Mangino, M.; Marongiu, M.; McArdle, P. F.; Smith, A. V.; Stolk, L.; Van Wingerden, S. H.; Zhao, J. H.; Albrecht, E.; Corre, T.; Ingelsson, E.; Hayward, C.; Magnusson, P. K. E.; Smith, E. N.; Ulivi, S.; Warrington, N. M.; Zgaga, L.; Alavere, H.; Amin, N.; Aspelund, T.; Bandinelli, S.; Barroso, I.; Berenson, G. S.; Bergmann, S.; Blackburn, H.; Boerwinkle, E.; Buring, J. E.; Busonero, F.; Campbell, H.; Chanock, S. J.; Chen, W.; Cornelis, M. C.; Couper, D.; Coviello, A. D.; D'Adamo, P.; De Faire, U.; De Geus, E. J. C.; Deloukas, P.; Döring, A.; Smith, G. D.; Easton, D. F.; Eiriksdottir, G.; Emilsson, V.; Eriksson, J.; Ferrucci, L.; Folsom, A. R.; Foroud, T.; Garcia, M.; Gasparini, P.; Geller, F.; Gieger, C.; Gudnason, V.; Hall, P.; Hankinson, S. E.; Ferreli, L.; Heath, A. C.; Hernandez, D. G.; Hofman, A.; Hu, F. B.; Illig, T.; Järvelin, M. R.; Johnson, A. D.; Karasik, D.; Khaw, K. T.; Kiel, D. P.; Kilpeläinen, T. O.; Kolcic, I.; Kraft, P.; Launer, L. J.; Laven, J. S. E.; Li, S.; Liu, J.; Levy, D.; Martin, N. G.; McArdle, W. L.; Melbye, M.; Mooser, V.; Murray, J. C.; Murray, S. S.; Nalls, M. A.; Navarro, P.; Nelis, M.; Ness, A. R.; Northstone, K.; Oostra, B. A.; Peacock, M.; Palmer, L. J.; Palotie, A.; Paré, G.; Parker, A. N.; Pedersen, N. L.; Peltonen, L.; Pennell, C. E.; Pharoah, P.; Polasek, O.; Plump, A. S.; Pouta, A.; Porcu, E.; Rafnar, T.; Rice, J. P.; Ring, S. M.; Rivadeneira, F.; Rudan, I.; Sala, C.; Salomaa, V.; Sanna, S.; Schlessinger, D.; Schork, N. J.; Scuteri, A.; Segrè, A. V.; Shuldiner, A. R.; Soranzo, N.; Sovio, U.; Srinivasan, S. R.; Strachan, D. P.; Tammesoo, M. L.; Tikkanen, E.; Toniolo, D.; Tsui, K.; Tryggvadottir, L.; Tyrer, J.; Uda, M.; Van Dam, R. M.; Van Meurs, J. B. J.; Vollenweider, P.; Waeber, G.; Wareham, N. J.; Waterworth, D. M.; Weedon, M. N.; Wichmann, H. E.; Willemsen, G.; Wilson, J. F.; Wright, A. F.; Young, L.;

Zhai, G.; Zhuang, W. V.; Bierut, L. J.; Boomsma, D. I.; Boyd, H. A.; Crisponi, L.; Demerath, E. W.; Van Duijn, C. M.; Econs, M. J.; Harris, T. B.; Hunter, D. J.; Loos, R. J. F.; Metspalu, A.; Montgomery, G. W.; Ridker, P. M.; Spector, T. D.; Streeten, E. A.; Stefansson, K.; Thorsteinsdottir, U.; Uitterlinden, A. G.; Widen, E.; Murabito, J. M.; Ong, K. K.; Murray, A. Thirty New Loci for Age at Menarche Identified by a Meta-Analysis of Genome-Wide Association Studies. *Nat. Genet.* **2010**, *42* (12), 1077–1085. https://doi.org/10.1038/ng.714.

(334) Liang, J.; Shang, Y. Estrogen and Cancer. *Annu. Rev. Physiol.* **2013**, *75*, 225–240. https://doi.org/10.1146/annurev-physiol-030212-183708.

(335) Regulski, M. J. Cellular Senescence: What, Why, and How. *Wounds* **2017**, *29* (6), 168–174.

(336) Maciel-Barón, L. A.; Morales-Rosales, S. L.; Aquino-Cruz, A. A.; Triana-Martínez, F.; Galván-Arzate, S.; Luna-López, A.; González-Puertos, V. Y.; López-Díazguerrero, N. E.; Torres, C.; Königsberg, M. Senescence Associated Secretory Phenotype Profile from Primary Lung Mice Fibroblasts Depends on the Senescence Induction Stimuli. *Age.* **2016**, *38* (1), 1–14. https://doi.org/10.1007/s11357-016-9886-1.

(337) Heckenbach, I.; Mkrtchyan, G. V.; Ezra, M. Ben; Bakula, D.; Madsen, J. S.; Nielsen, M. H.; Oró, D.; Osborne, B.; Covarrubias, A. J.; Idda, M. L.; Gorospe, M.; Mortensen, L.; Verdin, E.; Westendorp, R.; Scheibye-Knudsen, M. Nuclear Morphology Is a Deep Learning Biomarker of Cellular Senescence. *Nat. Aging* **2022**, *2* (8), 742–755. https://doi.org/10.1038/s43587-022-00263-3.

(338) Kuo, L. J.; Yang, L.-X. Phosphorylation of H2AX and Its Related Molecules.

in vivo. **2008**, *22* (3), 305–310.

(339) Collins, A. R. The Comet Assay for DNA Damage and Repair: Principles, Applications, and Limitations. *Mol. Biotechnol.* **2004**, *26* (3), 249–261. https://doi.org/10.1385/MB:26:3:249.

(340) Calimport, S. R. G.; Bentley, B. L.; Stewart, C. E.; Pawelec, G.; Scuteri, A.; Vinciguerra, M.; Slack, C.; Chen, D.; Harries, L. W.; Marchant, G.; Alexander Fleming, G.; Conboy, M.; Antebi, A.; Small, G. W.; Gil, J.; Lakatta, E. G.; Richardson, A.; Rosen, C.; Nikolich, K.; Wyss-Coray, T.; Steinman, L.; Montine, T.; de Magalhães, J. P.; Campisi, J.; Church, G. To Help Aging Populations, Classify Organismal Senescence: Comprehensive Disease Classification and Staging Is Required to Address Unmet Needs of Aging Populations. *Science* **2019**, *366* (6465), 576. https://doi.org/10.1126/SCIENCE.AAY7319.

(341) Gehm, B. D.; McAndrews, J. M.; Chien, P. Y.; Jameson, J. L. Resveratrol, a Polyphenolic Compound Found in Grapes and Wine, Is an Agonist for the Estrogen Receptor. *Proc. Natl. Acad. Sci. U. S. A.* **1997**, *94* (25), 14138–14143. https://doi.org/10.1073/pnas.94.25.14138.

(342) Acar, M. B.; Ayaz-Güner, Ş.; Gunaydin, Z.; Karakukcu, M.; Peluso, G.; Di Bernardo, G.; Özcan, S.; Galderisi, U. Proteomic and Biological Analysis of the Effects of Metformin Senomorphics on the Mesenchymal Stromal Cells. *Front. Bioeng. Biotechnol.* **2021**, *9* (October), 1–10. https://doi.org/10.3389/fbioe.2021.730813.

(343) Hirsch, H. A.; Iliopoulos, D.; Struhl, K. Metformin Inhibits the Inflammatory Response Associated with Cellular Transformation and Cancer Stem Cell Growth. *Proc. Natl. Acad. Sci. U. S. A.* **2013**, *110* (3), 972–977.

https://doi.org/10.1073/pnas.1221055110.

Appendices

Appendix 1: Portfolio of papers

Here, I give a list of my co-authored published journal articles from the last five years, with a copy attached of the published article “Targeting Alternative Splicing for Reversal of Cellular Senescence in the Context of Aesthetic Aging” as it has been referenced in this thesis.

K. A. Ayyappa, I. Shatwan, D. Bodhini, **L. R. Bramwell**, K. Ramya, V. Sudha, R. M. Anjana, J. A. Lovegrove, V. Mohan, V. Radha, and K. S. Vimaleswaran. **2017**. “High Fat Diet Modifies the Association of Lipoprotein Lipase Gene Polymorphism with High Density Lipoprotein Cholesterol in an Asian Indian Population.” *Nutrition & Metabolism* 14 (1): 8. https://doi.org/10.1186/s12986-016-0155-1.

L. J. McCulloch, **L. R. Bramwell**, B. Knight, and K. Kos. **2020**. “Circulating and Tissue Specific Transcription of Angiopoietin-like Protein 4 in Human Type 2 Diabetes.” *Metabolism: Clinical and Experimental* 106: 154192. https://doi.org/10.1016/j.metabol.2020.154192.

L. R. Bramwell, and L. W. Harries. **2021**. “Targeting Alternative Splicing for Reversal of Cellular Senescence in the Context of Aesthetic Aging.” Plastic & Reconstructive Surgery 147 (1S-2): 25S-32S. https://doi.org/10.1097/PRS.0000000000007618.

M. Davies, **L. R. Bramwell**, N. Jeffery, B. Bunce, B. P. Lee, B. Knight, C. Auckland, J. A. H. Masoli, and L. W. Harries. **2022**. “Persistence of

Clinically Relevant Levels of SARS-CoV2 Envelope Gene Subgenomic RNAs in Non-Immunocompromised Individuals.” *International Journal of Infectious Diseases* 116: 418–25. https://doi.org/10.1016/j.ijid.2021.12.312.

Targeting Alternative Splicing for Reversal of Cellular Senescence in the Context of Aesthetic Aging

Laura R. Bramwell, MRes
Lorna W. Harries, PhD
Exeter, United Kingdom

Summary: Cellular senescence is a state of stable cell cycle arrest that has increasingly been linked with cellular, tissue, and organismal aging; targeted removal of senescent cells brings healthspan and lifespan benefits in animal models. Newly emerging approaches to specifically ablate or rejuvenate senescent cells are now the subject of intense study to explore their utility to provide novel treatments for the aesthetic signs and diseases of aging in humans. Here, we discuss different strategies that are being trialed in vitro, and more recently in vivo, for the targeted removal or reversal of senescent cells. Finally, we describe the evidence for a newly emerging molecular mechanism that may underpin senescence; dysregulation of alternative splicing. We will explore the potential of restoring splicing regulation as a novel "senotherapeutic" approach and discuss strategies by which this could be integrated into the established portfolio of skin aging therapeutics. (*Plast. Reconstr. Surg.* 147: 25S, 2021.)

Aging is the primary risk factor for many of the common, chronic diseases of man, including changes to the skin; the largest organ of the body. The skin provides primary protection against external injuries and maintenance of general homeostasis, and is the first defence against environmental exposure to non-ingested chemicals and sun damage. Contrary to most other organs, its exposed position renders the effects of aging on the skin, particularly visible, although analogous changes do also occur in less visible organs. Aging brings profound changes to characteristics and quality of the skin and its substructure. Aged skin demonstrates changes in thickness, pigmentation, and elasticity, with loss of subdermal adipose deposits and increases in fragility and visibility of vascular architecture as well as compromised healing capacity. Age-related disease and the aesthetic signs of aging share many common underpinning cellular and molecular processes.[1] The cells that make up the layers and substructure of the skin are excellent models for the wider effects of aging on other organs and systems, and disease processes such as fibrosis, inflammation, and changes to the composition of the extracellular matrix are common to both age-related disease and aesthetic aging changes.

THE AGING EXTRACELLULAR MATRIX

The extracellular matrix (ECM) is a 3-dimensional noncellular macromolecular network comprising collagens, elastins, glycoproteins, glycosaminoglycans, proteoglycans, fibronectin, and laminins, as well as many other components. ECM macromolecules interact not only with each other but also with receptors present on the surface of cells to form a complex architecture within which cells may grow, communicate, and receive biochemical and metabolic support.[2,3] The ECM is primarily manufactured by fibroblast cells. Fibroblasts can be found in all major organ systems and secrete the macromolecules required for ECM formation in addition to their important role in the induction of inflammation in response to tissue injury.[4,5] Age-related ECM changes are

From the RNA-Mediated Mechanisms of Disease group, College of Medicine and Health, Institute of Biomedical and Clinical Science, University of Exeter.
Received for publication June 22, 2020; accepted August 27, 2020.

DOI: 10.1097/PRS.0000000000007618

Disclosure: *Dr. Harries is an inventor on patent PCT/GB2019/052125 and is a founder, chief science officer, and research and development lead for SENISCA, Ltd. Ms. Bramwell has no financial interest to declare in relation to the content of this article.*

characterized by changes in elastin and collagen fibers,[6,7] as well as alterations to the glycosaminoglycans and proteoglycans that associate with them (decorin, biglycan, versican, etc.).[8,9] Many of the age-related changes in skin composition and structure arise from age-related dysfunction of fibroblasts.[10] This dysfunction can take several forms, but ultimately is driven by the progressive failure of a number of basic health maintenance mechanisms collectively titled the "hallmarks of aging,"[11] which occur not only in skin but in all organ systems.

THE HALLMARKS OF AGING

The hallmarks of aging comprise a number of basic cellular and molecular mechanisms involved in the maintenance of cell and tissue homeostasis that demonstrate changes in activity or efficiency with age. These include genomic or proteomic changes such as genetic instability (the accumulation of mutations and other aspects of DNA damage), telomere attrition (the gradual erosion of telomeres), altered proteostasis (changes in protein production, trafficking or turnover), and epigenetic alterations (chemical modifications to DNA and RNA sequences). Dysregulated nutrient signaling (changes in the activity of signaling pathways such as mTOR) and dysfunctional cellular communication (deranged inflammatory profiles) also occur. Cellular changes such as stem cell exhaustion (depletion of the stem cell pool), mitochondrial dysfunction (morphological changes to mitochondrial and leakage of reactive oxygen species) and cellular senescence (the accumulation of "aged" cells) are also common.[11] The hallmarks are rarely seen in isolation, and have considerable interplay and overlap. Together, the hallmarks of aging are thought to drive much of the damage associated with aging of cells, tissues, organs, and organisms.

CELLULAR SENESCENCE

Cellular senescence is one of the hallmarks of aging that is currently the subject of intense study. Cellular senescence is defined by several characteristics which include cell cycle arrest, morphological changes (flattened and enlarged shape, heterochromatic foci), as well as altered cellular physiology [senescence-associated β-galactosidase positivity, G1 arrest and the secretion of the senescence-associated secretory phenotype (SASP)]. The SASP is a cocktail of proinflammatory and remodeling proteins,[12] which is thought to be a major contributor to the chronic sterile inflammation of aging ("inflammaging").[13] SASP has a paracrine action on nearby nonsenescent cells, driving them also into senescence or quiescence. Senescence arises in response to multiple insults including cellular stress, telomere attrition, mitochondrial dysfunction, DNA damage, and oncogene activation.[14] Senescence is an excellent example of antagonistic pleiotropy; in youth, the emergence of senescence guards cells against transformation[15] has importance in embryonic development[16] and aids in wound healing[17] but is deleterious in later life due to compromised senescent cell clearance from an aging immune system. There is no single biomarker for senescent cells, but they can be identified by changes in culture population doubling times or morphology, or by the use of biochemical or immunocytochemical markers such as senescence-associated beta galactosidase activity (elevated lysozyme activity), BrdU/Ki67 (loss of proliferation) and γ-H2AX protein (DNA damage). Additionally, changes in the expression and activity of DNA damage checkpoint genes (p16, p21) or SASP proteins (IL-6, IL-1β, IL-2, IL8) can be measured by quantitative PCR or ELISA (Fig. 1).

CELLULAR SENESCENCE AS A DRIVER OF AGING

Fibroblast and keratinocyte senescence, in particular, is thought to underpin many aspects of skin aging.[18] The most compelling evidence for senescent cells as systemic drivers of aging can be found in work where methods were found to bring about targeted ablation of senescent cells in a controlled manner in a mouse model system. Senescent cells express high levels of the cell cycle inhibitor $p16^{ink4a}$, which is encoded by the *CDKN2A* gene. Systems have been developed which allow selective ablation of cells expressing p16, under the control of a doxycycline induced switch in transgenic animals. The presence of p16 positive senescent cells has been demonstrated to shorten healthy lifespan,[19] and accordingly, the targeted removal of such cells has been demonstrated to prevent or ameliorate several features of aging.[20] Furthermore, removal of senescent cells brought about profound improvements to multiple aging phenotypes including renal, cardiac, and motor functions in these animals.[19–21] Therapies for the removal or reversal of senescent cells ("senotherapeutics") may therefore represent a relatively tractable target for the treatment or prevention of the aesthetic signs of aging, as well as providing a

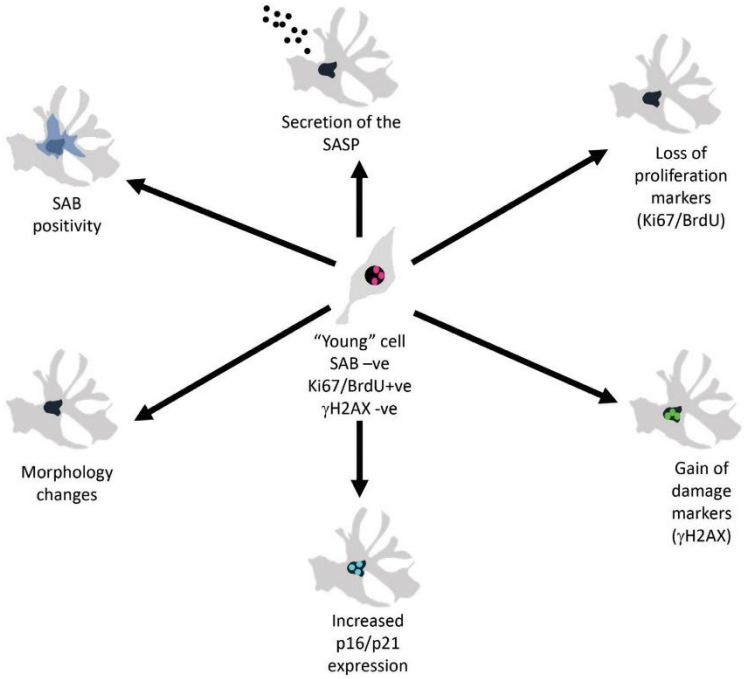

Fig. 1. Biomarkers to identify senescent cells. Senescent cells undergo a number of functional, morphological, and biochemical changes. These include the development of senescence-associated beta galactosidase positivity (senescence), secretion of the SASP, loss of proliferation markers such as Ki67 or BrdU, gain of markers of DNA damage such as γH2AX, gain of p16 and p21 positivity (cell cycle arrest) and characteristic morphology changes ("fried egg" morphology, gain of heterochromatic foci).

new approach to target the causes, not merely the effects of age-related disease.

EMERGING SENOTHERAPEUTIC STRATEGIES

There are 2 differing approaches to targeting senescent cells for therapeutic benefit. These are senolytic (cell killing) and senomorphic (cell rejuvenating) strategies. Senolysis involves the specific removal of senescent cells by induction of apoptosis. Senolytic small molecules (the tyrosine kinase inhibitor dasatinib, the plant polyphenol quercetin, as well as proprietary molecules ABT-263, ABT-737, A1331852, FOXO4-DR1 peptides) have been developed and tested in animal models, with suggested improvements to cardiac, vasomotor, bone, lung, hepatic, and hematopoietic function, as well as having positive effects on frailty, renal function, and hair growth.[22–29] Human trials are in their infancy, but initial small-scale phase 1 open-label trials of a combination of the dasatinib and quercetin in 14 human subjects with idiopathic pulmonary fibrosis, a disease characterized by lung fibrosis and accelerated cellular senescence,[30] and 9 subjects with chronic kidney disease[31] have been undertaken. In both these studies, removal of senescent cells was able to confer a small advantage in terms of improved physical functioning. These small studies require validation in larger trials, but are nevertheless encouraging. However, newly emerging data suggests that the complete ablation of senescent cells may not confer long term advantages, because some subsets of senescent cells are essential, with their removal resulting in fibrosis of the liver and perivascular system.[32] Others have suggested that removal of senescent cells may confer additional stresses onto remaining cells, driving them also into senescence and contribute to

accelerated tissue pathology and perhaps exacerbated disease.[33]

AN ALTERNATIVE TO SENOLYTICS

The alternative to senolytic technologies are senomorphic approaches. These are characterized not by the removal of senescent cells, but by the ablation of adverse effects such as secretion of the SASP. These approaches allow retention of cells in their original position within the tissues, which may be an advantage in some tissues, such as articular cartilage, that are relatively acellular. Approaches to achieve senomorphic outcomes include caloric restriction mimetics such as rapamycin and other mTOR inhibitors,[34] sirtuin activators,[35] antioxidants,[36] anti-inflammatory agents,[37] autophagy activators,[38] and proteasome activators.[39] Other approaches include the ectopic expression of telomerase, an enzyme that rebuilds telomeres, and ameliorates senescence-associated telomere attrition.[40] Restoration of telomeres has been shown to rescue chromosomal instability[41] and actively reverse tissue degeneration in mice.[42] However, concerns remain about the potential of telomerase therapy to result in increased cancer formation, because telomerase is frequently dysregulated in cancer cells.[43] Thus, the use of telomerase inactivation as a target for cancer therapeutics is more developed that strategies to activate it as an antiaging therapeutic.

ALTERNATIVE SPLICING: A NEW SENOTHERAPEUTIC TARGET?

Dysregulation of alternative splicing is emerging as a new hallmark of aging that can be targeted for senomorphic, rather than the senolytic effect. Alternative splicing is the process by which a single gene can produce a variety of mRNA isoforms in a regulated fashion. This process is responsible for genomic diversity, plasticity, and adaptability, comprises a key cellular response to stress,[44–46] and is known to be a major contributor to the development of senescence.[47] A primary RNA transcript (premessenger RNA) is expressed following successful transcription containing all of the noncoding sequences of the gene as well as the coding regions. It requires the modification of the 5′ end of the transcript by capping (the addition of a modified nucleotide that interacts with the translation machinery), the removal of the noncoding introns by splicing, and polyadenylation at the 3′ end (the addition of the poly-A tail which is important for posttranscriptional control of stability) (Fig. 2). Gene sequences are modular, consisting of coding sequences (exons) separated by noncoding sequences (introns). Exons can be retained or removed from the expressed transcripts according to the needs of the cell, yielding mRNA isoforms coding for subtly different proteins, which may have altered expression profiles or differential activity.[48] Splicing processes are coordinated by the spliceosome and occurs in the nuclear speckles.[49] The "cutting and pasting" activity is carried out by components of the spliceosome which bind to specific sequences around the splice sites to bring about splicing.[50] This is referred to as "constitutive" splicing, and these signals are necessary for splicing, but sometimes not sufficient. Regulated splicing, such as spatial, temporal, or developmental responses, and importantly the responses to external stimuli, often requires the binding of a battery of auxiliary proteins (termed splicing factors) to exon and intron enhancer or silencer binding sites. Splicing enhancers and silencers can sometimes be quite distant from the splice sites to bring about "alternative" splicing[51]; >95% of the human genome is capable of this.[52] There are thought to be over 100 different splicing factors, the most common classes of which are the serine/arginine-rich class of proteins which are usually, but not exclusively, splicing activators, and the heterogeneous nuclear ribonucleoprotein particles (hnRNPs) which are usually, but not exclusively, splicing inhibitors.[53,54] It is the combinational binding of activators and inhibitor proteins that regulates alternative splicing, so the balance of these is critical.[55]

There are multiple lines of evidence that suggest that splicing factors may have utility in a senotherapeutic arena. Transcripts encoding splicing regulators are enriched in age-associated pathways in human peripheral blood in multiple populations[56] and demonstrate predictive associations with aging outcomes in human populations.[57] Transcripts encoding splicing factors also demonstrate major dysregulation in senescent primary human cells of multiple lineages, including dermal and lung fibroblasts, cardiomyocytes, endothelial cells, and astrocytes.[58–60] Splicing factor expression is also associated with median strain lifespan and dietary restriction in animal models,[61,62] but is maintained in animals such as naked mole-rats, which demonstrate resistance to senescence.[63] Perhaps, most compellingly, the restoration of splicing factor levels to those comparable with younger cells through the use of small molecules capable of inducing splicing factor expression (polyphenols, hydrogen sulphide donors,

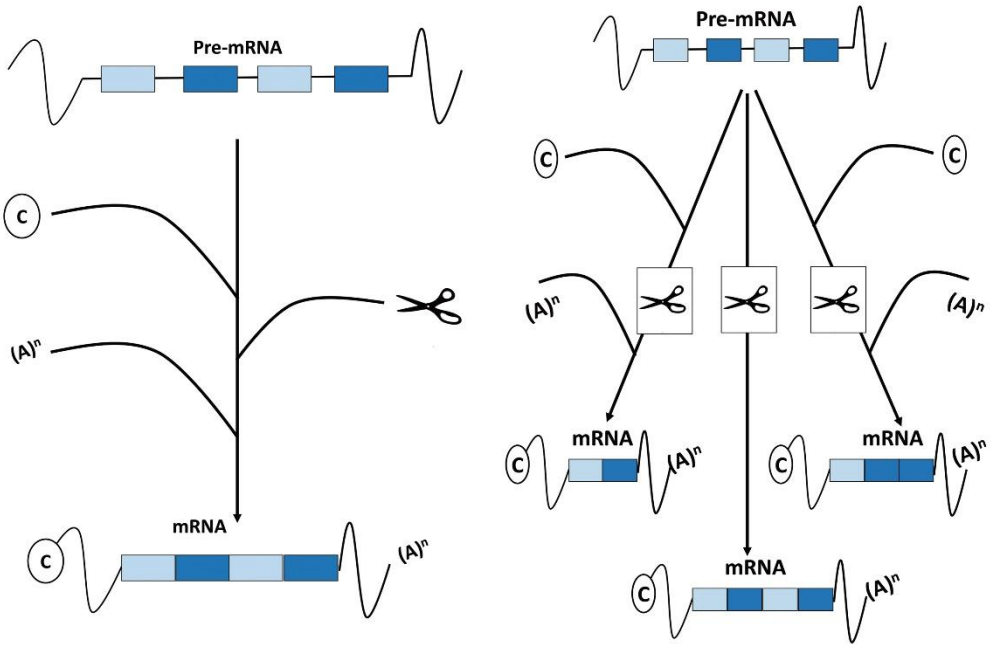

Fig. 2. Illustration of constitutive and alternative splicing. (*Left*) Constitutive splicing. Before it can be translated, a pre-mRNA must undergo capping (indicated with by the circle-enclosed "C"), spliced (indicated by the scissor graphic), and polyadenylated (indicated by $(A)^n$). The result of this is a spliced and processed mRNA. Introns and untranslated regions are indicated by black lines, exons by light or dark blue boxes. (*Right*) Alternative splicing. This is the production of multiple mRNA isoforms from a single gene. Alternatively-expressed isoforms are independently processed as indicated (the addition of the 5′ cap, given here by a circle-enclosed "C," splicing, indicated by the scissors and polyadenylation, shown by $(A)^n$), but undergo differential removal of exons (*blue boxes*) to produce distinct mRNA species, which may be temporally or spatially regulated.

ERK or AKT inhibitors) is able to bring about a senomorphic effect. This leads to the amelioration of multiple aspects of the senescent cell phenotype in both senescent primary human dermal fibroblasts and endothelial cells.[64–66] Furthermore, targeted ablation of the genes encoding *SRSF2* or *HNRNPD* splicing factors was able to induce senescence in early passage human endothelial cells.[66] These data suggest that some of the important cell types responsible for ECM dysfunction during aging are amenable to rejuvenation by restoration of splicing regulation, and that this may represent a fruitful avenue of exploration. The restoration of a more youthful pattern of alternative splicing patterns by targeted intervention could lead to reversal of cellular senescence phenotypes, remodeling of the ECM, restoration of collagen and elastin frameworks, and reversal of adipose tissue atrophy. The technology could also be applicable to ex vivo applications, whereby the senescent cells could be removed or rejuvenated in harvested preadipocytes before transplantation. These approaches could effectively rejuvenate the skin from within, reversing some of the visual signs of aging such as wrinkles, skin thinning, and pigmentation changes as well as rejuvenation of subdermal fat depots.

MANIPULATION OF SPLICING REGULATION AS A NEW THERAPY FOR AESTHETIC AGING

The restoration of alternative splicing patterns in aging ECM has the potential to allow rejuvenation of human skin by restoring younger physiology. If efficacious, it would effectively allow us to rejuvenate the skin from inside, restoring the ECM and reversing the age-related atrophy of subdermal fat depots that lead to unwanted changes in skin quality or function. There are 2

potential points of intervention. First, once the alternative splicing patterns that drive senescence in dermal fibroblasts and keratinocytes is fully elucidated, and those responsible for the emergence of senescence identified, it may be possible to modulate the expression of specific isoforms using splice switching oligonucleotides for therapeutic benefit. Splice switching oligonucleotides are small, synthetic, and modified nucleic acid fragments, that bind to the genomic regions controlling specific splice sites through Watson–Crick base pairing, and promote or suppress splice site choice by steric hindrance of access by splicing factors.[67] This is a new technology, but has been developed and licensed for a number of genetic diseases including spinal muscular atrophy[68] and Duchenne muscular dystrophy.[69] Their use for aesthetic aging purposes is some way off, because identification and functional validation of the specific isoform changes driving senescence is not trivial. It may thus be easier to target the splicing regulators themselves responsible for these changes. Splicing factors are regulated at the protein level by the action of the SRPK1, SRPK2, and CLK1 kinases,[70,71] and at the level of transcription by the activity of the ERK and AKT cell signaling pathways, through the action of the ETV6 and FOXO1 transcriptional regulators.[65] Small molecule or mRNA therapeutics targeting the "master controls" of splicing regulators may allow the moderation of modules of senescence-associated isoforms simultaneously, and bring about useful new tools with which we can target the aesthetic signs of aging.

CONCLUSIONS

Targeting the emergence of senescent cells in the dermis, and subdermal layers will bring about a new era in how we think about approaching not just the aesthetic signs of aging, but also a wider insight into aging physiology or organ systems. Skin is itself a useful first target; it is accessible, amenable to topical or injectable delivery of new treatments, and will allow the development of new small molecule or mRNA therapeutic approaches for the removal or rejuvenation of senescent cells. At present, these exciting new developments are unproven, and some work remains to translate their effects to the clinic. Realistically, we may be looking at several years before the safety profile for these new interventions are available, and appropriate formulations for topical, microneedle or injectable delivery established. In the meantime, it may be possible to influence the prevalence of senescent cells in aging skin by dietary modification; some naturally occurring small molecules such as polyphenols are also known to have activity in the regulation of splicing factors.[64] Other naturally occurring compounds such as quercetin or fisetin have also been demonstrated to have senolytic effects.[30,72] Naturally occurring compounds may, however, require substantial dosing to replicate the effect we see, because many of the promising compounds may have limited oral bioavailability. There may of course be some inherent risks associated with rejuvenation; cells of course remain aged, if not senescent, and retain their mutation load. This could be counteracted by tailoring interventions to produce senescence reversal, but not necessarily resumption of cell cycle, which we have found to be possible in the laboratory.[65,66]

In the future, these new approaches may become part of the battery of treatments available to aestheticians for the reversal of signs of aging. The inclusion of senotherapeutics such as moderators of alternative splicing into injectable fillers or topical creams may allow genuine rejuvenation, rather than just addressing the effects of aging on the skin and its substructure. We are now entering a new era of approaches to address not just the effects of aging, but also its systemic root causes. In addition to their role in skin aging, they also occur in most other tissues including those associated with common, chronic diseases. There is considerable work to do; the majority of these nascent observations currently remain preclinical. The time is ripe, however, for these new approaches to undergo more focused clinical evaluation to determine their utility as a new generation of interventions not just for skin aging, but also for other diseases of aging.

Lorna W. Harries, PhD
Institute of Biomedical and Clinical Sciences
University of Exeter College of Medicine and Health
RILD Building
Royal Devon and Exeter Hospital
Barrack Road
Exeter, Devon EX2 5DW, United Kingdom
L.W.Harries@exeter.ac.uk
Twitter: @miRNAgirl, @LauraBramwell1, @TeamRNA

ACKNOWLEDGMENT

The authors gratefully acknowledge funding from Animal Free Research UK.

REFERENCES

1. Kenessary A, Zhumadilov Z, Nurgozhin T, et al. Biomarkers, interventions and healthy ageing. *N Biotechnol.* 2013;30:373–377.

2. Haydont V, Bernard BA, Fortunel NO. Age-related evolutions of the dermis: Clinical signs, fibroblast and extracellular matrix dynamics. *Mech Ageing Dev.* 2019;177:150–156.
3. Theocharis AD, Skandalis SS, Gialeli C, et al. Extracellular matrix structure. *Adv Drug Deliv Rev.* 2016;97:4–27.
4. Smith RS, Smith TJ, Blieden TM, et al. Fibroblasts as sentinel cells. Synthesis of chemokines and regulation of inflammation. *Am J Pathol.* 1997;151:317–322.
5. Bonnans C, Chou J, Werb Z. Remodelling the extracellular matrix in development and disease. *Nat Rev Mol Cell Biol.* 2014;15:786–801.
6. Lovell CR, Smolenski KA, Duance VC, et al. Type I and III collagen content and fibre distribution in normal human skin during ageing. *Br J Dermatol.* 1987;117:419–428.
7. Montagna W, Carlisle K. Structural changes in aging human skin. *J Invest Dermatol.* 1979;73:47–53.
8. Carrino DA, Calabro A, Darr AB, et al. Age-related differences in human skin proteoglycans. *Glycobiology.* 2011;21:257–268.
9. Lee DH, Oh JH, Chung JH. Glycosaminoglycan and proteoglycan in skin aging. *J Dermatol Sci.* 2016;83:174–181.
10. Cole MA, Quan T, Voorhees JJ, et al. Extracellular matrix regulation of fibroblast function: redefining our perspective on skin aging. *J Cell Commun Signal.* 2018;12:35–43.
11. López-Otín C, Blasco MA, Partridge L, et al. The hallmarks of aging. *Cell.* 2013;153:1194–1217.
12. Campisi J, Robert L. Cell senescence: role in aging and age-related diseases. *Interdiscip Top Gerontol.* 2014;39:45–61.
13. McHugh D, Gil J. Senescence and aging: causes, consequences, and therapeutic avenues. *J Cell Biol.* 2018;217:65–77.
14. Childs BG, Durik M, Baker DJ, et al. Cellular senescence in aging and age-related disease: from mechanisms to therapy. *Nat Med.* 2015;21:1424–1435.
15. Pérez-Mancera PA, Young AR, Narita M. Inside and out: the activities of senescence in cancer. *Nat Rev Cancer.* 2014;14:547–558.
16. Muñoz-Espín D, Cañamero M, Maraver A, et al. Programmed cell senescence during mammalian embryonic development. *Cell.* 2013;155:1104–1118.
17. Demaria M, Ohtani N, Youssef SA, et al. An essential role for senescent cells in optimal wound healing through secretion of PDGF-AA. *Dev Cell.* 2014;31:722–733.
18. Gruber F, Kremslehner C, Eckhart L, et al. Cell aging and cellular senescence in skin aging - Recent advances in fibroblast and keratinocyte biology. *Exp Gerontol.* 2020;130:110780.
19. Baker DJ, Childs BG, Durik M, et al. Naturally occurring p16(Ink4a)-positive cells shorten healthy lifespan. *Nature.* 2016;530:184–189.
20. Baker DJ, Wijshake T, Tchkonia T, et al. Clearance of p16Ink4a-positive senescent cells delays ageing-associated disorders. *Nature.* 2011;479:232–236.
21. Baar MP, Brandt RMC, Putavet DA, et al. Targeted apoptosis of senescent cells restores tissue homeostasis in response to chemotoxicity and aging. *Cell.* 2017;169:132–147.e16.
22. Farr JN, Xu M, Weivoda MM, et al. Targeting cellular senescence prevents age-related bone loss in mice. *Nat Med.* 2017;23:1072–1079.
23. Xu M, Pirtskhalava T, Farr JN, et al. Senolytics improve physical function and increase lifespan in old age. *Nat Med.* 2018;24:1246–1256.
24. Zhu Y, Tchkonia T, Pirtskhalava T, et al. The Achilles' heel of senescent cells: from transcriptome to senolytic drugs. *Aging Cell.* 2015;14:644–658.
25. Schafer MJ, White TA, Iijima K, et al. Cellular senescence mediates fibrotic pulmonary disease. *Nat Commun.* 2017;8:14532.
26. Chang J, Wang Y, Shao L, et al. Clearance of senescent cells by ABT263 rejuvenates aged hematopoietic stem cells in mice. *Nat Med.* 2016;22:78–83.
27. Yosef R, Pilpel N, Tokarsky-Amiel R, et al. Directed elimination of senescent cells by inhibition of BCL-W and BCL-XL. *Nat Commun.* 2016;7:11190.
28. Moncsek A, Al-Suraih MS, Trussoni CE, et al. Targeting senescent cholangiocytes and activated fibroblasts with B-cell lymphoma-extra large inhibitors ameliorates fibrosis in multidrug resistance 2 gene knockout (Mdr2-/-) mice. *Hepatology.* 2018;67:247–259.
29. Baar MP, Brandt RMC, Putavet DA, et al. Targeted apoptosis of senescent cells restores tissue homeostasis in response to chemotoxicity and aging. *Cell.* 2017;169:132–147.e16.
30. Justice JN, Nambiar AM, Tchkonia T, et al. Senolytics in idiopathic pulmonary fibrosis: results from a first-in-human, open-label, pilot study. *EBioMedicine.* 2019;40:554–563.
31. Hickson LJ, Langhi Prata LGP, Bobart SA, et al. Senolytics decrease senescent cells in humans: preliminary report from a clinical trial of Dasatinib plus Quercetin in individuals with diabetic kidney disease. *EBioMedicine.* 2019;47:446–456.
32. Grosse L, Wagner N, Emelyanov A, et al. Defined p16High senescent cell types are indispensable for mouse healthspan. *Cell Metab.* 2020;32:87–99.e6.
33. Fossel M. Cell senescence, telomerase and senolytic therapy. *OBM Geriatrics.* 2019;3:14.
34. Lamming DW, Ye L, Sabatini DM, Baur JA. Rapalogs and mTOR inhibitors as anti-aging therapeutics. *J Clin Invest.* 2013;123:980–989.
35. Hubbard BP, Sinclair DA. Small molecule SIRT1 activators for the treatment of aging and age-related diseases. *Trends Pharmacol Sci.* 2014;35:146–154.
36. Si H, Liu D. Dietary antiaging phytochemicals and mechanisms associated with prolonged survival. *J Nutr Biochem.* 2014;25:581–591.
37. Soto-Gamez A, Demaria M. Therapeutic interventions for aging: the case of cellular senescence. *Drug Discov Today.* 2017;22:786–795.
38. Nakamura S, Yoshimori T. Autophagy and longevity. *Mol Cells.* 2018;41:65–72.
39. Chondrogianni N, Voutetakis K, Kapetanou M, et al. Proteasome activation: an innovative promising approach for delaying aging and retarding age-related diseases. *Ageing Res Rev.* 2015;23(Pt A):37–55.
40. Bonafè M, Sabbatinelli J, Olivieri F. Exploiting the telomere machinery to put the brakes on inflamm-aging. *Ageing Res Rev.* 2020;59:101027.
41. Samper E, Flores JM, Blasco MA. Restoration of telomerase activity rescues chromosomal instability and premature aging in Terc-/- mice with short telomeres. *EMBO Rep.* 2001;2:800–807.
42. Jaskelioff M, Muller FL, Paik JH, et al. Telomerase reactivation reverses tissue degeneration in aged telomerase-deficient mice. *Nature.* 2011;469:102–106.
43. Sansone V, Le Grazie M, Roselli J, et al. Telomerase reactivation is associated with hepatobiliary and pancreatic cancers. *Hepatobiliary Pancreat Dis Int.* 2020;19:420–428.
44. Carew NT, Nelson AM, Liang Z, Smith SM, Milcarek C. Linking endoplasmic reticular stress and alternative splicing. *Int J Mol Sci.* 2018;19:.
45. Filichkin S, Priest HD, Megraw M, Mockler TC. Alternative splicing in plants: directing traffic at the crossroads of adaptation and environmental stress. *Curr Opin Plant Biol.* 2015;24:125–135.
46. Melangath G, Sen T, Kumar R, Bawa P, Srinivasan S, Vijayraghavan U. Functions for fission yeast splicing

factors SpSlu7 and SpPrp18 in alternative splice-site choice and stress-specific regulated splicing. *PLoS One.* 2017;12:e0188159.
47. He S, Sharpless NE. Senescence in health and disease. *Cell.* 2017;169:1000–1011.
48. de Klerk E, 't Hoen PA. Alternative mRNA transcription, processing, and translation: insights from RNA sequencing. *Trends Genet.* 2015;31:128–139.
49. Galganski L, Urbanek MO, Krzyzosiak WJ. Nuclear speckles: molecular organization, biological function and role in disease. *Nucleic Acids Res.* 2017;45:10350–10368.
50. Will CL, Luhrmann R. Spliceosome structure and function. *Cold Spring Harb Perspect Biol.* 2011;3:a003707:1–23.
51. Cartegni L, Chew SL, Krainer AR. Listening to silence and understanding nonsense: exonic mutations that affect splicing. *Nat Rev Genet.* 2002;3:285–298.
52. Pan Q, Shai O, Lee LJ, Frey BJ, Blencowe BJ. Deep surveying of alternative splicing complexity in the human transcriptome by high-throughput sequencing. *Nat Genet.* 2008;40:1413–1415.
53. Valcárcel J, Green MR. The SR protein family: pleiotropic functions in pre-mRNA splicing. *Trends Biochem Sci.* 1996;21:296–301.
54. Martinez-Contreras R, Cloutier P, Shkreta L, Fisette JF, Revil T, Chabot B. hnRNP proteins and splicing control. *Adv Exp Med Biol.* 2007;623:123–147.
55. Smith CW, Valcárcel J. Alternative pre-mRNA splicing: the logic of combinatorial control. *Trends Biochem Sci.* 2000;25:381–388.
56. Harries LW, Hernandez D, Henley W, et al. Human aging is characterized by focused changes in gene expression and deregulation of alternative splicing. *Aging Cell.* 2011;10:868–878.
57. Lee BP, Pilling LC, Bandinelli S, Ferrucci L, Melzer D, Harries LW. The transcript expression levels of HNRNPM, HNRNPA0 and AKAP17A splicing factors may be predictively associated with ageing phenotypes in human peripheral blood. *Biogerontology.* 2019;20:649–663.
58. Holly AC, Melzer D, Pilling LC, et al. Changes in splicing factor expression are associated with advancing age in man. *Mech Ageing Dev.* 2013;134:356–366.
59. Latorre E, Pilling LC, Lee BP, et al. The VEGFA156b isoform is dysregulated in senescent endothelial cells and may be associated with prevalent and incident coronary heart disease. *Clin Sci (Lond).* 2018;132:313–325.
60. Lye J, Latorre E, Lee BJ, et al. Astrocyte senescence may drive alterations in GFAP(A), CDKN2A p14ARF and TAU3 transcript expression and contribute to cognitive decline. *Geroscience.* 2019;41:561–573.
61. Lee BP, Pilling LC, Emond F, et al. Changes in the expression of splicing factor transcripts and variations in alternative splicing are associated with lifespan in mice and humans. *Aging Cell.* 2016;15:903–913.
62. Lee BP, Mulvey L, Barr G, et al. Dietary restriction in ILSXISS mice is associated with widespread changes in splicing regulatory factor expression levels. *Exp Gerontol.* 2019;128:110736.
63. Lee BP, Smith M, Buffenstein R, et al. Negligible senescence in naked mole rats may be a consequence of well-maintained splicing regulation. *Geroscience.* 2020;42:633–651.
64. Latorre E, Birar VC, Sheerin AN, et al. Small molecule modulation of splicing factor expression is associated with rescue from cellular senescence. *BMC Cell Biol.* 2017;18:31.
65. Latorre E, Ostler EL, Faragher RGA, et al. FOXO1 and ETV6 genes may represent novel regulators of splicing factor expression in cellular senescence. *FASEB J.* 2019;33:1086–1097.
66. Latorre E, Torregrossa R, Wood ME, et al. Mitochondria-targeted hydrogen sulfide attenuates endothelial senescence by selective induction of splicing factors HNRNPD and SRSF2. *Aging (Albany NY).* 2018;10:1666–1681.
67. Havens MA, Hastings ML. Splice-switching antisense oligonucleotides as therapeutic drugs. *Nucleic Acids Res.* 2016;44:6549–6563.
68. Corey DR. Nusinersen, an antisense oligonucleotide drug for spinal muscular atrophy. *Nat Neurosci.* 2017;20:497–499.
69. Cirak S, Arechavala-Gomeza V, Guglieri M, et al. Exon skipping and dystrophin restoration in patients with Duchenne muscular dystrophy after systemic phosphorodiamidate morpholino oligomer treatment: an open-label, phase 2, dose-escalation study. *Lancet.* 2011;378:595–605.
70. Aubol BE, Plocinik RM, Hagopian JC, et al. Partitioning RS domain phosphorylation in an SR protein through the CLK and SRPK protein kinases. *J Mol Biol.* 2013;425:2894–2909.
71. Bates DO, Morris JC, Oltean S, Donaldson LF. Pharmacology of modulators of alternative splicing. *Pharmacol Rev.* 2017;69:63–79.
72. Yousefzadeh MJ, Zhu Y, McGowan SJ, et al. Fisetin is a senotherapeutic that extends health and lifespan. *EBioMedicine.* 2018;36:18–28.